



THE UNIVERSITY OF
WAIKATO
Te Whare Wānanga o Waikato

Research Commons

<http://researchcommons.waikato.ac.nz/>

Research Commons at the University of Waikato

Copyright Statement:

The digital copy of this thesis is protected by the Copyright Act 1994 (New Zealand).

The thesis may be consulted by you, provided you comply with the provisions of the Act and the following conditions of use:

- Any use you make of these documents or images must be for research or private study purposes only, and you may not make them available to any other person.
- Authors control the copyright of their thesis. You will recognise the author's right to be identified as the author of the thesis, and due acknowledgement will be made to the author where appropriate.
- You will obtain the author's permission before publishing any material from the thesis.

Stabilisation Effects of Ferrocenylalkyl Groups on Hydrides of Heavier Main Group Elements

A thesis
submitted in fulfilment
of the requirements for the degree
of
Doctor of Philosophy in Chemistry
at
The University of Waikato
by
Toshie Asamizu



THE UNIVERSITY OF
WAIKATO
Te Whare Wānanga o Waikato

2013

Abstract

New hydrides of heavier *p*-block main group elements with a ferrocenylalkyl moiety, $\text{Fc}(\text{CH}_2)_n\text{EH}_m$ ($\text{Fc} = (\text{CpFeC}_5\text{H}_4^-)$; $\text{E} = \text{P}, \text{As}, \text{Si}, \text{Ge}$ or Se ; $n = 1, 2, 4, 6$ or 11 ; $m = 1, 2$ or 3) and $\text{FcCH}_2\text{P}(\text{R})\text{H}$ ($\text{R} = \text{CH}_3, \text{C}_6\text{H}_{11}$ or *p*- $\text{CH}_2\text{C}_6\text{H}_4\text{NO}_2$), have been synthesised and characterised. Although some precursors of the desired hydrides, i.e. $\text{Fc}(\text{Cl})\text{C}=\text{C}(\text{SnCl}_3)\text{H}$ and $(\text{FcCH}_2\text{Te})_2$, which are also new compounds, could be prepared, the syntheses of the corresponding desired hydrides, FcCH_2EH_n , were unsuccessful probably due to their extreme instabilities. Some related primary phosphanes, $[\text{CpFeC}_5\text{H}_3(\text{CH}_2\text{OH})(\text{CH}_2\text{PH}_2)]$, RcCH_2PH_2 and $\text{Fc}(\text{CH}_2)_6\text{PH}_2\cdot\text{BH}_3$, phosphane oxide, $\text{FcCH}_2\text{P}(\text{O})\text{H}_2$, and phosphinic acid, $\text{FcCH}_2\text{P}(\text{O})(\text{OH})\text{H}$, were also synthesised and reported. The X-ray crystal structures of $\text{Fc}(\text{CH}_2)_6\text{PH}_2\cdot\text{BH}_3$ and FcCH_2SeCN are also presented in the present thesis.

The stability of the hydrides of heavier *p*-block main group elements with a ferrocenyl or ruthenocenylalkyl moiety under ambient conditions has been investigated using NMR and/or IR spectroscopy. Ferrocenylalkyl and ruthenocenylmethyl primary phosphanes, $\text{Fc}(\text{CH}_2)_n\text{PH}_2$ ($n = 4, 6$ or 11) and RcCH_2PH_2 , respectively, exhibited a remarkable stability towards air oxidation in solution, i.e. ~ 1 year. In contrast, the secondary phosphanes were not as stable as expected, rapidly oxidising over several weeks or months. General trend for the oxidative stability of the secondary phosphanes could not be elucidated on the basis of the electronegativity, size or degree of conjugation of the substituent on the phosphorus. Ferrocenylmethyl primary arsane, $\text{FcCH}_2\text{AsH}_2$, was also unexpectedly air-sensitive, having been readily oxidised as a neat liquid or in solution upon the exposure to air.

Ferrocenylethyl primary silane, $\text{Fc}(\text{CH}_2)_2\text{SiH}_3$, was stable both as a neat liquid and also in solution. It could be purified on a TLC plate in air and also stored in solution for up to 7 months. On the other hand, ferrocenylmethyl primary germane, $\text{FcCH}_2\text{GeH}_3$, was unstable, almost completely decomposing left overnight in solution,

which was indicated by the disappearance of the germane proton NMR signal by ^1H NMR spectroscopy.

Ferrocenylalkyl selenols, $\text{Fc}(\text{CH}_2)_n\text{SeH}$ ($n = 1$ or 4), were both found to be unstable as neat liquids or in solution. Handling the compounds in air caused significant oxidation, resulting in the formation of the corresponding diselenides which are the common oxidation products of selenols. Ferrocenylmethyl selenol, FcCH_2SeH , was completely oxidised in solution in air in 5 days while ferrocenylbutyl selenol, $\text{Fc}(\text{CH}_2)_4\text{SeH}$, in 3 days. The rapid oxidation of the latter was also observed by IR spectroscopy over a period of 10 minutes when exposed to air as a neat liquid.

The oxidative stability of the air-sensitive primary phosphanes, PhPH_2 and camphyl PH_2 , in the presence of ferrocene, FcH , or its derivative, FcCH_2PH_2 , in solution, was studied by ^{31}P NMR spectroscopy. The study showed that the primary phosphanes could be stabilised by simple addition of FcH or FcCH_2PH_2 . The corresponding ^{31}P NMR study using known antioxidants, diphenyl picryl hydrazyl (DPPH) or nitrosobutane, in place of the ferrocene species also exhibited that PhPH_2 could be stabilised by addition of an antioxidant. These results suggest that FcH and FcCH_2PH_2 can be used to stabilise air-sensitive primary phosphanes in solution by simply adding them, probably acting as radical scavengers.

In contrast, the corresponding ^{77}Se NMR study into the oxidative stability of PhSeH in solution in the presence of FcH under the analogous conditions showed not only that the selenol could not be stabilised but rather the oxidation was almost twice as fast in the presence of FcH . It may suggest that the oxidation of selenols does not involve the formation of free radicals and hence cannot be stabilised by FcH which acts as a radical inhibitor in solution.

While the incorporation of a $\text{Fc}(\text{CH}_2)_n$ group at the hydride centres of the hydrides of heavier main group elements was successful for providing a stability for phosphanes, especially primary phosphanes, it was not for the other hydrides, i.e. $\text{Fc}(\text{CH}_2)_n\text{EH}$ ($\text{E} = \text{As, Ge, Se}$; $n = 1$ or 4).

Acknowledgements

I would like to thank my supervisors, Prof. Bill Henderson and Prof. Brian K Nicholson, for their guidance, encouragement and assistance in every way throughout the course of my Ph.D studies over the last three years.

I would like to thank Prof. Dr. Evamarie Hey-Hawkins and her research group at Leipzig University in Germany for having me there for a month and allowing me to experience their excellent research facilities some of which are not available at Waikato University, enabling me to broaden my experiences in synthetic chemistry.

I would like to thank Prof. Alistair Wilkins, Dr. Michael Mucalo and Dr. Graham Saunders for their assistance with NMR spectroscopy and Dr. Joseph Lane for his help with computational calculation. Also, I would like to thank Wendy Jackson and Pat Gread for their kind help with everything from finding chemicals to having instruments repaired whenever needed.

Thanks also go to Dr. Tania Groutso at Auckland University in New Zealand for collection of X-ray crystallographic structural data and also the Campbell Microanalysis Laboratory at Otago University in New Zealand for performing elemental analyses.

I am grateful to the Marsden Fund of the Royal Society of New Zealand for providing me a Ph.D scholarship as well as financial support for this research during the course of this study.

Table of Contents

Abstract	ii
Acknowledgements	iv
Table of Contents	v
List of Schemes	xv
List of Figures	xvii
List of Tables.....	xxvi
List of Abbreviations.....	xxviii
Chapter 1: Introduction.....	1
1.1 Literature Review	1
1.1.1 Hydrides of <i>p</i> -Block Elements	1
1.1.1.1 Discovery of the Hydrides of the Group 14 and 15 Elements.....	4
1.1.1.2 Properties of Hydrides of Heavier <i>p</i> -Block Elements	5
1.1.1.3 Organoderivatives of the Hydrides of the Group 15 Elements	6
1.1.1.4 Organophosphorus Hydrides	6
1.1.1.5 Organoarsenic Hydrides	9
1.1.1.6 Organoantimony Hydrides	11
1.1.1.7 Organoderivatives of the Hydrides of the Group 14 Elements	12
1.1.1.8 Organosilicon Hydrides.....	13
1.1.1.9 Organogermanium Hydrides	16
1.1.1.10 Organotin Hydrides	20
1.1.1.11 Organolead Hydrides.....	22
1.1.1.12 Organoderivatives of the Group 16 Element Hydrides	24
1.1.1.13 Stabilisation of Highly Reactive Hydrides of Heavier Main Group Elements	25
1.1.1.14 Stabilisation of the Hydrides of Heavier Main Group Elements with $\text{Fc}(\text{CH}_2)_n$ ($n \geq 1$) Groups	26
1.1.1.15 Aims of Thesis.....	27

Chapter 2: Stabilisation Effects of Ferrocenylalkyl Groups on the Hydrides of the Heavier Group 15 Elements, P, As, Sb	28
2.1 Introduction	28
2.1.1 Hydrides of Phosphorus, Arsenic and Antimon	28
2.1.2 Organo-phosphanes, -arsanes and -stibanes	29
2.1.3 Stabilisation of Hydrides of Heavier Group 15 Elements	29
2.2 Results and Discussion	30
2.2.1 Synthesis and Characterisation of Ferrocenylmethyl Secondary Phosphanes; $[\text{Fe}(\eta\text{-C}_5\text{H}_5)(\eta\text{-C}_5\text{H}_4\text{CH}_2\text{PRH})]$ ($\text{R} = \text{C}_6\text{H}_{11}$ (3), CH_3 (4), $p\text{-CH}_2\text{C}_6\text{H}_4\text{NO}_2$) (5))	30
2.2.1.1 Synthesis of FcCH_2PRH ($\text{R} = \text{C}_6\text{H}_{11}$ (3), CH_3 (4) and $\text{CH}_2\text{C}_6\text{H}_4\text{NO}_2$ (5))	30
2.2.1.2 Characterisation of FcCH_2PRH ($\text{R} = \text{C}_6\text{H}_{11}$ (3), CH_3 (4) and $\text{CH}_2\text{C}_6\text{H}_4\text{NO}_2$ (5))	34
2.2.1.3 Characterisation of $(\text{FcCH}_2)_2\text{PCy}$ (11), $(\text{FcCH}_2)_2\text{PCH}_2\text{C}_6\text{H}_4\text{NO}_2$ (12) and $\text{FcCH}_2\text{P}(\text{CH}_2\text{C}_6\text{H}_4\text{NO}_2)_2$ (13)	38
2.2.2 Synthesis and Characterisation of Ferrocenylalkyl Primary Phosphanes; $[\text{Fe}(\eta\text{-C}_5\text{H}_5)\{\eta\text{-C}_5\text{H}_4(\text{CH}_2)_n\text{PH}_2\}]$ ($n = 4, 6, 11$)	40
2.2.2.1 Synthesis of $\text{Fc}(\text{CH}_2)_n\text{P}(\text{CH}_2\text{OH})_2$ ($n = 4$ (20), 6 (21), 11 (22))	41
2.2.2.2 Characterisation of $\text{Fc}(\text{CH}_2)_n\text{P}(\text{CH}_2\text{OH})_2$ ($n = 4$ (20), 6 (21) or 11 (22))	41
2.2.2.3 Synthesis of $\text{Fc}(\text{CH}_2)_n\text{PH}_2$ ($n = 4$ (14), 6 (15), 11 (16))	45
2.2.2.4 Characterisation of $\text{Fc}(\text{CH}_2)_n\text{PH}_2$ ($n = 4$ (14), 6 (15), 11 (16))	45
2.2.2.5 Synthesis of RcCH_2PH_2 (24)	50
2.2.2.6 Characterisation of RcCH_2PH_2 (24)	51
2.2.2.7 Isolation and Partial Characterisation of $\text{RcCH}_2\text{P}(\text{O})(\text{CH}_2\text{OH})\text{H}$ (28)	55
2.2.2.8 Synthesis and Characterisation of $[\text{CpFeC}_5\text{H}_3(\text{CH}_2\text{OH})\{\text{CH}_2\text{P}(\text{CH}_2\text{OH})_2\}]$ (31) and $[\text{CpFeC}_5\text{H}_3(\text{CH}_2\text{OH})(\text{CH}_2\text{PH}_2)]$ (32)	56

2.2.2.9	Synthesis of $\text{Fc}(\text{CH}_2)_6\text{PH}_2\cdot\text{BH}_3$ (34)	61
2.2.2.10	Characterisation of $\text{Fc}(\text{CH}_2)_6\text{PH}_2\cdot\text{BH}_3$ (34).....	61
2.2.2.11	X-ray Crystallographic Structure of $\text{Fc}(\text{CH}_2)_6\text{PH}_2\cdot\text{BH}_3$ (34)	64
2.2.3	Synthesis and Characterisation of Phosphane Oxides	67
2.2.3.1	Synthesis of $\text{FcCH}_2\text{P}(\text{O})\text{H}_2$ (30).....	68
2.2.3.2	Characterisation of $\text{FcCH}_2\text{P}(\text{O})\text{H}_2$ (30).....	70
2.2.3.3	Synthesis of $\text{FcCH}_2\text{P}(\text{O})(\text{OH})\text{H}$ (36).....	72
2.2.3.4	Characterisation of $\text{FcCH}_2\text{P}(\text{O})(\text{OH})\text{H}$ (36).....	73
2.2.4	^{31}P NMR Studies on Oxidative Stability of Ferrocenyl Primary and Secondary Phosphanes	75
2.2.4.1	Air-Stability of FcCH_2PRH ($\text{R} = \text{C}_6\text{H}_{11}$ (3), CH_3 (4) and $\text{CH}_2\text{C}_6\text{H}_4\text{NO}_2$ (5)).....	75
2.2.4.2	Air-stability of $\text{Fc}(\text{CH}_2)_n\text{PH}_2$ ($n = 4$ (14), 6 (15), 11 (16)) and RcCH_2PH_2 (24).....	79
2.2.4.3	^{31}P NMR Studies into Effect of Ferrocene and FcCH_2PH_2 (1) on Oxidative Stability of PhPH_2 and CamphylPH_2 (2) in Solution	86
2.2.4.4	^{31}P NMR Study on Oxidative Stability of PhPH_2 in Solution with Added FcH or FcCH_2PH_2 (1).....	87
2.2.4.5	^{31}P NMR Study on Oxidative Stability of CamphylPH_2 (2) in Solution with Added FcH and (1)	89
2.2.4.6	^{31}P NMR Study on Oxidative Stability of PhPH_2 in Solution with Added Antioxidants.....	92
2.2.4.7	Summary	96
2.2.5	Synthesis and Characterisation of Ferrocenylmethyl Arsane (38).....	97
2.2.5.1	Synthesis and Characterisation of $\text{FcCH}_2\text{AsCl}_2$ (39)	98
2.2.5.2	Synthesis of $\text{FcCH}_2\text{AsH}_2$ (38)	100
2.2.5.3	Characterisation of $\text{FcCH}_2\text{AsH}_2$ (38)	101
2.2.5.4	Air-Stability of $\text{FcCH}_2\text{AsH}_2$ (38)	103
2.2.5.5	Attempted Synthesis of $\text{Fc}(\text{CH}_2)_n\text{AsH}_2$ ($n = 4$ (42), 6 (43) and 11 (44)	105
2.2.6	Attempted Synthesis of Ferrocenylmethyl Stibane (45)	106
2.2.6.1	Attempted Synthesis of $\text{FcCH}_2\text{SbCl}_2$ (46).....	106

2.2.6.2	Attempted Synthesis of $\text{FcCH}_2\text{SbH}_2$ (45)	107
2.3	Conclusion	108
2.4	Experimental.....	110
2.4.1	Synthesis of Ferrocenylmethyl Secondary Phosphanes; $[\text{Fe}(\eta\text{-C}_5\text{H}_5)(\eta\text{-C}_5\text{H}_4\text{CH}_2\text{PRH})]$ ($\text{R} = \text{C}_6\text{H}_{11}$ (3), CH_3 (4), $p\text{-CH}_2(\text{C}_6\text{H}_4)\text{NO}_2$ (5)).....	110
2.4.1.1	Synthesis of $\text{FcCH}_2\text{P}(\text{CH}_2\text{OH})\text{Cy}$ (7).....	110
2.4.1.2	Synthesis of $\text{FcCH}_2\text{P}(\text{Cy})\text{H}$ (3)	110
2.4.1.3	Synthesis of $\text{FcCH}_2\text{P}(\text{Me})\text{H}$ (4).....	111
2.4.1.4	Synthesis of $\text{FcCH}_2\text{P}(\text{CH}_2\text{C}_6\text{H}_4\text{NO}_2)\text{H}$ (5).....	112
2.4.2	Syntheses of Ferrocenylalkyl Primary Phosphanes	113
2.4.2.1	Synthesis of $\text{Fc}(\text{CH}_2)_4\text{P}(\text{CH}_2\text{OH})_2$ (20).....	113
2.4.2.2	Synthesis of $\text{Fc}(\text{CH}_2)_4\text{PH}_2$ (14)	114
2.4.2.3	Synthesis of $\text{Fc}(\text{CH}_2)_6\text{P}(\text{CH}_2\text{OH})_2$ (21).....	115
2.4.2.4	Synthesis of $\text{Fc}(\text{CH}_2)_6\text{PH}_2$ (15)	115
2.4.2.5	Synthesis of $\text{Fc}(\text{CH}_2)_{11}\text{P}(\text{CH}_2\text{OH})_2$ (22).....	116
2.4.2.6	Synthesis of $\text{Fc}(\text{CH}_2)_{11}\text{PH}_2$ (16).....	117
2.4.2.7	Synthesis of $\text{Fc}(\text{CH}_2)_6\text{PH}_2 \cdot \text{BH}_3$ (34)	117
2.4.2.8	Synthesis of $\text{RcCH}_2\text{P}(\text{CH}_2\text{OH})_2$ (27)	118
2.4.2.9	Synthesis of RcCH_2PH_2 (24).....	119
2.4.2.10	Synthesis of $[\text{CpFeC}_5\text{H}_3(\text{CH}_2\text{OH})\{\text{CH}_2\text{P}(\text{CH}_2\text{OH})_2\}]$ (31)	120
2.4.2.11	Synthesis of $[\text{CpFeC}_5\text{H}_3(\text{CH}_2\text{OH})(\text{CH}_2\text{PH}_2)]$ (32).....	120
2.4.3	Synthesis of Ferrocenylmethyl Phosphane Oxide and Phosphinic Acid.....	121
2.4.3.1	Synthesis of $\text{FcCH}_2\text{P}(\text{O})\text{H}_2$ (30).....	121
2.4.3.2	Synthesis of $\text{FcCH}_2\text{P}(\text{O})(\text{OH})\text{H}$ (36).....	122
2.4.4	^{31}P NMR Studies on Oxidative Stability of PhPH_2 and CamphylPH_2 (2) in Solution	123
2.4.4.1	^{31}P NMR Investigation on Oxidative Stability of PhPH_2 in Solution with Added FcH or FcCH_2PH_2 (1)	123

2.4.4.2	³¹ P NMR Investigation on Oxidative Stability of CamphylPH ₂ (2) in Solution with Added FcH and FcCH ₂ PH ₂ (1)	123
2.4.4.3	³¹ P NMR Investigation on Oxidative Stability of PhPH ₂ in Solution with Added Antioxidants	124
2.4.4.4	³¹ P NMR Investigation on Oxidative Stability of PhPH ₂ in Solution with Added Phenylphosphinic Acid	124
2.4.5	Synthesis of Ferrocenylalkyl Arsanes	124
2.4.5.1	Synthesis of FcCH ₂ AsCl ₂ (39)	124
2.4.5.2	Synthesis of FcCH ₂ AsH ₂ (38)	125
2.4.5.3	Attempted Synthesis of Fc(CH ₂) ₄ AsH ₂ (42) from reaction of Fc(CH ₂) ₄ As(O)(OH) ₂ (48) with Zn/HCl	126
2.4.5.4	Attempted Synthesis of Fc(CH ₂) ₁₁ AsH ₂ (44) from reaction of Fc(CH ₂) ₁₁ As(O)(OH) ₂ (49) with Zn/HCl	127
2.4.5.5	Attempted Synthesis of Ferrocenylmethyl Stibane	128
2.4.5.6	Attempted Synthesis of FcCH ₂ SbCl ₂ (46)	128
2.4.5.7	Attempted Synthesis of FcCH ₂ SbH ₂ (45)	129
2.4.6	X-Ray Crystallography	129
Chapter 3: Stabilisation Effects of Ferrocenylalkyl Groups on the Hydrides of the Heavier Group 14 Elements, Si, Ge, Sn		131
3.1	Introduction	131
3.1.1	Hydrides of Heavier Group 14 Elements	131
3.1.2	Organo-silanes, -germanes and -stannanes	132
3.1.3	Stabilisation of Hydrides of Heavier Group 14 Elements	133
3.1.4	Synthesis of Hydrides of Heavier Group 14 Elements	134
3.2	Results and Discussion	135
3.2.1	Synthesis and Characterisation of Ferrocenylethyl Silane, FcCH ₂ CH ₂ SiH ₃ (50)	135
3.2.1.1	Synthesis and Characterisation of Fc(CH ₂) ₂ SiX ₃ (X = Cl (51) and OMe (52))	136
3.2.1.2	Synthesis of Fc(CH ₂) ₂ SiH ₃ (50)	139

3.2.1.3	Characterisation of $\text{Fc}(\text{CH}_2)_2\text{SiH}_3$ (50)	139
3.2.2	Air-Stability of $\text{Fc}(\text{CH}_2)_2\text{SiH}_3$ (50)	142
3.2.3	Synthesis and Characterisation of Ferrocenylmethyl Germane, $\text{FcCH}_2\text{GeH}_3$ (57)	143
3.2.3.1	Synthesis and Characterisation of $\text{FcCH}_2\text{GeCl}_3$ (58)	143
3.2.3.2	Synthesis of $\text{FcCH}_2\text{GeH}_3$ (57)	146
3.2.3.3	Characterisation of $\text{FcCH}_2\text{GeH}_3$ (57)	147
3.2.4	Stability of $\text{FcCH}_2\text{GeH}_3$ (57)	149
3.2.5	Attempted Syntheses and Characterisation of Ferrocenylalkyl Stannane	150
3.2.5.1	Attempted Syntheses of $\text{FcCH}_2\text{SnX}_3$ ($\text{X} = \text{Cl}$ (59), I (60)) and by Reaction of FcCH_2Li (40) with SnX_4	152
3.2.5.2	Attempted Synthesis of $\text{FcCH}_2\text{SnCl}_3$ (59) by Reaction of $[\text{FcCH}_2\text{NMe}_3]\text{I}$ (6) with SnCl_2	152
3.2.5.3	Synthesis and Characterisation of 1-Trichlorostannyl-2- ferrocenyl-ethene (62)	153
3.2.5.4	Attempted Synthesis of $\text{Fc}(\text{Cl})\text{C}=\text{C}(\text{H})\text{SnH}_3$ (64) or $\text{Fc}(\text{CH}_2)_2\text{SnH}_3$ (65) <i>via</i> $\text{Fc}(\text{Cl})\text{C}=\text{C}(\text{H})\text{SnCl}_3$ (62)	156
3.3	Conclusion	157
3.4	Experimental	158
3.4.1	Synthesis of $\text{Fc}(\text{CH}_2)_2\text{SiH}_3$ (50)	158
3.4.1.1	Synthesis of $\text{Fc}(\text{CH}_2)_2\text{Si}(\text{OMe})_3$ (52)	158
3.4.1.2	Synthesis of $\text{Fc}(\text{CH}_2)_2\text{SiH}_3$ (50) <i>via</i> $\text{Fc}(\text{CH}_2)_2\text{Si}(\text{OMe})_3$ (52)	159
3.4.1.3	Synthesis of $\text{Fc}(\text{CH}_2)_2\text{SiCl}_3$ (51)	159
3.4.1.4	Synthesis of $\text{Fc}(\text{CH}_2)_2\text{SiH}_3$ (50) <i>via</i> $\text{Fc}(\text{CH}_2)_2\text{SiCl}_3$ (51)	160
3.4.2	Synthesis of $\text{FcCH}_2\text{GeH}_3$ (57)	160
3.4.2.1	Synthesis of $\text{FcCH}_2\text{GeCl}_3$ (58)	160
3.4.2.2	Synthesis of $\text{FcCH}_2\text{GeH}_3$ (57)	161
3.4.3	Attempted Synthesis of Ferrocenylalkyl Stannane, $\text{FcCH}_2\text{SnH}_3$ (66)	162
3.4.3.1	Attempted Synthesis of $\text{FcCH}_2\text{SnCl}_3$ (59)	162

3.4.3.2	Attempted Synthesis of $\text{FcCH}_2\text{SnH}_3$ (66) via $\text{FcCH}_2\text{SnCl}_3$ (59)	163
3.4.3.3	Attempted Synthesis of $\text{FcCH}_2\text{SnI}_3$ (60) by Reaction of FcCH_2Li (40) with SnI_4	164
3.4.3.4	Attempted Synthesis of $\text{FcCH}_2\text{SnH}_3$ (66) via $\text{FcCH}_2\text{SnI}_3$ (60) ..	164
3.4.3.5	Attempted Synthesis of $\text{FcCH}_2\text{SnCl}_3$ (59) by Reaction of $[\text{FcCH}_2\text{NMe}_3]\text{I}$ (6) with SnCl_2	164
3.4.3.6	Synthesis of $\text{Fc}(\text{Cl})\text{C}=\text{C}(\text{H})\text{SnCl}_3$ (62).....	165
3.4.3.7	Attempted Synthesis of $\text{Fc}(\text{Cl})\text{C}=\text{C}(\text{H})\text{SnH}_3$ (64).....	166

Chapter 4: Stabilisation Effects of Ferrocenylalkyl Groups on the Hydrides of Heavier Group 16 Elements, Se, Te..... 167

4.1	Introduction	167
4.1.1	Hydrides of Heavier Group 16 Elements	167
4.1.2	Organo-selenols and -tellurols	167
4.1.3	Stabilisation of Hydrides of Heavier Group 16 Elements.....	168
4.1.4	Synthesis of Organo-selenols and -tellurols.....	169
4.2	Results and Discussion	170
4.2.1	Synthesis of Ferrocenylalkyl Selenols	170
4.2.1.1	Synthesis of $\text{Fc}(\text{CH}_2)_n\text{SeCN}$ ($n = 1$ (67), 4 (68)).....	171
4.2.1.2	Characterisation of $\text{Fc}(\text{CH}_2)_n\text{SeCN}$ ($n = 1$ (67), 4 (68)).....	172
4.2.1.3	Synthesis of $(\text{FcCH}_2\text{Se})_2$ (69) by Reaction of FcCH_2Li (40) with Elemental Se.....	178
4.2.1.4	Attempted Synthesis of $(\text{FcCH}_2\text{Se})_2$ (69) by Reaction of $[\text{FcCH}_2\text{NMe}_3]\text{I}$ (6) with Na_2Se_2	181
4.2.1.5	Synthesis of $(\text{FcCH}_2\text{Se})_2$ (69) by Reaction of FcCH_2Cl (71) with Na_2Se_2	182
4.2.1.6	Attempted Synthesis of FcCH_2SeH (72) by Reaction of FcCH_2Cl (71) with NaSeH	183
4.2.1.7	Synthesis of $\text{Fc}(\text{CH}_2)_n\text{SeH}$ ($n = 1$ (72), 4 (74)) by Reaction of $\text{Fc}(\text{CH}_2)_n\text{SeCN}$ ($n = 1$ (67), 4 (68)) with NaBH_4	184
4.2.1.8	Synthesis of FcCH_2SeH (72) by Reaction of $(\text{FcCH}_2\text{Se})_2$ (69) with Zn under Acidic Conditions	187

4.2.1.9	Synthesis of FcCH_2SeH (72) by Reduction of $(\text{FcCH}_2\text{Se})_2$ (69) with NaBH_4	188
4.2.1.10	Summary	189
4.2.1.11	Characterisation of $(\text{FcCH}_2\text{Se})_2$ (69), $(\text{FcCH}_2)_2\text{Se}$ (70) and $(\text{FcCH}_2)_2\text{Se}_3$ (76)	190
4.2.1.12	Characterisation of $\{\text{Fc}(\text{CH}_2)_4\text{Se}\}_2$ (75) and $\{\text{Fc}(\text{CH}_2)_4\}_2\text{Se}$ (77)	194
4.2.1.13	Characterisation of $\text{Fc}(\text{CH}_2)_n\text{SeH}$ ($n = 1$ (72), 4 (74))	197
4.2.1.14	Air-stability of $\text{Fc}(\text{CH}_2)_n\text{SeH}$ ($n = 1$ (72), 4 (74))	204
4.2.2	^{77}Se NMR Study on Effect of Ferrocene on Oxidative Stability of Phenyl Selenol (78) in Solution	206
4.2.3	Attempted Synthesis of Ferrocenylmethyl Tellurol (80)	209
4.2.3.1	Synthesis of KTeCN (86).....	210
4.2.3.2	Attempted Synthesis of FcCH_2TeCN (81) by Reaction of FcCH_2Cl (71) with KTeCN (86)	211
4.2.3.3	Attempted Synthesis of FcCH_2TeCN (81) by Reaction of $[\text{FcCH}_2\text{NMe}_3]\text{I}$ (6) with KTeCN (86)	211
4.2.3.4	Attempted Synthesis of $\text{Fc}(\text{CH}_2)_4\text{TeCN}$ (87) by Reaction of $\text{Fc}(\text{CH}_2)_4\text{Br}$ (17) with KTeCN (86)	212
4.2.3.5	Synthesis of $(\text{FcCH}_2\text{Te})_2$ (82) by Reaction of FcCH_2Li (40) with Te powder.....	212
4.2.3.6	Characterisation of $(\text{FcCH}_2\text{Te})_2$ (82) and $(\text{FcCH}_2)_2\text{Te}$ (88)	214
4.2.3.7	Attempted Synthesis of FcCH_2TeH (80).....	217
4.2.3.8	Attempted Synthesis of FcCH_2TeH (80) by Reduction of $(\text{FcCH}_2\text{Te})_2$ (82) with Zn/HCl	218
4.2.3.9	Attempted Synthesis of FcCH_2TeH (80) by Reduction of $(\text{FcCH}_2\text{Te})_2$ (82) with NaBH_4	218
4.3	Conclusion.....	218
4.4	Experimental.....	219
4.4.1	Synthesis of Ferrocenylalkyl Selenols, $[\text{Fe}(\eta\text{-C}_5\text{H}_5)\{\eta\text{-C}_5\text{H}_4(\text{CH}_2)_n\text{SeH}]$ ($n = 1$ (72) or 4 (74)).....	219
4.4.1.1	Synthesis of $(\text{FcCH}_2\text{Se})_2$ (69) from FcCH_2Li (40) with Elemental Se.....	220

4.4.1.2	Synthesis of FcCH ₂ SeCN (67)	222
4.4.1.3	Synthesis of FcCH ₂ SeH (72) by Reaction of (FcCH ₂ Se) ₂ (69) with Zn/HCl.....	222
4.4.1.4	Attempted Synthesis of (FcCH ₂ Se) ₂ (69) by Reaction of [FcCH ₂ NMe ₃]I (6) with Na ₂ Se ₂	223
4.4.1.5	Attempted Synthesis of (FcCH ₂ Se) ₂ (69) by Reaction of FcCH ₂ Cl (71) with Na ₂ Se ₂	223
4.4.1.6	Attempted Synthesis of FcCH ₂ SeH (72) from Reaction of FcCH ₂ Cl (71) with NaSeH.....	224
4.4.1.7	Synthesis of FcCH ₂ SeH (72) by Reaction of (FcCH ₂ Se) ₂ (69) with NaBH ₄	224
4.4.1.8	Synthesis of FcCH ₂ SeH (72) by Reaction of FcCH ₂ SeCN (67) with NaBH ₄	225
4.4.1.9	Synthesis of Fc(CH ₂) ₄ SeCN (68)	226
4.4.1.10	Synthesis of Fc(CH ₂) ₄ SeH (74) by Reaction of Fc(CH ₂) ₄ SeCN (68) with NaBH ₄	226
4.4.1.11	⁷⁷ Se NMR Study on Effect of Ferrocene on Oxidative Stability of PhSeH (78) in Solution.....	227
4.4.2	Attempted Synthesis of Ferrocenylmethyl Tellurol (80)	228
4.4.2.1	Attempted Synthesis of FcCH ₂ TeCN (81) by Reaction of FcCH ₂ Cl (71) with (86).....	228
4.4.2.2	Attempted Synthesis of FcCH ₂ TeCN (81) by Reaction of [FcCH ₂ NMe ₃]I (6) with (86)	229
4.4.2.3	Attempted Synthesis of Fc(CH ₂) ₄ TeCN (87) by Reaction of Fc(CH ₂) ₄ Br (17) with (86).....	229
4.4.2.4	Synthesis of (FcCH ₂ Te) ₂ (82).....	230
4.4.2.5	Attempted Synthesis of FcCH ₂ TeH (80) by Reaction of (FcCH ₂ Te) ₂ (82) with Zn/HCl.....	231
4.4.2.6	Attempted Synthesis of FcCH ₂ TeH (80) by Reaction of (FcCH ₂ Te) ₂ (82) with NaBH ₄	231
4.4.3	X-Ray Crystallography	231
Chapter 5: Overall Conclusion		233
Chapter 6: General Experimental Procedures and Materials		239
6.1	General Experimental Techniques.....	239

6.1.1	Schlenk Line.....	239
6.1.2	Chromatography.....	240
6.2	Instrumentation.....	241
6.2.1	FTIR Spectroscopy.....	241
6.2.2	ESI-Mass Spectrometry	241
6.2.3	GC-Mass Spectrometry.....	242
6.2.4	NMR Spectroscopy	242
6.2.5	X-ray Crystallography.....	244
6.3	Chemicals	245
6.3.1	Reaction Solvents.....	245
6.3.2	Commercial Chemicals	245
6.3.3	Synthesised Compounds	246
6.3.4	Other Compounds	246
	References	248

List of Schemes

Scheme 1-1:	<i>(a) Nucleophilic displacement of a negative ligand in organosilanes by a hydride ion H; (b) nucleophilic displacement of a negative ligand in substituted silicon hydrides by a carbanion R⁻; (c) protonation of an organosilylmetal compound; (d) abnormal Grignard reaction; (e) hydrosilation of alkenes and alkynes (adopted from Wiberg, E.; Amberger, E., Hydrides of the Elements of Main Groups I-IV, (1971))</i>	14
Scheme 1-2:	<i>Reactions of Si-H bonds (adopted from Wiberg, E.; Amberger, E., Hydrides of the Elements of Main Groups I-IV, (1971))</i>	16
Scheme 1-3:	<i>Reactions of Ge-H bonds (adopted from Wiberg, E.; Amberger, E., Hydrides of the Elements of Main Groups I-IV, (1971))</i>	19
Scheme 1-4:	<i>Reactions of Sn-H bonds (adopted from Wiberg, E.; Amberger, E., Hydrides of the Elements of Main Groups I-IV, (1971))</i>	21
Scheme 1-5:	<i>Synthesis of alkylplumbanes (adopted from Wiberg, E.; Amberger, E., Hydrides of the Elements of Main Groups I-IV, (1971))</i>	23
Scheme 2-1:	<i>Synthesis of 3, 4 and 5</i>	31
Scheme 2-2:	<i>Synthesis of ferrocenylalkyl primary phosphanes</i>	40
Scheme 2-3:	<i>Synthesis of 24</i>	50
Scheme 2-4:	<i>Synthesis of 32 via 31</i>	57
Scheme 2-5:	<i>Synthesis of 34</i>	61
Scheme 2-6:	<i>Synthesis of 30 and 36</i>	68
Scheme 2-7:	<i>Disproportionation of ferrocenylmethyl phosphane oxide</i>	69
Scheme 2-8:	<i>Typical oxidation of secondary phosphane</i>	76
Scheme 2-9:	<i>Typical oxidation of primary phosphane</i>	79
Scheme 2-10:	<i>Oxidation of primary phosphane of the type RPH₂⁹</i>	87
Scheme 2-11:	<i>Proposed photolytic oxidation mechanism of primary phosphane of the type RPH₂ by Higham et al.^{114, 119}</i>	95
Scheme 2-12:	<i>Proposed inhibition mechanism of phosphane oxidation by ferrocene</i>	96

Scheme 2-13:	<i>Synthesis of 38 via 39</i>	97
Scheme 2-14:	<i>Postulated oxidation of RAsH₂ with O₂</i>	104
Scheme 2-15:	<i>Attempted synthesis of 42, 43 and 44 by reduction of the corresponding arsonic acids with Zn/HCl</i>	106
Scheme 2-16:	<i>Attempted synthesis of 45 via 46</i>	106
Scheme 3-1:	<i>Hydrosilation of alkene using a Pt catalyst</i>	134
Scheme 3-2:	<i>Hydrosilation of ferrocenyl alkenes with a Pt catalyst</i>	134
Scheme 3-3:	<i>Synthesis of FcCH₂EH₂ (E = Ge or Sn) via FcCH₂ECl₃</i>	135
Scheme 3-4:	<i>Synthesis of 50</i>	135
Scheme 3-5:	<i>Synthesis of 57 via 58</i>	143
Scheme 3-6:	<i>Attempted syntheses of ferrocenyl stannic halides and stannane</i> ...	151
Scheme 4-1:	<i>Oxidation and reduction of organo-selenols and -tellurols and the corresponding dichalcogenides</i>	168
Scheme 4-2:	<i>Proposed synthetic routes to Fc(CH₂)_nEH (E = Se or Te)</i>	169
Scheme 4-3:	<i>Attempted synthesis of ferrocenyl-methyl 72 and -butyl 74 selenols</i>	170
Scheme 4-4:	<i>Proposed reaction of organoselenocyanate with metal hydride to give the corresponding organoselenol by Krief et al.¹⁶⁸</i>	186
Scheme 4-5:	<i>Attempted synthesis of 81 and synthesis of 82</i>	210
Scheme 4-6:	<i>Attempted synthesis of 80 via 82</i>	217

List of Figures

Figure 1-1:	<i>Tetrahedral configuration of the hydrides of the Group 14 elements</i>	2
Figure 1-2:	<i>Polarisation of the hydrogen atoms in the hydrides of the Group 15, EH₃, 16, EH₂, and 17, EH, elements¹</i>	2
Figure 1-3:	<i>Examples of dative bonds formed by HF, H₂O and H₃N·BH₃ to themselves or foreign electron acceptors¹</i>	3
Figure 1-4:	<i>Commonly utilised methods for the synthesis of hydrides of the main group elements (adopted from Wiberg, E.; Amberger, E., Hydrides of the Elements of Main Groups I-IV, (1971))</i>	4
Figure 1-5:	<i>(a) Phenylthiophosphonic anhydride; (b) 4-membered thiophosphane (c) secondary phosphane sulfide and selenide (adopted from Kosolapoff, G. M.; Maier, L., Organic Phosphorus Compounds, (1972))</i>	8
Figure 1-6:	<i>Sterically stabilised hydrides of heavier main group elements</i>	25
Figure 1-7:	<i>Primary phosphanes stabilised by conjugation in their backbones</i>	26
Figure 1-8:	<i>Air-stable primary phosphanes and arsane with a Fc(CH₂)_n (n = 1 or 2) group</i>	26
Figure 2-1:	<i>³¹P NMR spectra of (a) 3 and (b) 4 after being stored as neat liquids for 5 months at -18 °C in air</i>	32
Figure 2-2:	<i>Overalkylated by-products 11, 12 and 13 from the synthesis of 3 and 5</i>	34
Figure 2-3:	<i>Atom labelling used in NMR assignments of ferrocenyl secondary phosphanes; hydrogen atoms are numbered according to the carbon to which they are bonded</i>	36
Figure 2-4:	<i>Selected ^{1,2,3}J_{CH} and ³J_{HH} NMR correlations observed in the HMBC, HSQC, COSY and HETCOR NMR experiments for 3, 4, 5</i>	37
Figure 2-5:	<i>Selected ^{1,2,3}J_{CH} and ²J_{PH} correlations observed for 12 in the HMBC and HSQC and HETCOR, respectively, NMR experiments</i>	39
Figure 2-6:	<i>Selected ^{1,2,3}J_{CH} and ³J_{HH} correlations observed in the HMBC, HSQC and COSY NMR experiments for 13</i>	40

Figure 2-7:	<i>Selected $^{1,2,3}J_{CH}$ and $^3J_{HH}$ correlations observed for 20, 21 and 22 in the HMBC, HSQC and COSY NMR experiments</i>	42
Figure 2-8:	<i>Atom labelling used in assignment of ferrocenylalkyl phosphanes NMR signals; hydrogen atoms are numbered according to the carbon to which they are bonded</i>	43
Figure 2-9:	<i>Partial ESI-MS of 21 showing the observed and theoretical isotope distribution patterns of $[M + Ag]^+$ ion</i>	44
Figure 2-10:	<i>ESI-MS of (a) 20 (b) 21 (c) 22 with added aq. $AgNO_3$</i>	44
Figure 2-11:	<i>IR spectrum showing the ν P-H stretches for (a) 14, (b) 15 and (c) 16</i>	46
Figure 2-12:	<i>(a) Observed and (b) theoretical isotope pattern for the $[M]^+$ Ion of 15</i>	47
Figure 2-13:	<i>GC-MS of 14, 15 and 16</i>	48
Figure 2-14:	<i>Selected $^{1,2,3}J_{CH}$ and $^3J_{HH}$ correlations observed for 14, 15 and 16 in the HMBC, HSQC and COSY NMR experiments</i>	49
Figure 2-15:	<i>Partial IR spectrum of 24</i>	51
Figure 2-16:	<i>Selected $^{1,2,3}J_{CH}$ correlations observed for 24 in the HMBC and HSQC NMR experiments</i>	53
Figure 2-17:	<i>Atom labelling used in NMR assignments for 24; hydrogen atoms are numbered according to the carbon to which they are bonded</i>	53
Figure 2-18:	<i>EI-mass spectrum of 24</i>	53
Figure 2-19:	<i>Partial ESI-MS of 24 showing the observed and theoretical $[M - PH_2]^+$ ions ($M = \mathbf{24}$)</i>	54
Figure 2-20:	<i>Partial ESI-MS of 24 showing the observed and theoretical $[M + Ag]^+$ ion ($M = \mathbf{24}$)</i>	54
Figure 2-21:	<i>Proposed Structure of 29</i>	56
Figure 2-22:	<i>$^{1,2,3}J_{CH}$ and $^3J_{HH}$ correlations observed for 29 in the HMBC, HSQC and HETCOR NMR experiments</i>	56
Figure 2-23:	<i>$^{1,2,3}J_{CH}$ correlations observed for 31 in the HMBC and HSQC experiments</i>	58

Figure 2-24: <i>Atom labelling used in NMR assignments for 31 and 32; hydrogen atoms are numbered according to the carbon to which they are bonded</i>	58
Figure 2-25: <i>IR spectrum of 32</i>	59
Figure 2-26: <i>Selected $^{1,2,3}J_{CH}$ correlations observed for 32 in the HMBC and HSQC NMR experiments</i>	60
Figure 2-27: <i>IR spectrum of 34</i>	62
Figure 2-28: <i>Partial ESI-MS of 34 showing the observed and theoretical $[M]^+$ ion ($M = 34$)</i>	62
Figure 2-29: <i>^{31}P NMR spectrum of 34</i>	63
Figure 2-30: <i>Selected $^{1,2,3}J_{CH}$ and $^3J_{HH}$ correlations observed for 34 in the HMBC, HSQC and COSY NMR experiments</i>	64
Figure 2-31: <i>Crystal structure of 34</i>	65
Figure 2-32: <i>$^{31}P\{-^1H\}$ NMR spectrum of 30</i>	69
Figure 2-33: <i>IR spectrum of 30</i>	70
Figure 2-34: <i>Partial ESI-MS of 30 showing the observed and theoretical $[M + Na]^+$ ion ($M = 30$)</i>	71
Figure 2-35: <i>Atom labelling used in NMR assignments for 30 and 36; hydrogen atoms are numbered according to the carbon to which they are bonded</i>	72
Figure 2-36: <i>Selected $^{1,2,3}J_{CH}$ and $^3J_{HH}$ correlations observed for 30 in the HMBC, HSQC and COSY NMR experiments</i>	72
Figure 2-37: <i>IR spectrum of 36</i>	74
Figure 2-38: <i>Selected $^{1,2,3}J_{CH}$ correlations observed for 36 in the HMBC, HSQC and COSY NMR experiments</i>	75
Figure 2-39: <i>Oxidation progress of ferrocenyl secondary phosphanes 3, 4 and 5</i>	77
Figure 2-40: <i>$^{31}P\{-^1H\}$ NMR spectra showing the oxidation of 5 in solution at room temperature in air</i>	77
Figure 2-41: <i>$^{31}P\{-^1H\}$ NMR spectra showing the oxidation of 3 in solution at room temperature in air</i>	78

Figure 2-42:	<i>³¹P-¹H} NMR spectra showing the oxidation of 4 in solution at room temperature in air</i>	78
Figure 2-43:	<i>Oxidation progress of phenyl phosphane and ferrocenyl primary phosphanes 14, 15, 16 and 24 in solution at room temperature in air monitored by ³¹P NMR spectroscopy with ¹H decoupled mode.....</i>	81
Figure 2-44:	<i>³¹P NMR spectrum showing the air oxidation of Fc(CH₂)₄PH₂ 14 in solution at room temperature</i>	82
Figure 2-45:	<i>³¹P NMR spectrum showing the air oxidation of Fc(CH₂)₆PH₂ 15 in solution at room temperature</i>	83
Figure 2-46:	<i>³¹P NMR spectrum showing the air oxidation of Fc(CH₂)₁₁PH₂ 16 in solution at room temperature</i>	83
Figure 2-47:	<i>³¹P-¹H} NMR spectrum showing the air oxidation of 24 in solution at room temperature</i>	84
Figure 2-48:	<i>³¹P-¹H} NMR spectra showing the oxidation of PhPH₂ in solution at room temperature over 78 days.....</i>	88
Figure 2-49:	<i>³¹P-¹H} NMR spectra showing the oxidation of PhPH₂ in solution at room temperature in air with a 0.48 molar equivalent of added FcH</i>	88
Figure 2-50:	<i>³¹P-¹H} NMR spectra showing the oxidation of PhPH₂ in solution at room temperature in air with a 0.37 molar equivalent of 1 added</i>	89
Figure 2-51:	<i>Oxidation Progress of 2 in CDCl₃ at room temperature in air with FcH or 1 added.....</i>	90
Figure 2-52:	<i>³¹P-¹H} NMR spectra showing the oxidation of 2 in solution at room temperature in air</i>	91
Figure 2-53:	<i>³¹P-¹H} NMR spectra showing the oxidation of 2 in solution at room temperature in air with FcH added.....</i>	91
Figure 2-54:	<i>³¹P-¹H} NMR spectra showing the oxidation of 2 in solution at room temperature in air with 1 added.....</i>	92
Figure 2-55:	<i>³¹P-¹H} NMR spectra showing the oxidation of PhPH₂ in solution at room temperature</i>	93

Figure 2-56:	<i>³¹P-¹H} NMR spectra showing the oxidation of PhPH₂ in solution at room temperature with added nitrosobutane</i>	94
Figure 2-57:	<i>³¹P-¹H} NMR spectra showing the oxidation of PhPH₂ in solution at room temperature with added DPPH</i>	94
Figure 2-58:	<i>Selected ^{1,2,3}J_{CH} correlations observed for 39 in the HMBC and HSQC NMR experiments</i>	99
Figure 2-59:	<i>Partial ESI-MS of 39 showing the observed and theoretical [M - Cl]⁺ ion (M = 39)</i>	99
Figure 2-60:	<i>IR spectrum of 38</i>	101
Figure 2-61:	<i>Selected ^{2,3}J_{CH} Correlations Observed for 38 in the HMBC, HSQC COSY NMR Experiments</i>	102
Figure 2-62:	<i>GC-MS of 38</i>	102
Figure 2-63:	<i>Partial ESI-MS of 38 showing the observed and theoretical [M]⁺ ion (M = 38)</i>	103
Figure 2-64:	<i>¹H NMR spectrum showing the complete oxidation of 38 in CDCl₃ after 24 days at room temperature in air</i>	105
Figure 3-1:	<i>Stable primary organo-germane and -stannane</i>	133
Figure 3-2:	<i>Partial IR Spectrum of 51</i>	137
Figure 3-3:	<i>Selected ^{1,2,3}J_{CH} and ³J_{HH} correlations observed for 51 in the HMBC, HSQC and COSY NMR experiments</i>	137
Figure 3-4:	<i>Partial ESI-MS of 52 showing the observed and theoretical [M]⁺ ion (M = 52)</i>	138
Figure 3-5:	<i>Selected ^{1,2,3}J_{CH} and ³J_{HH} correlations observed for 52 in the HMBC, HSQC and COSY NMR experiments</i>	138
Figure 3-6:	<i>IR spectrum of 50</i>	140
Figure 3-7:	<i>Partial ¹H NMR spectrum showing the δ Si-H Signal of 50</i>	141
Figure 3-8:	<i>Selected ^{1,2,3}J_{CH} and ³J_{HH} correlations observed for 50 in the HMBC, HSQC and COSY NMR experiments</i>	141
Figure 3-9:	<i>Partial ESI-MS of 50 showing the observed and theoretical [M]⁺ ion (M = 50)</i>	142
Figure 3-10:	<i>Partial ¹H NMR spectra showing the oxidation of 50 in CDCl₃ at room temperature in a capped NMR tube in air over 218 days</i>	143

Figure 3-11:	<i>IR spectrum of 58</i>	144
Figure 3-12:	<i>Partial ESI-MS of 58 showing the observed and theoretical [M – Cl + OH]⁺ ion (M = 58)</i>	145
Figure 3-13:	<i>Selected ^{1,2,3}J_{CH} correlations observed for 58 in the HMBC and HSQC NMR experiments</i>	145
Figure 3-14:	<i>IR spectrum of 57</i>	147
Figure 3-15:	<i>Partial ESI-MS of 57 showing the observed and theoretical [M]⁺ ion (M = 57)</i>	148
Figure 3-16:	<i>GC-MS of 57</i>	148
Figure 3-17:	<i>Partial COSY NMR spectrum of 57</i>	149
Figure 3-18:	<i>Selected ^{1,2,3}J_{CH} and ³J_{HH} correlations observed for 57 in the HMBC, HSQC and COSY NMR experiments</i>	149
Figure 3-19:	<i>¹H NMR spectra of 57 in solution at 300 K over 20 hours</i>	150
Figure 3-20:	<i>IR spectrum of the crude product from the reaction of 59 (assumed) with LiAlH₄</i>	152
Figure 3-21:	<i>¹H NMR spectrum of the crude product of 62</i>	154
Figure 3-22:	<i>Partial ¹H NMR spectrum showing the alkene proton signal bonded cis to SnCl₃</i>	154
Figure 3-23:	<i>¹H NMR spectrum showing the decomposition of 62 after 2 h at room temperature in air</i>	155
Figure 3-24:	<i>Selected ^{1,2,3}J_{CH} and ³J_{HH} correlations observed for 62 in the HMBC, HSQC and COSY NMR experiments</i>	155
Figure 3-25:	<i>¹H NMR spectrum showing the decomposition of 62 at room temperature in a sealed NMR tube over 11 days</i>	156
Figure 4-1:	<i>Air-stable tellurol</i>	168
Figure 4-2:	<i>IR spectra showing the SeC≡N stretches of 67 and 68</i>	172
Figure 4-3:	<i>Selected ^{1,2,3}J_{CH} correlations observed in the HMBC and HSQC NMR experiments for 67 and 68</i>	173
Figure 4-4:	<i>^{1,2,3}J_{CH} correlations observed for 67 in the HMBC (in black) and HSQC (in red) NMR experiments</i>	173
Figure 4-5:	<i>^{1,2,3}J_{CH} correlations observed for 68 in the HMBC (in black) and HSQC (in red) NMR experiments</i>	174

Figure 4-6:	$^3J_{HH}$ correlations observed in the COSY NMR experiment for 68	174
Figure 4-7:	Partial ESI-MS showing the observed and theoretical $[M]^+$ ion of 68	175
Figure 4-8:	GC-MS of 68	175
Figure 4-9:	X-ray crystallographic structure of 67 showing the atom labelling scheme. Thermal ellipsoids are 50% probability and H atoms are arbitrary circles.	177
Figure 4-10:	1H NMR spectra showing the decomposition of 69 into 70 after multiple chromatography on preparative TLC plates: (a) the crude product, (b) after 1 st chromatography, (c) after 2 nd chromatography	179
Figure 4-11:	1H NMR spectra showing the decomposition of 69 into 70 (a) before the storage (b) after storage at $-18\text{ }^\circ\text{C}$ for 2 months	180
Figure 4-12:	ESI-MS of the product (a yellow solid) from the reaction of $[FcCH_2NMe_3]I$ 6 with Na_2Se_2 ($M = 6$)	182
Figure 4-13:	1H NMR Spectrum of the crude product from the reaction of $FcCH_2Cl$ 71 with Na_2Se_2	183
Figure 4-14:	Partial 1H NMR spectrum showing the selenol proton signal of 72 ...	185
Figure 4-15:	Partial 1H NMR spectrum showing the selenol proton signal of 74 ...	186
Figure 4-16:	Partial 1H NMR spectrum showing an approximately 4 : 1 : 3.75 mixture of 69 , 72 and 70 , respectively	188
Figure 4-17:	1H NMR Spectra of 69 (the crude product) obtained from reaction of $FcCH_2SeCN$ 67 with $NaBH_4$ and of $FcCH_2Li$ 40 with elemental Se	190
Figure 4-18:	^{77}Se NMR spectra showing the δ ^{77}Se NMR signals of 69 and 70 in the proton-coupled mode	191
Figure 4-19:	Selected $^{1,2,3}J_{CH}$ correlations observed for 69 and 70 in the HMBC and HSQC NMR experiments	192
Figure 4-20:	$^{1,2,3}J_{CH}$ correlations observed for 69 and 70 in the HMBC and HSQC NMR experiments	192
Figure 4-21:	Partial ESI spectra showing the (a) theoretical and (b) observed $[M]^+$ ions of 69 , 70 and 76	193

Figure 4-22:	<i>ESI-MS of the mixture of 70 (= [M₁]), 69 (= [M₂]) and 76 (= [M₃])</i>	193
Figure 4-23:	<i>GC-MS of 70</i>	194
Figure 4-24:	<i>Partial ⁷⁷Se NMR Spectra showing the δ ⁷⁷Se NMR signals of 75 in proton-coupled and –decoupled modes</i>	196
Figure 4-25:	<i>Selected ^{1,2,3}J_{CH and HH} correlations observed for 75 in the HMBC, HSQC and COSY NMR experiments</i>	196
Figure 4-26:	<i>Partial ESI-MS showing the observed and theoretical [M]⁺ ions of 75 and 77</i>	197
Figure 4-27:	<i>⁷⁷Se-¹H} NMR spectrum of a mixture of 69, 70 and 72</i>	198
Figure 4-28:	<i>Partial ⁷⁷Se NMR spectrum showing the δ ⁷⁷Se NMR signals of 74 in proton-coupled and -decoupled modes</i>	199
Figure 4-29:	<i>Partial ¹H NMR spectra showing the selenol proton signals for 72 and 74</i>	200
Figure 4-30:	<i>Selected ³J_{HH} correlation between the selenol proton and CH₂ proton signals observed for 72 and 74 in the COSY NMR experiment</i>	201
Figure 4-31:	<i>^{1,2,3}J_{CH} correlations observed for 72 in the HMBC (in black) and HSQC (in red and pink) NMR experiments</i>	201
Figure 4-32:	<i>^{1,2,3}J_{CH} correlations between the CH₂ and adjacent proton signals observed for 72 in the HMBC (in black) and HSQC (in red (CH₂ protons) and pink (CH protons)) NMR experiments</i>	202
Figure 4-33:	<i>Selected ^{1,2,3}J_{CH} correlations observed for 72 and 74 in the HMBC, HSQC and COSY NMR experiments</i>	202
Figure 4-34:	<i>IR Spectrum showing the Se–H stretch of 74</i>	203
Figure 4-35:	<i>GC-MS of 72 and 74</i>	203
Figure 4-36:	<i>Partial ESI-MS showing the observed and theoretical [M]⁺ ions of 74</i>	204
Figure 4-37:	<i>¹H NMR spectra showing the air oxidation of 72 in CDCl₃ at room temperature in a capped NMR tube in air over 5 days</i>	205
Figure 4-38:	<i>IR spectra showing the air oxidation of 74 in the neat state at room temperature by disappearance of the Se–H stretch</i>	205

Figure 4-39: ^1H NMR spectra showing the air oxidation of 74 in solution (in CDCl_3) at room temperature in a capped NMR tube	206
Figure 4-40: % of 79 in the sample against time.....	208
Figure 4-41: Selected $^{77}\text{Se}\{-^1\text{H}\}$ spectra showing the oxidation of 78 in CDCl_3 at room temperature in air in a capped NMR tube	208
Figure 4-42: Selected $^{77}\text{Se}\{-^1\text{H}\}$ spectra showing the oxidation of 78 in CDCl_3 at room temperature in air in a capped NMR tube with added FcH	208
Figure 4-43: Selected $^{1,2,3}J_{\text{CH}}$ correlations observed for 88 in the HMBC and HSQC NMR experiments	214
Figure 4-44: Selected $^{1,2,3}J_{\text{CH}}$ correlations observed in the HMBC and HSQC NMR experiments for 82	215
Figure 4-45: $^{1,2,3}J_{\text{CH}}$ correlations between the CH_2 proton and Cp carbons observed in the HMBC (in black) and HSQC (in red) NMR experiments for 82 and 88	215
Figure 4-46: Partial ESI-MS showing the observed and theoretical $[\text{M} + \text{Na}]^+$ ions of 82 and 88	216

List of Tables

Table 1-1:	<i>The first hydrides of the Group 14 and 15 elements and the years of their discovery</i>	4
Table 2-1:	<i>Selected spectroscopic and microanalytical data for 3, 4, 5</i>	35
Table 2-2:	<i>¹H, ¹³C and ³¹P NMR chemical shifts for 3, 4, 5</i>	37
Table 2-3:	<i>¹H, ¹³C and ³¹P NMR chemical shifts for 12 and 13</i>	39
Table 2-4:	<i>Selected spectroscopic data for Fc(CH₂)_nP(CH₂OH)₂ (n = 4 20, 6 21 and 11 22)</i>	41
Table 2-5:	<i>¹H, ¹³C and ³¹P NMR chemical shifts for 20, 21 and 22</i>	43
Table 2-6:	<i>Selected spectroscopic data for Fc(CH₂)_nPH₂ (n = 1 1, 2 23, 4 14, 6 15, 11 16)</i>	46
Table 2-7:	<i>¹H, ¹³C and ³¹P NMR chemical shifts for 14, 15 and 16</i>	50
Table 2-8:	<i>¹H, ¹³C and ³¹P NMR chemical shifts for 24</i>	52
Table 2-9:	<i>¹H, ¹³C and ³¹P NMR chemical shifts for 29</i>	56
Table 2-10:	<i>¹H, ¹³C and ³¹P NMR chemical shifts for 31</i>	58
Table 2-11:	<i>¹H, ¹³C and ³¹P NMR chemical shifts for 32</i>	60
Table 2-12:	<i>Crystal data and refinement details for 34</i>	65
Table 2-13:	<i>Selected bond lengths (Å) and angles (°) for 34</i>	66
Table 2-14:	<i>¹H and ¹³C NMR chemical shifts for 30</i>	72
Table 2-15:	<i>¹H, ¹³C and ³¹P NMR chemical shifts for 36</i>	75
Table 2-16:	<i>¹H and ¹³C NMR chemical shifts for 39</i>	98
Table 2-17:	<i>Selected spectroscopic data for 38 and 41</i>	101
Table 2-18:	<i>¹H and ¹³C NMR chemical shifts for 38</i>	102
Table 2-19:	<i>Bond lengths (Å) and angles (°) for 34</i>	130
Table 3-1:	<i>Selected spectroscopic data for 50</i>	140
Table 3-2:	<i>Selected reference spectroscopic values for primary stannanes</i>	151
Table 4-1:	<i>Selected spectroscopic data for 67 and 68</i>	172
Table 4-2:	<i>Crystal data and refinement details for 67</i>	176
Table 4-3:	<i>Selected bond lengths and angles for 67</i>	177
Table 4-4:	<i>The ⁷⁷Se NMR signals for 69 and 70</i>	190
Table 4-5:	<i>ESI mass spectrometric data for 69, 70 and 76</i>	194

Table 4-6:	<i>ESI mass spectrometric data for 75 and 77</i>	197
Table 4-7:	<i>Selected spectroscopic data for 72 and 74</i>	197
Table 4-8:	<i>Selected ESI-MS and NMR data for (PhCH₂Te)₂, (PhCH₂)₂Te, 82 and 88</i>	214
Table 4-9:	<i>Bond lengths (Å) and angles (°) for 67</i>	232

List of Abbreviations

Fc	[Fe(η -C ₅ H ₅)(η -C ₅ H ₄)] or η^1 -ferrocenyl
FcH ⁺	ferrocenium
FcH	ferrocene
Rc	[Ru(η -C ₅ H ₅)(η -C ₅ H ₄)] or η^1 -ruthenocenyl
Cp	η^5 -cyclopentadienyl
M	metal atom
E	main group element
X	inorganic group or atom
R	organic group
Me	methyl
Ar	aryl
Ph	phenyl
<i>t</i> -Bu	<i>tert</i> -butyl
Cy	cyclohexyl
THF	tetrahydrofuran
Et ₂ O	diethyl ether
MeOH	methanol
EtOH	ethanol
DMF	<i>N,N</i> -dimethylformamide
DMSO	dimethylsulfoxide
MeCN	acetonitrile
EtOAc	ethyl acetate
b.p.	boiling point
m.p.	melting point
<i>p</i>	<i>para</i> -
HOMO	highest occupied molecular orbital
SOMO	singly occupied molecular orbital
TLC	thin layer chromatography
R _f	retention factor

FTIR	Fourier transform infrared spectroscopy
ν	wavenumber in cm^{-1} (IR spectroscopy)
str	stretch
vs	very strong band (IR spectroscopy)
s	strong band (IR spectroscopy)
m	medium band (IR spectroscopy)
w	weak band (IR spectroscopy)
br	broad (IR spectroscopy)
sh	sharp band (IR spectroscopy)
ESI-MS	electrospray ionisation mass spectrometry
HR-MS	high resolution mass spectrometry
M	molecular ion
m/z	mass-to-charge ratio
NMR	nuclear magnetic resonance
DEPT	distortionless enhancement by polarisation transfer
SELTOCSY	selective excitation totally correlated spectroscopy
HSQC	heteronuclear single quantum correlation
HMBC	heteronuclear multiple bond correlation
COSY	correlated spectroscopy
HETCOR	heteronuclear correlation
1-D	one-dimensional
2-D	two-dimensional
δ	chemical shifts in ppm
J	coupling constant in Hz
s	singlet
d	doublet
t	triplet
q	quartet
sep	septet

m	multiplet
br	broad
Aq	acquisition
D ₁	relaxation delay
SPS	PureSolv solvent purification system model PS-SD-5

Numbered compounds are listed in a fold-out section inside the back cover for convenient reference.

Chapter 1: Introduction

1.1 Literature Review

1.1.1 Hydrides of *p*-Block Elements

Hydrides may be defined as compounds of elements formed with hydrogen, EH_n (E = element; $n \geq 1$)¹. There are four types of bonds by which hydrides can be classified¹. Hydrides containing a covalent bond without appreciable polarisation often form discrete molecules, i.e. CH_4 , or polymers, e.g. $(\text{BH})_n$ ¹. Hydrides containing a covalent bond in which the hydrogen is negatively polarised, $\text{H}^{\delta-}$, also form discrete molecules, e.g. $\text{SiH}_4^{\delta-}$ and/or salts, e.g. Cs^+H^- . Those containing a covalent bond with strongly positively polarised hydrogen, $\text{H}^{\delta+}$, form discrete molecules but often associated in the condensed phase, e.g. $\text{F}^{\delta-}\text{H}^{\delta+}$. Hydrides containing delocalised electrons forming metallic bonding to other metal atoms are often classified by different names such as interstitial hydrides, inclusion hydrides, alloy-like hydrides, solid solutions, or non-stoichiometric hydrides, i.e. $\text{Sm}^{\sim 2+}\text{-H}^{\sim 2-}_{1.93-2.55}$, $\text{Zr}^{\sim 2+}\text{D}^{\sim 2-}_{1.75-1.98}$ ¹. These hydrides often exist in a solid form with a metallic appearance which also possesses a conductivity band and conduct electricity¹. The actual state of hydrogen in this type is not known¹.

For the hydrides of the main group elements, the covalent character increases from the left to right and the bottom to top of the Periodic Table, while the ionic character of the hydrogen, $\text{H}^{\delta-}$, decreases¹. The Group 14 elements form hydrides with a formula, EH_4 ($\text{E} = \text{Si}, \text{Ge}, \text{Sn}$ or Pb)¹, containing covalent bonds with increasingly negatively polarised hydrogen atoms with the decrease in the electronegativity of the Group 14 element¹. The hydrides of the Group 14 elements are often in tetrahedral configurations in which the central atoms are located at the centres with four ligands located at the corners of tetrahedrons, and are electronically saturated (Figure 1-1)¹. The

hydrides are held by Van der Waals forces and are typically gases under ambient conditions¹.

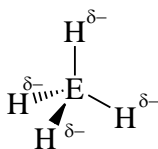


Figure 1-1: *Tetrahedral configuration of the hydrides of the Group 14 elements*

Except for a few examples, i.e. $\text{FCH}_2\text{CF}_2\text{SiH}_3\cdot\text{NMe}_3$, trigonal-bipyramidal sp^3d -configurations are rarely adopted by the hydrides of the Group 14 elements and only occur in intermediate states in reactions¹. Silicon, germanium and tin hydrides all form to a small extent alkane-like linear or branched oligomers or polymers, i.e. Si_4H_{10} , Ge_5H_{12} , Sn_2H_6 , $(\text{SiH}_2)_n$, $(\text{GeH}_2)_x$, as well as two-dimensional ones, i.e. $(\text{SiH})_n$ and $(\text{GeH})_n$, containing covalent bonds with predominantly negatively-polarised hydrogen¹.

The Group 15, 16 and 17 elements form hydrides containing covalent bonds with an ionic component and positively polarised hydrogen, $\text{H}^{\delta+}$, with formulae, EH_3 , EH_2 and EH , respectively, (Figure 1-2)¹. The more electronegative the elements are, the more positively the hydrogen atoms in the hydride are polarised¹. The polarisation of the hydrogen atoms in the hydrides of the Group 15 elements is generally weak while those in the hydrides of the Group 16 and 17 elements are stronger. The hydrogen atoms in the hydrides of the Group 15, 16 and 17, are also more polarised down the group with the rapid decrease in electronegativity¹. The polarisation is slight in the hydrides of the heavier elements, i.e. Sn, Sb, Te¹. These hydrides generally fill the transition from positive to negative hydrogen, following the preceding main group hydrides¹, e.g. NH_3 has $\text{H}^{\delta+}$ while P and the lower members have $\text{E}-\text{H}^{\delta-}$.

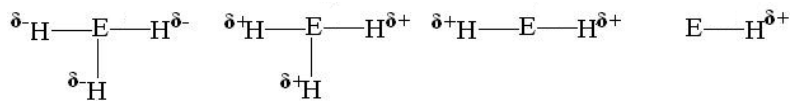


Figure 1-2: *Polarisation of the hydrogen atoms in the hydrides of the Group 15, EH_3 , 16, EH_2 , and 17, EH , elements¹*

Since the central atoms of the hydrides of the types, EH_3 , EH_2 and EH , all possess four occupied sp^3 -hybrid orbitals with appropriate number of ligands, i.e. 3, 2 or 1, they are generally electron-donors and the positively polarised hydrogen atoms are electron acceptors. The hydrides also form dative bonds with themselves or with foreign electron acceptors (Figure 1-3).

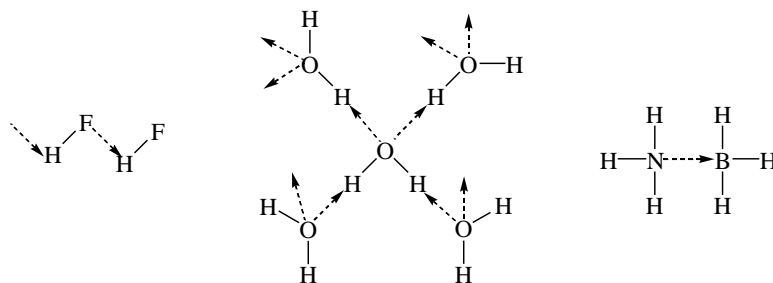


Figure 1-3: Examples of dative bonds formed by HF , H_2O and $\text{H}_3\text{N}\cdot\text{BH}_3$ to themselves or foreign electron acceptors¹

The hydrogen bonding between fluorine and hydrogen is stronger than that between oxygen and hydrogen atoms because fluorine is more electronegative than oxygen. In ammonia borane, a coordinated bond formed between nitrogen and boron atom is slightly weaker than that between fluorine and hydrogen atoms (the B-N distance is around 158 pm)², but stronger than that between oxygen and hydrogen atoms shown by the intermolecular distances of 155 , 158 and 197 pm (the typical length of a hydrogen bond is 197 pm) for F-H, B-N and O-H, respectively.

Hydrides are often synthesised by reactions of appropriate precursors. Common methods for the preparations of hydrides of the main group elements are summarised in Figure 1-4¹.

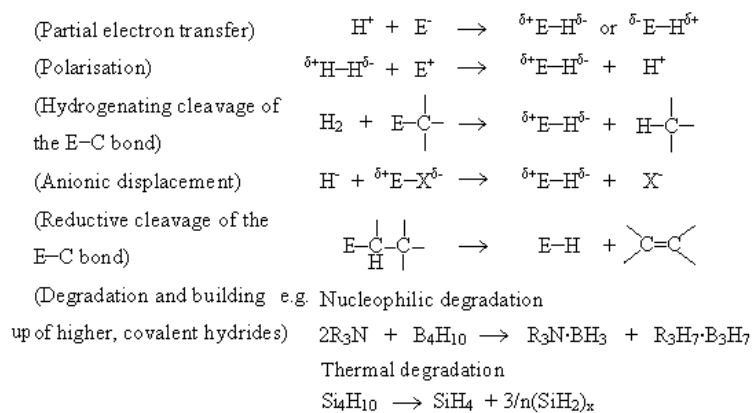


Figure 1-4: Commonly utilised methods for the synthesis of hydrides of the main group elements (adopted from Wiberg, E.; Amberger, E., *Hydrides of the Elements of Main Groups I-IV*, (1971))

1.1.1.1 Discovery of the Hydrides of the Group 14 and 15 Elements

Table 1-1: The first hydrides of the Group 14 and 15 elements and the years of their discovery

<u>Hydride</u>	<u>Year of discovery</u>
NH ₃	1774
AsH ₃	1775
CH ₄	1778
PH ₃	1812
SbH ₃	1837
SiH ₄	1857
GeH ₄	1902
BiH ₃	1918
SnH ₄	1919
PbH ₄	1920

The first hydrides of elements of the Group 14 and 15 were discovered over the last three centuries¹. Table 1-1 summarises the hydrides and the years of their discovery.

Ammonia, NH₃, arsane, AsH₃, and methane, CH₄, were first discovered in the mid-to-late 1770s. Ammonia was discovered in 1774 by Joseph Priestley³ followed by arsane in the subsequent year. The latter was synthesised by reduction of arsenic(III) oxide with Zn under acidic condition by Carl Scheele *et al*¹. Methane was isolated from natural gas and reported by Alessandro Volta later in the same decade. In the early 1800s, phosphane, PH₃, and stibane, SbH₃, were discovered. The first silicon hydride, silane, SiH₄, was reported by Wöhler and Buff in the mid 1800s. Silane was isolated as a gas formed from silicon-containing aluminium immersed in an aqueous salt solution at the positive pole of a galvanic circuit. The gas ignited in air, forming

silicon oxide, SiO_2 , and water while thermal decomposition gave silicon and hydrogen¹. Germanium hydride, germane, GeH_4 , was first synthesised in 1902 as a mixture of germanium hydride and hydrogen by Voegelen¹. In the next two years, the synthesis of stannane, SnH_4 , and also plumbane, PbH_4 , which is known to only form in a trace amount during the acid hydrolysis of magnesium-lead alloys^{4, 5}, were reported.

1.1.1.2 Properties of Hydrides of Heavier *p*-Block Elements

While the hydrides of lighter *p*-block elements such as BH_3 , C_nH_m , NH_3 and OH_2 are well-known, stable and ubiquitous molecules, those of the corresponding heavier *p*-block elements are often extremely reactive, poisonous and malodorous substances. Possibly due to the difficulties in handling the compounds, the chemistry of the hydrides of heavier *p*-block elements is relatively poorly exploited, despite them being potentially a very important class of chemicals. The hydrides of heavier *p*-block elements are used as ligands to transition metals in coordination chemistry, versatile precursors to many important chemicals in organic synthesis and also substrates for the chemical vapour deposition of semiconductor materials.

Hydrides of heavier *p*-block elements, EH_n (E = heavier *p*-block element; $n = 1 - 4$), are often colourless and odourless gases which are usually readily oxidised and some spontaneously ignite in air (pyrophoricity), i.e. AsH_3 , P_2H_4 , SiH_4 ¹. The reactivity of the hydrides towards oxygen generally decreases down the group, i.e. $\text{P} > \text{As} > \text{Sb} > \text{Bi}$ ⁵, and so does the strength of E-H bonds and hence the thermal stability of the compounds, i.e. $\text{Si} > \text{Ge} > \text{Sn}$. The stability of the compounds also decreases with the increased number of hydrogen on the element, i.e. $\text{R}_n\text{MH}_{3-n}$, $n = 1 > 2 > 3$, also depending on the organic substituents bonded to the elements, i.e. alkyl $>$ aryl. For example, while ammonia begins to decompose into nitrogen and hydrogen at ~ 2000 °C, a heavier element of the group, bismuthane, BiH_3 , decomposes within a few minutes at room temperature^{1, 4, 5}. The hydrides of the main group elements are also often strongly reducing⁴.

Hydrides of heavier main group elements are commonly prepared by reduction of the corresponding halides or oxides with an ionic or a metal hydride^{6,7}.



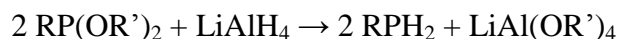
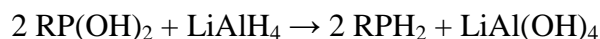
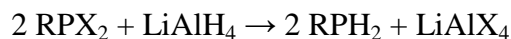
1.1.1.3 Organoderivatives of the Hydrides of the Group 15 Elements

Organoderivatives of the hydrides of the group 15 elements, $\text{R}_n\text{EH}_{3-n}$ (R = organic substituent; E = P, As, Sb or Bi; n = 0, 1 or 2), especially, organo-phosphanes and -arsanes, are very important substrates. The organoderivatives of phosphorus and arsenic hydrides, EH_3 (E = P or As), are often referred to as primary, REH_2 , and secondary, $\text{RR}'\text{EH}$, phosphanes and arsanes, depending on the number of the hydrogen atoms at their hydrogen centres. Primary and secondary phosphanes and arsanes are key precursors to many organo-phosphorus compounds^{8,9}, which are also important catalysts for metal ions^{8,10,11} and complexes^{9,10}, and organo-arsenic¹² compounds in organic syntheses. The organoderivatives of antimony and bismuth hydrides, also referred to as stibanes and bismuthanes, respectively, have, on the other hand, much less use and are also much less common probably because of their extreme instabilities under ambient conditions.

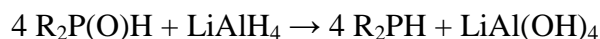
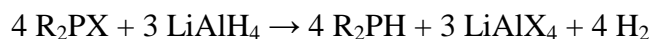
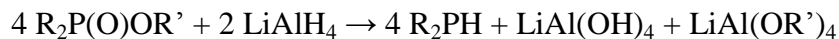
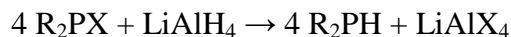
1.1.1.4 Organophosphorus Hydrides

Phosphanes are generally very reactive and extremely sensitive towards air oxidation. Those of the lower aliphatic radicals are pyrophoric, spontaneously igniting in air⁹. Primary phosphanes can be prepared in a number of ways, i.e. by reduction of the phosphorus and phosphonic derivatives with metal hydrides, by reactions of metal phosphides with alkylating agents and of elemental phosphorus with appropriate reagents, by hydrolysis of alkyl- or arylphosphorus dihalides, under Friedel-Crafts

conditions, by reactions of PH_3 or $[\text{PH}_4]^+\text{T}$ with suitable alkylating reagents, by photolysis of biphosphanes and triphosphanes and by miscellaneous methods etc.⁹ The most commonly utilised method for the preparation of primary phosphanes in laboratory syntheses is, however, probably by reduction of phosphorus and phosphinic derivatives, especially dihalides, with LiAlH_4 ⁹:



These methods are applicable to the preparation of secondary phosphanes. Other commonly used methods for the preparation of secondary phosphanes also include the followings:



Primary and secondary phosphanes react with a wide range of various chemicals. They generally readily react with oxygen, sulfur and selenium. Reaction with oxygen gives phosphorous and phosphonic acids⁹. With sulfur and selenium, the products may vary depending on the stoichiometry of the reaction and also the organic substituents on the phosphorus⁹. For instance, in the equimolar reaction of PhPH_2 and sulfur, the phosphane sulfide, PhP(S)H_2 is obtained. However, the phosphane sulphide is rather unstable and further reacts to give a tertiary phosphane sulphide $(\text{PhP})_4\text{S}$ ⁹. With two molar equivalents of sulfur, the main product will be $(\text{PhPS})_3$ ⁹.

With three molar equivalents of sulfur, phenyldithiophosphonic anhydride (Figure 1-5 (a)) can be obtained⁹. In contrast, aliphatic primary phosphanes exclusively give $(RPS)_4$, which forms a four-membered ring (Figure 1-5 (b)), regardless of the stoichiometry of the reaction⁹.

Reaction of $PhPH_2$ with selenium also yields a ring structured compound, i.e. $(PhSe)_x$ ⁹, under similar conditions to that with sulfur. An equimolar reaction of secondary phosphanes with sulfur yields dithiophosphinic acids, $R_2P(S)SH$. Selenium also forms the corresponding compound (Figure 1-5 (c)).

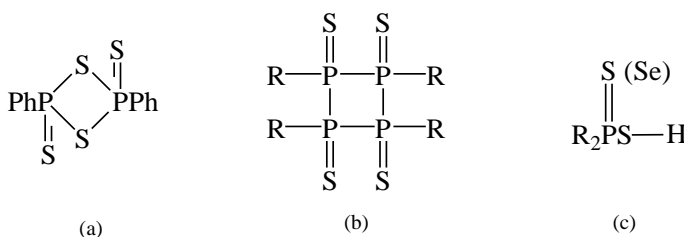


Figure 1-5: (a) Phenyldithiophosphonic anhydride; (b) 4-membered thiophosphane (c) secondary phosphane sulfide and selenide (adopted from Kosolapoff, G. M.; Maier, L., *Organic Phosphorus Compounds*, (1972))

Reaction with alkali metals or organoalkali compounds may give the monosubstituted metal phosphides, $RHPM$ ($M = Na, K$), or disubstituted metal phosphides, RPM_2 ($M = Li, Na, K$), depending on the reaction conditions⁹. Substitution at the hydride centre of primary phosphanes with Grignard reagents gives the product in which the hydrogen atom is replaced by the MgX group of the Grignard reagent⁹. Addition reactions of primary and secondary phosphanes to the unsaturated bonds of olefins or ketenes, alkynes, i.e. acetylenes, aldehydes, ketones or diketones, isocyanates, isothiocyanates, ethylene oxides and thionylanilines⁹, are also well-known. The reaction occurs more readily if the unsaturated bonds are activated by electron-withdrawing substituents although the reaction occurs at elevated temperatures without the activation or the presence of catalysts⁹. The reaction proceeds *via* a free-radical chain mechanism which can be initiated by UV light, X-rays, organic peroxides and also α, α' -azobisisobutyronitrile⁹. Addition of primary phosphanes to dienes and diacetylenes gives various cyclic tertiary phosphanes such as phospholanes, phospholes, phosphorinanes, phosphorinanones, 1,4-

dihydrophosphorin-4-ones, 1,4-oxaphosphorinanes, phosphapanes, bicyclic phosphanes and tricyclic phosphanes⁹.

Reaction of primary and secondary phosphanes with acid halides such as phosgene and thionylchloride usually yields the corresponding halophosphanes in excellent yields⁹. Primary and secondary phosphanes also readily react with phosphonous and phosphinous halides, metal and transition metal halides⁹. They react with halogens to give phosphinous halides. When treated with a stoichiometric amount of the halogen, the corresponding phosphane dihalides can be obtained. Reaction of primary and secondary phosphanes with Lewis acids such as trimethylborane and diborane gives the addition products⁹. In Freon solution, both primary and secondary phosphanes form the SO₃ adducts although the primary phosphane adducts are only stable at very low temperatures, i.e. -78 °C⁹. Primary phosphanes form phosphonium salts with alkyl halides which decompose upon addition of water or through base hydrolysis⁹. Secondary phosphanes form salts with alkyl halides which are stable in water but decompose in the presence of alkaline reagents⁹. The C-P bonds of primary and secondary phosphanes are generally stable towards hydrolysis⁹. A strongly electron-withdrawing organic substitute, however, makes the phosphorus susceptible to nucleophilic attack and C-P bond fission occurs⁹. Secondary phosphanes readily react with azides such as Ph₃SiN₃, Ph₂P(O)N₃, PhN₃ and PhCON₃, to ultimately give phosphane imine derivatives⁹.

1.1.1.5 Organoarsenic Hydrides

The physical properties of organoarsanes are relatively unknown because of the fewer investigations possibly owing to their high toxicity as well as air-sensitivity¹². Primary, RAsH₂, and secondary, R₂AsH, arsanes are, like the corresponding phosphanes, highly reactive substances which may be pyrophoric, i.e. Me₂AsH, Et₂AsH, MePhAsH¹², or very easily oxidised in air. Primary and secondary arsanes are commonly prepared by reduction of the corresponding halides or oxides with suitable reducing reagents. Any arsenical containing one or two R groups bonded to arsenic can be reduced to the corresponding primary and secondary arsane with a

suitable reducing agent. Arsenic and arsenic acids or their salts, halo or dihalo arsanes are well reduced to the corresponding arsanes¹². Zinc dust with hydrochloric acid, amalgamated zinc, zinc-copper couple and platinised zinc with hydrochloric acid are all suitable reducing agents¹². Although lithium aluminium hydride has also been used in the synthesis of primary and secondary arsanes, satisfactory yields may not be obtained¹². Other known but less commonly used preparations of primary and secondary arsanes are from metallic arsenides, the Friedel-Crafts reactions and addition of arsanes to carbonyl compounds and also electrical reduction to arsanes¹².

Primary and secondary arsanes, e.g. PhAsH₂, MeAsH₂, Ph₂AsH, Me₂AsH, react vigorously with oxygen, producing arseno or arsenoso compounds or arsenic acids¹². They are generally powerful reducing agents¹².

Primary and secondary arsanes undergo addition reactions with the C=C bonds of acrylonitrile, 2-vinyl pyridine and hexafluoropropene, giving RAs(CH₂CH₂CN)₂ or R₂AsCH₂CH₂CN, CH₂(Ph₂As)CHNC₅H₃ and CF₂(Me₂As)CFCF₃, respectively, and also with arylisocyanates. Secondary arsanes can add to the C≡C bonds of alkynes to give the *cis*- and/or *trans*-isomers and/or substitution product of the expected alkene, depending on the secondary arsanes and alkynes used. Additions with aldehydes yield three products, RAs(CHOHR')₂, (RAsOCHR')₂ and (C₆H₅As)_n, depending on the reaction conditions¹². Primary and secondary arsanes also add to ketones, i.e. hexafluoroacetone, to give the corresponding arseno derivatives, i.e. Me₂AsC(CF₃)₂OH and MeAs(H)C(CF₃)₂OH¹².

Reaction of primary and secondary arsanes with alkyl halides gives the corresponding tertiary haloarsanes. Symmetrical tetraalkyl- or tetraaryldiarsanes can be prepared by reacting dialkyl- or diarylarsanes with dialkyl- or diaryllhaloarsanes. Reaction of primary and secondary arsanes with alkyl halides may also give quaternary arsonium salts. Some organometallic and thioarseno compounds are derived from primary and secondary arsanes¹². Primary and secondary arsanes also form borane adducts with diboranes at very low temperatures although the adducts are much more unstable than the corresponding phosphane compounds¹².

1.1.1.6 Organoantimony Hydrides

Stibanes, primary, RSbH_2 , and secondary, R_2SbH , stibanes, are often thermally unstable and readily decompose at room temperature¹³. Some are also sensitive towards air as well as light¹³. The number of the known primary and secondary stibanes is very small. Except for few melting and boiling points, the physical properties of stibanes are, therefore, not known. Alkyl primary and secondary stibanes, CH_3SbH_2 and $(\text{CH}_3)_2\text{SbH}$, respectively, have been synthesised from dimethylbromo stibane and sodium borohydride in diglyme at $-78\text{ }^\circ\text{C}$. The primary stibane slowly decomposes above $-78\text{ }^\circ\text{C}$ into hydrogen and a black solid of unknown composition. The secondary stibane decomposes at room temperature into hydrogen and tetramethyldistibane¹². Some other alkyl primary and secondary stibanes, RSbH_2 ($\text{R} = \text{Mes}(2,4,6\text{-}(\text{CH}_3)_3\text{C}_6\text{H}_2)$ or $2\text{-}(\text{Me}_2\text{NCH}_2)\text{C}_6\text{H}_2$)¹³ and R_2SbH ($\text{R} = \text{C}_6\text{H}_{11}$, Et or *tert*-Bu)¹², prepared by reduction of the corresponding halides with LiAlH_4 in Et_2O , have been also known.

Phenyl and diphenyl stibanes, which are the only examples of aryl primary and secondary stibanes, have been prepared by reaction of $[\text{C}_6\text{H}_5\text{SbCl}_4]^- \text{NH}_4^+$ or $\text{C}_6\text{H}_5\text{SbI}_3$ with lithium borohydride or lithium aluminium hydride in Et_2O at $-50\text{ }^\circ\text{C}$. Phenyl stibane is a colourless liquid with a phosphane-like odour, which is readily oxidised in air and gives a white solid which is believed to be either $\text{C}_6\text{H}_5\text{Sb}(\text{OH})_2$ or a mixture of $\text{C}_6\text{H}_5\text{SbO}$ and $\text{C}_6\text{H}_5\text{SbO}_3\text{H}_2$. Phenyl stibane reacts with iodine to give phenyldiiodo stibane which readily decomposes in air into hydrogen and a brownish solid which is thought to be a highly polymerised form of antimonobenzene¹². Phenyldiiodo stibane also further reacts with phenyl stibane to give an ether-insoluble dark brown solid which is believed to be $(\text{C}_6\text{H}_5\text{Sb})_x$, with the evolution of H_2 and also HI ¹².

Diphenyl stibane has also been prepared by reduction of diphenylchloro stibane with lithium borohydrides or lithium aluminium hydride at $< -50\text{ }^\circ\text{C}$ ¹². It is a colourless oil, readily oxidised in solution to diphenylstibinic acid and also a powerful reducing agent. When reacted with chlorine, the secondary stibane converts into

diphenylantimony trichloride. Reaction of the secondary stibane with iodine also gives the corresponding diphenyliodo stibane as a yellow solid. Diphenystibane adds to the C≡C bond of phenylacetylene to yield the *trans* isomer of the corresponding alkene¹². Diphenystibane and dibutylstibane undergo addition reactions with diphenylethynylstibane or dibutylethynylstibane. Diphenystibane forms tetraphenyldistibane and triethylvinylsilane by treatment with triethylethynylsilane¹². Reaction of diphenylstibane with acids such as hydrochloric, acetic and benzoic acids gives the corresponding tertiary stibanes with the evolution of H₂. With alkyl chlorides such as carbon tetrachloride and benzotrichlorides, the corresponding diphenylchlorostibanes are obtained as a mixture with by-products such as hydrogen or benzylidene chlorides, benzene and an unidentified solid which is believed to be antimonobenzene¹².

Stibanes are useful intermediates to organoantimony compounds in organic synthesis. Metalation of secondary stibanes of the type R₂SbH with organolithium compounds or reactions of tertiary stibanes or distibanes with alkali metals gives well-known alkalimetal diorganoantimonides, R₂SbM (R = alkyl or aryl), which can then be reacted further *in situ* to yield the desired organoantimony derivatives¹⁴⁻¹⁷. PhSbNa₂ and (PhSb)₃Na₂ can also be prepared by reactions of PhSbH₂^{18, 19}. Me₂SbH reacts with HCl and bromodiborane, to give Me₂SbCl and Me₂SbBr, respectively, which can also be used in further reactions.

1.1.1.7 Organoderivatives of the Hydrides of the Group 14 Elements

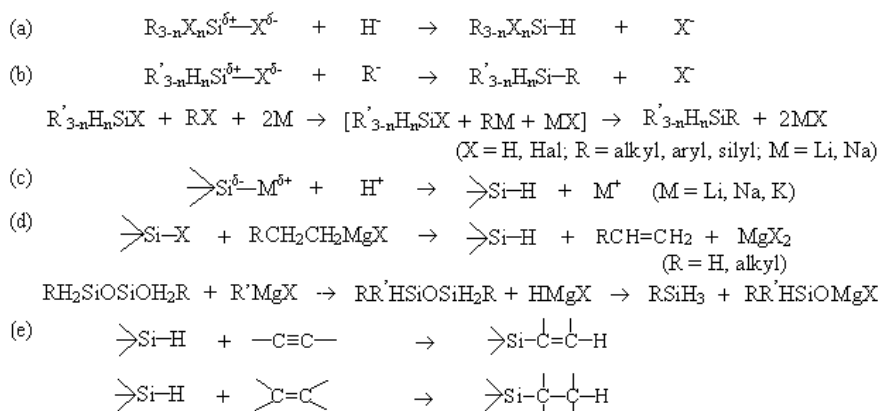
Many examples of organosilicon hydrides are known, but there are relatively fewer hydrides of the other Group 14 elements i.e. Ge, Sn and Pb, partly due to the difficulties in preparing suitable precursors or in carrying out suitable syntheses⁵. The general formula for the hydrides of the Group 14 elements is R_{4-n}EH_n (E = Si, Ge, Sn, Pb; E = 1, 2 or 3)⁵. The number of hydrogen atoms bonded to the element, i.e. 3 > 2 > 1, and the nature of the substituent, i.e. R = alkyl > aryl²⁰, affect the stability of the hydrides⁵. The more hydrogen atoms on the element the less stable the hydride

becomes. The aryl hydrides are generally more unstable than the alkyl ones. This may be because the electron-releasing ability of an alkyl group stabilises the hydrides by increasing an electron density around the element to which it is bonded or an alkyl group is also known as an electron insulator which may be able to stabilise the hydrides whose oxidation/decomposition proceeds *via* a free radical pathway. In contrast, an aryl group, which is electron-withdrawing, may destabilise the hydride centre by pulling an electron density away from the main group element.

1.1.1.8 Organosilicon Hydrides

The chemistry of organosilanes containing at least one Si–H bond has been extensively studied^{1, 14, 21-24}. Organosilanes, R_nSiH_{4-n} ($n = 0 - 3$), are generally stable under ambient conditions, i.e. in air at room temperature²⁰. Monoorganosilanes, $RSiH_3$, with relatively large organic substituents such as $C_2H_5SiH_3$, cyclo- $C_6H_{11}SiH_3$, $C_6H_5SiH_3$, $CH_2(SiH_3)_2$, can, for example, be distilled satisfactorily in air. *n*-Alkyl silanes, $CH_3(CH_2)_nSiH_3$ ($n = 0 - 7$), are slightly more thermally stable than SiH_4 and decompose at 440 – 460 °C into hydrogen, hydrocarbons and silane¹. The physical properties of organosilanes are between those of the corresponding tetraalkyl silanes, R_3Si , and SiH_4 and also depend on the nature of ligands¹. Di- and tri-organosilanes are also generally more stable than monoorganosilanes¹.

Organosilanes are commonly prepared as in Scheme 1-1¹. Hydrogenation of organosilyl cations^{1, 25} (Scheme 1-1 (a)) or by reaction of the corresponding halides, $R_{4-n}SiX_n$ ($X = \text{halides}, n = 1 - 3$), with metal hydrides, i.e. LiH , R_2AlH , $NaBH_4$, $LiAlH_4$, $Al(BH_4)_3$, $LiAlD_4$, in dry solvents, i.e. Et_2O , THF, diglyme, dioxane, $LiCl$ - KCl melts, give the corresponding organosilanes in excellent yields. Very dry solvents, an appropriate reaction temperature and strict exclusion of air are crucial for better yields¹. Organosilanes of higher boiling are usually insensitive to air and can be prepared between 0 °C and the boiling point of the solvent¹.



Scheme 1-1: (a) Nucleophilic displacement of a negative ligand in organosilanes by a hydride ion H^- ; (b) nucleophilic displacement of a negative ligand in substituted silicon hydrides by a carbanion R^- ; (c) protonation of an organosilylmetal compound; (d) abnormal Grignard reaction; (e) hydrosilation of alkenes and alkynes (adopted from Wiberg, E.; Amberger, E., *Hydrides of the Elements of Main Groups I-IV*, (1971))

The highly reactive Si–H bonds make organosilanes very useful substances. Silicon is less electronegative than carbon and hence forms more polar and weaker Si–H bonds, leading to the higher reactivity of the hydrides than the corresponding carbon hydrides. A larger covalent radius of silicon and the availability of d-orbitals also allows greater coordination numbers in intermediate stages, resulting in lower activation energy and hence higher reactivity.

One or more of the hydrogen atoms on the silicon can be replaced by foreign elements or groups such as halogens, nitrogen or oxygen groups, alkali metals or organic radicals, leading to the extremely large number of its derivatives¹. Organosilanes react with (a) halogens, i.e. Cl_2 , Br , I_2 , (b) metal halides, MX_n , non-metal halides, i.e. HSO_3Cl , metal pseudohalides, i.e. AgNCO , AgNCS , (c) organic halides, i.e. alkyl halides, RX , alkenyl halides, i.e. $\text{CH}_2=\text{CHCH}_2\text{X}$, acid halides, RCOX , (d) oxygen (e) water both in basic and acidic conditions, (f) PH_3 and GeH_4 , (g) anhydrous proton-active compounds, (h) methane and benzene, (i) ketones, (j) alkenes, (k) alkynes (Scheme 1-2). Organosilanes also react with R_2S , RSH , RN_3 , RNH_2 , R_2NH and AsH_3 , $\text{C}\equiv\text{N}$, and undergo ligand exchange reactions with metal salts and alkyl metals¹.

Hydrosilation reaction(s) of alkene or ketones catalysed by transition metal complexes, i.e. H_2PtCl_6 or $\text{RhCl}(\text{PPh}_3)_3$ ⁴, $\text{Co}_2(\text{CO})_8$ ²⁶ or copper containing catalysts, i.e. copper acetate, CuCl_2 , CuSO_4 , $\text{Cu}(\text{OH})_2$, $\text{Cu}(\text{NO}_3)_2$, $\text{Cu}(\text{CN})_2$ ²⁷, is probably the most utilised application of organosilanes²⁰. An excellent-yielding synthesis of the corresponding silanols with a Pd-catalyst by oxidation of organosilanes with H_2O has also been reported²⁸.

Other applications of organosilanes include self-assembled monolayers, SAMs, formed by reaction of organosilanes with solid surfaces²⁹, Pd-catalysed cross-coupling reactions³⁰, photosensitive films by low energy induction of dehydrogenative polymer of various monosubstituted silanes³¹, arylsilicon monomers made by reaction of aryl halides with silicon hydrides³², silicon-containing diene polymers formed by cross-linkage of diolefin polymers by addition of organosilanes³³, precursors to organosilicon derivatives^{34, 35}, i.e. $\text{EtSiH}_3\text{-EtSiF}_3$, $\text{Et}_2\text{SiH}_2\text{-Et}_2\text{SiF}_2$, $\text{Et}_3\text{SiH-Et}_2\text{SiF}$, Et_4Si , which also are useful as reducing reagents, propellants and fuels³⁶. Tertiary silanes such as Cl_3SiH and Me_3SiH are themselves commercially important substances¹.



Scheme 1-2: *Reactions of Si-H bonds (adopted from Wiberg, E.; Amberger, E., Hydrides of the Elements of Main Groups I-IV, (1971))*

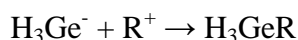
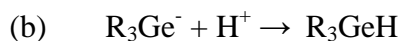
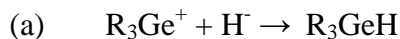
1.1.1.9 Organogermanium Hydrides

The chemistry of organogermanes has recently been reviewed by Bulten³⁷. Although the number of tetraorganyl germanes is large, that of organogermanes containing at least one Ge-H bond, i.e. R_nGeH_{4-n} ($n = 1 - 3$), is limited. The physical properties of organogermanes are, therefore, little known^{1, 38}. The properties of organogermanes are generally considered to be between those of the hydrides and the peralkylated germanes¹ and also depend on the nature, number and size of the organic groups substituted on the germanium. Alkyl germanes are more stable than aryl germanes and their stability can be compared with that of the corresponding silanes. The

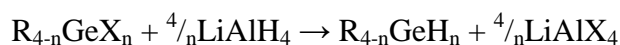
stability of organogermanium hydrides also increases with the loss of hydrogen on the germanium in order of $\text{RGeH}_3 < \text{R}_2\text{GeH}_2 < \text{R}_3\text{GeH}^{39}$.

While organosilanes are stable in air, the corresponding germanes, including primary, RGeH_3 , secondary, R_2GeH_2 , and tertiary, R_3GeH , germanes³⁹, slowly oxidise at room temperature in air to the corresponding oxides or hydroxides, i.e. $(\text{R}_3\text{Ge})_2\text{O}$, (R_2GeO) , $(\text{RGeO})_2\text{O}$, $\text{R}_3\text{GeOH}^{20, 39}$. Alkyl germanes are, however, much less oxidisable than the corresponding alkyl stannanes^{1, 39} and the sensitivity of organogermanes to oxidising agents is almost comparable to that of the corresponding silanes³⁹. Organogermanes are generally less thermally stable than the corresponding silanes¹.

Organogermanes are prepared similarly to organosilanes. Germanium compounds containing a germanium-halogen bond, $\text{RGe}^{\delta+}-\text{X}^{\delta-}$ (X = halogen), or -metal, $\text{RGe}^{\delta-}-\text{M}^{\delta+}$ (M = metal), can be either (a) hydrogenated or (b) protonated to give the corresponding organogermanium hydrides¹.



Reaction of organohalogeno germanes, $\text{R}_{4-n}\text{GeX}_n$, with LiAlH_4 in appropriate organic solvents, e.g. Et_2O , often gives satisfactory yields of the corresponding germanes¹.

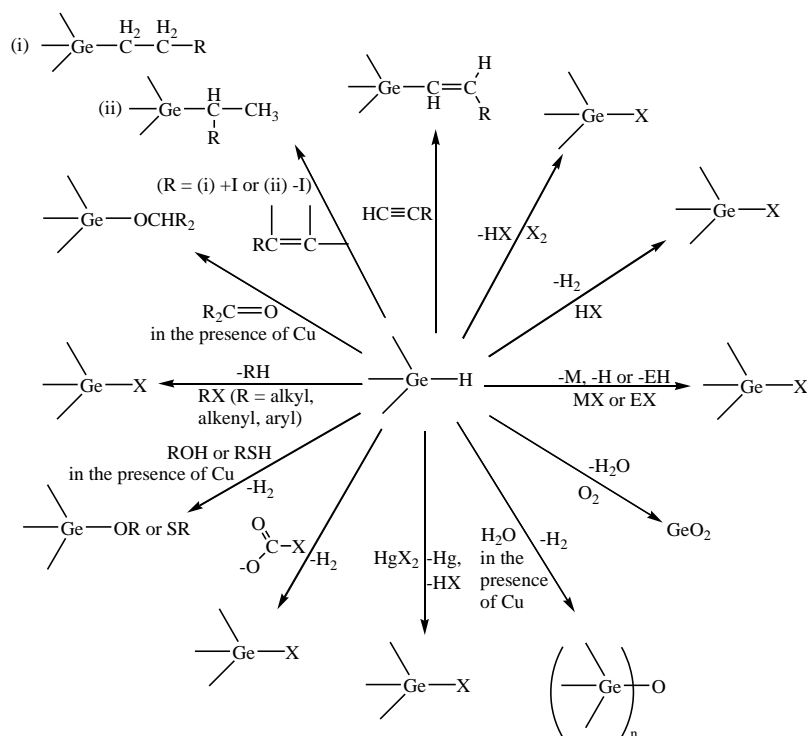


Organogermynyl hydroxides, R_3GeOH , and bis(triorganogermynyl) oxides, $(\text{R}_3\text{-Ge})_2\text{O}$, can also be easily reduced with LiAlH_4 in Et_2O to yield the corresponding germanes¹.



Organogermanes have also been made by reduction of the corresponding halides with Zn and HCl⁴⁰, from organogermyl lithium, R₃GeLi, e.g. Et₃GeLi, or organogermyl sodium, R₃GeNa, e.g. Ph₃GeNa, derivatives with appropriate alkyl halides, by reduction of germanium halides, e.g. Ph₃GeBr, and sulfides, e.g. Me₂GeS, with zinc amalgam and aqueous HCl, by reduction of organohalogeno germanes with lithium hydride, lithium deuteride, sodium hydride or sodium borohydride, by reaction of Grignard reagents on germanium tetrachloride and by cleavage reaction with hydrogenosilanes and hydrogenogermanes in the presence of chloroplatinic acid³⁹.

The Ge–H bonds react in similar manners to the Si–H bonds except that they are less polarised¹. The Ge–H bonds react with halogen, i.e. X₂, HX, RX, MX, HgX₂, oxygen, i.e. O₂, OH[•], RCOOH, acids, i.e. H₂SO₄, HgSO₄, sulfur, i.e. Ag₂S, RSH, nitrogen, i.e. NH₃, N₂R, carbon, i.e. N₂CHR, LiR, alkene, alkyne, carbene, halocarbenes, alkali metals or alkali metal hydrides, i.e. M (in liquid ammonia or in polyethers), MH, MOH, MR, transition metal π-complexes, i.e. HMn(CO)₅¹, selenium, i.e. Se, Et₂Se, tellurium, i.e. Et₂Te, Et₃GeTeEt, M–N bonds, i.e. R₃SnNEt₂, R₃PbNEt₂, and M–O bonds, i.e. Et₃SnOMe, organometallic derivatives, i.e. RLi, and also Grignard reagents, i.e. R_nM (M = Hg, Zn, Cd, Sb, Pb), Fe₃(CO)₁₂³⁹ (Scheme 1-3).



Scheme 1-3: *Reactions of Ge-H bonds (adopted from Wiberg, E.; Amberger, E., Hydrides of the Elements of Main Groups I-IV, (1971))*

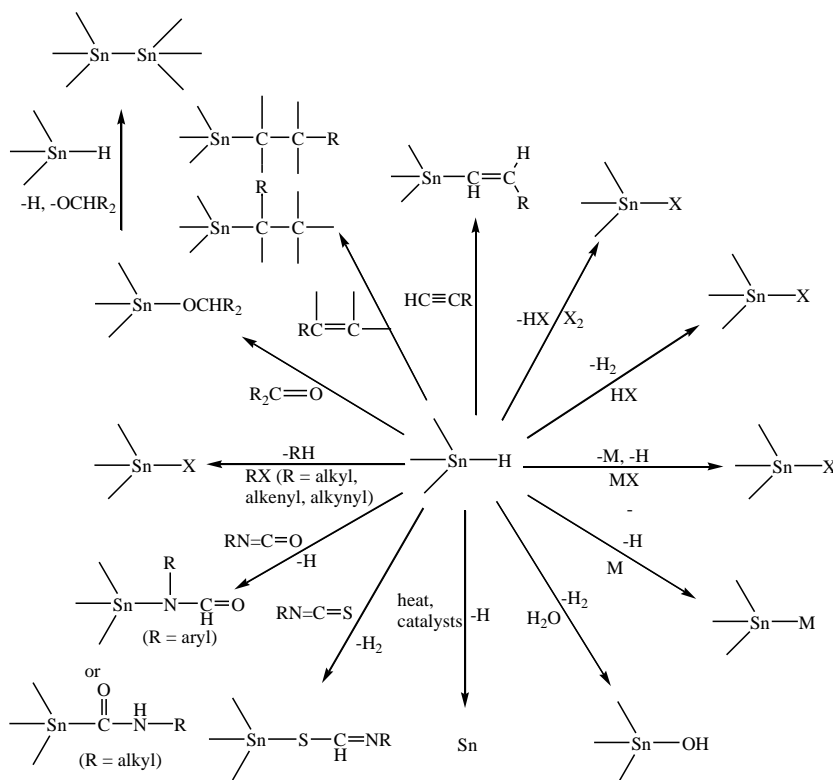
Organogermanes are useful precursors to many organogermanium compounds^{7, 41-47}, e.g. $(C_6H_5)_3GeCu(PPh_3)_2$ ⁴⁸, oligogermanes *via* hydrogermolysis reaction which is useful for providing Ge-Ge bonds⁴⁹. Hydrogenations of unsaturated compounds such as alkenes, alkynes, carbonylated compounds, imines, nitrones etc., to give a range of acyclic or cyclic carbon functionalised germanium compounds are probably the most common application of organogermanes²⁰. Organogermanes also react with saturated halides and, in certain cases, with alkenyl and alkyl halides in which the hydrogen of the halide will be replaced by the hydrogen on the germanium¹. They are also used industrially as activators of titanium and molybdenum Ziegler-Natta catalysts of alkene polymers. Germanium-containing polymers prepared from organogermanes often exhibit semiconducting properties and used as conducting surface material in semiconductor industry. Organogermanes are also used as reagents for enantioselectivity reducing prochiral carbon centred radical in the presence of Lewis acid⁵⁰.

1.1.1.10 Organotin Hydrides

Organostannanes are generally susceptible to oxygen. They are also much more thermally unstable than the corresponding silanes and germanes and reduction to Sn^{2+} and Sn^0 is much more likely to occur¹. Alkyl stannanes are often colourless liquids with unpleasant odours while aryl stannanes are sometimes isolated as crystalline solids at room temperature⁵¹. Organostannanes are usually soluble in most common organic solvents⁵¹. The instability of organostannanes increases with the increase in the number of the hydrogen atoms on the tin, i.e. $\text{R}_3\text{SnH} < \text{R}_2\text{SnH}_2 < \text{RSnH}_3$ ¹. Triorganostannanes, R_3SnH , may, for instance, be stable up to 150 °C while monorganostannanes, RSnH_3 , begin to decompose at 0 °C⁵¹. Aryl stannanes are also generally less stable than alkyl ones⁵¹. The decomposition of organostannanes can be promoted by the nature of the organic substituents on the tin, temperature, time of pyrolysis, short-wave UV irradiation, the presence of catalyst, especially, bases and heavy metals including Sn itself^{1, 51}. The presence of impurities may also lead to the decomposition of the organostannane at ambient temperature⁵¹. In their pure states, however, organostannanes may unexpectedly be stable in the absence of air⁵¹. Since the cleavage of bonds occurs not only at the Sn–H but also at the Sn–C bond, the formation of ditins and polytins as well as tetraalkyltins and elemental tin is common upon the decomposition organostannanes⁵¹.

Both alkyl and aryl stannanes, $\text{R}_{4-n}\text{SnH}_n$ (R = alkyl or aryl; n = 1 or 2), are generally prepared in excellent yields by reduction of the corresponding halides, i.e. generally Cl but may also be Br, I, or alkoxides, i.e. OMe or OEt, with metal hydrides such as LiAlH_4 , NaBH_4 or R_2AlH in dry organic solvent¹. The synthesis of organotin trihydrides, RSnH_3 , is rarely known probably because of their extreme thermal instabilities.

The reactions of stannanes, $\text{Sn}_n\text{H}_{2n-2}$, and their organoderivatives, $\text{R}_{4-n}\text{SnH}_n$, are similar to those of the corresponding silanes and germanes. The Sn–H bonds react with halogens, hydrogen halides, alkyl halides, alkenes, alkynes, the double bonds of the C=O, C=S, C=N and also alkali metals (Scheme 1-4).



Scheme 1-4: Reactions of Sn-H bonds (adopted from Wiberg, E.; Amberger, E., *Hydrides of the Elements of Main Groups I-IV*, (1971))

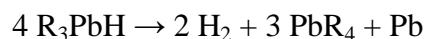
The Sn-H bonds react vigorously towards free radicals (by far more than the C-H, Si-H and Ge-H bonds) and many organostannanes are, therefore, often excellent radical scavengers⁵¹. Organostannanes react with the protons of acids with the loss of H₂. In the reactions of aryl stannanes with inorganic acids, the cleavage of aryl-tin bonds is favoured by that of Sn-H bonds. Ligand exchange reactions occur with nucleophilic groups of other stannyl compounds such as trialkyl tin oxides and sulfides, organotin methoxides and cyanides, stannyl phosphanes and stannyl amines⁵¹. Condensation reactions to form Sn-Sn bonds are known between excess stannanes and stannyl compounds carrying negative substituents such as stannyl alkoxides, dibutylphosphides, stannoxanes and diethylamide and stannylamines⁵¹. Organostannanes react with alkyl metals, i.e. R₃Al, exchanging the hydrogen of the organostannane with one of the organic groups of the alkyl metal⁵¹. Reaction with aliphatic diazo-compounds give ultimately the corresponding tetraorganotin, in most cases with a copper as catalyst⁵¹. Hydrostannation of carbon-carbon multiple bonds

and polar double bonds is the most well-established application of organostannanes⁵¹. The stannyl group is added to the terminal carbon or at the inner carbon of the double bond. The addition reaction proceeds almost exclusively by a radical mechanism for stannanes while both a radical or polar mechanism are possible for silanes and germanes although germanes almost exclusively add by a polar mechanism¹. In reactions of phenyl stannanes, $\text{Ph}_{4-n}\text{SnH}_n$, with HBr like the corresponding silanes, the cleavage of Sn–Ph bond is favoured over that of Sn–H bond and, therefore, the formation of PhSnHBr_2 dominates the reaction products. Phenyl stannanes also undergo hydrolysis *via* electrophilic addition in neutral or, more rapidly, in alkaline media¹.

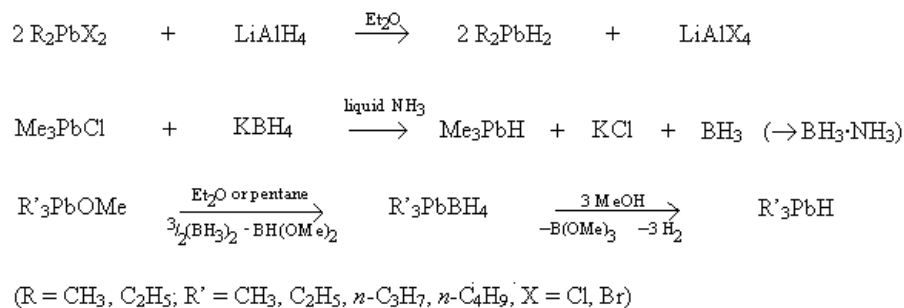
Organostannanes are diverse as precursors to many organotin compounds in organic syntheses^{1, 51-57}. Tertiary organostannanes, R_3SnH , are routinely used as reductants and important reagents in synthetic and mechanistic organic studies involving free radical intermediates²⁰. Chains, $\text{H}(\text{R}_2\text{Sn})_n\text{H}$ ($n \leq 8$), and rings, $(\text{R}_2\text{Sn})_2$, are obtained by thermal decomposition of disubstituted secondary stannanes, R_2SnH_2 (R = alkyl or aryl)¹.

1.1.1.11 Organolead Hydrides

Secondary and tertiary organolead hydrides, $\text{R}_{4-n}\text{PbH}_n$ ($n = 1$ or 2), also referred as secondary and tertiary plumbanes, respectively, are extremely thermally unstable. For example, R_3PbH and R_2PbH_2 (R = Me or Et), decompose even at -30 to -20 °C and -50 °C, respectively¹. Monoalkyl plumbanes, RPbH_3 , are not known probably due to the great difficulties in synthesising the corresponding halides¹. Organoplumbanes are also air- as well as light-sensitive^{20, 58}. Alkyl plumbanes are often colourless liquids which decompose at room temperature or even at below 0 °C¹. The decomposition of monoalkylated plumbane typically occurs as follows:

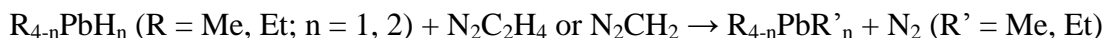


Alkyl plumbanes are synthesised in moderate to good yields by hydrogenation of the corresponding halides, $R_{4-n}PbX_n$, i.e. $X = Cl$ or Br , with double hydrides, i.e. KBH_4 or $LiAlH_4$, in organic solvents, e.g. Et_2O ^{1,58} at very low temperatures, i.e. $\leq -60\text{ }^\circ C$ ²⁰ or quantitatively by reaction of the corresponding methoxides with diborane also at low temperatures (Scheme 1-5)¹.

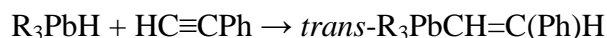


Scheme 1-5: *Synthesis of alkylplumbanes (adopted from Wiberg, E.; Amberger, E., Hydrides of the Elements of Main Groups I-IV, (1971))*

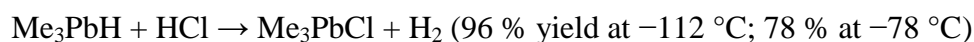
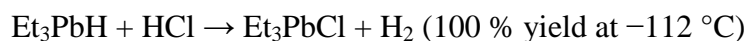
Probably because of the extreme instabilities, only a few reactions of alkyl plumbanes are known¹. Alkyl plumbanes react in the same manner as for the hydrides of the lighter Group 14 elements. Only the $Pb-H$ bonds are more polarised than those of the lighter Group 14 element hydrides and thus more reactive^{59,60}. Reactions of trimethyl and triethyl plumbanes with diazoalkanes give the corresponding alkylated derivatives¹.



Similarly to silanes, germanes and stannanes, plumbanes also undergo addition reactions with the double bonds of the $C=C$, $C=N$ and $C\equiv C$, also referred as hydroplumbalation. The addition reaction proceeds *via* either a polar or free radical mechanism¹. Plumbanes tend to be more reactive towards olefins than the corresponding silanes and germanes. Trialkyl plumbanes, R_3PbH , add to the $C=C$ bond under pressure without activation by neighbouring groups or to the $C=N$ even at $0\text{ }^\circ C$ without pressure or a catalyst.



Trimethyl plumbane, Me_3PbH , reacts with NH_3 at low temperatures to give the corresponding ammonium salt, $\text{NH}_4^+\text{PbMe}_3^-$, which decomposes on heating to give various products, i.e. Pb , $\text{Me}_3\text{PbPbMe}_3$, PbMe_4 , NH_3 , MeH and H_2 . Trialkyl plumbanes also react with EtI to give R_3PbI with the evolution of EtH^1 . Reaction of trialkyl plumbanes with HCl gives the corresponding chlorides, R_3PbCl , with the generation of H_2 . Although the reaction of Me_3PbH with HCl is faster than that of Et_3PbH , it will be disturbed by thermolysis at $> -112^\circ\text{C}$.



1.1.1.12 Organoderivatives of the Group 16 Element Hydrides

While organosulfur hydrides, also referred as thiols, are well-studied, only a few organo-selenium and -tellurium hydrides, also known as selenols and tellurols, respectively, are known. Although selenols and tellurols are often used as intermediates in the syntheses of organo-selenium^{61, 62} and -tellurium compounds, in many cases, they are not isolated probably owing to their extreme instabilities towards oxidation. Organo-thiols, -selenols and -tellurols are prepared by reaction of elemental sulfur, selenium and tellurium with organolithiums and then deoxygenated water^{63, 64}. Organo-thiols, -selenols and -tellurols undergo addition reactions with activated olefins (hydrochalcogenation (chalcogens = O, S, Se or Te))⁶³. For organotellurols, hydrotelluration reactions of terminal unactivated alkynes to give vinyl tellurides are well established⁶⁵⁻⁷¹. *In Situ* addition reactions of organotellurols to alkynyl phosphonates and alkynyl sulfonates have also been reported⁷².

1.1.1.13 Stabilisation of Highly Reactive Hydrides of Heavier Main Group Elements

There has been a growing interest in the stabilisation of highly reactive hydrides of main group elements, which are often unstable, volatile and extremely toxic with offensive odours but are otherwise very useful substances because of their highly reactive hydride centres. One of the key strategies employed in the recent developments in the stabilisation of the main group element hydrides such as primary phosphanes^{10, 11, 73-75}, germanes⁷⁶, stannane or stibane, i.e. RSbH_2 ($\text{R} = [2,4,6\text{-}^i\text{Pr}_3\text{C}_6\text{H}_2]_2\text{C}_5\text{H}_3$)¹⁹, is to sterically hinder the hydride centres with bulky R groups⁷⁶ (Figure 1-6). By sterically protecting the highly reactive hydride centres, the unstable hydrides can be stabilised. However, this strategy, which is often successful, runs a risk of compromising the chemistry of the highly reactive hydride centres in part by physically preventing an organic substrate from approaching the reactive site and may not be desirable in some cases.

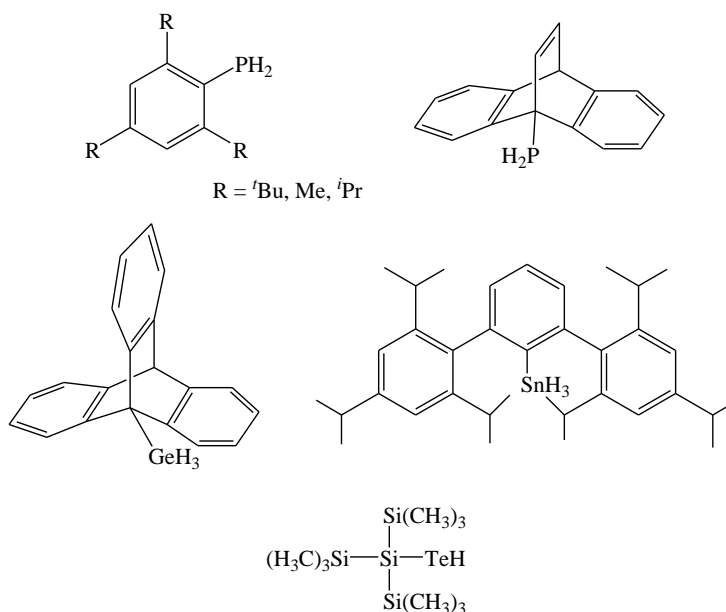


Figure 1-6: Sterically stabilised hydrides of heavier main group elements

Another strategy employed in the stabilisation of primary phosphanes is to incorporate an appropriate conjugation system in the molecular skeleton (Figure 1-7)⁷⁶. This type is also successful at stabilising primary phosphanes and exhibits a

remarkable air-stability under ambient conditions. The more conjugation there is in the molecule, the more stable the primary phosphane becomes⁷⁶.

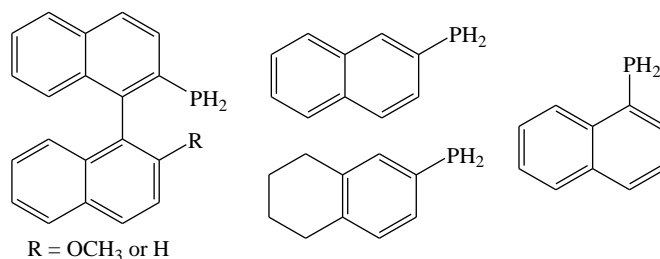


Figure 1-7: Primary phosphanes stabilised by conjugation in their backbones

1.1.1.14 Stabilisation of the Hydrides of Heavier Main Group Elements with Fc(CH₂)_n (n ≥ 1) Groups

Air-stable main group element hydrides with non-bulky R groups are relatively rare and only a few examples such as H₂N(CH₂)₃PH₂⁷⁷, Br(CH₂)₃PH₂⁷⁷ and PhNHC(O)C(CH₂PH₂)₂⁷⁶, have been known. Earlier, Goodwin *et al.*⁷⁸ and Alley *et al.*⁷⁹ have reported that primary phosphanes and a primary arsane with a ferrocenylalkyl group incorporated at the hydride centre, Fc(CH₂)_nPH₂ (n = 1 **1** or 2 **23**) and Fc(CH₂)₂AsH₂ **41**, respectively, (Figure 1-8), were completely air-stable. The primary phosphane **1** was stable even as a solid, showing no oxidation after being exposed to air in an unsealed vial for 61 days at ambient temperature and also for 2 years in a closed vessel⁷⁸. The improved air-stabilities of other closely related primary phosphanes, 1,1-Fc'- and 1,2-Fc''-((CH₂PH₂)₂) [Fc' = Fe(η⁵-C₅H₄); Fc'' = (η⁵-C₅H₅)(η⁵-C₅H₃)], ranging from several weeks to months, were also reported in the literature⁷⁹.

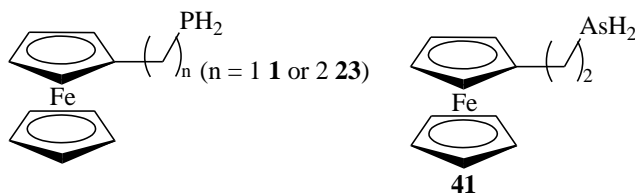


Figure 1-8: Air-stable primary phosphanes and arsane with a Fc(CH₂)_n (n = 1 or 2) group

Although the significantly improved air-stabilities of the primary phosphanes and arsane were not fully explained, the studies demonstrated that highly reactive hydrides could be stabilised by non-steric or -conjugative means, which may be advantageous because of the absence of steric hindrance at their hydride centres. Ferrocene is also a stable, versatile, readily accessible and well-studied chemical with redox properties^{80, 81} as well as planar chirality⁸²⁻⁸⁴ which may also be added to the hydrides.

1.1.1.15 Aims of Thesis

Building on the earlier studies by Goodwin *et al.*⁷⁸ and Alley *et al.*⁷⁹, the present study investigates the ferrocene-based stabilisation effects on air-sensitive primary phosphanes and arsane. The study also extends into the hydrides of other heavier main group elements, i.e. Ge, Sb, Si, Sn, Se, Te. The syntheses of the heavier main group element hydrides with Fc(CH₂)_n groups incorporated at the hydride centres and their stabilities under ambient conditions were investigated mainly using spectroscopic techniques, i.e. NMR and IR spectroscopy.

The syntheses, characterisations and determination of the air-stability of the hydrides of the heavier Group 15 element hydrides, i.e. P, As and Sb, are reported in Chapter 2. The chapter also reports the ³¹P NMR studies on the stabilisation effects of ferrocene, FcH, and the ferrocenyl compound, FcCH₂PH₂ **1**, on the highly air-sensitive primary phosphanes, PhPH₂ and camphylPH₂ **2**, in solution by simple addition. Chapter 3 describes the syntheses, characterisations and determination of the stability of the hydrides of the heavier Group 14 elements, i.e. Si, Ge and Sn. The syntheses, characterisations and determination of the stability of the hydrides of the heavier Group 16 elements, i.e. Se and Te, under ambient conditions are reported in Chapter 4. The ⁷⁷Se NMR study on the stabilisation effects of FcH on an air-sensitive selenol, PhSeH **78**, in solution is also described in Chapter 4.

Chapter 2: Stabilisation Effects of Ferrocenylalkyl Groups on the Hydrides of the Heavier Group 15 Elements, P, As, Sb

2.1 Introduction

2.1.1 Hydrides of Phosphorus, Arsenic and Antimony

While, in the pure state, phosphane, PH_3 , is a stable and odourless gas, it is extremely pyrophoric⁹ and has an offensive odour which is often described as a garlic or rotten fish, in the presence of P_2H_4 . Arsane, AsH_3 , is also a colourless, extremely poisonous, air-sensitive and pyrophoric gas with a noxious odour⁴. In the presence of oxygen, it is readily oxidised to arsenic oxide, As_2O_3 ⁴. Arsane is thermally stable and decomposes only slowly at room temperature and more rapidly at 230 °C into elemental arsenic and hydrogen, depositing a metallic mirror, which can be used in the detection of thermal decomposition⁴. The decomposition of arsane is also catalysed by the presence of elemental arsenic as is often expected for heavier elements of the group⁴. An autocatalytic decomposition takes place in their presence. Both phosphane and arsane are used as a means of depositing the elements onto material surfaces (chemical vapour deposition) in the semiconductor industry, which can then be functionalised (i.e. conductivity)⁸⁵.

Stibane, SbH_3 , and bismuthane, BiH_3 , are also both extremely toxic gases with revolting odours. They are extremely thermally unstable and little is known about their chemistry. The chemistry of SbH_3 is very similar to that of AsH_3 but only less thermally stable^{4, 86}. Stibane decomposes slowly at room temperature and more rapidly at 200 °C. An autocatalytic decomposition also takes place in the presence of elemental Sb. It is readily oxidised in air to give the corresponding stibanic oxide, Sb_2O_3 , and water. Stibane is also used in the semiconductor industry as a means of depositing elemental Sb onto material surfaces. Bismuthane is extremely unstable and

does not have many applications⁴. It decomposes below 0 °C to hydrogen and elemental Bi, which also catalyses the decomposition of the hydride. One of the main uses of BiH₃ may be as a reaction intermediate to organobismuth compounds in organic syntheses.

2.1.2 Organo-phosphanes, -arsanes and -stibanes

Organoderivatives of primary, REH₂, and secondary, R₂EH (E = P, As or Sb), phosphanes, arsanes and stibanes are also often toxic, air-sensitive and potentially pyrophoric substances with noxious odours^{9, 12}. They are, however, very important substances because of their highly reactive E–H bonds^{9, 12}. Organophosphanes are used as ligands to transition metals^{84, 87} in coordination chemistry^{10, 88, 89} and as precursors^{77-79, 84, 90, 91} to many organophosphorus compounds⁹. Organo-arsanes and -stibanes are also used as precursors to many arsenic¹² and stibanic compounds in organic syntheses. Despite their extensive uses, the chemistry of the hydrides has been rather poorly understood probably due to their toxicity and difficulties in handling.

2.1.3 Stabilisation of Hydrides of Heavier Group 15 Elements

As mentioned earlier in Chapter 1, the most utilised strategies for the stabilisation of highly reactive primary phosphanes are to sterically protect their hydride centres with bulky R groups^{10, 11, 73-75} or to incorporate appropriate conjugation in the molecule⁷⁵. Since stable primary phosphanes without steric protections are relatively rare and also it runs a risk of compromising the chemistry of the highly reactive hydride centre, it was of great interest to synthesise air-stable phosphanes and arsanes with a small and readily accessible R group, i.e. Fc(CH₂)_n, building on the earlier studies by Goodwin *et al.*⁷⁸ and Alley *et al.*⁷⁹ which showed the completely air-stable primary phosphanes and arsanes by incorporation of a Fc(CH₂)_n group at their hydride centres.

The present research extends the earlier studies by Goodwin *et al.*⁷⁸, and Alley *et al.*⁷⁹, by synthesising ferrocenyl primary phosphanes and arsanes with an extended alkyl

spacer, $\text{Fc}(\text{CH}_2)_n\text{EH}_2$ ($\text{E} = \text{P}$ or As ; $n \geq 2$), in order to find the key factors of the stabilisation effects of the ferrocenylalkyl groups on primary phosphanes and arsanes and also by the syntheses of secondary phosphanes and primary stibanes with a FcCH_2 group incorporated at their hydride centres so as to investigate if the ferrocene-based stabilisation effects would extend to secondary phosphanes and primary stibanes as well.

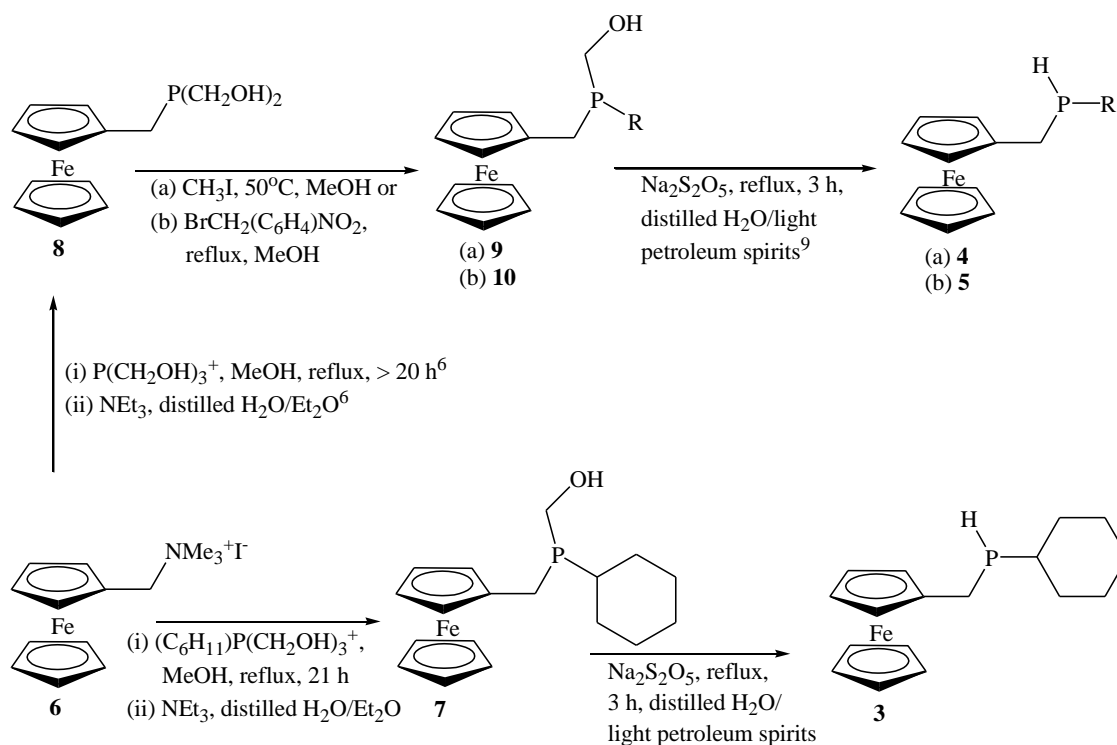
This chapter reports the stabilisation effects of a $\text{Fc}(\text{CH}_2)_n$ group on the hydrides of the heavier Group 15 elements, i.e. P, As, Sb. The syntheses, characterisation and air-stabilities of a series of ferrocenylalkyl and related primary and secondary phosphanes and arsane are described. Attempts to synthesise ferrocenyl primary arsanes with the extended alkyl spacer, $\text{Fc}(\text{CH}_2)_n$ ($n = 4, 6$ or 11), and ferrocenylmethyl stibane are also presented. The ^{31}P NMR studies on the oxidative stability of PhPH_2 and camphyl PH_2 **2** in solution under ambient conditions in the presence of FcH or **1** are also described.

2.2 Results and Discussion

2.2.1 Synthesis and Characterisation of Ferrocenylmethyl Secondary Phosphanes; $[\text{Fe}(\eta\text{-C}_5\text{H}_5)(\eta\text{-C}_5\text{H}_4\text{CH}_2\text{PRH})]$ ($\text{R} = \text{C}_6\text{H}_{11}$ (**3**), CH_3 (**4**), $p\text{-CH}_2\text{C}_6\text{H}_4\text{NO}_2$) (**5**))

2.2.1.1 Synthesis of FcCH_2PRH ($\text{R} = \text{C}_6\text{H}_{11}$ (**3**), CH_3 (**4**) and $\text{CH}_2\text{C}_6\text{H}_4\text{NO}_2$ (**5**))

The secondary phosphanes **3**, **4** and **5** were prepared according to the literature methods^{78,92} with minor modifications where needed. Scheme 2-1 shows the syntheses.



Scheme 2-1: Synthesis of **3**, **4** and **5**

Compounds **7**, **9** and **10** were neither purified nor isolated but used as obtained in the subsequent reduction reactions. Compounds **7** and **8** were prepared, with reference to the literature methods^{92, 93}. Compound **7** was prepared by reaction of **6**⁹³ with $\text{CyP}(\text{CH}_2\text{OH})_3^+$ and **8** by reaction of **6**⁹³ with excess $\text{P}(\text{CH}_2\text{OH})_3$ prepared *in situ* from $[\text{P}(\text{CH}_2\text{OH})_4]\text{Cl}$ and KOH according to the literature method⁹², in MeOH at reflux for > 20 h under an N_2 atmosphere. After the methanol from the mixture had been removed under reduced pressure, the residue was stirred in a mixture of NEt_3 , distilled H_2O and Et_2O for 1 h to ensure the full conversion of the phosphonium salt to the hydroxymethyl phosphane. The organic phase was separated and washed thoroughly with distilled H_2O . Removal of the solvent from the organic phase gave the hydroxymethyl phosphanes **7** and **8** as orange-red oils.

The hydroxymethyl phosphane **8** was further reacted with an appropriate alkylating agent to yield the hydroxymethyl phosphanes **9** and **10**. After adding the alkylating agent to the methanol solution of **8**, the mixture was stirred under the given

conditions. After removal of the solvent from the mixture under reduced pressure, the hydroxymethyl phosphanes **9** and **10** were obtained as orange-red oils.

The hydroxymethyl phosphanes **7**, **9** and **10** were reacted without further purifications with $\text{Na}_2\text{S}_2\text{O}_5$ in a two solvent system consisting of distilled H_2O and light petroleum spirits in the same pot at reflux for 3 h under an N_2 atmosphere. After separating and washing the organic phase with distilled H_2O , removal of the solvent from the organic phase yielded the desired secondary phosphanes **3**, **4**, **5** as orange-red oils in moderate to good yields.

The distinctive phosphane odour was detected from all three secondary phosphanes. The crude products were purified by chromatography on a preparative TLC plate, eluting with a solvent mixture of an appropriate ratio. The desired bands were collected and extracted with CH_2Cl_2 . Removal of the CH_2Cl_2 gave the pure secondary phosphanes **3**, **4**, **5** as orange-red oils which solidified at $-18\text{ }^\circ\text{C}$.

The ^{31}P NMR spectra showed that the neat states of the secondary phosphanes **3** and **4** could be stored at $-18\text{ }^\circ\text{C}$ for at least 5 months without significant oxidation (Figure 2-1; the ^{31}P NMR signals for the corresponding oxides of **3** and **4** appear at δ 42.1 and 30.0 ppm, respectively). Since the secondary phosphane **5** was never stored for a long period of time, the long term stability of the compound under the given conditions is not known.

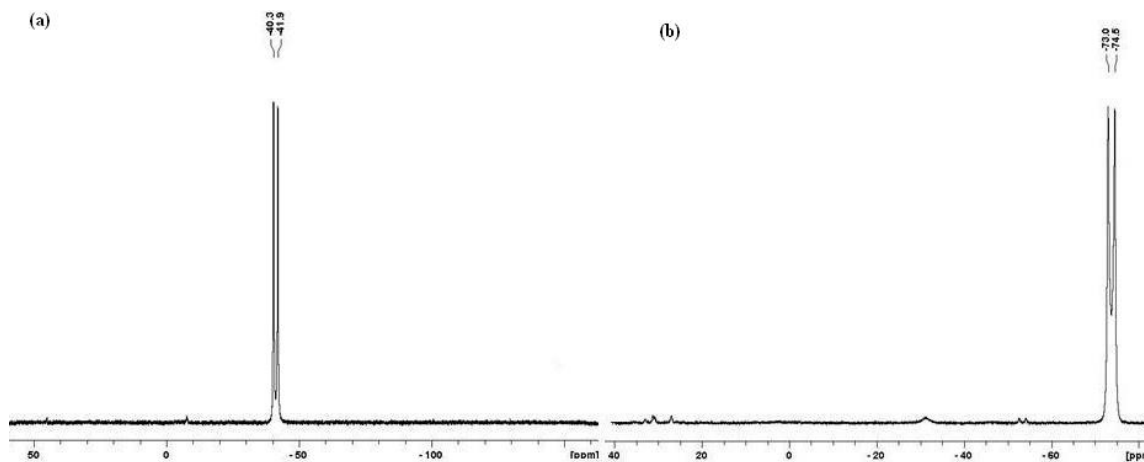


Figure 2-1: ^{31}P NMR spectra of (a) **3** and (b) **4** after being stored as neat liquids for 5 months at $-18\text{ }^\circ\text{C}$ in air

The overalkylated by-products (Figure 2-2) were also isolated from the synthesis of **3** and **5**. Compound **11** was isolated from the synthesis of **3** as a yellow solid in poor yield (3 %), precipitating out upon re-extraction of the crude product with Et₂O or with a mixture of Et₂O and light petroleum spirits.

Compounds **12** and **13** were isolated from the synthesis of **5**. Chromatography of the crude product on a TLC plate, eluting with a 1 : 1 mixture of CH₂Cl₂ and light petroleum spirits gave compound **13**. Compound **12** was obtained as a red oil in very poor yield (0.8 %) from the fraction at R_f 0.33 and the latter as a red solid in moderate yield (24 %) from the fraction at R_f 0.66 after removal of the organic solvents under reduced pressure. Characterisations of **11**, **12** and **13** are given in 2.2.1.3.

A trace amount of (C₆H₁₁)PH₂ was also observed by ³¹P NMR spectroscopy carried out on the crude product of **3**. The triplet at δ -110.2 ppm with a ¹J_{PH} coupling constant of 194 Hz was consistent with the literature values^{9, 94}. No attempt was made to isolate the compound as it is a well-known compound.

These by-products may have been avoided if the reactions had been carried out separately, isolating and purifying the compounds at each step and the stoichiometric amount of each reagent had been used. The yields of the secondary phosphanes may hence be improved.

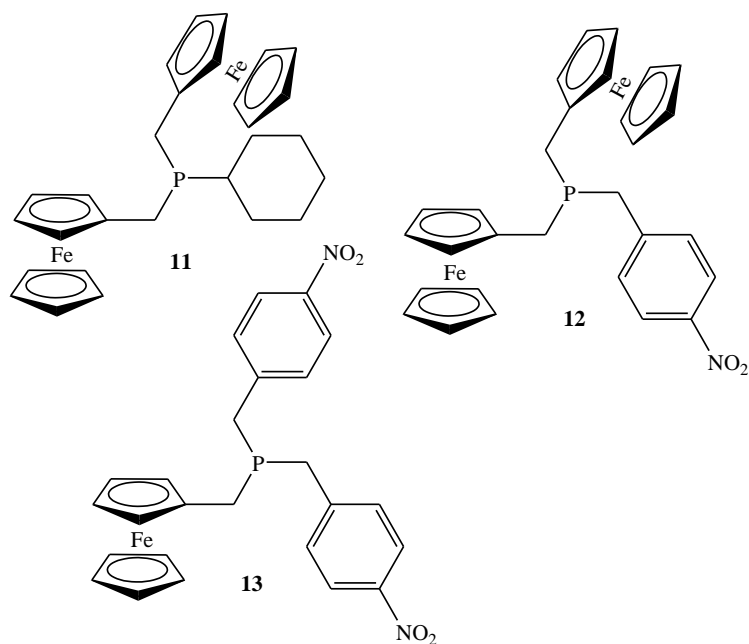


Figure 2-2: Overalkylated by-products **11**, **12** and **13** from the synthesis of **3** and **5**

2.2.1.2 Characterisation of FcCH_2PRH ($\text{R} = \text{C}_6\text{H}_{11}$ (**3**), CH_3 (**4**) and $\text{CH}_2\text{C}_6\text{H}_4\text{NO}_2$ (**5**))

The secondary phosphanes **3**, **4** and **5** were characterised by IR and NMR spectroscopy, ESI-MS and elemental analysis. The selected spectroscopic data for **3**, **4** and **5** are summarised in Table 2-1.

Mass Spectrometry: Mass spectrometric data for **4** were not obtained because of the satisfactory microanalytical data. The ESI-MS was carried out for **3** and **5** in MeOH as a mobile phase. The parent ions $[M]^+$ of compounds **3** and **5** were observed at the expected m/z in the positive ion mode. The observation of $[M]^+$ ion in ESI-MS in positive ion mode is common for ferrocenyl compounds while a positively charged ion *via in situ* formation of $[M + H]^+$ or $[M + Na]^+$ ions are generally observed.

An ESI-MS technique of *in situ* formation of silver adducts such as $[M + \text{Ag}]^+$, $[2M + \text{Ag}]^+$ and/or $[3M + \text{Ag}]^+$ for characterisation of ferrocenyl phosphanes has been described in the literature⁹⁵. Such distinctive silver isotope distribution patterns and stronger intensity of the ions can be advantageous when characterising compounds

which ionise poorly. Some ferrocenyl phosphanes have been characterised using the technique described in the literature⁹². ESI-MS was therefore carried out on **3** using the established literature technique⁹⁵ in order to investigate whether it was applicable to these secondary phosphanes. When a half drop of a 0.1 mol L⁻¹ AgNO₃ solution was added to a methanol solution containing a very small amount of **3**, the corresponding silver adducts formed and were easily observed as $[M + Ag]^+$ and $[2M + Ag]^+$ ions in the positive ion mode. The intensities of the ions were much stronger than that of $[M]^+$ without added Ag⁺ and the isotope distribution pattern, agreed with the theoretical one. It was much easier to identify the ions of interest because of the high intensity and the unique isotope distribution patterns of the desired signals.

Table 2-1: Selected spectroscopic and microanalytical data for **3**, **4**, **5**

	3	4	5
ν (PH) / cm ⁻¹	2268s	2276s	2278m
³¹ P NMR (CDCl ₃) / δ_P ppm	-41.1 (d, ¹ J _{PH} = 199 Hz)	-73.5 (d, ¹ J _{PH} = 199 Hz)	-49.1 (d, ¹ J _{PH} = 192 Hz)
¹ H NMR (CDCl ₃) / δ_{PH} ppm	3.1 (d of unresolved m, ¹ J _{PH} = 198 Hz)	3.1 (d of q, ¹ J _{PH} = 194, ³ J _{HH} = 4 Hz)	3.4 (d of p, ¹ J _{PH} = 198 Hz, ³ J _{HH} = 7 Hz)
ESI-MS (MeOH) / m/z	314 [M] ⁺ , 422 [M + Ag] ⁺ , 736 [2M + Ag] ⁺ (with aq. AgNO ₃ added)	Not attempted.	367.0433 [M] ⁺
Elemental Analysis / %	C 65.18; H 7.56 (calcd. C 64.99; H 7.38)	C 59.00; H 6.19 (calcd. C 58.57; H 6.14)	C 59.63; H 4.92; N 3.95 (calcd. C 58.88; H 4.94; N 3.81)

IR Spectroscopy: The P–H stretches of **3**, **4** and **5** appeared at ν 2268, 2276 and 2278 cm⁻¹, respectively, as a medium to strong band. The frequencies are consistent for the class of compounds concerned (cf. 2280 ± 10 cm⁻¹ for the type RR'PH)⁹.

NMR Spectroscopy: The ³¹P NMR signals for **3**, **4** and **5** appeared at δ -41.1, -73.5 and -49.1 ppm, respectively, as doublets with ¹J_{PH} coupling constants of 192 – 199 Hz. The splitting of the signals and the coupling constant range are consistent with the expected compounds. The ³¹P NMR signal for **4** was observed at the furthest upfield of the three (by ~ δ 30 ppm further upfield than those for **3** and **5**). This is consistent with the fact that the methyl group is the most electron-donating and hence the most shielding of the three organic substituents on the phosphorus. The chemical shifts of the ³¹P NMR signals for **3** and **5** are about the same. It appears that the *p*-(CH₂C₆H₄NO₂) group is only slightly more shielding than the C₆H₁₁ group which is

contrary to the fact that the C₆H₁₁ group is generally more electron-donating than the *p*-(CH₂C₆H₄NO₂) group.

In the ¹H NMR spectrum, the phosphane proton signal of **3**, **4**, **5** appeared at ~ δ 3.3 ppm as a doublet of multiplets with ¹J_{PH} and ³J_{HH} coupling constants of ~196 and ~6 Hz, respectively. The phosphane proton signals were shifted further downfield by ~ δ 0.4 ppm than that for the corresponding primary phosphane **1** (cf. δ 2.9 ppm)⁷⁸. This may be expected as an organic substituent is more electron-withdrawing and hence more deshielding than hydrogen. Since magnetically equivalent NMR active nucleus do not split, the observation of H₃ atoms as a triplet suggests that the two H₃ proton atoms are not totally magnetically equivalent. This may be because it is a second order A2B2 spin system, or hindered rotation about the P-C-C system could also account for this. In the ¹³C-¹H NMR spectrum, the ^{1,2,3}J_{PC} couplings were observed for the respective carbon signals. The signals appeared as doublets with ^{1,2,3}J_{PC} coupling constants of 12 – 14, 4 – 6 and 3 Hz, respectively, which are comparable to the literature values for **1**⁷⁸. The assignments of the chemical shifts (Table 2-2) were made according to the 2-D NMR data. The 2-D correlations observed in the respective 2-D NMR experiments were consistent with the structure of the expected compounds. The selected ^{1,2,3}J_{CH} and ³J_{HH} NMR correlations observed in the respective HMBC, HSQC and COSY NMR experiments are shown in Figure 2-4. The HETCOR experiment was carried out only for **5**.

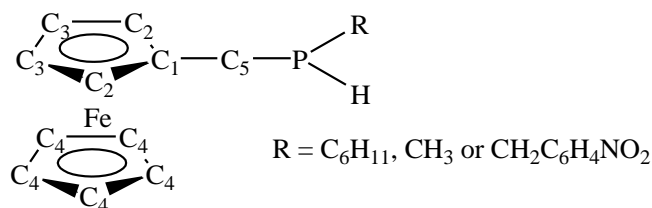


Figure 2-3: Atom labelling used in NMR assignments of ferrocenyl secondary phosphanes; hydrogen atoms are numbered according to the carbon to which they are bonded

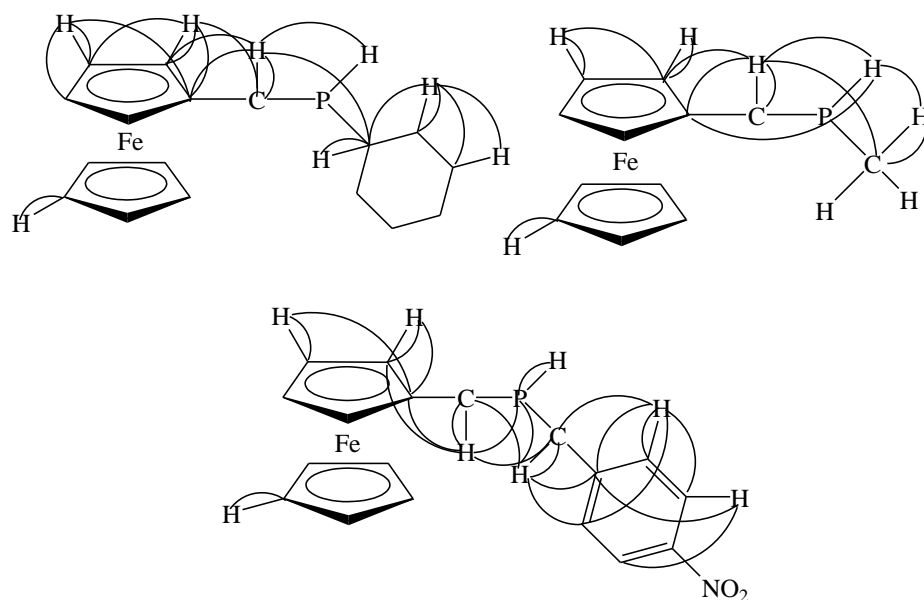


Figure 2-4: Selected $^{1,2,3}J_{CH}$ and $^3J_{HH}$ NMR correlations observed in the HMBC, HSQC, COSY and HETCOR NMR experiments for 3, 4, 5

Table 2-2: 1H , ^{13}C and ^{31}P NMR chemical shifts for 3, 4, 5

δ / ppm	3	4	5
1H NMR			
H_2	4.10 (t, $^3J_{HH} = 2$ Hz, 2 H)	4.10 (t, $^3J_{HH} = 2$ Hz, 2 H)	4.08 (unresolved m, 4 H)
H_3	4.04 (t, $^3J_{HH} = 2$ Hz, 2 H)	4.04 (t, $^3J_{HH} = 2$ Hz, 2 H)	
H_4	4.12 (s, 5 H)	4.11 (s, 5 H)	4.11 (s, 5 H)
H_5	2.7 (d of m, $^2J_{PH} = 37$ Hz, 2 H)	2.7 (d of m, 2 H)	2.6 (m, 2 H)
PH	3.1 (d, $^1J_{PH} = 198$ Hz, 1 H)	3.1 (d of m, $^1J_{PH} = 194$, $^3J_{HH} = 4$ Hz, 1 H)	3.4 (d of pentet, $^1J_{PH} = 198$ Hz, $^3J_{HH} = 7$ Hz, 1 H)
	1.3 – 1.7 (C_6H_{11} , unresolved m, 11 H)	1.7 (CH_3 , unresolved m, 3 H)	3.0 ($PCH_2C_6H_4$, d of p, 2 H)
			7.3 ($PCH_2C_6H_4$, d, $^3J_{HH} = 8$ Hz, 2 H)
			8.1 ($C_6H_4NO_2$, d, $^3J_{HH} = 9$ Hz, 2 H)
$^{13}C\{-^1H\}$ NMR			
C_1	87.0 (C, d, $^2J_{PC} = 5$ Hz)	87.0 (C, d, $^2J_{PC} = 6$ Hz)	85.6 (C, d, $^2J_{PC} = 7$ Hz)
C_2	68.3 (CH, s)	68.3 (CH, d, $^3J_{PC} = 26$, 4 Hz)	68.6 (CH, d, $^3J_{PC} =$ not determined)
C_3	67.3 (2 CH, s)	67.3 (2 CH, d, $^4J_{PC} = 13$ Hz)	68.1 (2 CH, d, $J_{PC} =$ not determined)
C_4	68.8 (5 CH, s)	68.8 (5 CH, s)	68.9 (5 CH, s)
C_5	19.8 (CH_2 , d, $^1J_{PC} = 13$ Hz)	19.8 (CH_2 , d, $^1J_{PC} = 14$ Hz)	21.6 (Cp $\underline{C}H_2$, d, $^1J_{PC} = 14$ Hz)
	31.2 (CH, d, $^1J_{PC} = 7$ Hz)	31.2 (CH_3 , d, $^1J_{PC} = 8$ Hz)	28.8 ($PCH_2C_6H_4$, d, $^1J_{PC} = 17$ Hz)
	27.0 (2 CH_2 , d, $^2J_{PC} = 8$ Hz)		148.7 (PCH_2C , d, $^2J_{PC} = 3$ Hz)
	26.5 (C_6H_{11} , s)		129.3 ($PCH_2C_6H_4$, d, $^3J_{PC} = 4$ Hz)
	32.0 (br)		123.9 ($C_6H_4NO_2$, s)
			129.5 (CNO_2 , s)
^{31}P NMR			
PH	-41.0 (d, $^1J_{PH} = 199$ Hz)	-73.5 (d, $^1J_{PH} = 199$ Hz)	-49.1 (d, $^1J_{PH} = 192$ Hz)

2.2.1.3 Characterisation of $(\text{FcCH}_2)_2\text{PCy}$ (**11**), $(\text{FcCH}_2)_2\text{PCH}_2\text{C}_6\text{H}_4\text{NO}_2$ (**12**) and $\text{FcCH}_2\text{P}(\text{CH}_2\text{C}_6\text{H}_4\text{NO}_2)_2$ (**13**)

Compound **11** was characterised by ^{31}P , ^1H and $^{13}\text{C}\{-^1\text{H}\}$ NMR spectroscopy and ESI-MS. The ^{31}P NMR signal appeared at $\delta -7.6$ ppm as a singlet. The signal was shifted by $\delta 34$ ppm further downfield than the corresponding secondary phosphane **3**. This is consistent with the addition of an extra bulky FcCH_2 group on the phosphorus. In the ^1H NMR spectrum, the CH_2 proton signal appeared at $\delta 2.5$ ppm as a singlet and those corresponding to the cyclohexyl protons at $\delta 1.2 - 1.8$ as unresolved multiplets. The Cp proton signals appeared at $\delta 4.0$ and 4.1 ppm as unresolved peaks. The integration of the signals agreed with the number of protons for the proposed compound ($\text{CH}_2 : \text{C}_6\text{H}_{11} : \text{Fc} = 4 : 11 : 18$). The mass spectrometric data were obtained by ESI-MS using MeOH as a mobile phase with a very small amount of AgNO_3 solution added. The corresponding silver adducts were observed as $[M + \text{Ag}]^+$ (m/z 620), and $[2M + \text{Ag}]^+$ (m/z 1132) in the positive ion mode. Compound **11** in solution (in CDCl_3) decomposed after 2 weeks at room temperature in a capped NMR tube in air. The ^{31}P NMR signal disappeared and the solution turned from yellow to dark brown.

Compound **12** was only partially characterised by ^{31}P , ^1H and $^{13}\text{C}\{-^1\text{H}\}$ NMR spectroscopy as it was obtained only in a small amount. The ^{31}P NMR signal was observed at $\delta -12.3$ ppm as a singlet. The signal was shifted further downfield by $\delta 37$ ppm than that for the corresponding secondary phosphane **5**. It was also slightly further upfield by $\delta 3.6$ ppm than that for **13**, suggesting that a FcCH_2 group is less deshielding than $p\text{-CH}_2\text{C}_6\text{H}_4\text{NO}_2$. The chemical shifts were assigned according to the 2-D NMR data including HMBC, HSQC and HETCOR NMR experiments (Table 2-3) (for atom labelling, see Figure 2-3). The selected $^{1,2,3}J_{\text{CH}}$ and $^2J_{\text{PH}}$ correlations observed in the respective NMR experiments are shown in Figure 2-5.

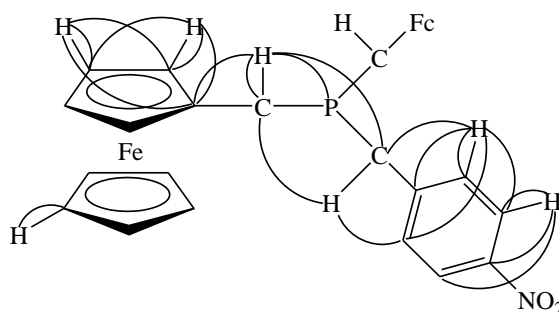


Figure 2-5: Selected $^{1,2,3}J_{CH}$ and $^2J_{PH}$ correlations observed for **12** in the HMBC and HSQC and HETCOR, respectively, NMR experiments

Compound **13** was characterised by elemental analysis, ^{31}P , ^1H and $^{13}\text{C}\{-^1\text{H}\}$ NMR, IR spectroscopy and ESI-MS. The composition of the red solid was found to be C 59.79; H 4.78; N 5.71% which agreed with the calculated values of C 59.76; H 4.62; N 5.58 %. The ^{31}P NMR signal appeared at δ -8.7 ppm as a singlet. The signal was shifted further downfield by δ 41 ppm than the corresponding secondary phosphane **5**. The shift is consistent with the addition of extra *p*-nitrobenzyl group on the phosphorus. The 2-D NMR data including HMBC, HSQC and COSY were also collected and the chemical shifts were assigned accordingly (Table 2-3) (for atom labelling, see Figure 2-3). The selected $^{1,2,3}J_{CH}$ and $^3J_{HH}$ correlations observed in the respective 2-D NMR experiments are shown in Figure 2-6.

Table 2-3: ^1H , ^{13}C and ^{31}P NMR chemical shifts for **12** and **13**

δ / ppm	12	13
^1H NMR		
$H_{2,3}$	4.03 (H_3 , d, $^3J_{HH} = 2$ Hz, 4 H); 4.07 (H_2 , d, $^3J_{HH} = 2$ Hz, 4 H)	4.03 (H_3 , unresolved m, 2 H); 4.11 (H_2 , unresolved m, 2 H)
H_4	4.08 (CH, s, 10 H)	4.08 (CH, s, 5 H)
H_5	2.5 (CH_2 , q of d, $^4J_{HH} = 8$ Hz, 6 H)	2.6 (CH_2 , s, 2 H)
PCH_2R	Could not be assigned.	2.9 (CH_2 , q, $^4J_{HH} = 19$ Hz, 4 H)
CH_2CCH	7.3 (CH, d of d, $^3J_{HH} = 8$, $^4J_{HH} = 1$ Hz, 2 H)	7.3 (CH, d, $^3J_{HH} = 8$ Hz, 4 H)
CHCNO_2	8.1 (CH, d, $^3J_{HH} = 9$ Hz, 2 H)	8.1 (CH, d, $^3J_{HH} = 8$ Hz, 4 H)
$^{13}\text{C}\{-^1\text{H}\}$ NMR		
C_1	83.6 (C, d, $^2J_{PC} = 10$ Hz)	82.2 (C, d, $^2J_{PC} = 8$ Hz)
C_2	67.7 (CH, d, $^3J_{PC} = 4$ Hz)	68.9 (CH, d, $^3J_{PC} = 3$ Hz)
C_3	67.7 (CH, d, $^3J_{PC} = 4$ Hz)	68.0 (CH, s)
C_4	68.9 (CH, s)	69.0 (CH, s)
C_5	27.9 (CH_2 , d, $^1J_{PC} = 19$ Hz)	27.7 (CH_2 , d, $^1J_{PC} = 19$ Hz)
PCH_2R	34.4 (CH_2 , d, $^1J_{PC} = 21$ Hz)	34.1 (CH_2 , d, $^1J_{PC} = 19$ Hz)
PCH_2C	147.0 (C, d, $^2J_{PC} = 7$ Hz)	145.5 (C, t, $^2J_{PC} = 4$ Hz)
CH_2CCH	129.9 (CH, d, $^3J_{PC} = 6$ Hz)	129.9 (CH, d, $^3J_{PC} = 6$ Hz)
CHCNO_2	123.6 (CH, s)	123.9 (CH, s)
CNO_2	146.2 (C, s)	146.5 (C, s)
^{31}P NMR		
P	-12.3 (P, s)	-8.7 (P, s)

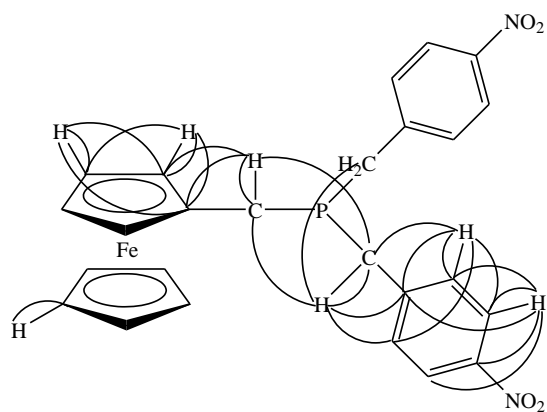
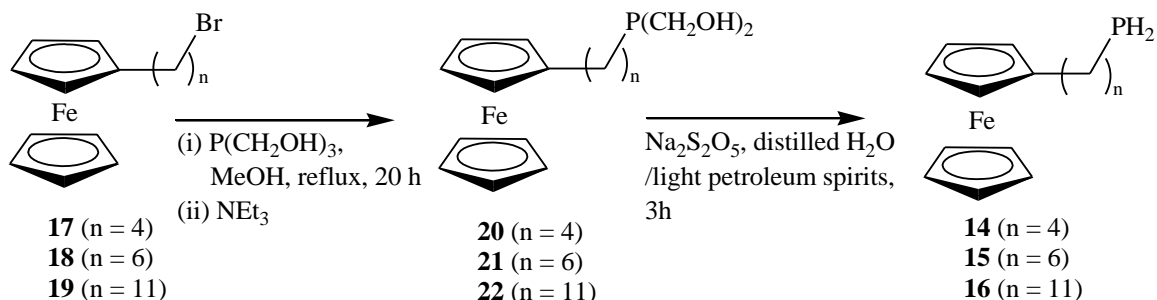


Figure 2-6: Selected $^{1,2,3}J_{CH}$ and $^3J_{HH}$ correlations observed in the HMBC, HSQC and COSY NMR experiments for **13**

The ESI-MS in MeOH with a small amount of added AgNO_3 solution added showed the molecular ion, $[M]^+$ (m/z observed. 502.074; calcd. 502.073), and the corresponding silver adduct, $[M + \text{Ag}]^+$ (m/z observed 608.978; calcd. 608.979), in the positive ion mode. In the IR spectrum, the $N-O$ stretches of **13** were observed at 1513 and 1343 cm^{-1} as very strong bands.

2.2.2 Synthesis and Characterisation of Ferrocenylalkyl Primary Phosphanes; $[\text{Fe}(\eta\text{-C}_5\text{H}_5)\{\eta\text{-C}_5\text{H}_4(\text{CH}_2)_n\text{PH}_2\}]$ ($n = 4, 6, 11$)

The new ferrocenyl-butyl **14**, -hexyl **15** and -undecyl **16** primary phosphanes were prepared by applications of the literature methods^{78, 92} with minor modifications where needed. Scheme 2-2 shows the synthesis.



Scheme 2-2: Synthesis of ferrocenylalkyl primary phosphanes

2.2.2.1 Synthesis of $\text{Fc}(\text{CH}_2)_n\text{P}(\text{CH}_2\text{OH})_2$ ($n = 4$ (**20**), **6** (**21**), **11** (**22**))

The reaction of $\text{P}(\text{CH}_2\text{OH})_3$, generated *in situ* from $[\text{P}(\text{CH}_2\text{OH})_4]\text{Cl}$ and KOH in MeOH ⁹², with ferrocenylalkyl bromides, $\text{Fc}(\text{CH}_2)_n\text{Br}$ ($n = 4$ **17**, **6** **18** or **11** **19**), prepared according to the literature methods⁹⁶⁻⁹⁸, gave the desired hydroxymethyl phosphanes, $\text{Fc}(\text{CH}_2)_n\text{P}(\text{CH}_2\text{OH})_2$ ($n = 4$ **20**, **6** **21** or **11** **22**), as red oils in good yields.

Attempted crystallisations of the crude hydroxymethyl phosphanes **20** and **21** from $\text{MeOH}/\text{CH}_2\text{Cl}_2$ with a few drops of light petroleum spirits added at $-18\text{ }^\circ\text{C}$ were not successful. The hydroxymethyl phosphanes were used as obtained without further purification. The hydroxymethyl phosphane **22** gave, however, a yellow solid from which satisfactory microanalytical data could be obtained.

2.2.2.2 Characterisation of $\text{Fc}(\text{CH}_2)_n\text{P}(\text{CH}_2\text{OH})_2$ ($n = 4$ (**20**), **6** (**21**) or **11** (**22**))

The hydroxymethyl phosphanes **20**, **21** and **22** were characterised by IR, NMR spectroscopy and ESI-MS; Selected spectroscopic data for **20**, **21** and **22** are summarised in Table 2-4.

Table 2-4: Selected spectroscopic data for $\text{Fc}(\text{CH}_2)_n\text{P}(\text{CH}_2\text{OH})_2$ ($n = 4$ **20**, **6** **21** and **11** **22**)

	20	21	22
³¹ P NMR ^{*1} / δ ppm	-22.7, singlet	-22.9, singlet	-22.7, singlet
ESI-MS ^{*2} / m/z	775.061 $[2M + \text{Ag}]^+$ (calcd. 775.061 for $\text{C}_{32}\text{H}_{46}\text{Ag}_1\text{Fe}_2\text{O}_4\text{P}_2$); 440.984 $[M + \text{Ag}]^+$ (calcd. 440.983 for $\text{C}_{16}\text{H}_{23}\text{Ag}_1\text{Fe}_1\text{O}_2\text{P}_1$); 334.078 $[M]^+$ (calcd. 334.078 for $\text{C}_{16}\text{H}_{23}\text{Fe}_1\text{O}_2\text{P}_1$)	831.123 $[2M + \text{Ag}]^+$ (calcd. 831.124 for $\text{C}_{36}\text{H}_{54}\text{Ag}_1\text{Fe}_2\text{O}_4\text{P}_2$); 469.014 $[M + \text{Ag}]^+$ (calcd. 469.014 for $\text{C}_{18}\text{H}_{27}\text{Ag}_1\text{Fe}_1\text{O}_2\text{P}_1$); 385.099 $[M + \text{Na}]^+$ (calcd. 385.099 for $\text{C}_{18}\text{H}_{27}\text{Fe}_1\text{Na}_1\text{O}_2\text{P}_1$); 362.108 $[M]^+$ (calcd. 362.109 for $\text{C}_{18}\text{H}_{27}\text{Fe}_1\text{O}_2\text{P}_1$)	539.093 $[M + \text{Ag}]^+$ (calcd. 539.092 for $\text{C}_{23}\text{H}_{37}\text{Ag}_1\text{Fe}_1\text{O}_2\text{P}_1$); 432.186 $[M]^+$ (calcd. 432.187 for $\text{C}_{23}\text{H}_{37}\text{Fe}_1\text{O}_2\text{P}_1$)
Elemental analysis / %	Not attempted.	Not attempted.	C 63.95; H 8.76 (calcd. C 63.87 H 8.63)

^{*1} in CDCl_3 ; ^{*2} in MeOH with added aq. AgNO_3

NMR Spectroscopy: The ³¹P NMR signals for **20**, **21** and **22** appeared at $\sim \delta -22$ ppm as a singlet in each case. The signals were shifted further downfield by $\delta 3$ ppm than

that for **8**⁹². This is consistent with the extended length of the alkyl spacer. The deshielding effect of ferrocene on the phosphorus becomes negligible in **20**, **21** and **22** due to the greater distance between ferrocene and the phosphorus.

In the ¹³C-¹H NMR spectra, ^{1,2,3}J_{PC} couplings were observed for the respective carbon signals with ^{1,2,3}J_{PC} coupling constants of 9, 15, 12 Hz, respectively, on the Fc(CH₂)_n moiety. The ¹J_{PC} coupling constant becomes larger for the hydroxymethylene carbon due to the presence of oxygen and was 21 Hz.

The assignments of the chemical shifts were made according to the 2-D NMR data obtained by HMBC, HSQC and COSY NMR experiments (Table 2-5). The selected ^{1,2,3}J_{CH} and ³J_{HH} correlations observed in the HMBC, HSQC and COSY NMR experiments are shown in Figure 2-7.

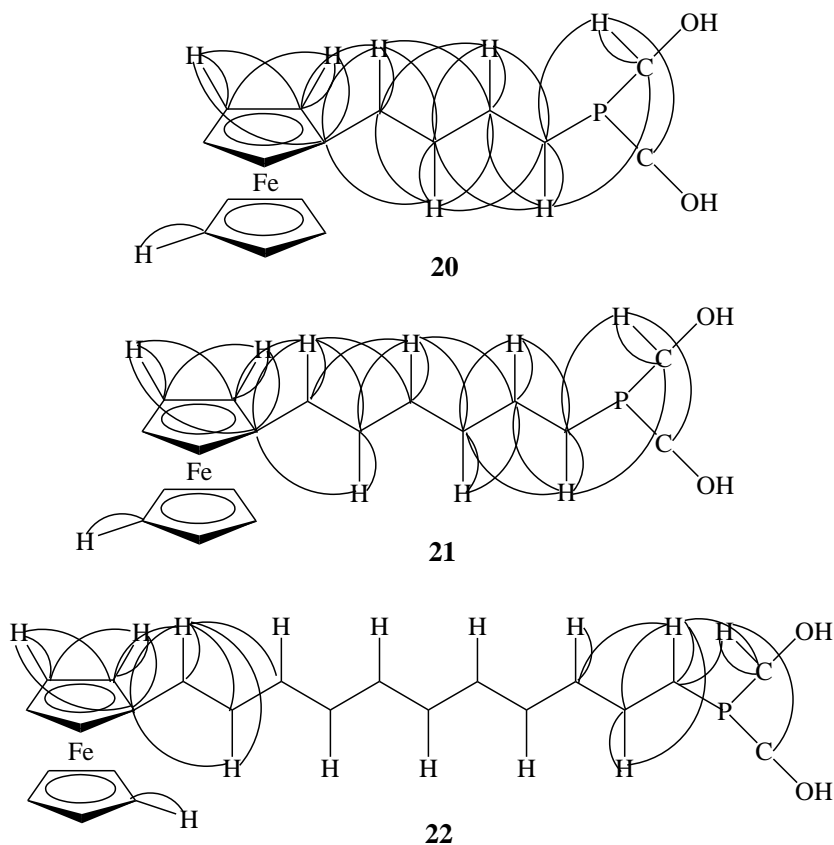


Figure 2-7: Selected ^{1,2,3}J_{CH} and ³J_{HH} correlations observed for **20**, **21** and **22** in the HMBC, HSQC and COSY NMR experiments

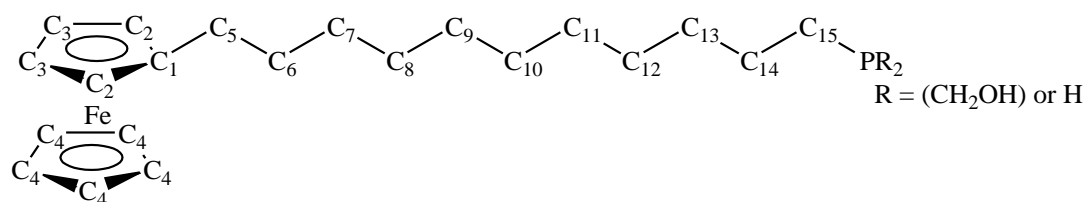


Figure 2-8: Atom labelling used in assignment of ferrocenylalkyl phosphanes NMR signals; hydrogen atoms are numbered according to the carbon to which they are bonded

Table 2-5: ^1H , ^{13}C and ^{31}P NMR chemical shifts for **20**, **21** and **22**

δ / ppm	20	21	22
^1H NMR			
H _{2,3}	4.05 (m, 4 H)	4.04 (m, 4 H)	4.04 (m, 4 H)
H ₄	4.10 (s, 5 H)	4.09 (s, 5 H)	4.09 (s, 5 H)
H ₅	2.4 (unresolved m, 2 H)	2.3 (t, $^3J_{\text{HH}} = 8$ Hz, 2 H)	2.3 (t, $^3J_{\text{HH}} = 8$ Hz, 2 H)
H ₆	-	1.5 (m, 2 H)	-
H ₇	-	1.4 (m, 2 H)	-
H ₈₋₁₂	-	-	1.4 & 1.5 (m, 18 H)
H ₁₃	1.7 (m, 2 H)	1.5(m, 4 H)	-
H ₁₄	1.6 (m, 2 H)	-	-
H ₁₅	1.8 (m, 2 H)	1.8 (m, 2 H)	1.8 (m, 2 H)
P(<u>CH</u> ₂ OH) ₂	4.2 (d of m, $^2J_{\text{PH}} = 85$ Hz, 4 H)	4.2 (d of m, $^2J_{\text{PH}} = 92$ Hz, 4 H)	4.2 (d of m, $^2J_{\text{PH}} = 89$ Hz, 4 H)
^{13}C - $\{^1\text{H}\}$ NMR			
C ₁	89.1 (C)	89.4 (C)	89.6 (C)
C ₂	68.1 (CH)	68.1 (CH)	68.1 (CH)
C ₃	67.1 (CH)	67.0 (CH)	67.0 (CH)
C ₄	68.5 (CH)	68.5 (CH)	68.5 (CH)
C ₅	29.3 (CH ₂)	29.5 (CH ₂)	29.6 (CH ₂)
C ₆	-	31.0 (CH ₂)	31.1 (CH ₂)
C ₇	-	29.3 (CH ₂)	29.6 (CH ₂)
C ₈₋₁₂	-	-	28.2 – 31.1 (CH ₂)
C ₁₃	32.7 (d, $^3J_{\text{PC}} = 12$ Hz, CH ₂)	31.2 (d, $^3J_{\text{PC}} = 12$ Hz, CH ₂)	31.3 (d, $^3J_{\text{PC}} = 12$ Hz, CH ₂)
C ₁₄	25.8 (d, $^2J_{\text{PC}} = 15$ Hz, CH ₂)	25.8 (d, $^2J_{\text{PC}} = 15$ Hz, CH ₂)	25.9 (d, $^2J_{\text{PC}} = 15$ Hz, CH ₂)
C ₁₅	16.7 (d, $^1J_{\text{PC}} = 9$ Hz, CH ₂)	16.8 (d, $^1J_{\text{PC}} = 8$ Hz, CH ₂)	16.9 (d, $^1J_{\text{PC}} = 8$ Hz, CH ₂)
P(<u>CH</u> ₂ OH) ₂	61.9 (d, $^1J_{\text{PC}} = 21$ Hz, CH ₂)	61.9 (d, $^1J_{\text{PC}} = 21$ Hz, CH ₂)	61.8 (d, $^1J_{\text{PC}} = 20$ Hz, CH ₂)
^{31}P NMR			
P	-22.7 (P, s)	-22.9 (P, s)	-22.7 (P, s)

ESI-Mass Spectrometry: Mass spectrometric data were obtained by ESI-MS using MeOH as a mobile phase and also aqueous AgNO₃ was added where appropriate⁹⁵. Without aqueous AgNO₃, the molecular ions, $[M]^+$, were observed in the positive-ion mode (Table 2-4). When a small amount of aqueous AgNO₃ was added to the solutions of **20**, **21** and **22** in MeOH, the corresponding silver adducts readily formed and were observed as $[M + \text{Ag}]^+$ and/or $[2M + \text{Ag}]^+$ in the positive-ion mode (Table 2-4). The

ions could easily be identified because of the distinctive silver isotope distribution patterns (Figure 2-9) and also of the much stronger intensity of the ions (Figure 2-10).

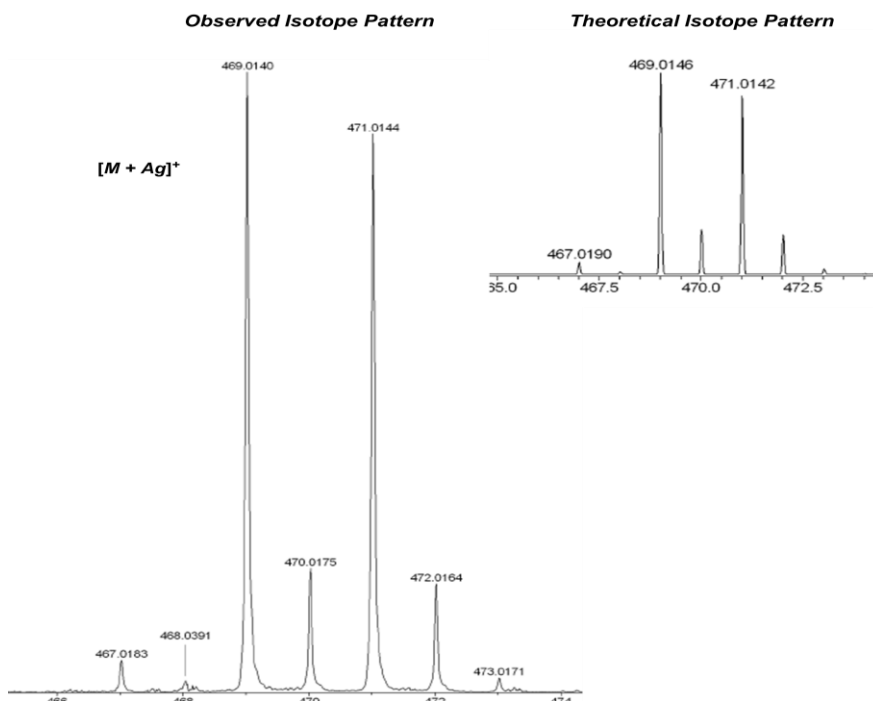


Figure 2-9: Partial ESI-MS of **21** showing the observed and theoretical isotope distribution patterns of $[M + Ag]^+$ ion

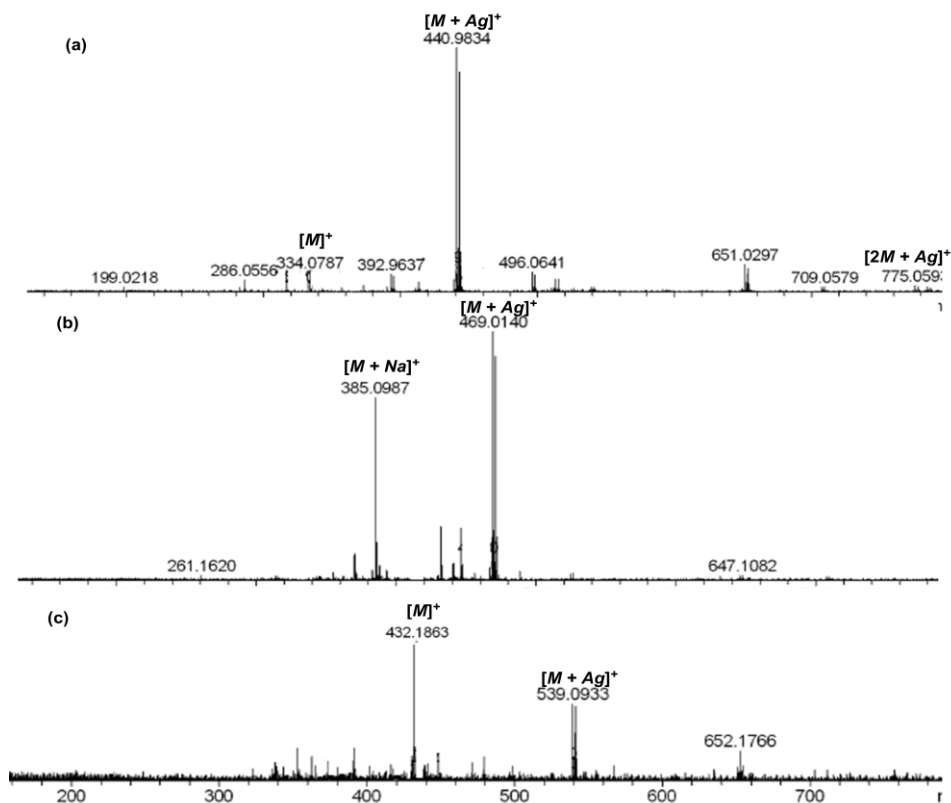


Figure 2-10: ESI-MS of (a) **20** (b) **21** (c) **22** with added aq. $AgNO_3$

Elemental Analysis: The composition of the yellow solid of **22** crystallised from CH₂Cl₂/MeOH/light petroleum spirits at -18 °C was found to be C 63.95; H 8.76 % consistent with the calculated values of C 63.87; H 8.63 %. Since the primary phosphanes **20** and **21** could not be satisfactorily purified (i.e. **20**: calcd. for C₁₆H₂₃Fe₁P₁O₂: C 57.49; H 6.94; N 0.00 %; found: C 58.84; H 6.73; N < 0.2 %; **21**: calcd. for C₁₈H₂₇Fe₁P₁O₂: C 59.67; H 7.52; N 0.00 %; found: C 62.48; H 7.90; N < 0.2 %), their microanalytical data could not be obtained.

2.2.2.3 Synthesis of Fc(CH₂)_nPH₂ (n = 4 (**14**), 6 (**15**), 11 (**16**))

The hydroxymethyl phosphanes **20**, **21** and **22** were heating to reflux with an equimolar quantity of Na₂S₂O₅ in a two-solvent system consisting of distilled H₂O and light petroleum spirits⁷⁸ in air or under an N₂ atmosphere for 3 h. After the subsequent work-ups, removal of the solvent from the organic phase gave the desired primary phosphanes **14**, **15** and **16** as yellow-red oils in moderate to good yields (**14** 28 %; **15** 83 %; **16** 35 %). Distinctive phosphane odours were noted from the oils. The crude products were purified by chromatography on a preparative TLC plate, eluting with light petroleum spirits or a mixture of light petroleum spirits/Et₂O or CH₂Cl₂. The desired bands were collected and extracted with CH₂Cl₂. Removal of the CH₂Cl₂ gave purer **14**, **15** and **16** as yellow oils. The primary phosphane **14** was purified further by distillation under 10⁻⁶ torr at 65 °C for 12 h, and obtained as a red oil.

2.2.2.4 Characterisation of Fc(CH₂)_nPH₂ (n = 4 (**14**), 6 (**15**), 11 (**16**))

The primary phosphanes **14**, **15** and **16** were characterised by ³¹P, ¹H and ¹³C-{¹H} NMR and IR spectroscopy, ESI- and GC-MS. Microanalytical results were unsatisfactory for **15** (i.e. calcd. for C₁₆H₂₃Fe₁P₁: C 63.58; H 7.68 %; found: C 62.04; H 7.99 %) and **16** (i.e. calcd. for C₂₁H₃₃Fe₁P₁: C 67.73; H 8.94; N 0.00 %; found: C 71.08; H 9.36; N < 0.2 %). The primary phosphanes **15** and **16** could not be completely purified by chromatography on a preparative TLC plate or by

recrystallisation. The composition of the red oil obtained for **14** as above was found to be C 61.64, H 6.61 % which is consistent with the calculated values of C 61.34, H 6.99 %. The selected spectroscopic data for **14**, **15** and **16** are summarised in Table 2-6. The data for **1**⁷⁸ and $\text{Fc}(\text{CH}_2)_2\text{PH}_2$ **23**⁷⁹ adopted from the respective literature are also included in the table for comparative purposes.

Table 2-6: Selected spectroscopic data for $\text{Fc}(\text{CH}_2)_n\text{PH}_2$ ($n = 1$ **1**, 2 **23**, 4 **14**, 6 **15**, 11 **16**)

	1 ⁷⁸	23 ⁷⁹	14	15	16
IR / $\nu \text{ cm}^{-1}$	2285s	2294m	2289s	2283m	2290m
³¹ P NMR / δ ppm	-129.1 (t, ¹ J _{PH} = 194 Hz)	-135.8 (t, ¹ J _{PH} = 195 Hz)	-136.9 (t, ¹ J _{PH} = 194 Hz)	-136.5 (t, ¹ J _{PH} = 195 Hz)	-136.7 (t, ¹ J _{PH} = 195 Hz)
¹ H NMR / δ ppm	2.9 (d of t, ¹ J _{PH} = 192, ³ J _{HH} = 8 Hz)	2.7 (d of t, ¹ J _{PH} = 194, ³ J _{HH} = 7 Hz)	2.7 (d of t, ¹ J _{PH} = 194, ³ J _{HH} = 7 Hz)	2.7 (d of t, ¹ J _{PH} = 195, ³ J _{HH} = 7 Hz)	2.7 (d of t, ¹ J _{PH} = 195, ³ J _{HH} = 7 Hz)
MS / m/z	232 [M] ⁺	246 [M] ⁺	274.056 [M] ⁺ (calcd. 274.056 for C ₁₄ H ₁₉ Fe ₁ P ₁)	302.088 [M] ⁺ (calcd. 302.088 for C ₁₆ H ₂₃ Fe ₁ P ₁)	372.165 [M] ⁺ (calcd. 372.166 for C ₂₁ H ₃₃ Fe ₁ P ₁)

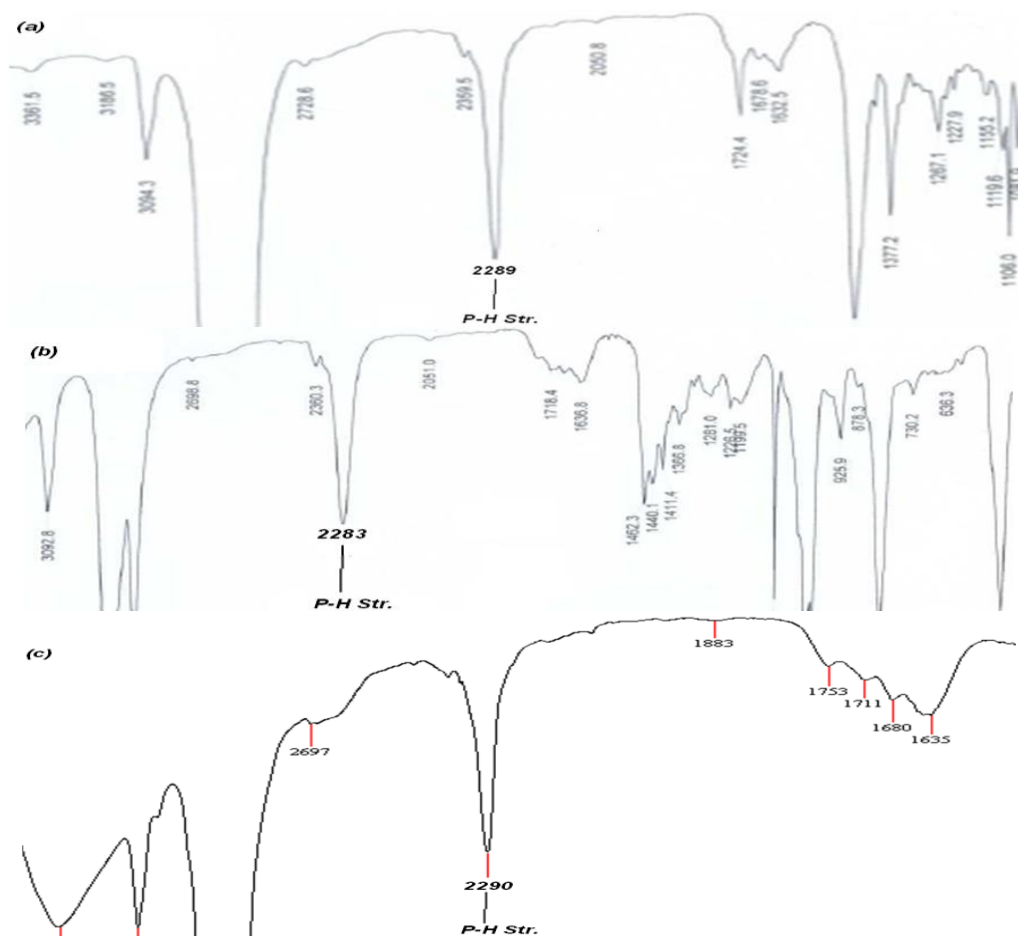


Figure 2-11: IR spectrum showing the ν P–H stretches for (a) **14**, (b) **15** and (c) **16**

IR Spectroscopy: The *P-H* stretches for $\text{Fc}(\text{CH}_2)_n\text{PH}_2$ ($n = 4$ **14**, 6 **15** or 11 **16**) were observed at 2289, 2283 and 2290 cm^{-1} , respectively, as a medium or strong band (Figure 2-11). The frequencies and intensity of the bands are consistent with the literature values for $\text{Fc}(\text{CH}_2)_n\text{PH}_2$ ($n = 1$ **1**⁷⁸ or 2 **23**⁷⁹) (cf. **1**: 2285 cm^{-1} ; **23**: 2294 cm^{-1}) and also for the class of compounds concerned (cf. $2280 \pm 10 \text{ cm}^{-1}$)⁹.

ESI-Mass Spectrometry: The mass spectrometric data were obtained by ESI- and/or GC- mass spectrometry. ESI-MS was carried out using MeOH as a mobile phase. The molecular ions, $[M]^+$, were easily observed in positive ion mode at capillary exit voltage of 150 V (Table 2-6). The isotope distribution patterns were consistent with the theoretical ones (i.e. **15**: Figure 2-12).

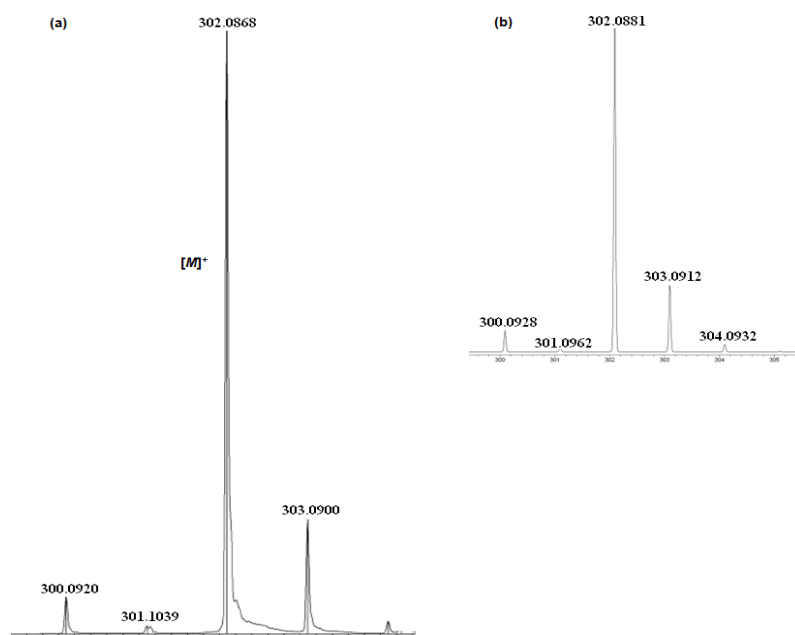


Figure 2-12: (a) Observed and (b) theoretical isotope pattern for the $[M]^+$ Ion of **15**

GC-MS showed the molecular ions of **14**, **15** and **16** with the ions corresponding to the fragmentation of the parent ion into $[\text{FcCH}_2]^+$, $[\text{CpFe}]^+$ and $[\text{Fe}]^+$ (Figure 2-13). The fragmentation of the parent ion into those ions has been observed for **23**⁷⁹ as well.

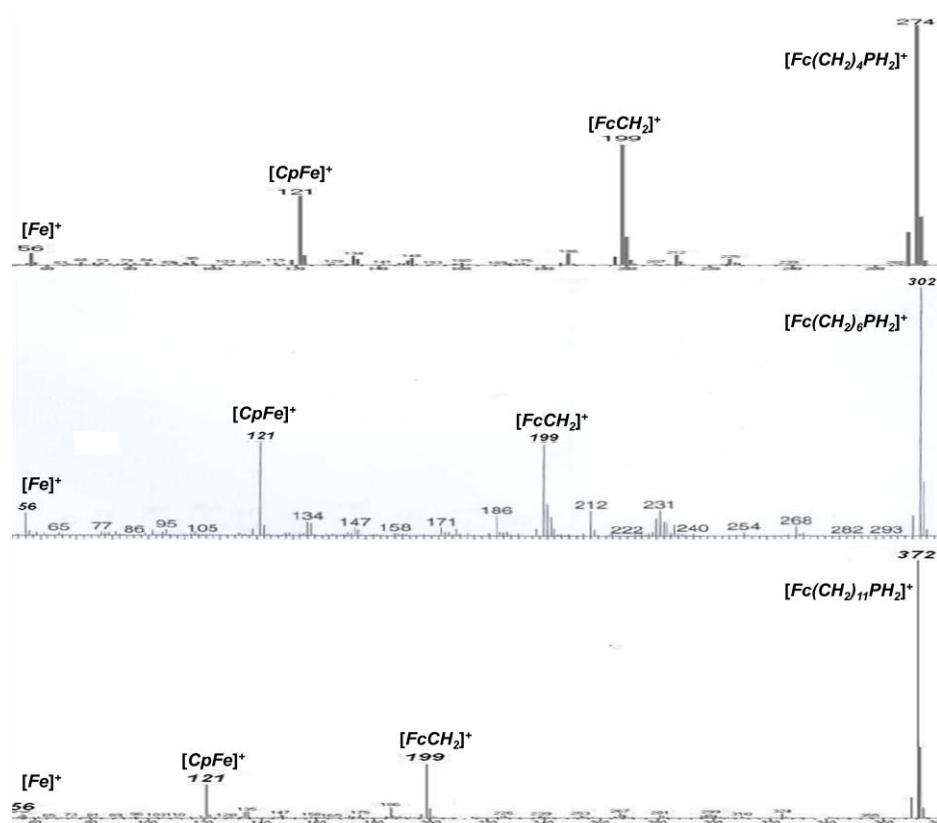


Figure 2-13: GC-MS of **14**, **15** and **16**

NMR Spectroscopy: The ^{31}P NMR signals for **14**, **15** and **16** appeared at $\sim \delta -136$ ppm as triplets with $^1J_{PH}$ coupling constants of ~ 194 Hz. The chemical shifts and $^1J_{PH}$ coupling constants are consistent with the literature values for **1**⁷⁸ and **23**⁷⁹ (Table 2-6). The signals were shifted further upfield by $\sim \delta 7$ ppm than that for **1** (cf. $\delta -129.1$ ppm)⁷⁸ which is consistent with the absence of deshielding effect from ferrocene in **14**, **15** and **16** due to the greater distance from the phosphorus. The signals are the same as that for **23** (cf. $\delta -135.8$ ppm)⁷⁹, suggesting that the deshielding effect of ferrocene becomes negligible beyond 2 σ -bonds. The $^1J_{PH}$ coupling constant was consistent with that for **1** and **23** and also for the class of compounds concerned⁹.

In the ^1H NMR spectra, the phosphane proton signal for **14**, **15** and **16** appeared at $\delta 2.7$ ppm which is expected considering the same surrounding chemical environments around the protons. The chemical shift was the same as that for **23**⁷⁹. It was, however, slightly shifted upfield by $\delta 0.2$ ppm than that for **1**⁷⁸ which may be expected due to

the lack of deshielding effect from ferrocene. The $^1J_{PH}$ and $^3J_{HH}$ coupling constants of 194 – 5 and 7 Hz, respectively, also agree with the literature values for **1**⁷⁸ and **23**⁷⁹.

In the $^{13}\text{C}\{-^1\text{H}\}$ NMR spectra, the $^{1,2,3}J_{PC}$ couplings were also observed for the respective carbon signals. The assignments of the chemical shifts were made according to the 2-D NMR data (Table 2-7). The selected $^{1,2,3}J_{CH}$ and $^3J_{HH}$ correlations observed in the respective HMBC, HSQC and COSY NMR experiments are shown in Figure 2-14. For atom labelling, see Scheme 2-8. Attempts to grow single crystals of the primary phosphanes by fractional recrystallisation or sublimation were also unsuccessful.

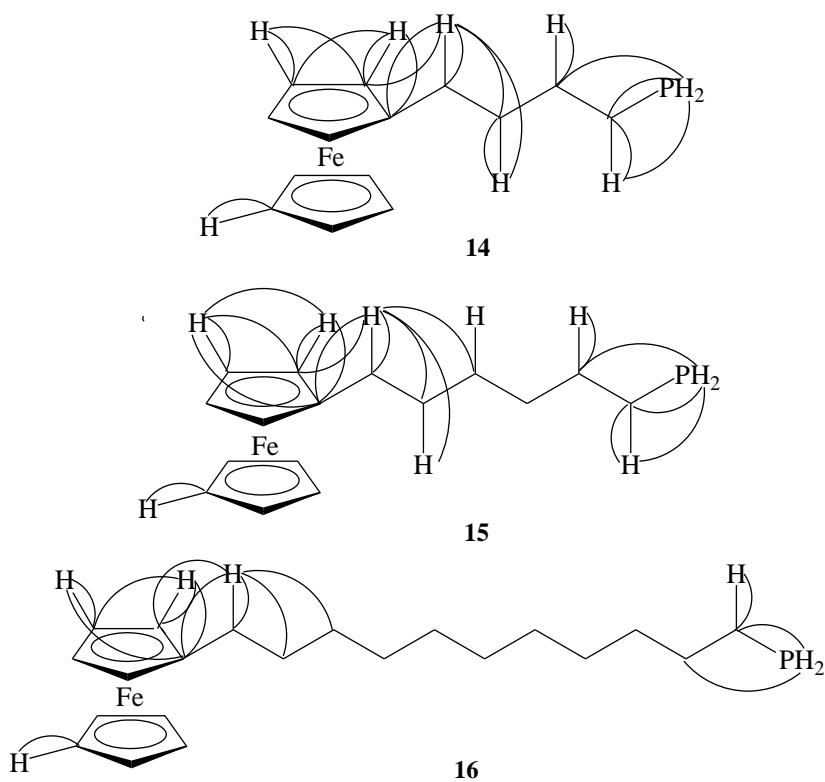


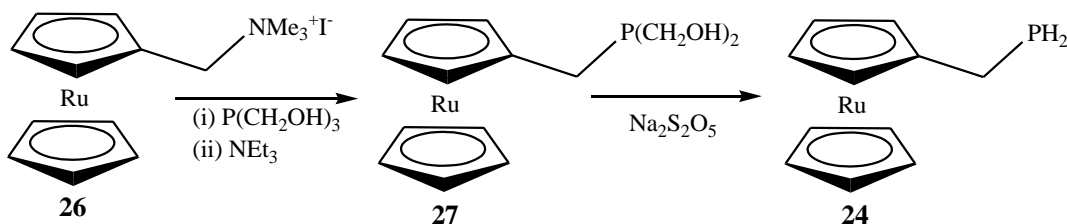
Figure 2-14: Selected $^{1,2,3}J_{CH}$ and $^3J_{HH}$ correlations observed for **14**, **15** and **16** in the HMBC, HSQC and COSY NMR experiments

Table 2-7: ^1H , ^{13}C and ^{31}P NMR chemical shifts for **14**, **15** and **16**

δ / ppm	14	15	16
^1H NMR			
$H_{2,3}$	4.05 (unresolved m, 4 H)	4.05 (d, $^3J_{\text{HH}} = 2$ Hz, 4 H)	4.04 (d, $^3J_{\text{HH}} = 2$ Hz, 4 H)
H_4	4.09 (s, 5 H)	4.09 (s, 5 H)	4.09 (s, 5 H)
H_5	2.3 (t, $^3J_{\text{HH}} = 7$ Hz, 2 H)	2.3 (t, $^3J_{\text{HH}} = 8$ Hz, 2 H)	2.3 (t, $^3J_{\text{HH}} = 8$ Hz, 2 H)
H_{6-15}	1.5 – 1.6 (unresolved m, 6 H)	1.3 – 1.6 (unresolved m, 10 H)	1.3 – 1.5 (m, 22 H)
PH_2	2.7 (d of t, $^1J_{\text{PH}} = 194$, $^3J_{\text{HH}} = 7$ Hz, 2 H)	2.7 (d of t, $^1J_{\text{PH}} = 195$, $^3J_{\text{HH}} = 7$ Hz, 2 H)	2.7 (d of t, $^1J_{\text{PH}} = 195$ Hz, $^3J_{\text{HH}} = 7$ Hz, 2 H)
$^{13}\text{C}\{-^1\text{H}\}$ NMR			
C_1	89.1 (C, s)	89.4 (C, s)	89.6 (C, s)
C_2	68.1 (CH, s)	68.1 (CH, s)	68.0 (CH, s)
C_3	67.1 (CH, s)	67.0 (CH, s)	67.0 (CH, s)
C_4	68.5 (CH, s)	68.5 (CH, s)	68.4 (CH, s)
C_5	29.2 (CH ₂ , s)	29.2 (CH ₂ , s)	29.2 (CH ₂ , s)
C_6	Not applicable.	29.6 (CH ₂ , s)	29.6 (CH ₂ , s)
C_7	Not applicable.	31.0 (CH ₂ , s)	31.1 (CH ₂ , s)
C_{8-12}	Not applicable.	Not applicable.	29.6 (CH ₂ , s)
C_{13}	32.8 (CH ₂ , d, $^3J_{\text{PC}} = 3$ Hz)	32.9 (CH ₂ , d, $^3J_{\text{PC}} = 4$ Hz)	32.9 (CH ₂ , d, $^3J_{\text{PC}} = 3$ Hz)
C_{14}	32.0 (CH ₂ , d, $^2J_{\text{PC}} = 6$ Hz)	30.5 (CH ₂ , d, $^2J_{\text{PC}} = 6$ Hz)	30.5 (CH ₂ , d, $^2J_{\text{PC}} = 6$ Hz)
C_{15}	13.7 (CH ₂ , d, $^1J_{\text{PC}} = 7$ Hz)	13.7 (CH ₂ , d, $^1J_{\text{PC}} = 7$ Hz)	13.7 (CH ₂ , d, $^1J_{\text{PC}} = 7$ Hz)
^{31}P NMR			
	-136.9 (PH_2 , t of unresolved m, $^1J_{\text{PH}} = 194$ Hz)	-136.5 (PH_2 , t of p, $^1J_{\text{PH}} = 195$; $^2J_{\text{PH}} = 6$ Hz)	-136.7 (PH_2 , t of p, $^1J_{\text{PH}} = 195$; $^2J_{\text{PH}} = 6$ Hz)

2.2.2.5 Synthesis of RcCH_2PH_2 (**24**)

To investigate whether the stabilisation effect of a $\text{Fc}(\text{CH}_2)_n$ moiety incorporated at the hydride centre of air-sensitive primary phosphanes was unique to ferrocene or would extended to other metallocenes, the title compound was prepared. Ruthenocenylmethyl phosphane **24** was prepared analogously to the corresponding ferrocenyl phosphanes⁷⁸. Ruthenocene **25**⁹⁹ and $[\text{RcCH}_2\text{NMe}_3]^+\text{I}^-$ **26**^{92, 100} were prepared using the literature methods. Scheme 2-3 describes the synthesis of **24**.

Scheme 2-3: Synthesis of **24**

Compound **26** was heated to reflux with excess $\text{P}(\text{CH}_2\text{OH})_3$ in MeOH under an N_2 atmosphere for > 20 h and stirred with NEt_3 in distilled H_2O and Et_2O for 1 h. After separating and washing the organic phase with distilled H_2O , removal of the solvent

from the organic phase gave the desired hydroxymethyl phosphane **27** as a pale-yellow oil in moderate yield (10 %). The entire yield of the crude hydroxymethyl phosphane **27** was heating to reflux with Na₂S₂O₅ in a two-solvent system containing distilled H₂O and light petroleum spirits for 3 h under an N₂ atmosphere. After separating, washing and drying the organic phase, removal of the solvent gave the desired primary phosphane **24** as a pale-yellow oil in moderate yield (43 %). The distinctive phosphane odour was noted from the oil. The crude product was purified by chromatography on a preparative TLC plate, eluting with a 1 : 1 mixture of CH₂Cl₂/light petroleum spirits. The pale yellow fraction at R_f 0.76 was collected and extracted with CH₂Cl₂. Removal of the solvent from the extract under reduced pressure gave purer **24** as a pale-yellow oil in poor yield (10 %). The yield may have been improved if the hydroxymethyl phosphane **27** had been purified and the stoichiometric amount of each reagent had been used in the reduction reaction.

2.2.2.6 Characterisation of RcCH₂PH₂ (**24**)

The title compound was characterised by IR and NMR spectroscopy and ESI-MS. The *P-H* stretch was observed at 2290 cm⁻¹ as a medium intensity peak (Figure 2-15). The frequency is consistent with that for the corresponding ferrocenyl primary phosphane, FcCH₂PH₂ (**1**), and also those for the ferrocenyl analogues with extended alkyl spacers, Fc(CH₂)_nPH₂ (n = 4 (**14**), 6 (**15**) or 11 (**16**)) (Table 2-6).

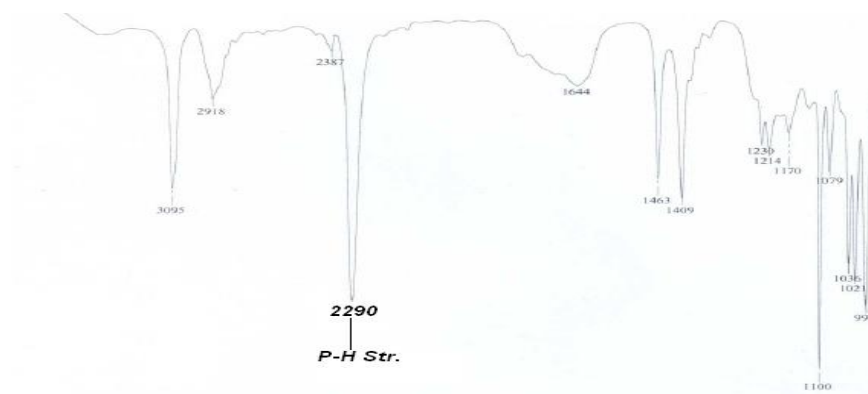


Figure 2-15: Partial IR spectrum of **24**

The ^{31}P NMR signal of **24** appeared at $\delta -132.5$ ppm as a triplet with a $^1J_{\text{PH}}$ coupling constant of 193 Hz. The signal was shifted further upfield by $\delta 3$ ppm than that for the corresponding ferrocenyl primary phosphane **1**⁷⁸, suggesting that the phosphorus in **24** is more shielded than that in **1**. The $^1J_{\text{PH}}$ coupling constant was consistent with **1**⁷⁸ and also with those for **14**, **15**, **16** and **23**⁷⁹, (Table 2-6). In the ^1H NMR spectrum, the phosphane proton signal appeared at $\delta 2.9$ ppm as a doublet of triplets with a $^1J_{\text{PH}}$ and $^3J_{\text{HH}}$ coupling constant of 194 and 7 Hz, respectively. The chemical shift was consistent with that for **1** and further downfield by $\delta 0.2$ ppm compared to those for **14**, **15**, **16** and **23**⁷⁹ which is consistent with the shift in **1** due to the deshielding effect from the metallocene. The $^1J_{\text{PH}}$ and $^3J_{\text{HH}}$ coupling constants are also consistent with those for the ferrocenyl analogues **1**, **14**, **15**, **16** and **23**⁷⁹. The Cp proton signals were shifted further downfield by an average of $\delta 0.5$ ppm than the corresponding signals for the corresponding ferrocenyl analogue **1**. The Cp proton signals for **26**¹⁰⁰ were also shifted further downfield by about the same amount as for the corresponding signals for the ferrocenyl analogue **6**. In the $^{13}\text{C}\{-^1\text{H}\}$ NMR spectrum, the $^{1,3}J_{\text{PC}}$ couplings were observed for the respective carbon signals with a $^1J_{\text{PC}}$ and $^3J_{\text{PC}}$ coupling constant of 8 and 3 Hz, respectively. The $^2J_{\text{PC}}$ coupling on the C_1 carbon was not observed. The chemical shifts were assigned according to the 2-D NMR data and listed in Table 2-8. The selected $^{1,2,3}J_{\text{CH}}$ correlations observed in the respective HMBC and HSQC NMR experiments are shown in Figure 2-16.

Table 2-8: ^1H , ^{13}C and ^{31}P NMR chemical shifts for **24**

δ / ppm	24
^1H NMR	
H_2	4.57 (t, $^3J_{\text{HH}} = 2$ Hz, 2 H)
H_3	4.46 (t, $^3J_{\text{HH}} = 2$ Hz, 2 H)
H_4	4.56 (s, 5 H)
H_5	2.5 (m, $^3J_{\text{HH}} = 4$ Hz, 2 H)
PH	2.9 (d of t, $^1J_{\text{PH}} = 194$, $^3J_{\text{HH}} = 7$ Hz, 2 H)
$^{13}\text{C}\{-^1\text{H}\}$ NMR	
C_1	92.6 (C)
C_2	70.9 (CH, d, $^3J_{\text{PC}} = 3$ Hz)
C_3	69.5 (CH, s)
C_4	70.7 (CH, s)
C_5	14.0 (CH ₂ , d, $^1J_{\text{PC}} = 8$ Hz)
^{31}P NMR	
P	-132.5 (t, $^1J_{\text{PH}} = 193$ Hz)

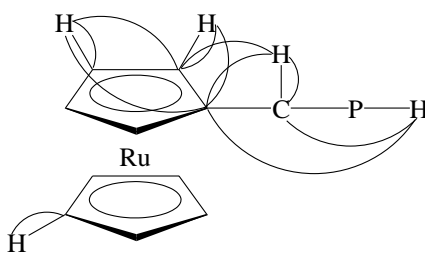


Figure 2-16: Selected $^{1,2,3}J_{CH}$ correlations observed for **24** in the HMBC and HSQC NMR experiments

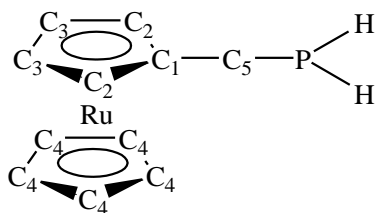


Figure 2-17: Atom labelling used in NMR assignments for **24**; hydrogen atoms are numbered according to the carbon to which they are bonded

Mass spectrometric data could be obtained by GC- and ESI-MS. In the EI mass spectrum, the fragmentation of the molecular ion, $[M]^+$, into $[RcCH_2]^+$ and $[CpRu]^+$, analogously to those of the ferrocenyl primary phosphanes **1**, **14**, **15**, **16** and **23**, could also be observed (Figure 2-18).

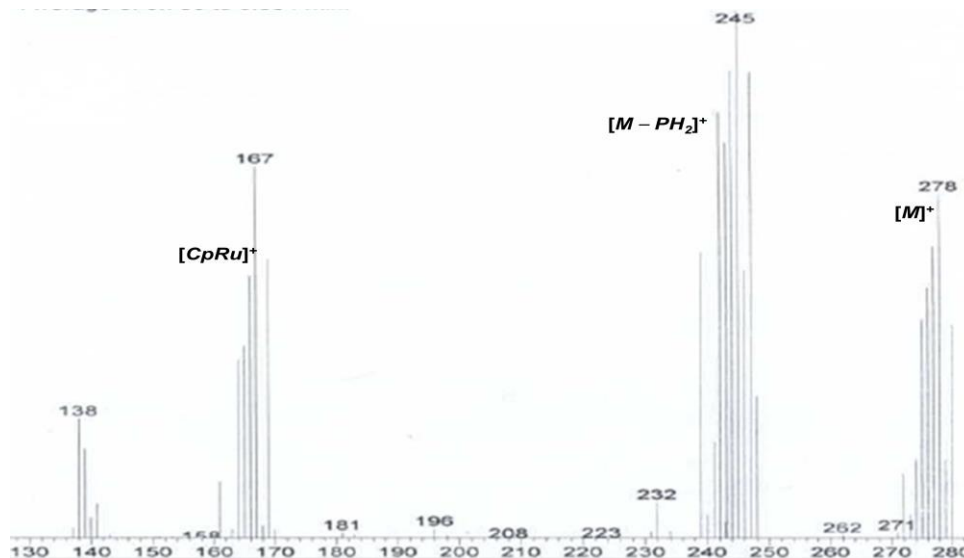


Figure 2-18: EI-mass spectrum of **24**

ESI-MS was carried out using MeOH as a mobile phase at capillary exit voltage of 150 V. Although the molecular ion, $[M]^+$, could not be observed, an ion which may

be assigned as $[M - PH_2]^+$ (m/z observed 244.989; calcd. 244.989 for $C_{11}H_{11}Ru_1$) was observed in positive ion mode (Figure 2-19).

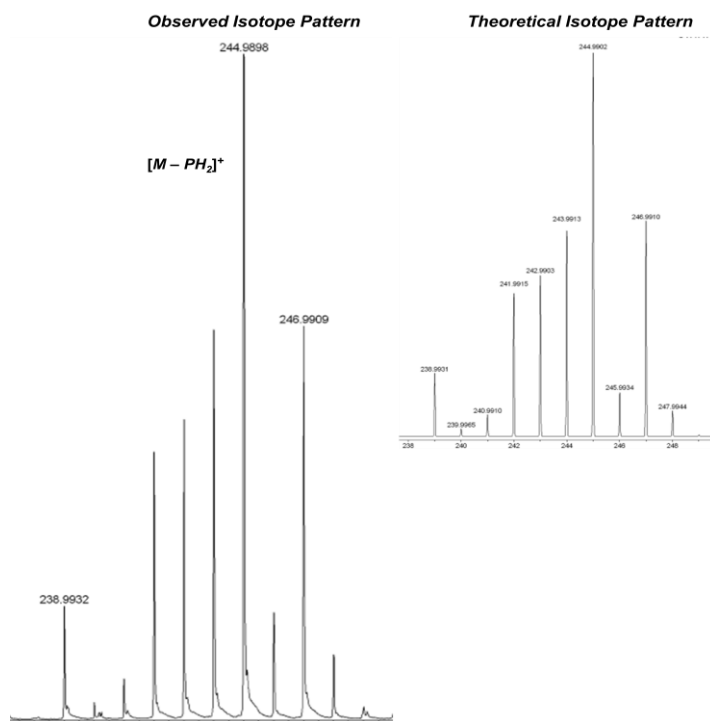


Figure 2-19: Partial ESI-MS of **24** showing the observed and theoretical $[M - PH_2]^+$ ions ($M = 24$)

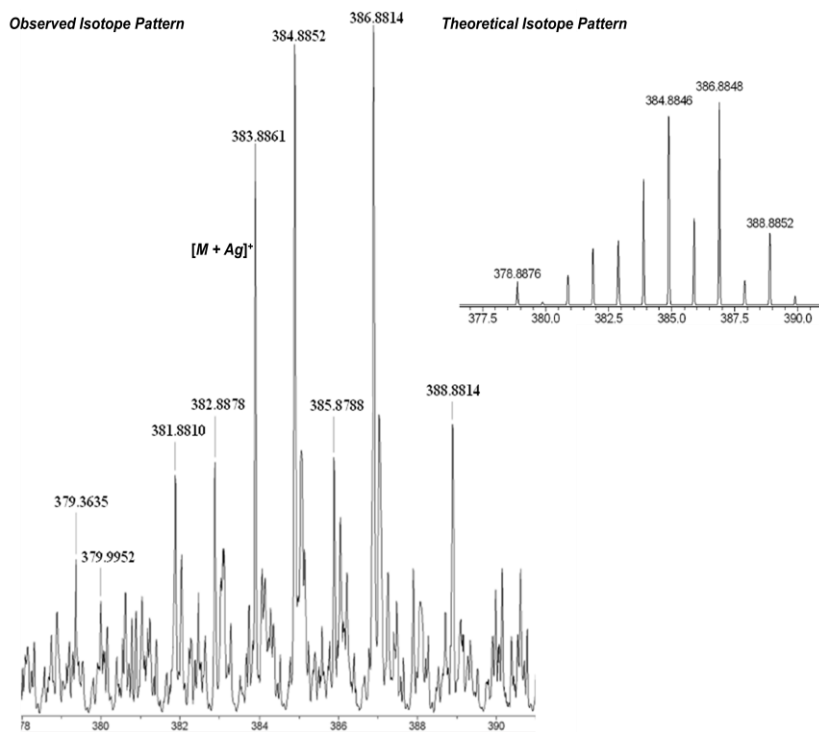


Figure 2-20: Partial ESI-MS of **24** showing the observed and theoretical $[M + Ag]^+$ ion ($M = 24$)

When a small quantity of aqueous AgNO₃ was added, the silver adduct formed and was observed as $[M + Ag]^+$ (m/z observed 384.885; calcd. 384.884 for C₁₁H₁₃Ag₁P₁Ru₁) at capillary exit voltage of 130 V in positive ion mode (Figure 2-20).

Attempts to obtain microanalytical and X-ray crystallographic structural data for **24** were unsuccessful. Satisfactory samples for the analyses could not be obtained by chromatography on a preparative TLC plate or crystallisation (i.e. calcd. for C₁₁H₁₃P₁Ru₁: C 47.65; H 4.73 %; found: C 45.03; H 4.44%).

2.2.2.7 Isolation and Partial Characterisation of R_cCH₂P(O)(CH₂OH)H (**28**)

A white solid was isolated after removal of the solvent from the aqueous phase separated from the reaction mixture in the synthesis of **24**. The white solid was tentatively characterised as **28** according to its NMR data. In the ³¹P NMR spectrum, the ³¹P NMR signal was observed at δ 35.7 ppm as a doublet of triplets with a ¹J_{PH} and ²J_{PH} coupling constant of 467 and 14 Hz, respectively. The chemical shift and coupling constant are consistent with a secondary phosphane oxide and also comparable to those for the phosphinic acids, FcCH₂P(O)(CH₂OH)OH⁷⁸ **29**, (³¹P NMR: δ 37.4 ppm in D₂O; ²J_{PH} = 15 Hz), FcCH₂P(O)(OH)H **36** (³¹P NMR: δ 36.9 ppm in CDCl₃; ¹J_{PH} = 557, ²J_{PH} = 17 Hz (see 2.2.3.4)) and the phosphane oxide, FcCH₂P(O)H₂ **30**, (³¹P NMR: δ 9.5 ppm in CDCl₃; ¹J_{PH} = 470, ³J_{HH} = 16 Hz (see 2.2.3.2)).

The Cp and CH₂ proton and carbon signals were observed in the same region for **24** and also comparable to those for [R_cCH₂NMe₃]I **26**¹⁰⁰. According to the 2-D NMR data, the structure in Figure 2-21 was proposed. The ^{1,2,3}J_{CH} and ³J_{HH} correlations observed in the respective HMBC, HSQC and HETCOR NMR experiments are shown in Figure 2-22 and the assignments of the chemical shifts are listed in Table

2-9. No attempt was made to further characterise the compound as it was only a by-product and also obtained in a minor amount (0.05 g, 5 % yield).

Table 2-9: ^1H , ^{13}C and ^{31}P NMR chemical shifts for **29**

δ / ppm	29
^1H NMR	
H_2	4.7 (unresolved m, 2 H)
H_3	4.5 (d, $^3J_{\text{HH}} = 1$ Hz, 2 H)
H_4	4.6 (s, 5 H)
H_5	3.0 (d of t, $^3J_{\text{HH}} = 13$; $^4J_{\text{HH}} = 4$ Hz, 2 H)
PH	6.8 (d of unresolved m, $^1J_{\text{PH}} = 467$ Hz, 1 H)
CH_2OH	4.0 (m, 2 H)
^{13}C - $\{^1\text{H}\}$ NMR	
C_1	80.0 (C)
C_2	71.9 (CH)
C_3	70.6 (CH)
C_4	71.2 (CH)
C_5	26.7 (CH ₂)
CH_2OH	58.7 (d, $^1J_{\text{PC}} = 74$ Hz)
^{31}P NMR	
PH	35.7 (d of m, $^1J_{\text{PH}} = 467$; $^2J_{\text{PH}} = 14$ Hz)

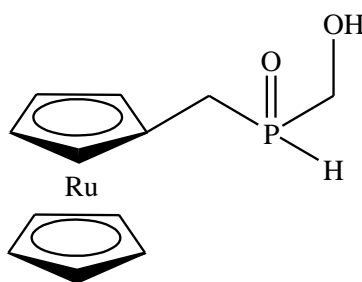


Figure 2-21: Proposed Structure of **29**

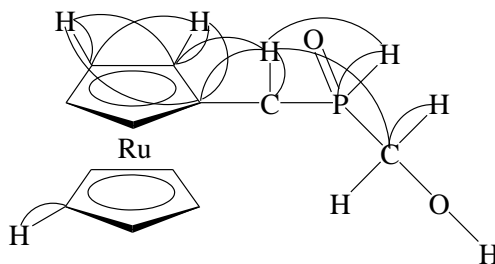
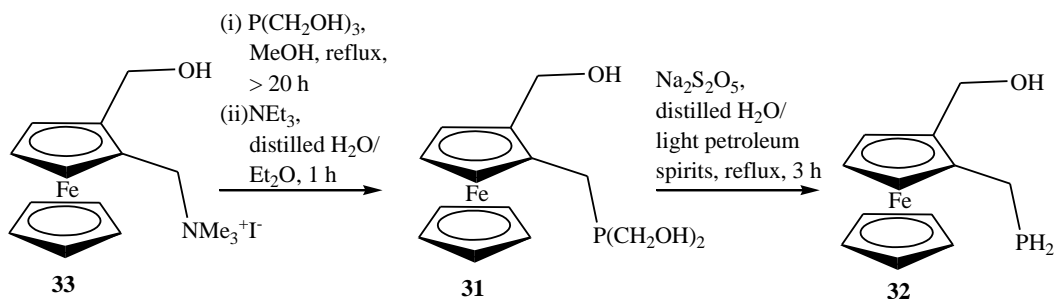


Figure 2-22: $^{1,2,3}J_{\text{CH}}$ and $^3J_{\text{HH}}$ correlations observed for **29** in the HMBC, HSQC and HETCOR NMR experiments

2.2.2.8 Synthesis and Characterisation of $[\text{CpFeC}_5\text{H}_3(\text{CH}_2\text{OH})\{\text{CH}_2\text{P}(\text{CH}_2\text{OH})_2\}]$ (31) and $[\text{CpFeC}_5\text{H}_3(\text{CH}_2\text{OH})(\text{CH}_2\text{PH}_2)]$ (32)

Compound **32** was synthesised analogously to **1**⁷⁸. Scheme 2-4 shows the synthesis of **32** via the corresponding hydroxymethyl primary phosphane **31**.



Scheme 2-4: Synthesis of **32** via **31**

Compound **33**¹⁰¹ was heated to reflux with $\text{P}(\text{CH}_2\text{OH})_3$ generated *in situ* from $[\text{P}(\text{CH}_2\text{OH})_4]\text{Cl}$ and KOH , in MeOH for 20 h under an N_2 atmosphere and the solvent was removed under reduced pressure. After stirring the residue with NEt_3 in distilled H_2O and Et_2O for 1 h, the organic phase was separated, washed with distilled H_2O and dried. Removal of the solvent from the organic phase gave the hydroxymethyl phosphane **31** as a mixture of a crystalline yellow solid and oil in good yield (88 %). The hydroxymethyl phosphane **31** was partially characterised by ^{31}P , ^1H and $^{13}\text{C}\{-^1\text{H}\}$ NMR spectroscopy and used as obtained without further purification.

The ^{31}P NMR signal appeared at $\delta -19.3$ ppm as a septet with a $^2J_{\text{PH}}$ coupling constant of 6 Hz. The chemical shift was consistent with the literature value of $\delta -19.3$ ppm for the analogue $\text{FcCH}_2\text{P}(\text{CH}_2\text{OH})_2$ **8**⁹². Since the $^2J_{\text{PH}}$ coupling constant was not reported in the literature⁹², a direct comparison of the $^2J_{\text{PH}}$ coupling constants could not be made. The ^1H and ^{13}C NMR chemical shifts are comparable to those for **8**⁹². In the $^{13}\text{C}\{-^1\text{H}\}$ NMR spectrum, the $^{1,2,3}J_{\text{PC}}$ couplings were observed for the respective carbon signals (Table 2-10). The assignments were made according to the 2-D data and also by analogy to those for **8**⁹² (Table 2-10). The unambiguous assignment for $\text{C}_{2\text{a}}$ could not be made due to the overlap of the signals. The $^{1,2,3}J_{\text{CH}}$ correlations observed in the HMBC and HSQC experiment are shown in Figure 2-23.

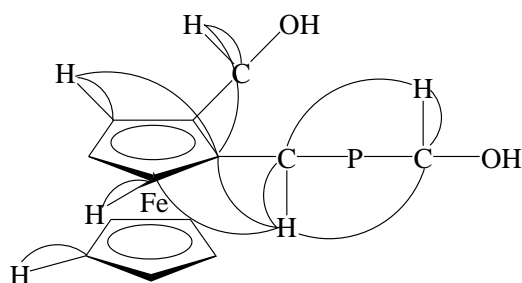


Figure 2-23: $^{1,2,3}J_{CH}$ correlations observed for **31** in the HMBC and HSQC experiments

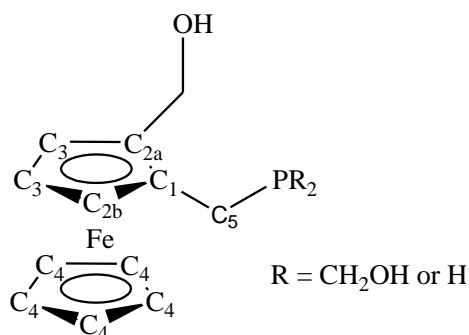


Figure 2-24: Atom labelling used in NMR assignments for **31** and **32**; hydrogen atoms are numbered according to the carbon to which they are bonded

Table 2-10: 1H , ^{13}C and ^{31}P NMR chemical shifts for **31**

δ / ppm		31
1H NMR		
$H_{2b,3}$	4.05	(unresolved m, 3 H)
H_4	4.07	(s, 5 H)
H_5	3.1	(p of d, $^4J_{HH} = 15$; $^2J_{PH} = 4$, Hz, 2 H)
\underline{CH}_2OH	4.26	(d, $^4J_{HH} = 2$ Hz, 2 H)
\underline{PCH}_2OH	4.29	(m, 4 H)
^{13}C - $\{^1H\}$ NMR		
C_1	82.9	(C, d, $^2J_{PC} = 8$ Hz)
C_{2a}		Could not be assigned.
C_{2b}	69.9	(CH, d, $^3J_{PC} = 4$ Hz)
C_3	66.4	(CH, s)
C_4	70.0	(CH, s)
C_5	16.6	(CH ₂ , d, $^1J_{PC} = 9$ Hz)
\underline{CH}_2OH	68.6	(CH ₂ , d, $^3J_{PC} = 3$ Hz)
\underline{PCH}_2OH	60.9	(CH ₂ , d, $^1J_{PC} = 26$ Hz)
^{31}P NMR		
P	-19.3	(seven-line multiplet, $^2J_{PH} = 6$ Hz)

The crude hydroxymethyl phosphane **31** was heated to reflux with $Na_2S_2O_5$ in a two-solvent system consisting of distilled H_2O and light petroleum spirits for 3 hours under an N_2 atmosphere. After separating and washing the organic phase with distilled H_2O , removal of the solvent gave the desired primary phosphane **32** as a yellow oil in moderate yield (56 %). The distinctive phosphane odour was noted from the yellow oil.

The primary phosphane **32** was characterised by IR and NMR spectroscopy. The $P-H$ stretch was observed at 2291 cm^{-1} as a medium intensity band (Figure 2-25). The frequency is consistent with those for the primary phosphanes **1**, **14**, **15**, **16** and **23** (see 2.2.2.3 for the frequencies).

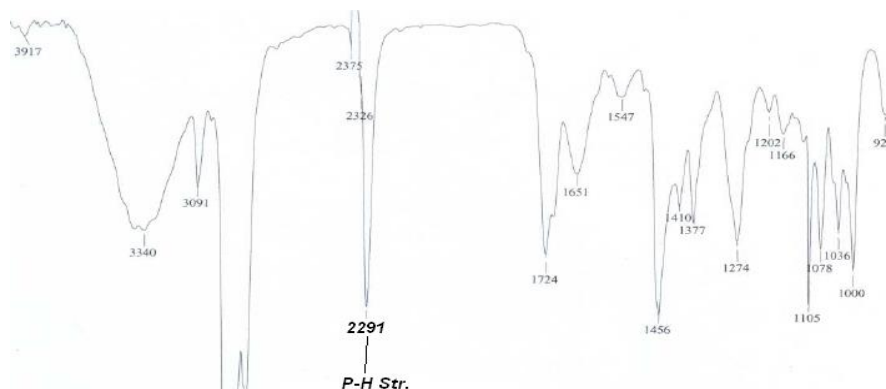


Figure 2-25: IR spectrum of **32**

The ^{31}P NMR signal was observed at $\delta -129.8$ ppm as a triplet with a $^1J_{PH}$ coupling constant of 197 Hz. The chemical shift and $^1J_{PH}$ coupling constant are consistent with those for the ferrocenyl primary phosphane **1** and also for the class of compounds concerned⁹. In the ^1H NMR spectrum, the phosphane proton signal appeared at $\delta 2.9$ ppm as a doublet of multiplets with a $^1J_{PH}$ and $^3J_{HH}$ coupling constant of 200 and 5 Hz, respectively, which also agree with those for **1**. In the $^{13}\text{C}\{-^1\text{H}\}$ NMR spectrum, the $^{1,2,3}J_{CP}$ couplings with constants of 9, 8, 1 Hz, respectively, were also observed for the respective carbon signals. The chemical shifts were assigned according to the 2-D data (Table 2-11). The definite assignment of the C_{2a} carbon signal could not be made due to the overlap of the signals. The selected $^{1,2,3}J_{CH}$ correlations observed in the respective HMBC and HSQC NMR experiments are shown in Figure 2-26.

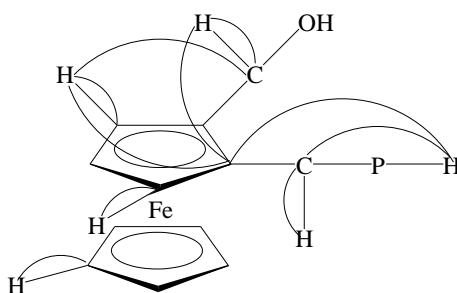


Figure 2-26: Selected $^{1,2,3}J_{CH}$ correlations observed for **32** in the HMBC and HSQC NMR experiments

Table 2-11: 1H , ^{13}C and ^{31}P NMR chemical shifts for **32**

δ / ppm	32
1H NMR	
H_{2b}	4.07 (d, $^3J_{HH} = 1$ Hz, 1 H)
H_3	4.01 (t, $^3J_{HH} = 2$ Hz, 2 H)
H_4	4.06 (s, 5 H)
H_5	2.7 (m, 2 H)
CH_2OH	4.1 (m, $^4J_{HH} = 6$ Hz, 2 H)
PH_2	2.9 (d of m, $^1J_{PH} = 200$; $^3J_{HH} = 5$ Hz, 2 H)
^{13}C - $\{^1H\}$ NMR	
C_1	86.9 (C, d, $^2J_{PC} = 8$ Hz)
C_{2a}	Could not be assigned.
C_{2b}	69.6 (CH, d, $^3J_{PC} = 1$ Hz)
C_3	65.7 (CH, s)
C_4	69.5 (CH, s)
C_5	12.9 (CH ₂ , d, $^1J_{PC} = 9$ Hz)
CH_2OH	67.4 (CH ₂)
^{31}P NMR	
PH_2	-129.8 (t, $^1J_{PH} = 197$ Hz)

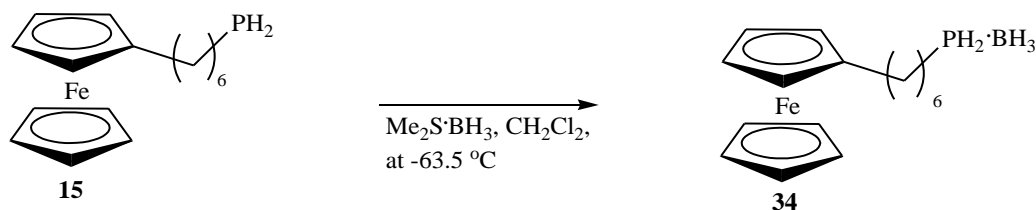
For atom labelling, see Figure 2-24.

Attempts to obtain mass spectrometric data by GC- and ESI-MS were unsuccessful. Neither the molecular ion nor silver adducts when a half drop of aqueous $AgNO_3$ was added could be observed. Satisfactory microanalytical data could also not be obtained. The attempts to purify the yellow oil by crystallisation from warm light petroleum spirits, cooling at -18 °C or by chromatography on a preparative TLC plate was unsuccessful and satisfactory microanalytical data could not be obtained (i.e. calcd. for $C_{12}H_{15}O_1P_1Fe_1$: C 54.98; H 5.77; N 0.00 %; found: C 59.30; H 7.74; N < 0.2 %). Since the compound has a CH_2OH group, purification by chromatography on a PLC plate was not very useful. A broad yellow coloured line containing the desired compound resulted on the plate upon elution with the solvent mixture probably due to H bonding formed between the H atom of the group and the O atom of the silicon dioxide. Therefore, satisfactory separation of each component of the sample could not be achieved. Since the found percentages of C and H atoms were higher than those

calculated, there might also have been a residual organic solvent such as petroleum spirits in the sample sent for elemental analysis.

2.2.2.9 Synthesis of $\text{Fc}(\text{CH}_2)_6\text{PH}_2\cdot\text{BH}_3$ (**34**)

Glueck *et al.*⁹⁰ reported that the ferrocenyl primary phosphane **1** forms a crystalline product upon reaction with $\text{Me}_2\text{S}\cdot\text{BH}_3$. Since it has been found to be difficult to grow a single crystal of the primary phosphanes prepared in this study, the present synthesis was carried out in order to obtain X-ray crystallographic structural data of one of the primary phosphanes as a borane complex. Scheme 2-5 illustrates the synthesis of **34**.



Scheme 2-5: Synthesis of **34**

The primary phosphane **15** was treated with $\text{Me}_2\text{S}\cdot\text{BH}_3$ in dry hexane at $-63.5\text{ }^\circ\text{C}$ under an N_2 atmosphere. Removal of the volatiles under reduced pressure, slowly warming up to room temperature, initially gave a yellow solid. During the further evacuation for 15 mins at room temperature, the yellow solid turned to a yellow oil. Slow recrystallisation of the yellow oil from hexane at $-18\text{ }^\circ\text{C}$ gave the desired borane complex **34** as orange needles, which were suitable for X-ray crystallographic structural determination, in moderate yield (26 %). The adduct was also stable in air at ambient temperature. Neither decomposition nor oxidation of the compound was noted upon handling or storing for at least 1 week in air at room temperature.

2.2.2.10 Characterisation of $\text{Fc}(\text{CH}_2)_6\text{PH}_2\cdot\text{BH}_3$ (**34**)

Satisfactory microanalytical data for the compound were obtained on the orange needles (Found: C 60.84; H 8.19 %; Calcd. C 60.75, H 8.29 %). The $P-H$ and $B-H$

stretches were observed as overlapping strong broad bands at around 2398 cm^{-1} (Figure 2-27). The increased frequency of the $P-H$ stretch from 2280 to 2398 cm^{-1} upon the addition of BH_3 was consistent with that observed for $\text{FcCH}_2\text{PH}_2\cdot\text{BH}_3$ ⁹⁰ **35**.

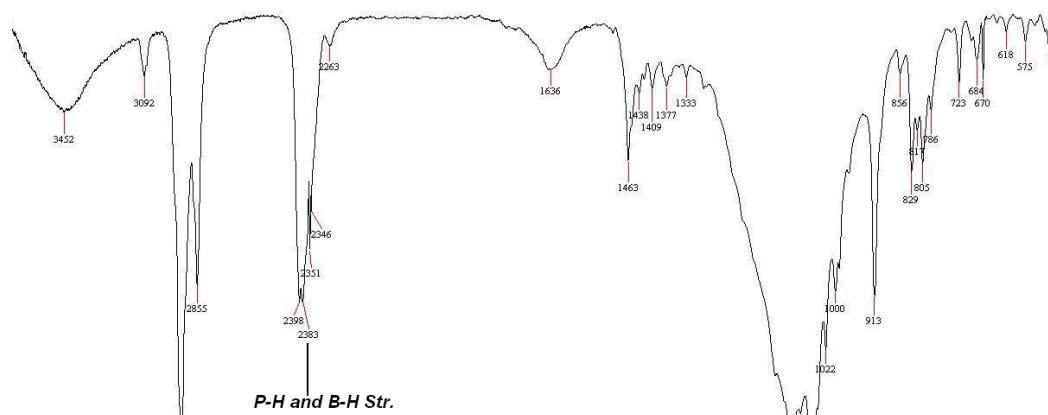


Figure 2-27: IR spectrum of **34**

ESI-MS was carried out in MeOH as a mobile phase with a drop of CH_2Cl_2 added to aid solubility. At a capillary exit voltage of 100 V, the molecular ion, $[M]^+$, (m/z observed 316.119; calcd. 316.120 for $\text{C}_{16}\text{H}_{26}\text{B}_1\text{Fe}_1\text{P}_1$) (Figure 2-28) and the sodium and potassium adducts, $[M + \text{Na}]^+$ (m/z observed 339.109; calcd. 339.111 for $\text{C}_{16}\text{H}_{26}\text{B}_1\text{Fe}_1\text{Na}_1\text{P}_1$) and $[M + \text{K}]^+$ (m/z observed 355.058; calcd. 355.084 for $\text{C}_{16}\text{H}_{26}\text{B}_1\text{Fe}_1\text{K}_1\text{P}_1$), respectively, were observed in the positive ion mode.

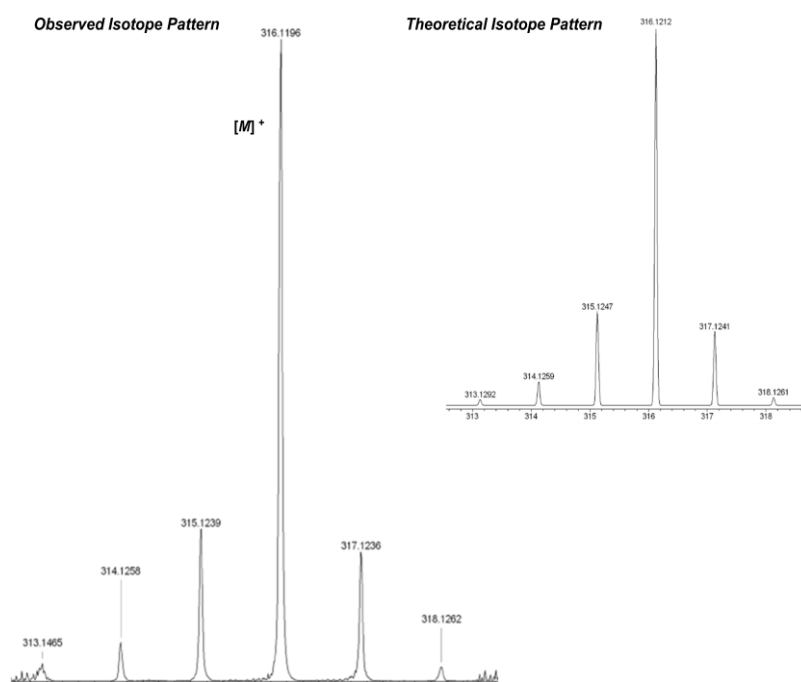


Figure 2-28: Partial ESI-MS of **34** showing the observed and theoretical $[M]^+$ ion ($M = \mathbf{34}$)

The ^{31}P NMR signal appeared at $\delta -52.3$ ppm as a broad triplet of unresolved multiplets with a $^1J_{PH}$ coupling constant of 362 Hz (Figure 2-29). The broadening comes from coupling to the boron atom of the ^{31}P NMR signal by addition of BH_3 , consistent with the description in the literature⁹⁰ for $\text{FcCH}_2\text{PH}_2\cdot\text{BH}_3$ **35**.

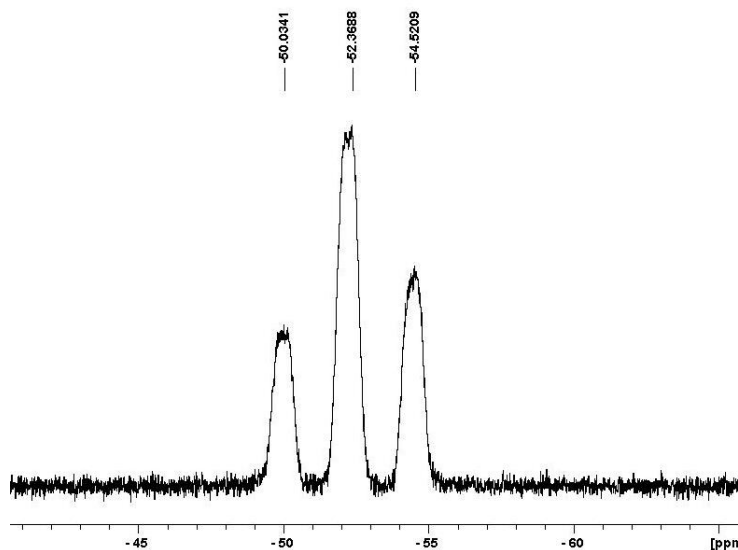


Figure 2-29: ^{31}P NMR spectrum of **34**

In the ^1H NMR spectrum, the phosphane proton signal appeared at $\delta 4.5$ ppm as a doublet of six-line multiplet with a $^1J_{PH}$ and $^3J_{HH}$ coupling constant of 360 and 1 Hz, respectively. The borane proton signal was observed at $\delta 1.4$ ppm as an unresolved multiplet. In the $^{13}\text{C}\{-^1\text{H}\}$ NMR spectrum, the $^{1,2,3}J_{PC}$ couplings were also observed for the respective carbon signals with constants of 35, 11 and 6 Hz, respectively. The $^1J_{PC}$ coupling constant was consistent with that for **35**⁹⁰. The chemical shifts were assigned according to the 2-D NMR data (see 2.4.2.7 for the assignments). The definitive assignments could not be made for the methylene proton signals of the alkyl chain due to the overlap. The selected $^{1,2,3}J_{CH}$ and $^3J_{HH}$ correlations observed in the HMBC, HSQC and COSY NMR experiments are shown in Figure 2-30.

Boron has two naturally occurring NMR active nuclei i.e. ^{10}B and ^{11}B . Due to the often dominant quadrupolar relaxation mechanism of the nucleus, their NMR signals are usually broad i.e. > 10 Hz in B NMR spectroscopy. The broadening of signal is also observed for the signal of nucleus attached to the $^{11}\text{B}/^{10}\text{B}$ nuclei. In ^{31}P NMR

spectrum, the ^{31}P NMR signal of a phosphine-borane complex bonded to borane through a dative bond is broad and usually is not resolved too well¹⁰². This was consistent with the observation of the ^{31}P NMR signal of compound **34**. $^1J_{PB}$ coupling is common in ^{31}P NMR spectroscopy for the complexes, containing a phosphine-borane covalent and also dative bond such as a phosphine-borane adduct of primary phosphane. For a phosphine-borane adduct, a typical $^1J_{PB}$ coupling constant is about 45 Hz e.g. 43.5 Hz for $\text{CH}_3\text{PH}_2\cdot\text{BH}_3$ ¹⁰² which was also consistent with that for **34**.

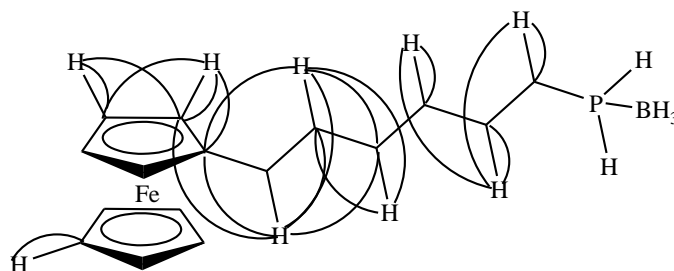


Figure 2-30: Selected $^{1,2,3}J_{\text{CH}}$ and $^3J_{\text{HH}}$ correlations observed for **34** in the HMBC, HSQC and COSY NMR experiments

2.2.2.11 X-ray Crystallographic Structure of $\text{Fc}(\text{CH}_2)_6\text{PH}_2\cdot\text{BH}_3$ (**34**)

Since it was difficult to obtain a single crystal of any of the primary phosphanes, $\text{Fc}(\text{CH}_2)_n\text{PH}_2$ ($n = 4$ **14**, 6 **15** or 11 **16**), X-ray crystallographic structural determination was carried out on the borane adduct of **16** which gave a single crystal as an orange needle suitable for the analysis. Crystals of **34** could be obtained by recrystallisation from hexane at $-18\text{ }^\circ\text{C}$. Intensity data were obtained on a Bruker SMART diffractometer with Mo-K α X-rays and corrected for absorption using a multi-scan procedure. The structures were solved by direct methods and developed and refined on F_o^2 .

All calculations were with the SHELX97 programs^{103, 104} run under WinGX¹⁰⁵ with Prof. Nicholson. Figures were generated with ORTEP-3¹⁰⁶. Figure 2-31 shows the crystal structure of **34** and Table 2-12 and Table 2-13 crystal data and refinement details and the selected bond parameters of **34**, respectively. H atoms on the CH_2 chain and

the Cp rings were in calculated positions, the PH₂ and BH₃ atoms were located and refined with isotropic temperature factors.

Table 2-12: *Crystal data and refinement details for 34*

34	
Empirical Formula	C ₁₆ H ₂₆ B ₁ Fe ₁ P ₁
M _r	316.00
T / K	89(2)
Wavelength / Å	0.71073
Crystal System	Monoclinic
Space Group	P2 ₁ /n
a / Å	14.9861(4)
b / Å	5.8093(1)
c / Å	19.7607(5)
α / °	90
β / °	110.711(1)
γ / °	90
V / Å ³	1609.17(7)
Z	4
ρ / mg m ⁻³	1.304
μ / mm ⁻¹	1.021
F (000)	672
Crystal Size / mm ³	0.37 × 0.12 × 0.08
θ range / °	1.48 to 27.96
Limiting Indices	-19 ≤ h ≤ 19, -7 ≤ k ≤ 7, -26 ≤ l ≤ 26
Reflection Collected	20240
Unique Reflections	3871 [R _{int} 0.0300]
Completeness to θ ° (%)	27.96 (99.8)
Absorption Correction	Semi-empirical from equivalents
T _{max} and T _{min}	0.9228 and 0.7039
Refinement Method	Full-matrix least-squares on F ²
Data / Restraints / Parameters	3871 / 0 / 192
GoF on F ²	1.037
Final RIndices	R ₁ 0.0243,
[I > 2σ(I)]	wR ₂ 0.0616
R Indices (all data)	R ₁ 0.0289,
	wR ₂ 0.0645
Largest Diff. Peak and Hole / eÅ ⁻³	0.440 and -0.211

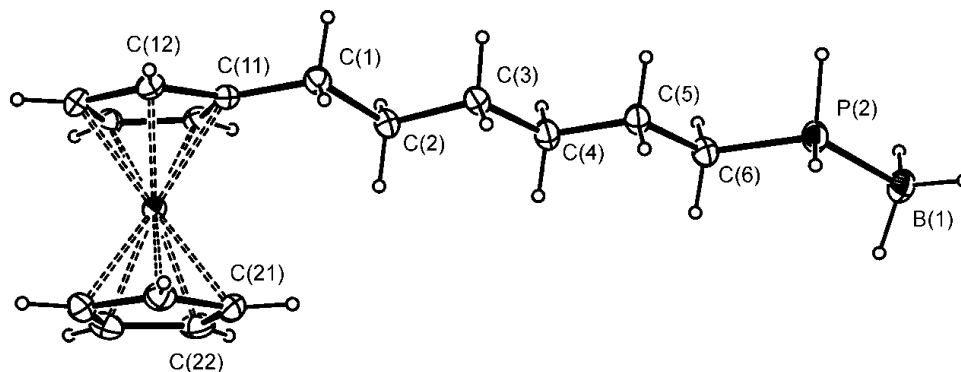


Figure 2-31: *Crystal structure of 34*

Table 2-13: Selected bond lengths (Å) and angles (°) for **34**

Bond Length / Å		Bond Angle / °	
<i>B(1)–H</i>	1.074(18), 1.127(18), 1.11(2)	<i>H–B(1)–H</i>	114.8(14), 113.4(14), 112.2(13)
<i>P(2)–B(1)</i>	1.9204(17)	<i>B(1)–P(2)–H</i>	115.0(8), 113.8(9)
		<i>P(2)–B(1)–H</i>	106.1(10), 102.9(10), 106.2(10)
<i>P(2)–H</i>	1.305(19), 1.29(2)	<i>H–P(2)–H</i>	102.0(12)
<i>P(2)–C(6)</i>	1.8164(13)	<i>C(6)–P(2)–H</i>	103.0(8), 104.0(8)
		<i>C(6)–P(2)–B(1)</i>	117.18(7)
		<i>C(5)–C(6)–P(2)</i>	113.65(9)
<i>alkyl C–C (range)</i>	1.5227(18) – 1.5301(17)	<i>alkyl C–C–C (range)</i>	111.08(11) – 114.09(11)
<i>alkyl C–C (average)</i>	1.5271	<i>alkyl C–C–C (average)</i>	112.57
<i>C(11)–C(1)</i>	1.5040(18)	<i>C(11)–C(1)–C(2)</i>	116.46(11)
		<i>C(12)–C(11)–C(1)</i>	124.22(12)
		<i>C(15)–C(11)–C(1)</i>	128.46(12)
<i>Cp C–C (range)</i>	1.424(2) – 1.4287(18)	<i>substituted Cp ring C–C–C</i>	107.20(11) – 108.80(11)
		<i>range</i>	
<i>Cp C–C (average)</i>	1.4259	<i>unsubstituted Cp ring C–C–C</i>	107.90(12) – 108.10(12)
		<i>range</i>	
<i>Fe–C (range)</i>	2.0391(13) – 2.0657(13)		
<i>Fe–C (average)</i>	2.0498		

As expected the structure consists of a ferrocenyl group with a (CH₂)₆ link to the PH₂ which is coordinated to BH₃. Related parts of the molecules of **34** are structurally very similar to those of FcCH₂PH₂·BH₃ **35**⁹⁰ except the extended alkyl spacer was absent in **35**. The B–H bond lengths and angles were comparable to those for **35** (**34**: 1.074(18) – 1.127(18) Å and 112.2(13) – 114.8(14)° v.s. **35**: 1.08(2) – 1.10(2) Å and 111.1(15) – 113.9(15)°, respectively)⁹⁰. The P–B length and B–P–H and P–B–H angles were also consistent with those for **35**⁹⁰ (**34**: 1.9204(17) Å and 113.8(9) – 115.0(8) and 102.9(10) – 106.2(10)° v.s. **35**: 1.9230(17) Å and 115.7(9) – 115.8(9) and 102.6(10) – 109.1(11)°, respectively).

The P–H bond lengths and H–P–H bond angle agree with those for **35** (**34**: 1.305(19) and 1.29(2) Å and 102.0(12)° v.s. **35**: 1.30(2) and 1.29(2) Å and 102.2(13)°, respectively)⁹⁰. The P–C bond length and C–P–H and C–C–P angles are also consistent with those for **35** (**34**: 1.8164(13) Å and 103.0(8), 104.0(8) and 113.65(9)° v.s. **35**: 1.8233(15) Å, 104.0(9) and 104.7(9) and 114.68(10)°)⁹⁰. The C–P–B angle of 117.18(7)° was greater by 4° than that of 113.01(7)° for **35**⁹⁰.

The C(11)–C(1) bond length and C(11)–C(1)–C(2) angle of 1.5040(18) Å and 116.46(11)°, respectively, were also in good agreement with the literature values of 1.5004(19) Å and 114.68(10)° for **35**⁹⁰.

The Cp C–C bond lengths of 1.424(2) – 1.4287(18) Å are statistically indistinguishable to those of 1.420(2) – 1.4344(19) Å for **35**⁹⁰ and also comparable to those of 1.379(7) – 1.428(6) Å reported for FcCH₂CH₂AsH₂ **41**⁷⁹. The substituted and unsubstituted Cp ring C–C–C angles were found to be between 107.20(11) – 108.80(11) and 107.90(12) – 108.10(12)°, respectively, and were consistent with those of 107.79(12) – 108.27(13) and 107.79(14) – 108.28(14)° for **35**⁹⁰ and also with those of 107.2(4) – 108.8(4) and 107.3(4) – 108.7(4)° for **41**⁷⁹.

The C(12)–C(11)–C(1) and C(15)–C(11)–C(1) angles of 124.22(12) and 128.46(12)° were also consistent with the literature values of 126.18(13) and 126.03(13)°, reported for **35**⁹⁰ and also with that of 121.2(5)° (only one angle was reported in the literature) for **41**⁷⁹. The (CH₂)₆ chain is in the extended (*anti*) conformation.

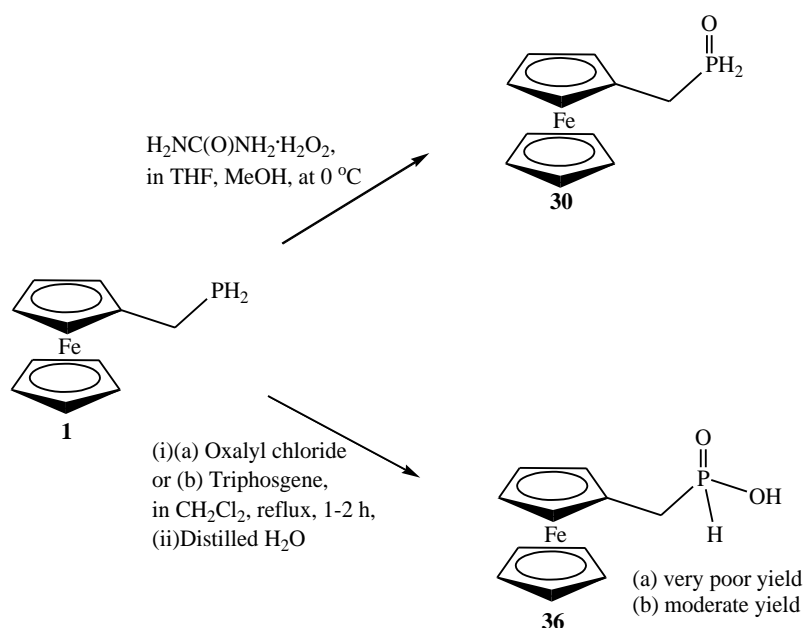
The Fe–C bond lengths were found to be between 2.0391(13) – 2.0657(13) Å which were consistent with the literature values of 2.0371(16) – 2.0578(15) Å reported for **35**⁹⁰, those of 2.022(3) – 2.042(2) Å for **1**⁷⁸ and also of 2.032(4) – 2.045(4) Å for **41**⁷⁹.

2.2.3 Synthesis and Characterisation of Phosphane Oxides

As an extension of the present study, the unpublished synthesis of the phosphane oxide **30** and FcCH₂P(O)(OH)H **36** in the earlier work¹⁰¹ was also re-investigated. In the earlier work¹⁰¹, although the phosphane oxide **30** was prepared by reaction of **1** with aqueous hydrogen peroxide, satisfactory microanalytical data could not be obtained. Since aqueous hydrogen peroxide is unstable and the concentration may vary, despite the fact that it could successfully provide the desired phosphane oxide **30**, it may not be best suited for the synthesis. It is also undesirable to use excess oxidant as it may cause the further oxidation⁹ of **30** and the corresponding phosphinic acid **36** would form. In the present study, the phosphane oxide **30** was, therefore,

synthesised using urea hydrogen peroxide as an alternative oxidant as it is more stable in the solid state and, therefore, the required amount of the oxidant for the reaction can precisely be obtained.

The synthesis of the phosphinic acid **36**, which was partially characterised in the earlier study¹⁰¹, was also re-investigated. The phosphinic acid **36** was synthesised using oxalyl chloride as an alternative chlorinating agent instead of triphosgene used in the earlier study¹⁰¹. The synthesis was also carried out with triphosgene subsequently due to the unsatisfactory yield of the desired product **36** in the synthesis with using oxalyl chloride. Scheme 2-6 summarises the syntheses of **30** and **36**.



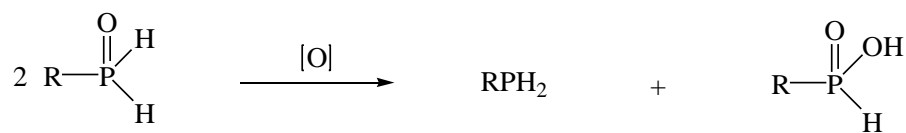
Scheme 2-6: Synthesis of **30** and **36**

2.2.3.1 Synthesis of $\text{FcCH}_2\text{P(O)H}_2$ (**30**)

In air, to a mixture of **1** and urea hydrogen peroxide in THF at 0°C , MeOH was slowly added and stirred for 15 minutes. After adding distilled H_2O , the reaction mixture was extracted with CH_2Cl_2 and the organic phase was washed with a 0.067 M NaOH solution and then distilled H_2O . Removal of the solvent from the organic phase gave the desired phosphane oxide **30** as a yellow solid in moderate yield (45 %). A strong distinctive phosphane odour was noted from the yellow solid.

Attempted purification of the crude product either by recrystallisation from $\text{CH}_2\text{Cl}_2/\text{MeOH}$ or $\text{CH}_2\text{Cl}_2/\text{light petroleum spirits}$ at $-18\text{ }^\circ\text{C}$ or by column chromatography on a silica gel, eluting with CH_2Cl_2 or using a 95 : 5 mixture of $\text{CH}_2\text{Cl}_2/\text{MeOH}$ were unsuccessful. Although the column chromatography on a silica gel, eluting with a 95 : 5 mixture of $\text{CH}_2\text{Cl}_2/\text{MeOH}$ gave the purest sample, satisfactory microanalytical data could not be obtained for the sample.

Phosphane oxides are generally unstable towards further oxidation. Disproportionation of the phosphane oxides to give the corresponding phosphinic acids occurs upon exposure to air (Scheme 2-7)^{9, 107}. The formation of the corresponding phosphinic acid **36** was always observed in the $^{31}\text{P}\{-^1\text{H}\}$ NMR spectrum of **30** (Figure 2-32) after the attempted purifications. The garlic-like phosphane odour from the samples also suggested the formation of RPH_2 . The phosphane oxide **30** may, therefore, also be more unstable than expected and readily undergo the further oxidation. The unsatisfactory microanalytical result may have been due to the instability of **30**.



Scheme 2-7: Disproportionation of ferrocenylmethyl phosphane oxide

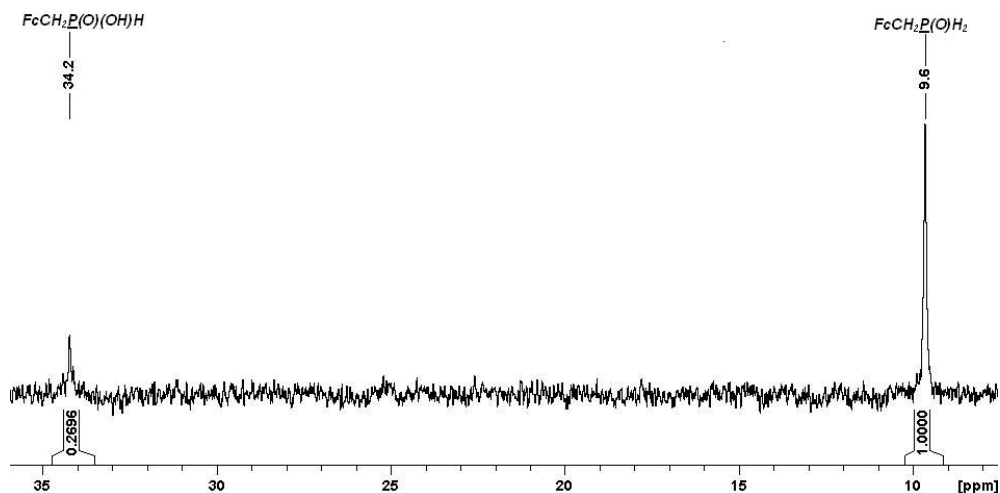


Figure 2-32: $^{31}\text{P}\{-^1\text{H}\}$ NMR spectrum of **30**

2.2.3.2 Characterisation of $\text{FcCH}_2\text{P}(\text{O})\text{H}_2$ (**30**)

The $P-H$ stretch was observed at 2390 cm^{-1} as a broad medium intensity peak (Figure 2-33) which is consistent for the class of compounds concerned¹⁰⁷.

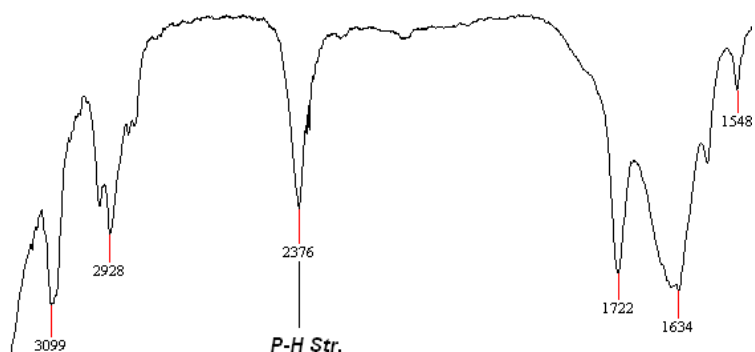


Figure 2-33 IR spectrum of **30**

An unambiguous assignment for the $P=O$ stretch, which typically appears between $1286 - 1170\text{ cm}^{-1}$ ¹⁰⁷, could not be made due to the presence of several bands in the region.

The mass spectrometric data were obtained by ESI-MS using MeOH as mobile phase at capillary exit voltage of 100 V. Although the molecular ion, $[M]^+$ could not be observed, the ions corresponding to the adducts could be observed in the positive ion mode i.e. $[M + Na]^+$ (m/z observed 270.999; calcd. 270.994 for $\text{C}_{11}\text{H}_{13}\text{Fe}_1\text{Na}_1\text{O}_1\text{P}_1$) (Figure 2-34), $[M + K]^+$ (m/z observed 286.969; calcd. 286.968 for $\text{C}_{11}\text{H}_{13}\text{Fe}_1\text{K}_1\text{O}_1\text{P}_1$) and $[2M + Na]^+$ (m/z observed 518.999; calcd. 518.999 for $\text{C}_{22}\text{H}_{26}\text{Fe}_2\text{Na}_1\text{O}_2\text{P}_2$). Since $P=O$ is a hard Lewis base and has strong affinity for alkali metal ions, the formation of adducts is consistent with the presence of the desired phosphane oxide **30**.

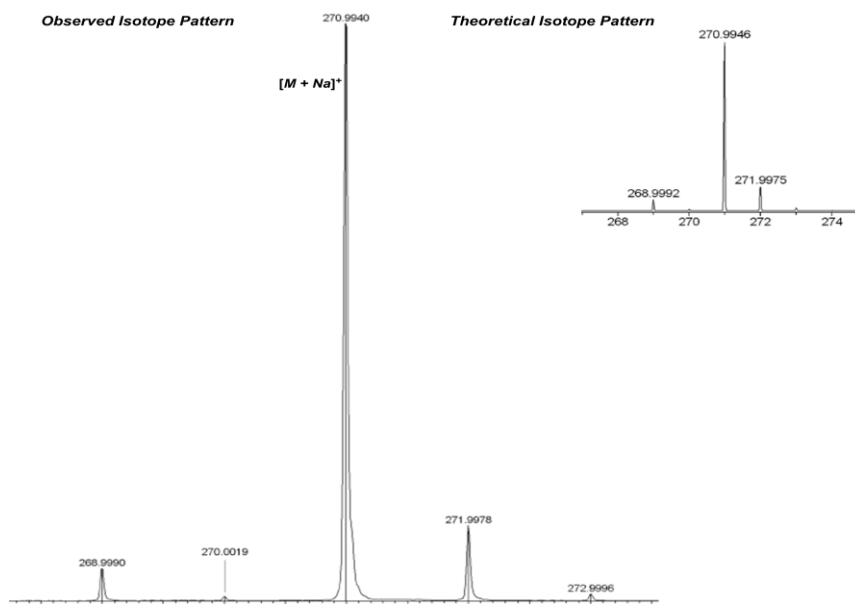
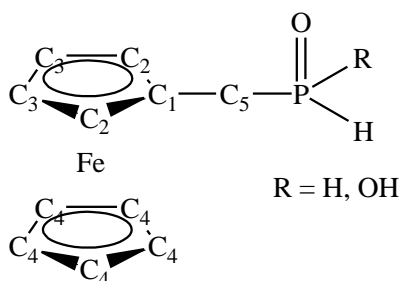
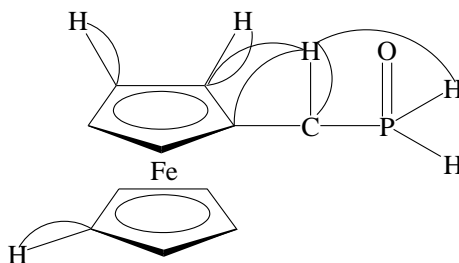


Figure 2-34: Partial ESI-MS of **30** showing the observed and theoretical $[M + Na]^+$ ion ($M = 30$)

The ^{31}P NMR signal appeared at δ 9.5 ppm as a triplet of triplets with a $^1J_{\text{PH}}$ and $^2J_{\text{PH}}$ coupling constant of 470 and 16 Hz, respectively, which are consistent with the class of compounds concerned (cf. $^1J_{\text{PH}} = 470 - 510$ Hz and $^2J_{\text{PH}} = 10 - 20$ Hz for $\text{RP}(\text{O})\text{H}_2$)¹⁰⁷. In the ^1H NMR spectrum, the phosphane proton signal appeared at δ 6.9 ppm as a doublet of triplets with a $^1J_{\text{PH}}$ and $^3J_{\text{HH}}$ coupling constant of 470 and 5 Hz, respectively, which are again typical for the class of compounds concerned¹⁰⁷. The methylene proton signal, which was observed at δ 3.1 ppm, also appeared as a doublet of triplets with a $^2J_{\text{PH}}$ and $^3J_{\text{HH}}$ constant of 16 and 5 Hz, respectively. The $^2J_{\text{PH}}$ coupling to the methylene proton signal was not observed for the primary phosphane **1** and also the other ferrocenyl phosphanes synthesised in the present study. The presence of oxygen often leads to a greater coupling constant of nearby NMR active nucleus. The observation of the $^2J_{\text{PH}}$ coupling for the phosphane oxide **30** may, therefore, be due to the presence of the oxygen bonded directly to the phosphorus. In the $^{13}\text{C}\{-^1\text{H}\}$ NMR spectrum, only the $^3J_{\text{PC}}$ coupling was observed for the C_2 carbon signal which appeared as a doublet with a coupling constant of 4 Hz. The assignments of the chemical shifts (Table 2-14) were made according to the 2-D NMR data including HMBC, HSQC and COSY NMR experiments and the selected $^{1,2,3}J_{\text{CH}}$ correlations are shown in Figure 2-36.

Table 2-14: ^1H and ^{13}C NMR chemical shifts for **30**

δ / ppm	30
^1H NMR	
H_2	4.14 (unresolved m, 2 H)
H_3	4.11 (unresolved m, 2 H)
H_4	4.18 (s, 5 H)
H_5	3.1 (d of t, $^2J_{PH} = 16$, $^3J_{HH} = 5$ Hz, 2 H)
PH	6.9 (d of t, $^1J_{PH} = 470$, $^3J_{HH} = 5$ Hz, 2 H)
^{13}C - $\{^1\text{H}\}$ NMR	
C_1	75.2 (C, s)
C_2	68.9 (CH, d, $^3J_{PC} = 4$ Hz)
C_3	68.7 (CH, s)
C_4	69.1 (CH, s)
C_5	29.7 (CH ₂ , s)
^{31}P NMR	
P	9.5 (t of t, $^1J_{PH} = 470$, $^3J_{HH} = 16$ Hz)

Figure 2-35: Atom labelling used in NMR assignments for **30** and **36**; hydrogen atoms are numbered according to the carbon to which they are bondedFigure 2-36: Selected $^{1,2,3}J_{CH}$ and $^3J_{HH}$ correlations observed for **30** in the HMBC, HSQC and COSY NMR experiments

Attempts to obtain satisfactory microanalytical data were unsuccessful (i.e. calcd. for $\text{C}_{11}\text{H}_{13}\text{O}_1\text{P}_1\text{Fe}_1$: C 53.24; H 5.28; N 0.00 %; found: C 56.44; H 5.39; N 0.5 %). The higher percentages of the found compositions of the C and H atoms for the sample might have been due to the residual organic solvent used during the work-up.

2.2.3.3 Synthesis of $\text{FcCH}_2\text{P}(\text{O})(\text{OH})\text{H}$ (**36**)

A mixture of **1** and oxalyl chloride in dry CH_2Cl_2 was heating to reflux for 2 h under an N_2 atmosphere and hydrolysed with distilled H_2O . The residual **1** was removed by

extracting with CH₂Cl₂ under basic conditions and the desired product **36** was then isolated by extraction with CH₂Cl₂ under acid condition. Removal of the solvent from the extract containing the desired compound gave a brown oil. The ³¹P NMR spectrum of the brown oil indicated that it was a mixture of the desired compound **36** and a phosphane whose ³¹P NMR signal appeared at δ 50.0 ppm as pentet. Although the desired compound **36** formed, it was only minor amount. The undesired phosphane was by far major in the mixture. Despite the attempts, neither product could be isolated. Attempted recrystallisation from CH₂Cl₂ at -18 °C gave no precipitate. The undesired side-product was, therefore, unidentified.

Compound **36** was again synthesised using triphosgene as chlorinating agent. The mixture of **1** and triphosgene in CH₂Cl₂ was heating to reflux for 1 h under an N₂ atmosphere. After removing the CH₂Cl₂, the residue was hydrolysed with distilled H₂O and the solution was stirred overnight. After removal of the excess **1** by extraction with CH₂Cl₂ under basic condition, acidification of the aqueous phase and the subsequent extraction with CH₂Cl₂, removal of the solvent from the CH₂Cl₂ extract under reduced pressure gave the desired phosphinic acid **36** as a yellow solid in moderate yield (64 %). The yellow solid was sufficiently pure for elementary analysis. Satisfactory microanalytical data could be obtained for the yellow solid (Found: C 50.12, H 4.95; calcd. C 50.02, H 4.96 %).

2.2.3.4 Characterisation of FcCH₂P(O)(OH)H (**36**)

The *P-H*, *P=O* and *P-OH* stretches were observed at 2378, 1181 and 2568 cm⁻¹, respectively (Figure 2-37). The frequencies are consistent with those expected for the class of compounds concerned (cf. 2440 – 2280 cm⁻¹ for *ν*(P-H); 1286 – 1170 cm⁻¹ for *ν*(P=O); 2900 – 2500 cm⁻¹ for *ν*(P-O-H))¹⁰⁷. *ν*(*P-H*) bands generally appear as a doublet in RP(O)(OR')H owing to the presence of the rotational isomers¹⁰⁷ which is also consistent with the bands observed for **36** (Figure 2-37).

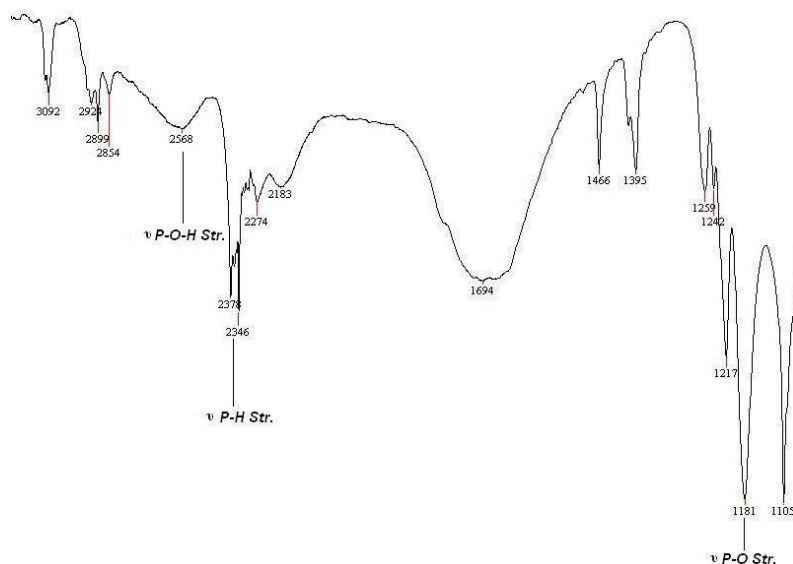


Figure 2-37: IR spectrum of **36**

The ^{31}P NMR signal was observed at δ 36.9 ppm as a doublet of triplets with a $^1J_{\text{PH}}$ and $^2J_{\text{PH}}$ coupling constant of 557 and 17 Hz, respectively, which are consistent with the compounds of the type $\text{RP}(\text{O})(\text{OH})\text{H}$ (cf. $^1J_{\text{PH}} = 470 - 700$ Hz; $^2J_{\text{PH}} = 10 - 20$ Hz)¹⁰⁷. In the ^1H NMR spectrum, as for the corresponding phosphane oxide **30**, the proton signal bonded to the phosphorus appeared further downfield at δ 7.0 ppm as a doublet of triplets with a greater $^1J_{\text{PH}}$ and $^3J_{\text{HH}}$ coupling constant of 557 and 2 Hz, respectively. The $^2J_{\text{PH}}$ coupling to the methylene proton signal was also observed for **36**. The signal appeared at δ 2.9 ppm as a doublet of doublets with a $^2J_{\text{PH}}$ and $^3J_{\text{HH}}$ coupling constant of 15 and 2 Hz, respectively. In the $^{13}\text{C}\{-^1\text{H}\}$ NMR spectrum, the $^{1,3}J_{\text{PC}}$ couplings were observed for the respective carbon signals which appeared as a doublet with a $^1J_{\text{PC}}$ and $^3J_{\text{PC}}$ coupling constant of 91 and 4 Hz, respectively. The assignments of the chemical shifts were made according to the 2-D data and summarised in Table 2-15. The selected $^{1,2,3}J_{\text{CH}}$ correlations observed in the HMBC, HSQC and COSY NMR experiments are shown in Figure 2-38. The atom labelling used is shown in Figure 2-35.

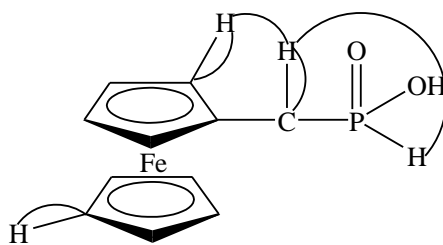


Figure 2-38: Selected $^{1,2,3}J_{CH}$ correlations observed for **36** in the HMBC, HSQC and COSY NMR experiments

Table 2-15: 1H , ^{13}C and ^{31}P NMR chemical shifts for **36**

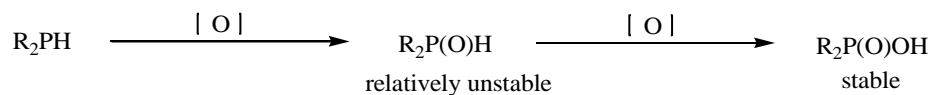
δ / ppm	36
1H NMR	
H_2	4.20 (unresolved m, $^3J_{HH} = 1$ Hz, 2 H)
H_3	4.15 (unresolved m, $^3J_{HH} = 2$ Hz, 2 H)
H_4	4.14 (s, 5 H)
H_5	2.9 (d of d, $^2J_{PH} = 15$, $^3J_{HH} = 2$ Hz, 2 H)
PH	7.0 (d of t, $^1J_{PH} = 557$, $^3J_{HH} = 2$ Hz, 1 H)
$^{13}C\{-^1H\}$ NMR	
C_1	Not Observed.
C_2	69.3 (CH, d, $^3J_{PC} = 4$ Hz)
C_3	68.4 (CH, s)
C_4	69.0 (CH, s)
C_5	31.8 (CH ₂ , d, $^1J_{PC} = 91$ Hz)
^{31}P NMR	
P	36.9 (d of t, $^1J_{PH} = 557$, $^2J_{PH} = 17$ Hz)

Despite the attempts, mass spectrometric data for **36** could not be obtained. ESI-MS was carried out in MeOH. Despite using various exit voltages, ranging from 80 to 220 V, the molecular ion or any related ions could not be observed in either ion mode.

2.2.4 ^{31}P NMR Studies on Oxidative Stability of Ferrocenyl Primary and Secondary Phosphanes

2.2.4.1 Air-Stability of $FcCH_2PRH$ ($R = C_6H_{11}$ (**3**), CH_3 (**4**) and $CH_2C_6H_4NO_2$ (**5**))

Secondary phosphanes are generally readily oxidised in air to form the corresponding oxides, $R_2P(O)H$, which are also relatively unstable towards further oxidation and often further oxidised to give the stable phosphinic acid, $R_2P(O)OH$ (Scheme 2-8)⁹.



Scheme 2-8: *Typical oxidation of secondary phosphane*

The oxidative stability of the secondary phosphanes **3**, **4** and **5** in solution i.e. in CDCl₃ at room temperature in air was studied by ³¹P NMR spectroscopy with ¹H decoupled. The samples were kept in capped NMR tubes the rate of oxygen diffusion into which might have varied due to the inconsistency of the NMR caps i.e. some were loosen by repeated use. However, since no significant increase in the amount of the oxidation products for each sample was observed even when a non-deoxygenated solvent was occasionally filled in air due to the loss by evaporation, the rate of oxygen diffusion into each sample through the cap was assumed to be negligible. The oxidation progress was monitored at intervals until the ³¹P NMR signals of the original secondary phosphanes had completely disappeared. The NMR samples were prepared in air. Small portions of the secondary phosphanes, which were not accurately measured but roughly the same amount, were dissolved in CDCl₃ and placed separately in clean and dry NMR tubes. The tubes were then sealed with plastic NMR lids. Immediately after the preparations, their first ³¹P-¹H NMR spectra were recorded. During the intervals, the NMR samples were placed on a bench at room temperature in air with their lids on. Additional NMR solvents were occasionally added due to the loss by slow evaporation.

The degree of oxidation was determined by comparison between the integrals of the ³¹P NMR signals corresponding to the original secondary phosphane and the oxides. The integrals of the ³¹P NMR signals for the original secondary phosphanes were set as the reference value (i.e. as 1) and those for the oxides were determined accordingly using an auto-integration function of Bruker TopSpin 3.0 software version 2.1. The integrals of the corresponding oxides, both the oxides and phosphinic acids (if present), were combined and used as the integral for the oxidation product. The integrals are converted into percentages by division of the combined integrals of the oxides and phosphinic acids over that of the original secondary phosphanes followed by multiplication by 100. The results are plotted in Figure 2-39. The vertical axis

shows the percentages of the combined amounts of the oxides present in the sample and the time taken is shown in days on the horizontal axis.

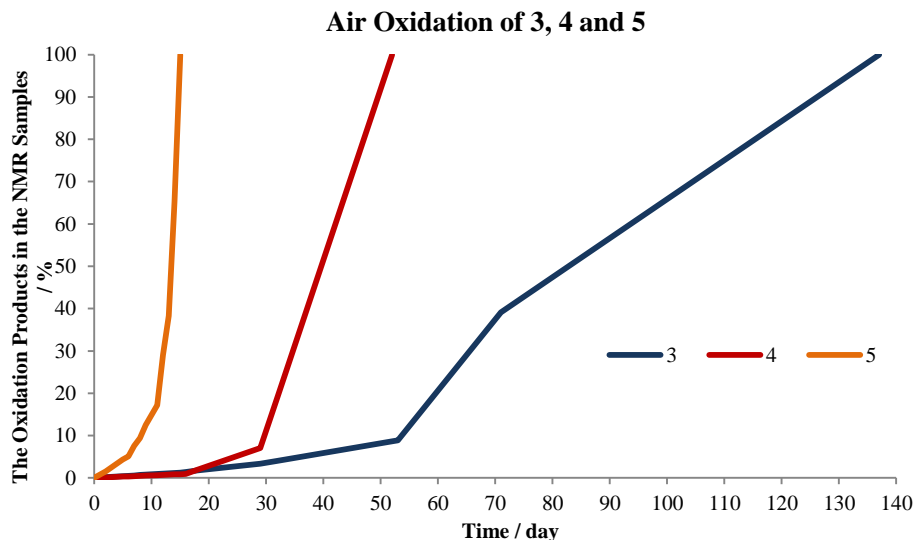


Figure 2-39: Oxidation progress of ferrocenyl secondary phosphanes **3**, **4** and **5**

As seen from Figure 2-39, the secondary phosphane **5** was the least air stable of the three secondary phosphanes. The actual $^{31}\text{P}\{-^1\text{H}\}$ NMR spectra showing the oxidation of **5** are also shown in Figure 2-40. The secondary phosphane was completely oxidised in little over 2 weeks. Since the *p*-nitrobenzyl group is generally electron-withdrawing, it may be expected to destabilise the hydride and seemed to be the case for **5**.

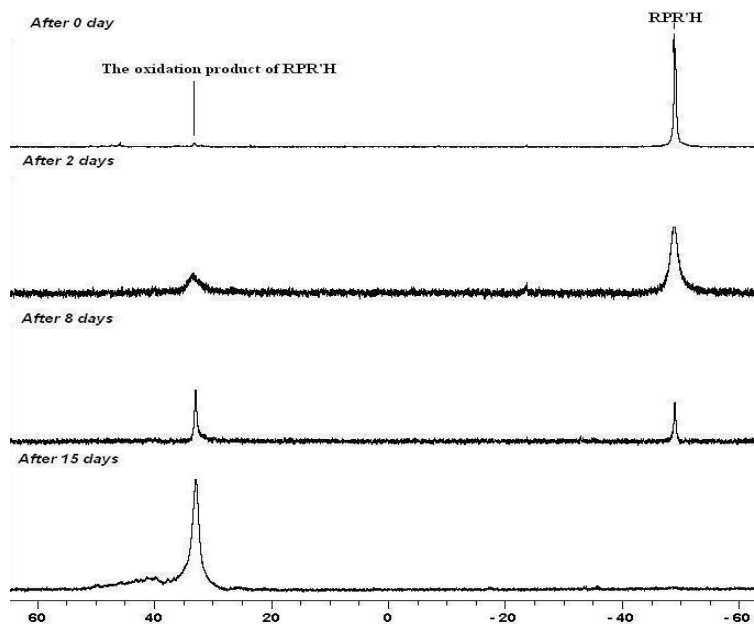


Figure 2-40: $^{31}\text{P}\{-^1\text{H}\}$ NMR spectra showing the oxidation of **5** in solution at room temperature in air

By contrast, the secondary phosphane **3** showed remarkable air stability under the analogous conditions. The ^{31}P NMR signal was kept being observed for more than 4 months (Figure 2-41). Since a cyclohexyl group is electron-donating, a stabilisation effect on the hydride centre may be expected. The result of the experiment seemed to agree.

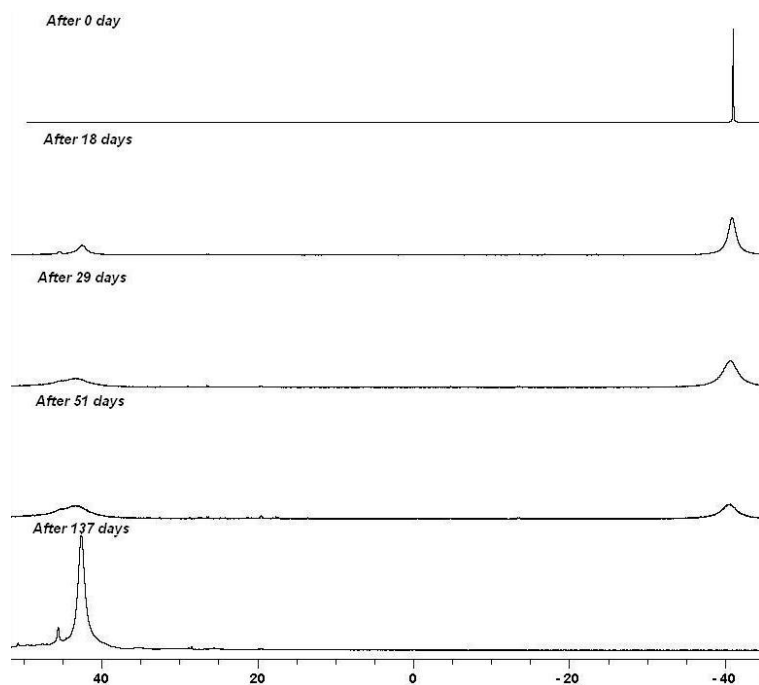


Figure 2-41: ^{31}P - $\{^1\text{H}\}$ NMR spectra showing the oxidation of **3** in solution at room temperature in air

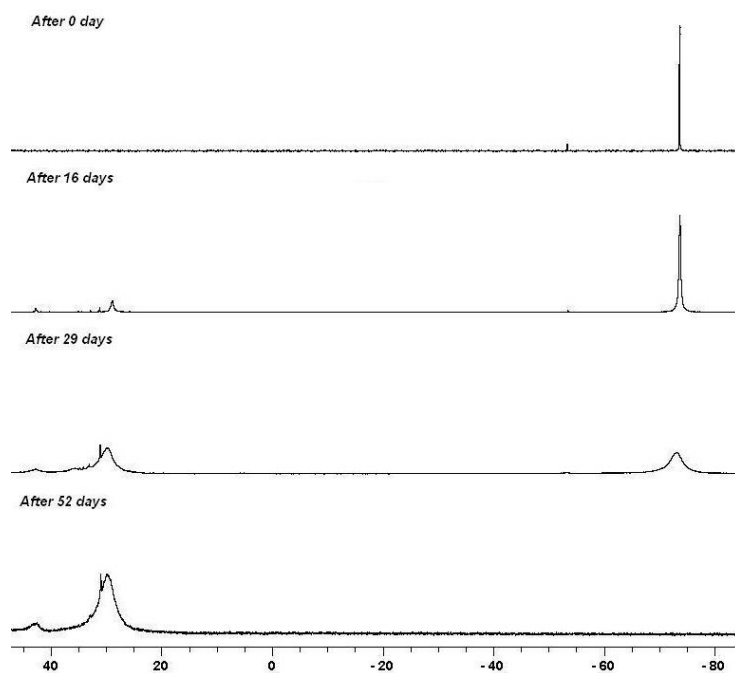


Figure 2-42: ^{31}P - $\{^1\text{H}\}$ NMR spectra showing the oxidation of **4** in solution at room temperature in air

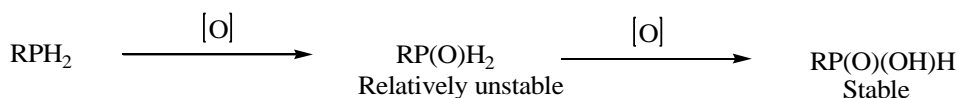
The air-stability of **4** was similar to **5**. It was fully oxidised after ~1.5 month under the analogous conditions (Figure 2-42 and Figure 2-40, respectively). These results may suggest that the more electron-donating the substituent on the phosphorus is, the more stable the secondary phosphane becomes and vice versa.

While *p*-O₂NC₆H₄CH₂ was the most electron-withdrawing of the three organic substituents and the secondary phosphane **5** was oxidised the most rapidly, the secondary phosphanes **3** and **4** with electron-donating substituents were rather stable in air. The complete oxidations of the secondary phosphanes **3** and **4** were observed after 1.5 and 4 months, respectively, at room temperature in air. The substitution of an electron-withdrawing organic group at the phosphorus appears to destabilise the secondary phosphane while that of an electron-donating substituent stabilises. Also, the more electron-donating the substituent was, the more stable the secondary phosphane was.

Since only a limited number of the secondary phosphanes was studied and the experiments were carried out using non-equimolar amounts, although electron-donating organic substituents on the phosphorus appeared to stabilise secondary phosphanes, the result may not be conclusive. The study may, therefore, be repeated with using an equimolar amount of various secondary phosphanes so that a more direct and comprehensive comparison can be made.

2.2.4.2 Air-stability of Fc(CH₂)_nPH₂ (n = 4 (**14**), 6 (**15**), 11 (**16**)) and R_cCH₂PH₂ (**24**)

Primary phosphanes of the type RPH₂ e.g. PhPH₂ are generally air-sensitive. They are readily oxidised in air to ultimately yield the phosphonic acids, RP(O)(OH)₂, via the formation of the corresponding oxides, RP(O)H₂ (Scheme 2-9)⁹.



Scheme 2-9: Typical oxidation of primary phosphane

The oxidative stability of the primary phosphanes **14**, **15**, **16** and **24** in solution i.e. CDCl_3 at room temperature in air was studied by ^{31}P NMR spectroscopy. The primary phosphanes were placed in capped NMR tubes dissolved in CDCl_3 and kept at room temperature in air. The oxidation progresses of the primary phosphanes were monitored by ^{31}P NMR spectroscopy with ^1H decoupled and also coupled modes at intervals until the ^{31}P NMR signals for the original primary phosphanes completely disappeared. The NMR samples were prepared in air. Small portions of the primary phosphanes, which were not accurately measured, were placed in dry and clean separate NMR tubes, dissolved in CDCl_3 and the tubes were then sealed with plastic NMR lids. The first ^{31}P NMR spectra were immediately recorded after the preparations. The samples of **16** and **24** used had not been purified prior to the experiment. The ^{31}P NMR signals of their corresponding oxides and phosphinic acids were, therefore, already seen in the spectra “after 0 day”. The oxides were likely to have been produced during the preparation of the compound because their ^{31}P NMR signals were also already observed in the spectrum of the crude product. The formation of the oxides and phosphinic acids in minor amounts during the preparation of the compounds was also observed for **14** and **15** probably due to the slight excess $\text{Na}_2\text{S}_2\text{O}_5$ used in order to ensure the completion of the reactions, which could cause further oxidations of the primary phosphanes. The oxidation products of **14** and **15** had, however, been removed by chromatography on a preparative TLC plate prior to the experiments so no ^{31}P NMR signals corresponding to the oxides and phosphinic acids were seen in their spectra at the beginning of the experiments. The rate of oxygen diffusion into each sample through the lid might have varied because of the inconsistency of the plastic NMR caps. The caps could be loosen by repeated use. At the beginning, it sealed well but towards the end it might have not. However, since the oxidations of these primary phosphanes were very moderate i.e. even when the filling of the solvents were carried out in air using non-deoxygenated solvents due to the loss by slow evaporation, there were no significant increases in the amounts of the oxidation products of the primary phosphanes, the rate of oxygen diffusion into each sample through the lid was assumed to be negligible. Since these experiments were qualitative surveys in order to look at major differences in stability, no duplicates

were also carried out. An NMR sample of PhPH_2 , which was obtained from a commercial source, was also prepared in the same manner as above and the oxidation progress under the same conditions was also monitored by ^{31}P NMR spectroscopy with ^1H decoupled and coupled modes for comparison purposes.

The degree of oxidation was determined as before (see 2.2.4.1) by comparison of the integrals between the ^{31}P NMR signals for the original primary phosphane and the oxidised products. The integrals of the ^{31}P NMR signals for the original primary phosphanes were used as the reference value (i.e. set as 1) and those for the corresponding oxides and phosphinic acids were determined accordingly using the auto-integration function of Bruker TopSpin 3.0 software version 2.1. The integrals of the ^{31}P NMR signals corresponding to the oxides and phosphinic acids were combined and converted into percentages by dividing the combined integrals for the oxides and phosphinic acids over those for the original primary phosphanes followed by multiplication by 100. The results are plotted as a graph and shown in Figure 2-43. The vertical axis shows the percentages of the combined amounts of the oxides present in the sample and the time taken is shown in days on the horizontal axis.

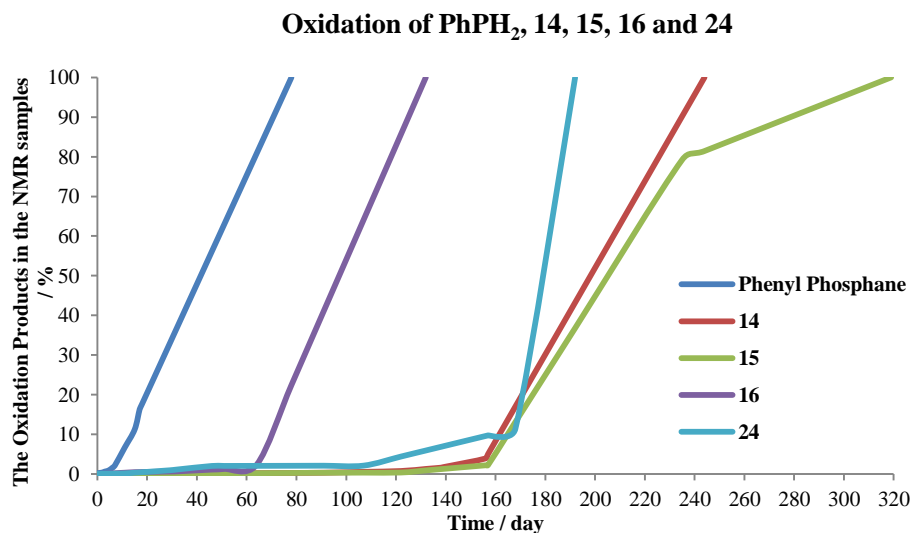


Figure 2-43: Oxidation progress of phenyl phosphane and ferrocenyl primary phosphanes **14**, **15**, **16** and **24** in solution at room temperature in air monitored by ^{31}P NMR spectroscopy with ^1H decoupled mode

PhPH₂ was completely oxidised after ~2 months. The oxidation rate of PhPH₂ in CDCl₃ appeared rather moderate, considering the highly air-sensitive nature of the compound (i.e. pyrophoric)⁹. It has been reported by Higham and Gilheany *et al.*⁷⁵ that the oxidation of air sensitive primary phosphanes can be slower in solution than as the neat state. Their NMR experiments in which the oxidation of the selected primary phosphanes, including PhPH₂, were monitored both as the neat and solution states (in CDCl₃) exposed to air in uncapped NMR tubes for the subsequent 7 days, showed that the oxidation was much faster as the neat states than in solution. The rather slow oxidation of PhPH₂ in the present study may, therefore, be explained by the fact that the experiment was carried out in solution state. Moreover, since the samples were kept sealed with their plastic NMR lids on as opposed to the uncapped literature condition, the partially limited exposure of the sample to air might have resulted in the unexpected slower oxidation of PhPH₂. The same argument may also apply to the other phosphanes used in the present study. Although they exhibited a remarkable air-stability under the given conditions, their oxidation may be much faster than the time frame indicated in Figure 2-43 if in their neat states or fully exposed to air as in the literature⁷⁵.

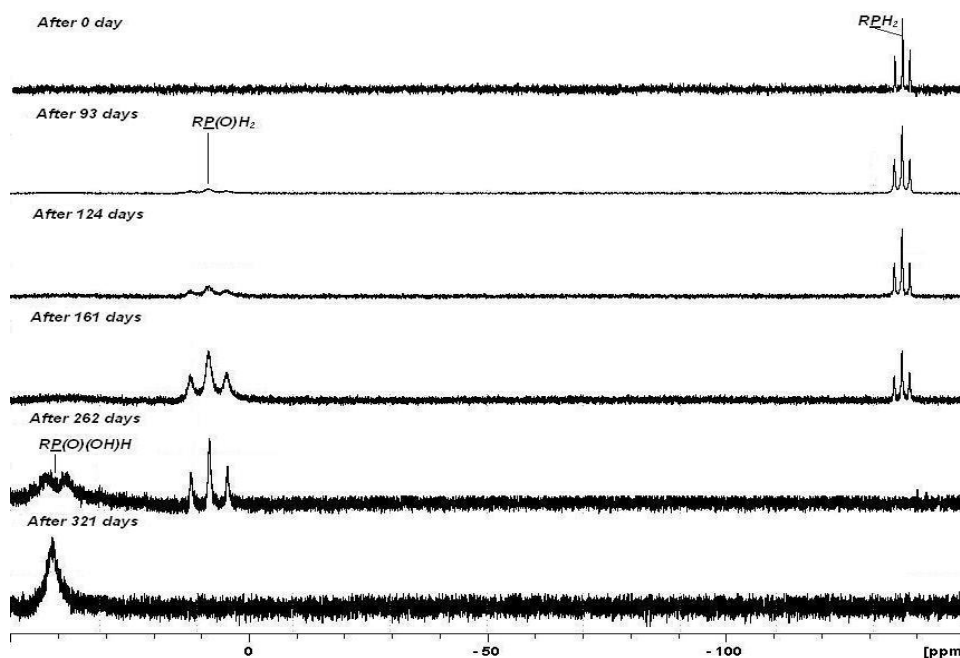


Figure 2-44: ³¹P NMR spectrum showing the air oxidation of Fc(CH₂)₄PH₂ **14** in solution at room temperature

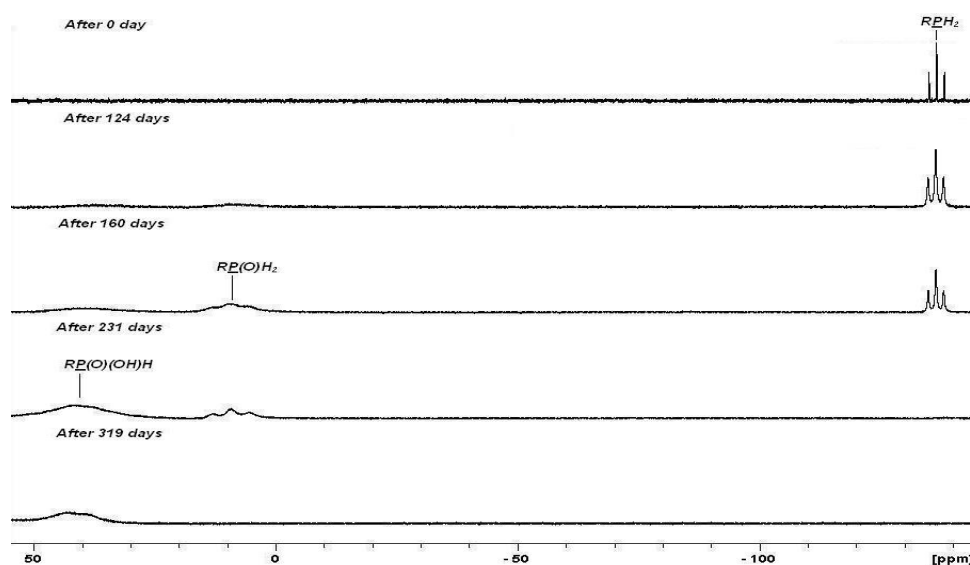


Figure 2-45: ^{31}P NMR spectrum showing the air oxidation of $\text{Fc}(\text{CH}_2)_6\text{PH}_2$ **15** in solution at room temperature

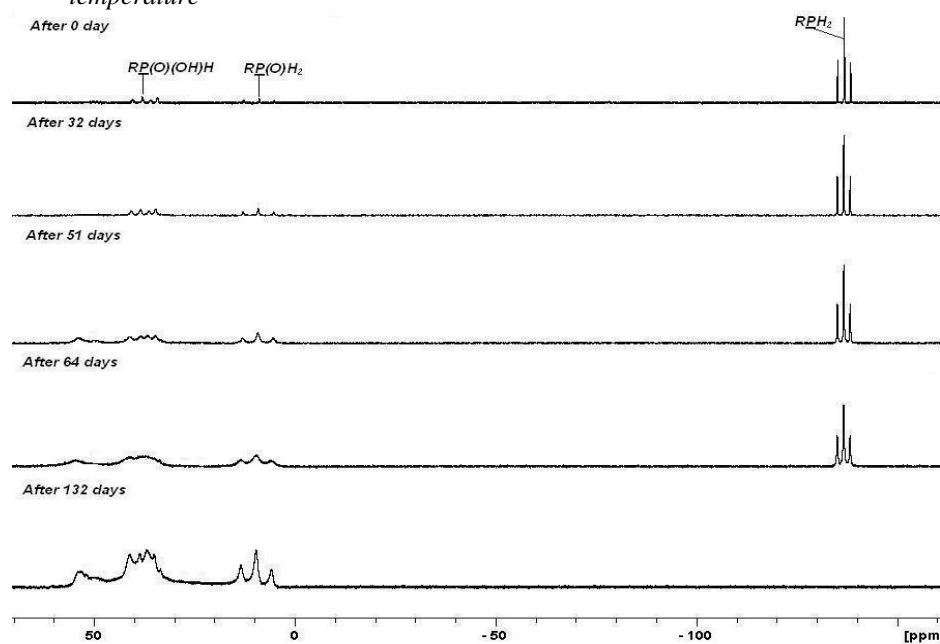


Figure 2-46: ^{31}P NMR spectrum showing the air oxidation of $\text{Fc}(\text{CH}_2)_{11}\text{PH}_2$ **16** in solution at room temperature

While PhPH_2 was completely oxidised after ~ 2 months, the oxidation of the ferrocenyl primary phosphanes **14**, **15**, **16** after 2 months was relatively minor (Figure 2-43; Figure 2-44; Figure 2-45; Figure 2-46). The primary phosphane **16** was fully oxidised after ~ 4 months and was the least air stable of the series. The primary phosphanes **14** and **15** were stable for ~ 4 months. The primary phosphane **14** was almost oxidised after 8 months and 9 months later the ^{31}P NMR signal completely disappeared (Figure 2-44). The oxidation of the primary phosphane **15** resembled to

that of **14**. The primary phosphane **15** underwent complete oxidation after ~7 months (Figure 2-45).

The primary phosphanes **14**, **15**, **16** were also sufficiently air stable to be handled in air for general work-ups or purification even on a preparative TLC plate. No oxidation was indicated in their $^{31}\text{P}\{-^1\text{H}\}$ NMR spectra upon handling in air.

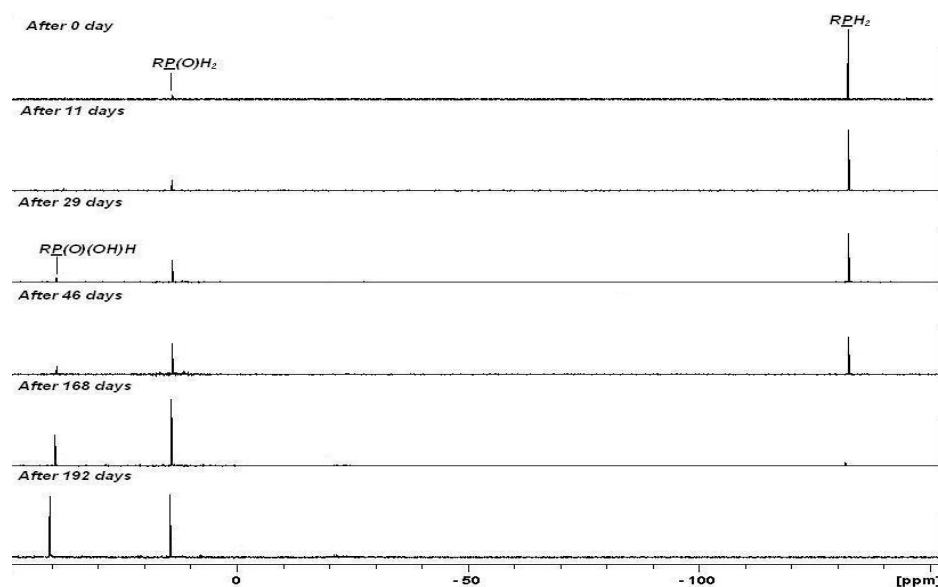


Figure 2-47: $^{31}\text{P}\{-^1\text{H}\}$ NMR spectrum showing the air oxidation of **24** in solution at room temperature

Nearly half the ruthenocenyl primary phosphane **24** was oxidised after ~1 month, indicating that it is much less air stable than the corresponding ferrocene analogue **1** which is completely stable in air for as long as 2 years in the neat state⁷⁸. The entire sample of **24** was nearly completely oxidised after ~5 months (Figure 2-47). Since ruthenocene has greater resistance towards oxidation than ferrocene and its derivatives do^{108, 109} and while the ferrocenium cation of ferrocene or of its derivatives can readily undergo oxidation and also the reaction is readily reversible^{110, 111}, the oxidation of the ruthenocenium cation of ruthenocene or of its derivatives is often irreversible^{108, 112, 113}.

The ruthenocenium cation of the ruthenocenyl moiety may undergo oxidation reaction. However, once the ruthenocenium cation is oxidised, it may not be reduced

and therefore there would no more stabilisation effect present in the molecule or in the system. This may explain the moderate air-stability of **24** compared to **1**.

Higham *et al.*¹¹⁴, in a paper published during the course of the present study, have shown that the air stability of primary phosphanes may be predicted by their electronic nature using DFT calculations. Primary phosphanes have been known to be stabilised through steric protection around the hydride centre or appropriate conjugation incorporated in the molecular skeleton. The DFT calculations on the air stable primary phosphanes with no steric protection around the hydride centre have shown that they are predicted to have the highest occupied molecular orbital (HOMO) energy of neutral phosphanes and also singly occupied molecular orbital (SOMO) energy of their radical counterparts above -10 eV. They argue that the increases in the HOMO and SOMO energies are through the conjugation or pseudo conjugation through a heteroatom in the molecular skeleton which leads to the shift in the localisation of the neutral molecular HOMO away from the phosphorus.

In order to investigate whether the literature theory¹¹⁴ would agree with the air stability of the primary phosphanes in the present study, the SOMO energies of the primary phosphanes were also calculated using DFT theory according to the literature method¹¹⁴. The DFT calculations were carried out by Dr. J. Lane. The result showed that the primary phosphanes, $\text{Fc}(\text{CH}_2)_n\text{PH}_2$ ($n = 1$ **1**, 2 **23**, 4 **14**, 6 **15**, 11 **16**) and RcCH_2PH_2 **24**, were all predicted to have a value of about -6 eV which is higher than the threshold value of -10 eV between the air-stable and -sensitive phosphanes calculated by Higham *et al.*¹¹⁴, suggesting the primary phosphanes should be kinetically stable in air and it is consistent with the results of the ^{31}P NMR studies. Since the hydride centre of these primary phosphanes is neither sterically protected nor has conjugation to render the HOMO or SOMO energies of the neutral molecules or its radical counterparts, respectively, the air stability of the primary phosphanes must be accounted for non-steric and -conjugation reasons. In the same paper, Higham *et al.* argue that the alkyl spacer group (a $(\text{CH}_2)_2$ group in their study) between the ferrocene and phosphorus in these primary phosphanes may act as “electronic insulator”, leading to the raise in the energy of the radical cation SOMO

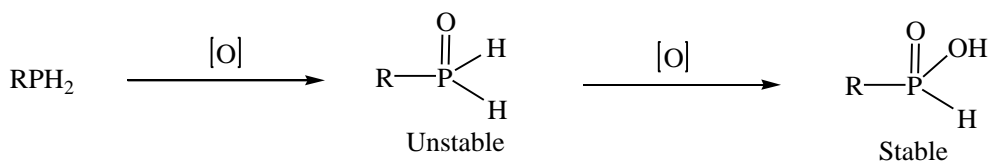
above -10 eV^{114} , stabilising the hydrides. This appears to be consistent with the fact that, regardless of the length of the alkyl spacer, the ferrocenyl primary phosphanes with a $(\text{CH}_2)_n$ ($n = 1^{78}$, 2^{115} , 4, 6 or 11) spacer exhibit remarkable air-stability while FcPH_2 and $1,1'\text{-Fc}'(\text{PH}_2)_2$ without an alkyl spacer are found to be air-sensitive⁷⁹.

Narasimhan *et al.*¹¹⁶ and Stafford *et al.*¹¹⁷ have also shown the involvement of the lone electron pair on the phosphorus in the chemical bonding of the ethyl group to the phosphorus of Et_3P by ^1H NMR. The increase in the energy of the radical cation SOMO of the ferrocenyl and ruthenocenyl primary phosphanes studied in this chapter may, therefore, also be explained by the involvement of the lone electron pair on the phosphorus in the bonding to the CH_2 group, resulting in reduction of the p -orbital character of the lone pair on phosphorus and reactivity towards oxygen and hence the increased air stability of the primary phosphane. A chemical bonding of a CH_2 group to the hydride centre may be important in the air stability of primary phosphanes without steric protection or conjugation in the molecule.

2.2.4.3 ^{31}P NMR Studies into Effect of Ferrocene and FcCH_2PH_2 (1) on Oxidative Stability of PhPH_2 and CamphylPH_2 (2) in Solution

Incorporation of a $\text{Fc}(\text{CH}_2)_n$ group into the hydride centre of air-sensitive primary phosphane has been shown to provide a remarkable air stabilisation to the primary phosphane as, for example, seen for the indefinite air-stability of **1**⁷⁸ and **23**¹¹⁵. Extending the earlier studies^{78, 115} on the stabilisation effect of a $\text{Fc}(\text{CH}_2)_n$ group on primary phosphanes, the subsequent ^{31}P NMR studies were carried out in order to investigate whether air-sensitive primary phosphanes such as PhPH_2 and **2** can also be stabilised in solution by simple addition of ferrocene itself or the derivative **1**.

Primary phosphanes of the type RPH_2 typically oxidise as follows;



Scheme 2-10: Oxidation of primary phosphane of the type RPH_2 ⁹

The primary phosphane is first oxidised to the corresponding phosphane oxide which is unstable and undergoes further oxidation with O_2 to ultimately give the air stable phosphinic acid⁹. The phosphane oxide and phosphinic acid formed can be distinguished by ^{31}P NMR spectroscopy. The signal corresponding to the phosphinic acid often appears further downfield than that of the corresponding phosphane oxide (i.e. $\delta \text{RP}(\text{O})(\text{OH})\text{H} > \delta \text{RP}(\text{O})\text{H}_2$)¹⁰⁷.

Phenyl phosphane, PhPH_2 , was obtained from a commercial source and **2** was synthesised *via* camphyl $\text{P}(\text{O})(\text{OH})\text{H}$ **37** prepared from camphene and hypophosphorous acid according to the literature method¹¹⁸.

2.2.4.4 ^{31}P NMR Study on Oxidative Stability of PhPH_2 in Solution with Added FcH or FcCH_2PH_2 (**1**)

Three NMR samples, consisting of PhPH_2 (“control”), 1 : 0.48 of PhPH_2 and ferrocene, and 1 : 0.37 of PhPH_2 and **1**, were prepared by placing ferrocene and **1** in separate clean and dry NMR tubes and dissolving them in CDCl_3 followed by addition of PhPH_2 under an N_2 atmosphere. After sealing the tubes with plastic NMR lids, they were removed from the inert atmosphere into air. The first $^{31}\text{P}\{-^1\text{H}\}$ NMR spectra were immediately recorded after the preparations. The oxidation of PhPH_2 in the samples was monitored by $^{31}\text{P}\{-^1\text{H}\}$ NMR spectroscopy until fully oxidised (disappearance of the signal). During the intervals, the samples were placed on a bench at room temperature in air with their lids on.

The PhPH_2 in the control sample was spontaneously oxidised. After 14 days, more than half of the PhPH_2 had been oxidised and, after approximately 2 months, the ^{31}P NMR signal could not be observed (Figure 2-48).

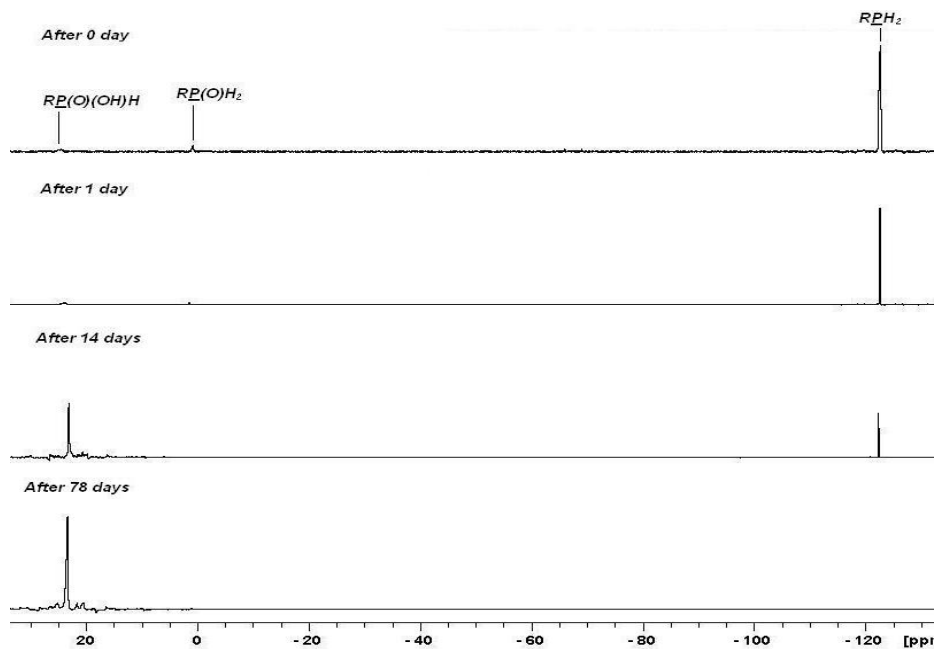


Figure 2-48: $^{31}\text{P}\{-^1\text{H}\}$ NMR spectra showing the oxidation of PhPH_2 in solution at room temperature over 78 days

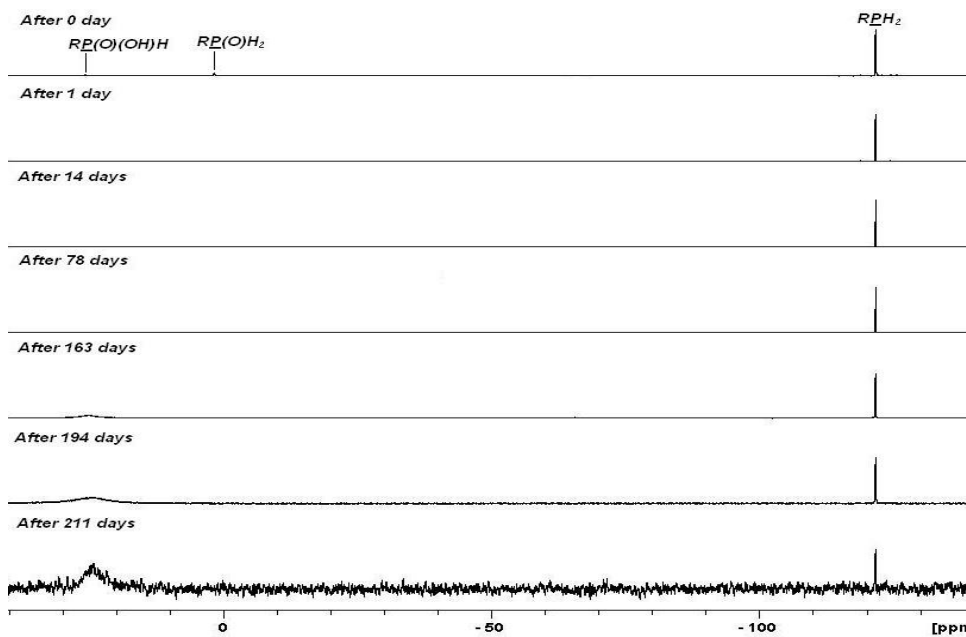


Figure 2-49: $^{31}\text{P}\{-^1\text{H}\}$ NMR spectra showing the oxidation of PhPH_2 in solution at room temperature in air with a 0.48 molar equivalent of added FcH

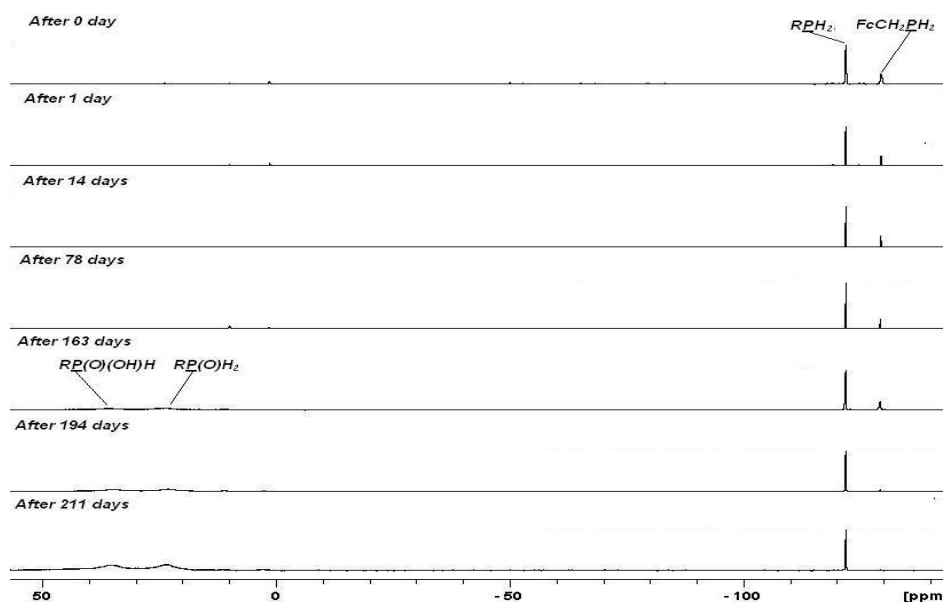


Figure 2-50: $^{31}\text{P}\{-^1\text{H}\}$ NMR spectra showing the oxidation of PhPH_2 in solution at room temperature in air with a 0.37 molar equivalent of **1** added

By contrast, the oxidation of the PhPH_2 in solution with ferrocene or **1** added was significantly slowed (Figure 2-49 & Figure 2-50). They were significantly stable for at least 163 days and then the significant amount of the oxidised products started to appear in their spectra (Figure 2-49 & Figure 2-50).

While it took a little over 2 weeks for more than half of the control to oxidise, those with more than 2 molar equivalent of ferrocene or **1** added remained significantly stable, showing little oxidation over a period of 6 months. The result of these NMR experiments suggests that PhPH_2 and other air-sensitive primary phosphanes in solution may be stabilised by simply addition of ferrocene or **1**. The amounts of ferrocene and **1** used in these experiments were experimental. Much fewer amounts might also be able to stabilise the phosphane.

2.2.4.5 ^{31}P NMR Study on Oxidative Stability of Camphyl PH_2 (**2**) in Solution with Added FcH and (**1**)

As an extension of the experiment above, an analogous ^{31}P NMR experiment was also carried out on another air-sensitive primary phosphane, Camphyl PH_2 **2**, in order

to investigate whether or not the ferrocene stabilisation effect would be extended to other air-sensitive primary phosphanes. Three NMR samples consisting of **2** (“control”), **2** and ferrocene, and **2** and **1**, were prepared analogously as in 2.2.4.4. Ferrocene and **1** were placed in separate clean dry NMR tubes and dissolved in CDCl_3 in air. The primary phosphane **2** was then added to each tube under an N_2 atmosphere. After sealing the tubes with plastic NMR lids, they were removed from the inert atmosphere into air. The first $^{31}\text{P}\{-^1\text{H}\}$ NMR spectrum was immediately recorded after the preparations. The oxidation of **2** was monitored also analogously to the earlier experiment i.e. 2.2.4.4, by $^{31}\text{P}\{-^1\text{H}\}$ NMR spectroscopy until fully oxidised (disappearance of the signal). During the intervals, the samples were placed on a bench at room temperature in air with their lids on.

More than a half of the primary phosphane **2** in the control sample was oxidised after about 2 months under the given conditions and the ^{31}P NMR signal could not be observed after ~6 months (Figure 2-51 & Figure 2-52).

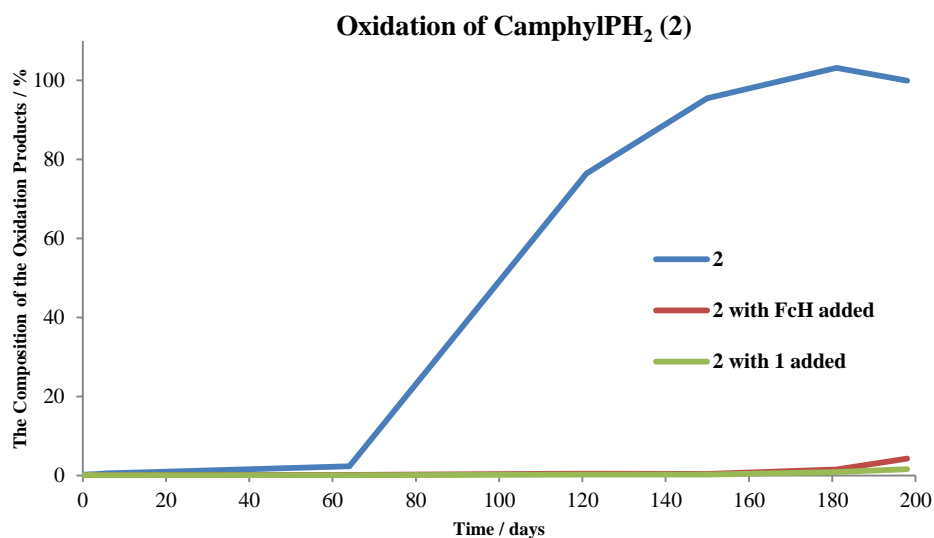


Figure 2-51: Oxidation Progress of **2** in CDCl_3 at room temperature in air with FcH or **1** added

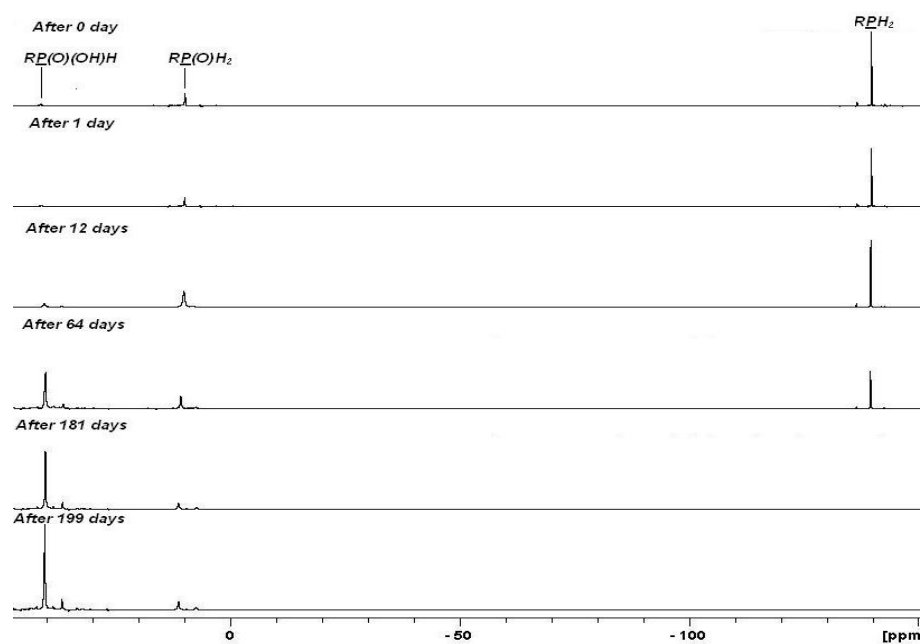


Figure 2-52: $^{31}\text{P}\{-^1\text{H}\}$ NMR spectra showing the oxidation of **2** in solution at room temperature in air

However, the oxidation of **2** in solution was again significantly slowed by addition of ferrocene or **1**. Those with FcH and **1** were moderately oxidised during the first 6 months by which time the control was fully oxidised (Figure 2-53 & Figure 2-54).

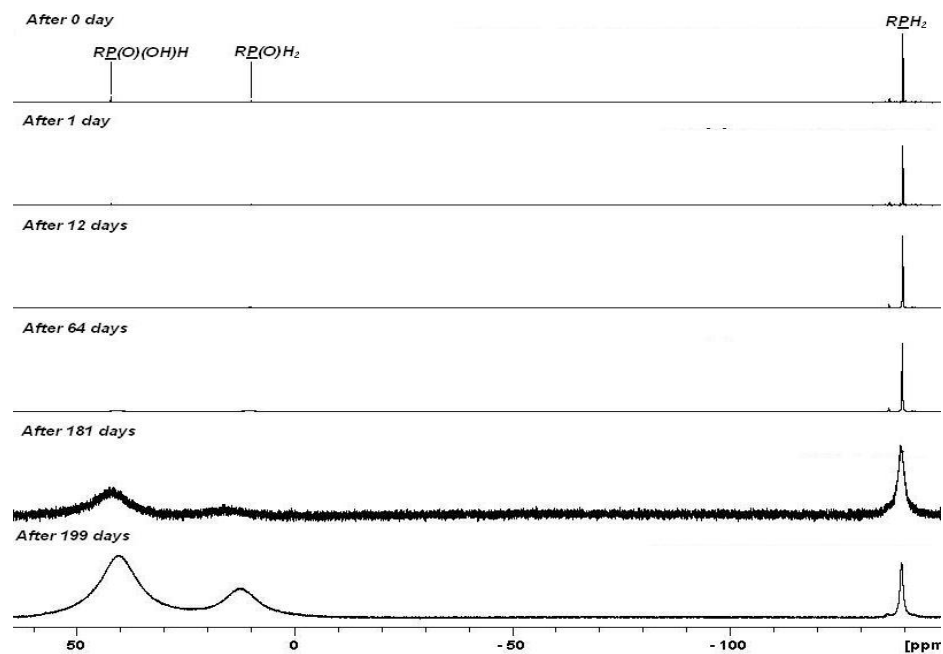


Figure 2-53: $^{31}\text{P}\{-^1\text{H}\}$ NMR spectra showing the oxidation of **2** in solution at room temperature in air with FcH added

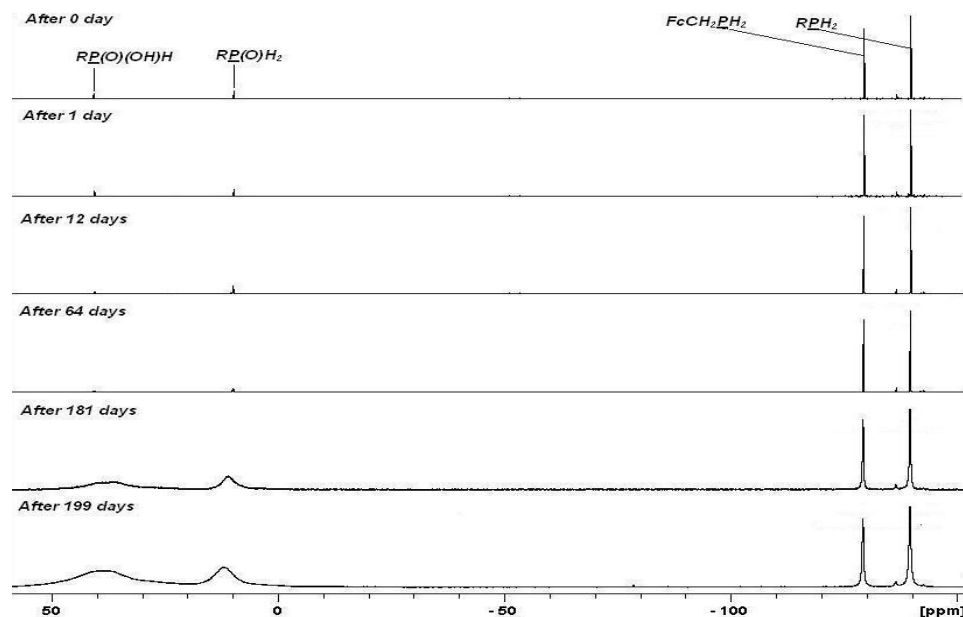


Figure 2-54: $^{31}\text{P}\{-^1\text{H}\}$ NMR spectra showing the oxidation of **2** in solution at room temperature in air with **1** added

The oxidation rate of **2** with ferrocene or **1** added appears the same. Therefore, it seems that FcH and the ferrocenyl moiety of **1** play a key role in this stabilisation effect. The oxidative stability of **2** in solution was significantly improved by addition of FcH and **1**. Therefore, it may be concluded that ferrocene-based stabilisation effect can be extended to **2** and possibly to other air-sensitive primary phosphanes.

2.2.4.6 ^{31}P NMR Study on Oxidative Stability of PhPH_2 in Solution with Added Antioxidants

Since the ^{31}P NMR studies on the stability of the primary and secondary phosphanes towards air oxidation all seemed to indicate that the oxidation of the phosphanes underwent *via* free radical pathways by the presence of the induction and rapidly oxidising periods in their graphs, in order to investigate whether or not the oxidation of PhPH_2 could also be inhibited by addition of antioxidant, this ^{31}P NMR study was carried out. Two known antioxidants, nitrosobutane and 2,2-diphenyl-1-picrylhydrazyl free radicals, DPPH, were used in the study because were available in the lab. Three NMR samples were prepared as before. Either of the antioxidants was

added in place of FcH or **1**. The oxidation of PhPH₂ in each sample was monitored by ³¹P-¹H NMR spectroscopy as before for the period of 3 months.

During the sample preparations, the colour changes of the solutions of PhPH₂ with either DPPH or nitrosobutane added in CDCl₃ were observed. After 10 minutes of PhPH₂ being added to the CDCl₃ solution of DPPH, the solution turned brown from purple. A brown solid was also precipitated out and the precipitation continued throughout the course of the experiment. Also, when PhPH₂ was added to the CDCl₃ solution of nitrosobutane, the solution turned colourless from blue overnight. The study was, nonetheless, continued because the ³¹P NMR signal for PhPH₂ in each sample could still be observed, indicating that there were still significant amounts left in both the samples.

As in the earlier experiments, PhPH₂ in the control sample was spontaneously oxidised and more than half of PhPH₂ was oxidised after 3 months (Figure 2-55). On the other hand, for the same period, the oxidations of PhPH₂ in the samples with the antioxidants added were almost negligible. Almost no or little oxidation could be observed for those samples (Figure 2-56 & Figure 2-57).

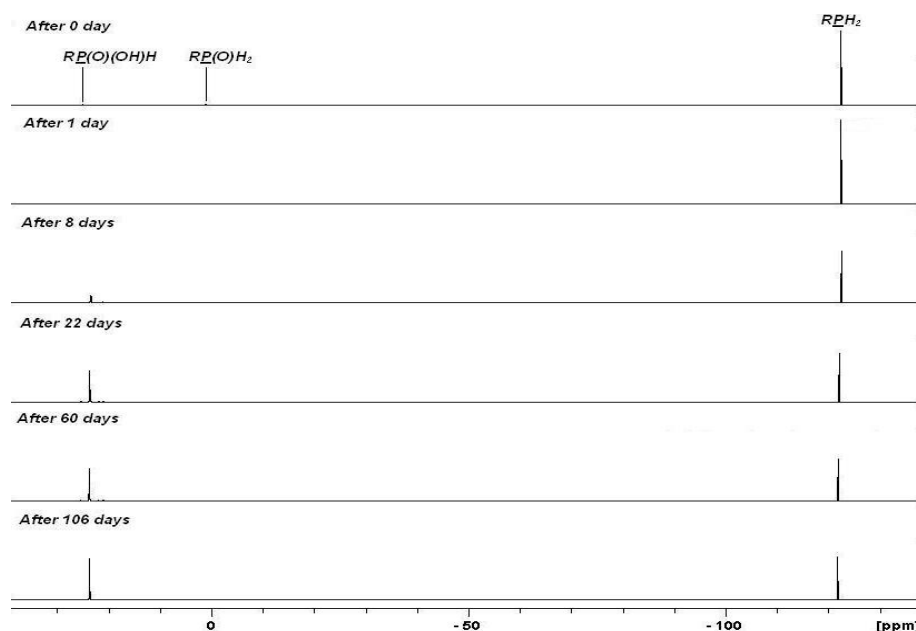


Figure 2-55: ³¹P-¹H NMR spectra showing the oxidation of PhPH₂ in solution at room temperature

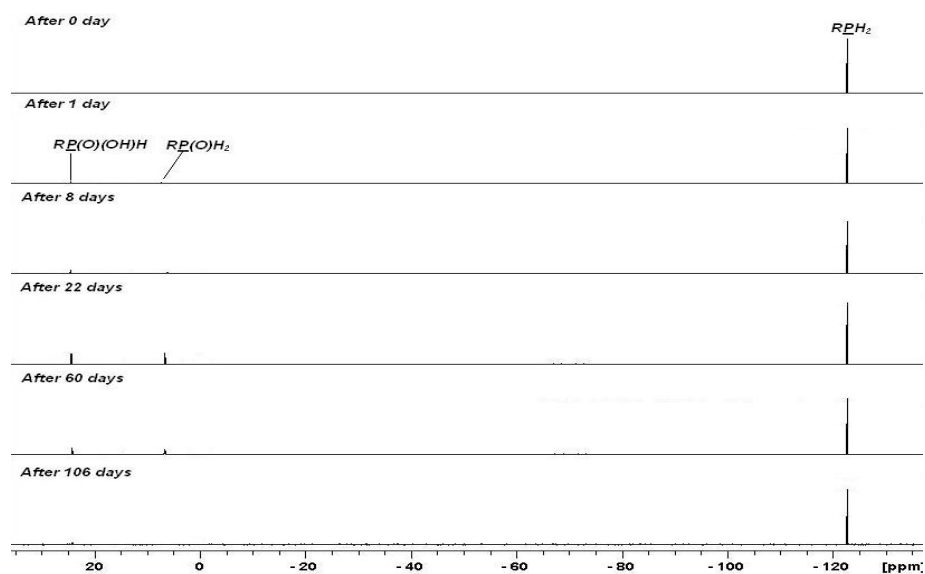


Figure 2-56: $^{31}\text{P}\{-^1\text{H}\}$ NMR spectra showing the oxidation of PhPH_2 in solution at room temperature with added nitrosobutane

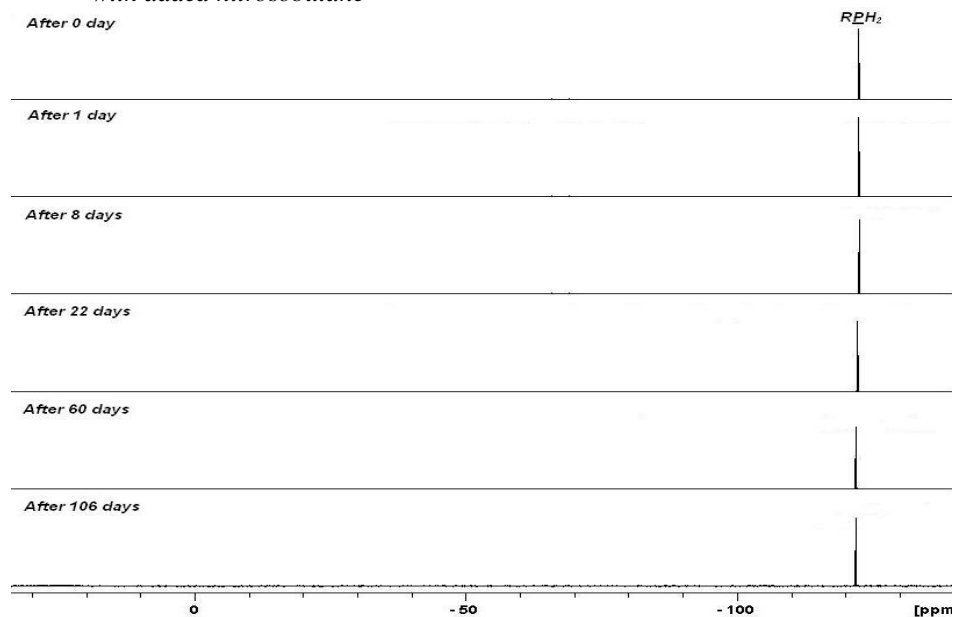
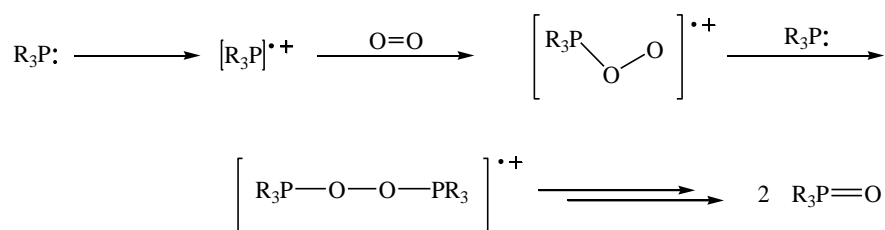


Figure 2-57: $^{31}\text{P}\{-^1\text{H}\}$ NMR spectra showing the oxidation of PhPH_2 in solution at room temperature with added DPPH

The result may suggest that the oxidation of PhPH_2 can also be inhibited by addition of an antioxidant and is consistent with the free radical cation mechanism theory for the oxidation of primary phosphanes suggested by Higham¹¹⁹ and others¹¹⁴. The oxidation of primary phosphanes proceeds *via* the formation of a free radical cation, $[\text{R}_3\text{P}]^+$, which reacts further with molecular oxygen, generating a peroxy radical, $[\text{R}_3\text{PO}_2]^\cdot$, to ultimately give 2 moles of phosphane oxide, $\text{R}_3\text{P}(\text{O})$, (Scheme 2-11)¹¹⁹.



Scheme 2-11: Proposed photolytic oxidation mechanism of primary phosphane of the type RPH_2 by Higham et al.^{114, 119}

The result of the ^{31}P NMR experiment with the antioxidants was consistent with the free radical cation mechanism theory for the oxidation of primary phosphanes (Scheme 2-11)^{114, 119}. The formation of a free radical cation may be inhibited by a radical inhibitor so that the further oxidation cannot proceed, giving rise to the significantly improved oxidative stability of the otherwise very air-sensitive primary phosphane.

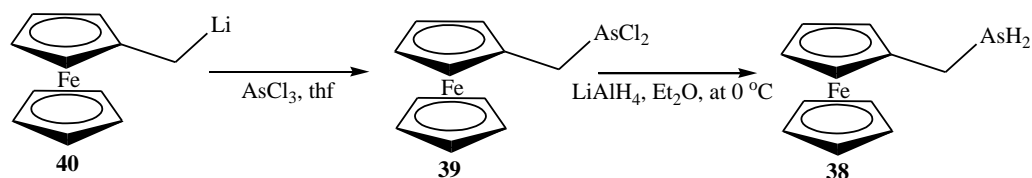
Ferrocene and some ferrocene derivatives have been implicated in free radical mechanisms¹²⁰. The results of the ^{31}P NMR studies on the stability of PhPH_2 and **2** towards air oxidation with either ferrocene or **1** added may, therefore, suggest that ferrocene and **1** can act as free radical inhibitor, preventing the corresponding free radical cations, $[\text{RPH}_2]^+$, from forming or further reacting to ultimately give the oxides, $\text{RP}(\text{O})\text{H}_2$, leading to the remarkably improved air-stability of the primary phosphanes (Scheme 2-12).

molar equivalent, respectively, or an antioxidant, DPPH or nitrosobutane, i.e. 0.13 and 0.69 molar equivalent, respectively, to the solution of PhPH₂. While the spontaneous oxidation of PhPH₂ (δ -122.3 ppm) without either of the additives was observed by the increase in the amounts of the corresponding oxides, PhP(O)H₂ (δ 9.6 ppm) and PhP(O)(OH)H (δ 34.2 ppm) by ³¹P NMR spectroscopy, the oxidation of PhPH₂ with either of the additives was significantly slowed, showing no or little oxidation for more than 3 months by which time the PhPH₂ in the control sample had been almost fully oxidised. The amounts of the additives used were experimental. Much fewer amounts of them might also be able to stabilise the phosphane as effectively.

2.2.5 Synthesis and Characterisation of Ferrocenylmethyl Arsane (38)

Primary arsanes are generally prepared by reduction of any arsenical containing a single R group bonded to arsenic with a suitable reducing agent. Reduction of arsonic and arsenic acids, or their salts, with zinc dust and hydrochloric acid is one of the most satisfactory preparation for primary arsanes¹². Other arsenicals including halo- or dihaloarsanes, arseno compounds or diaryl- or dialkylarsenic oxides are also known to be reduced equally well¹².

With reference to the syntheses of related arsenic compounds^{121, 122}, FcCH₂AsH₂ **38**, could be prepared by the reaction of the corresponding dichloroarsine, FcCH₂AsCl₂ **39**, which was also new and could be prepared by the reaction of the known FcCH₂Li^{122, 123} **40** and AsCl₃, with LiAlH₄ in dry Et₂O at 0 °C under an inert atmosphere. The syntheses are summarised in Scheme 2-13.



Scheme 2-13: Synthesis of **38** via **39**

2.2.5.1 Synthesis and Characterisation of $\text{FcCH}_2\text{AsCl}_2$ (**39**)

Synthesis: Compound **39** was prepared by reaction of **40** with AsCl_3 in dry THF at room temperature under an Ar atmosphere. Removal of the reaction solvent under reduced pressure afforded the crude **39** as a dark brown oil. The crude product was extracted with dry Et_2O and the insoluble materials were filtered with a #4 frit under an inert atmosphere. Removal of the solvent gave **39** as a brown oil. Attempted purification of the brown oil by recrystallisation from a mixture of hexane/ Et_2O at $-18\text{ }^\circ\text{C}$ gave no precipitate. Further purifications were not carried out because of the high moisture-sensitivity of the dichloroarsine **39**. Therefore, the dichloroarsine was used as obtained in the subsequent reaction.

Characterisation: Compound **39** was characterised by ^1H and $^{13}\text{C}\{-^1\text{H}\}$ NMR spectroscopy and ESI-MS. The NMR data were consistent for the class of compounds concerned^{124, 125}. The 2-D NMR data including HMBC and HSQC NMR data are also consistent with the structure of the expected compound (Figure 2-58). The selected $^{1,2,3}J_{\text{CH}}$ correlations observed in the HMBC and HSQC NMR experiments are shown Figure 2-58. Assignments were made according to the 2-D NMR data (Table 2-16).

Table 2-16: ^1H and ^{13}C NMR chemical shifts for **39**

δ / ppm	39
^1H NMR	
H_2	4.24 (unresolved m, 2 H)
H_3	4.23 (unresolved m, 2H),
H_4	4.22 (s, 5H),
H_5	3.6 (s, 2H),
$^{13}\text{C}\{-^1\text{H}\}$ NMR	
C_1	78.7 (C)
C_2	69.6 (CH),
C_3	69.0 (CH),
C_4	69.1 (CH)
C_5	46.7 (CH_2),

For atom labelling, see Figure 2-35.

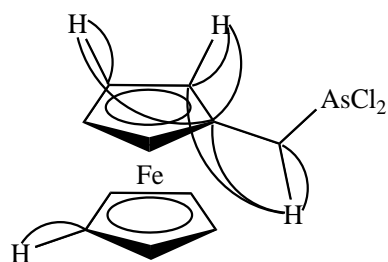


Figure 2-58: Selected $^{1,2,3}J_{CH}$ correlations observed for **39** in the HMBC and HSQC NMR experiments

The methylene proton signal was observed at δ 3.6 ppm which was consistent with the literature value for $\text{PhCH}_2\text{AsCl}_2$ i.e. δ 3.8 ppm¹²⁴. The signal was shifted little further upfield than the corresponding signal for $\text{PhCH}_2\text{AsCl}_2$ which was also consistent with the greater electron-withdrawing and hence deshielding effect of the benzyl moiety than a ferrocenylalkyl one. The Cp proton and carbon NMR signals could also be observed in the expected regions for the respective signals.

ESI mass spectrometry was carried out in CH_3CN as a mobile phase. At a capillary exit voltage of 100 V, the molecular ion could be observed as $[M - \text{Cl}]^+$ in the positive ion mode. The observed and calculated m/z values also agreed (Figure 2-59).

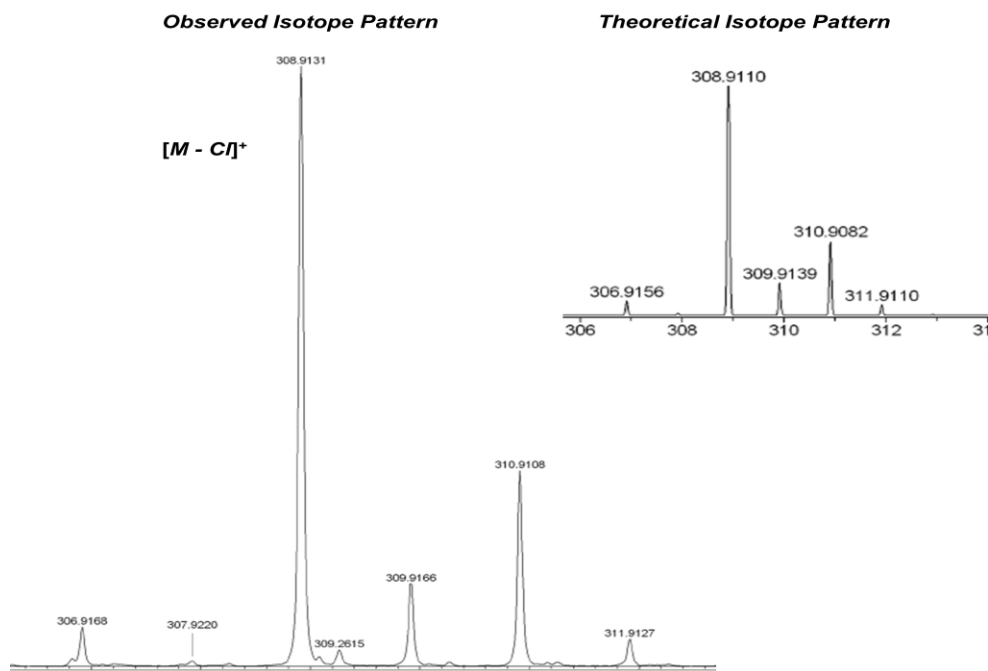


Figure 2-59: Partial ESI-MS of **39** showing the observed and theoretical $[M - \text{Cl}]^+$ ion ($M = \mathbf{39}$)

Compound **39** appeared to be unstable under ambient conditions. It may probably be moisture-sensitive as expected for the type of compounds concerned i.e. main group element chlorides¹². The decomposition of **39** was observed by NMR spectroscopy by the disappearance of the corresponding signals and also by darkening of the solution of the NMR sample after 18 h at room temperature in air. Satisfactory microanalytical data or a single crystal for X-ray crystallographic structural determination could not be obtained.

2.2.5.2 Synthesis of FcCH₂AsH₂ (**38**)

Reduction of **39** with LiAlH₄ in Et₂O at 0 °C under an N₂ atmosphere afforded a yellow oil after removal of the solvent from the reaction mixture under reduced pressure. The crude product was extracted with dry hexane and the insoluble materials were filtered with a #4 frit under an N₂ atmosphere. Removal of the solvent from the organic extract under reduced pressure gave **38** as a yellow oil in moderate yield (40 %). The work-up by removal of the excess LiAlH₄ using aqueous HCl resulted in much poorer yield (~5 %).

Attempted purification of **38** was also unsuccessful. GC-MS indicated that the crude product contained **38** but also other unwanted by-products i.e. FcCH₃ and FcCH₂CH₂Fc. Chromatography of the crude product on a preparative TLC plate, eluting with light petroleum spirits gave three yellow bands. The yellow bands were collected separately and analysed by ¹H NMR spectroscopy. The yellow oil obtained from the fraction at R_f 0.77 contained **38**. GC-MS showed that there were still some FcCH₃ left that could not be isolated during the purification, and **38**. Attempted purification by recrystallisation of the yellow oil from CH₂Cl₂/light petroleum spirits or hexane at -18 °C yielded a yellow solid. The yellow solid was, however, too fine to collect even with a #4 sintered glass or by centrifugation the exposure to air during which decomposed the compound into a grey solid.

2.2.5.3 Characterisation of FcCH₂AsH₂ (**38**)

Compound **38** was characterised by ¹H and ¹³C-¹H NMR, IR spectroscopy and ESI-MS. The selected spectroscopic data are summarised in Table 2-17. Those for FcCH₂CH₂AsH₂ **41**⁷⁹ are also included for comparative purposes.

Table 2-17: Selected spectroscopic data for **38** and **41**

	38	41 ⁷⁹
IR / ν cm ⁻¹	2088	Not given.
GC-MS / m/z	[M] ⁺	[M] ⁺
¹ H NMR / δ ppm	2.5 (AsH ₂ , t, ³ J _{HH} = 6 Hz)	2.2 (AsH ₂ , t, ³ J _{HH} = 6 Hz)
¹³ C- ¹ H NMR / δ ppm	12.6 (AsCH ₂)	14.02 (AsCH ₂)

The spectroscopic data were consistent with those expected for the type of compounds concerned¹²⁵. In the IR spectrum, the As-H stretch was observed at 2087 cm⁻¹ as a medium peak (cf. ~ 2100 cm⁻¹ for RAsH₂¹²) (Figure 2-60).

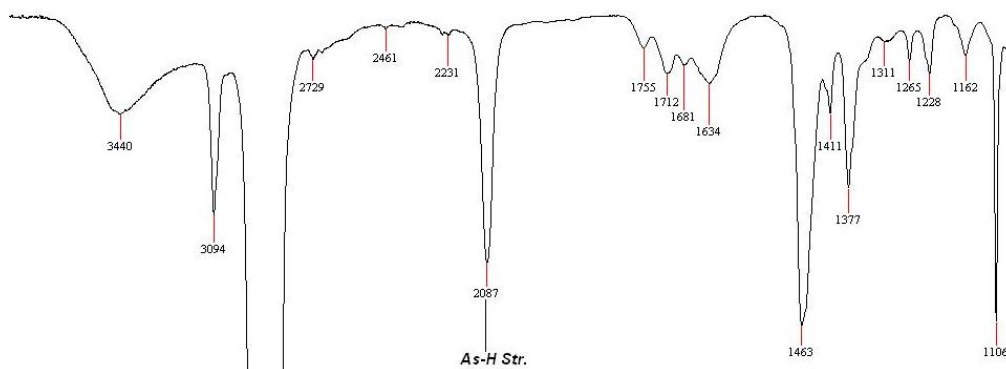


Figure 2-60: IR spectrum of **38**

In the ¹H NMR spectrum, the arsane proton signal appeared at δ 2.5 ppm as a triplet with a ³J_{HH} coupling constant of 6 Hz. The signal was shifted further downfield by about δ 0.3 ppm than that for **41** whose signal appeared at δ 2.2 ppm also as a triplet. The shift of the methylene proton signal further downfield is consistent with the shorter distance between ferrocene, which is deshielding, and the arsane protons and the same trend was observed for the corresponding primary phosphanes (cf. δ 2.62 *v.s.* δ 2.57 ppm for **1**⁷⁸ and **23**⁷⁹, respectively). The ³J_{HH} coupling constant of 6 Hz also agrees with that for **41**. The ¹³C and the 2-D NMR data were also consistent with the structure of the expected compound. The selected ^{2,3}J_{CH} correlations observed for **38**

in the HMBC, HSQC and COSY NMR experiments are shown in Figure 2-61. The assignments of the chemical shifts were made according to the 2-D NMR data and summarised in Table 2-18.

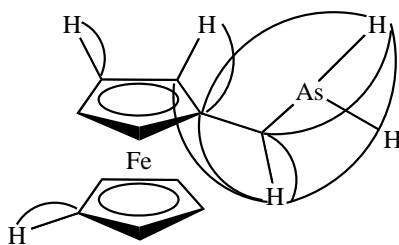


Figure 2-61: Selected $^{2,3}J_{CH}$ Correlations Observed for **38** in the HMBC, HSQC COSY NMR Experiments

Table 2-18: 1H and ^{13}C NMR chemical shifts for **38**

δ / ppm	38
1H NMR	
H_2	4.06 (t, $^3J_{HH} = 2$ Hz, 2 H)
H_3	4.02 (t, $^3J_{HH} = 2$ Hz, 2 H)
H_4	4.09 (s, 5 H)
H_5	2.7 (t, $^3J_{HH} = 6$ Hz, 2 H)
AsH_2	2.5 (t, $^3J_{HH} = 6$ Hz, 2 H)
^{13}C - $\{^1H\}$ NMR	
C_1	89.7 (C)
C_2	67.6 (CH)
C_3	67.3 (CH)
C_4	68.8 (CH)
C_5	12.6 (CH ₂)

For atom labelling, see Figure 2-35.

Mass spectrometric data could be obtained both by GC- and ESI-MS. In the GC-mass spectrum, the $[M]^+$ ion as well as those corresponding to the fragmentation of the parent molecule i.e. $[FcCH_2]^+$, $[CpFe]^+$ and $[Fe]^+$, which were also seen for **41**⁷⁹, were observed (Figure 2-62).

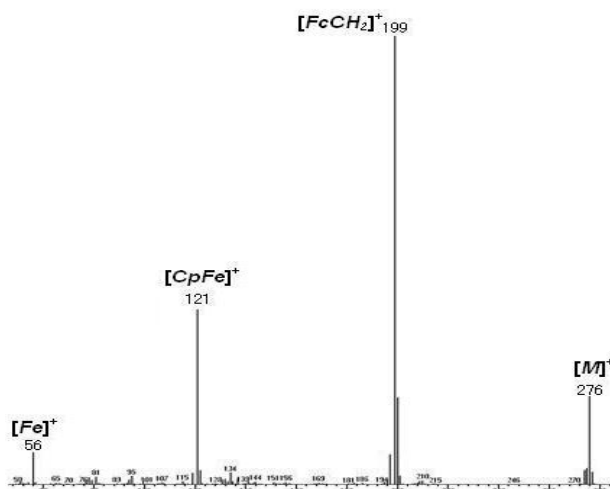


Figure 2-62: GC-MS of **38**

ESI-MS was carried out in MeOH as a mobile phase. At a capillary exit voltage of 90 V, the parent ion, $[M]^+$, was observed in positive ion mode (Figure 2-63). Attempts were made to generate a silver adduct *in situ*. It was, however, unsuccessful.

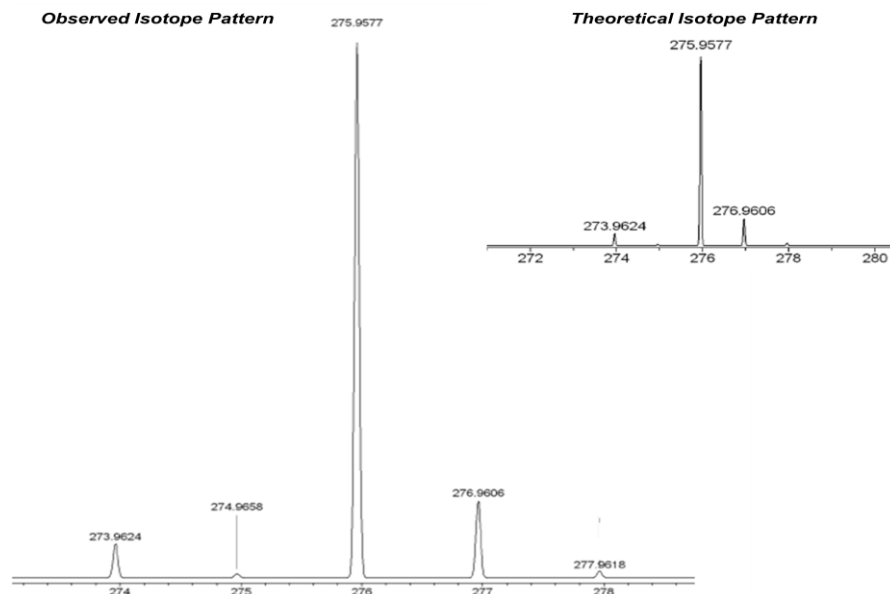
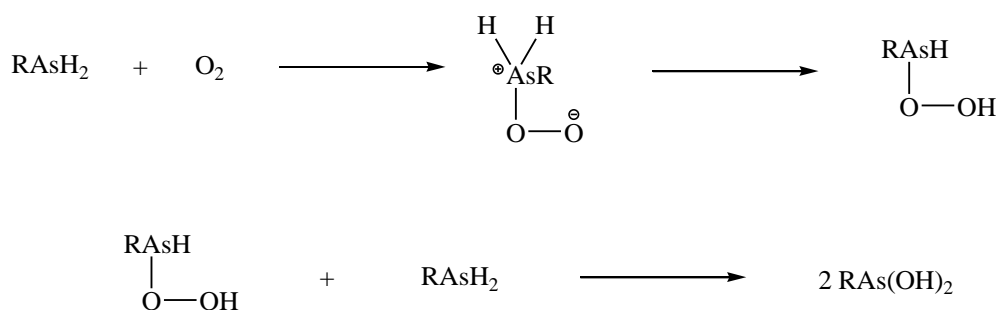


Figure 2-63: Partial ESI-MS of **38** showing the observed and theoretical $[M]^+$ ion ($M = 38$)

2.2.5.4 Air-Stability of $\text{FcCH}_2\text{AsH}_2$ (**38**)

The oxidation products of primary arsanes may be either arseno or arsenoso compounds or arsonic acids¹². It is thought that the oxidation of primary organoarsanes of the type RAsH_2 proceeds in a similar manner (Scheme 2-14) to many other organometallic compounds. Attack of oxygen molecule on the arsenic results in the formation of peroxide which will then be reduced by unreacted arsane to give the arsonic acid¹².



Scheme 2-14: *Postulated oxidation of RAsH₂ with O₂*

While the ethyl analogue, $\text{Fc}(\text{CH}_2)_2\text{AsH}_2$ **41**, had been reported as air-stable⁷⁹, compound **38** was surprisingly air-sensitive although it may be much more stable than typical aliphatic or aromatic primary arsanes such as PhAsH_2 , Me_2AsH and Et_2AsH which are often extremely reactive, either spontaneously flammable or rapidly oxidised in air¹². The strongest intensity of the arsane or methylene proton signals by NMR spectroscopy or of the IR band for the As–H stretch for **38** was always observed for the crude product of a freshly prepared sample before any work-up. Significant oxidation occurred during work-up or purification in air. The arsane proton signal and the band corresponding to the As–H stretch in the IR spectrum both weakened after the work-up handling in air. The arsane proton NMR signal completely disappeared after 24 days in solution at room temperature in air with a plastic NMR cap on (Figure 2-64).

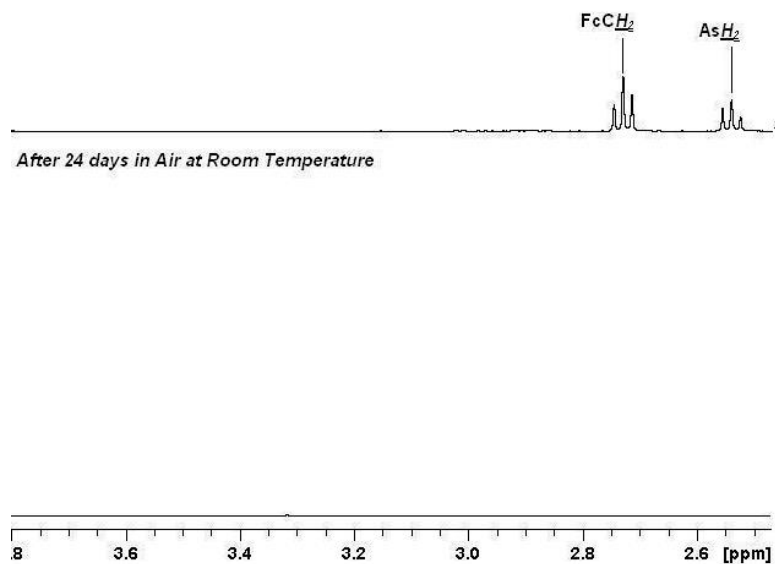
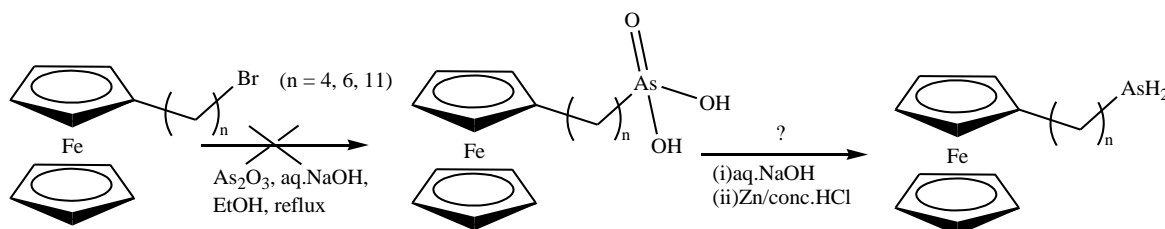


Figure 2-64: ¹H NMR spectrum showing the complete oxidation of **38** in CDCl₃ after 24 days at room temperature in air

2.2.5.5 Attempted Synthesis of Fc(CH₂)_nAsH₂ (n = 4 (**42**), 6 (**43**) and 11 (**44**))

Attempted preparations of ferrocenyl primary arsanes with extended CH₂ spacers i.e. butyl **42**, hexyl **43** and decyl **44**, by reaction of the corresponding arsonic acids under Zn/HCl conditions following the literature methods^{12, 79, 126} used for the synthesis of FcCH₂CH₂AsH₂ **41** were unsuccessful (Scheme 2-15). Despite the attempts, the preparation of the corresponding arsonic acids by reaction of the respective ferrocenylalkyl bromide with As₂O₃ in aq. NaOH with few drops of EtOH as a co-solvent⁷⁹ proved to be difficult. No precipitation of a yellow solid upon acidification of the reaction mixture with aq. HCl after refluxing for 20 h in aq. NaOH could be observed. Neither the increased amount of EtOH to aid solubilisation of the bromides in the aqueous solvent in which they were very poorly soluble, nor the prolonged reaction time gave the desired arsonic acids. Only unreacted bromides were recovered after the reactions. Neither ¹H NMR spectroscopy nor ESI-MS suggested the formation of the desired arsonic acids at any stage of the synthesis. Further reactions

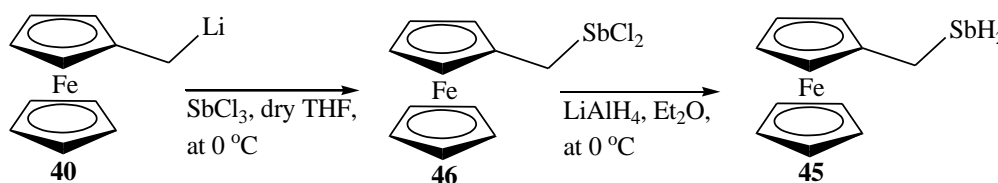
of the residues obtained from the above attempted syntheses in order to see if the desired arsonic acids did form or not, with Zn/HCl in distilled H₂O and light petroleum spirits were carried out. They did, however, not yield the desired arsanes either. The spectroscopic analyses using ¹H NMR spectroscopy and ESI-MS did not suggest the formation of the desired arsanes.



Scheme 2-15: Attempted synthesis of **42**, **43** and **44** by reduction of the corresponding arsonic acids with Zn/HCl

2.2.6 Attempted Synthesis of Ferrocenylmethyl Stibane (**45**)

Attempts were also made to synthesise ferrocenylmethyl stibane, FcCH₂SbH₂ **45**, analogously to the corresponding arsane **38**. Scheme 2-16 shows the attempted synthesis of **45** via FcCH₂SbCl₂ **46**.



Scheme 2-16: Attempted synthesis of **45** via **46**

2.2.6.1 Attempted Synthesis of FcCH₂SbCl₂ (**46**)

The reaction of **40** with SbCl₃ in dry THF at 0 °C under an Ar atmosphere yielded a brown oil after removing the solvent under reduced pressure. Attempts to obtain the spectroscopic data for the residue were not very successful. The resolution of the ¹H NMR spectrum was very poor maybe due to the impurities such as excess SbCl₃, THF, paramagnetic impurities from Fc oxidation to Fc⁺ which broadens NMR spectra

or other undesired side-products in the sample. In order to confirm the formation of **46**, it was further reacted without further purification with LiAlH₄ in Et₂O at 0 °C. The corresponding primary stibane **45** could, however, not be obtained or the formation could not be confirmed spectroscopically.

2.2.6.2 Attempted Synthesis of FcCH₂SbH₂ (**45**)

The reduction of the crude **46** obtained as above with LiAlH₄ in dry Et₂O at 0 °C under an N₂ atmosphere quantitatively deposited a metallic black solid (metallic mirror) on the wall of the reaction vessel. After removing the insoluble materials with a #4 frit under an N₂ atmosphere, removal of the reaction solvent at 0 °C gave a yellow semi-solid. Despite the attempts, the yellow semi-solid could not be identified; ESI-MS, IR and NMR spectroscopy did not show the formation of the desired compound **45**.

Primary stibanes appear to commonly ionise, losing a hydrogen to give a positively charged ion, $[M - H]^{+125}$. ESI-MS on the yellow semi-solid using MeOH as a mobile phase at capillary exit voltage of 50 V in positive ion mode did not show ions which could be assigned for **45**.

Even though only a limited number of IR spectra of primary and secondary stibanes have been reported, the Sb-H stretch for dibutylstibane and diphenylstibane is known to occur at 1847 and 1835 cm⁻¹, respectively, as an intense band¹². Other literature Sb-H stretching frequencies include 1842 – 45 and 1850 cm⁻¹ for dicyclohexyl- and di-*tert*-butylstibane, respectively¹²⁷. The Sb-H stretch for the type RSbH₂¹²⁵ is also suggested to occur at ~1880 cm⁻¹. Therefore, no band which could be assigned for the Sb-H stretch of **45** was observed in the IR spectrum of the reaction residue. Useful NMR data could not be obtained on the reaction residue either.

2.3 Conclusion

A series of new ferrocenyl phosphanes with extended CH₂ spacers between the cyclopentadienyl ring and the hydride centre **3**, **4**, **5**, **14**, **15**, **16**, **20**, **21**, **22** and **24** and ferrocenylmethyl phosphane oxide **30** and phosphinic acid **36** were prepared by application of the literature methods with minor modifications. For all the phosphanes, the intense distinctive phosphane odour was noted. The ferrocenyl primary, secondary and hydroxymethyl phosphanes were isolated as yellow-red oils with yields ranging from moderate to excellent. The primary phosphane **16** could be isolated as a yellow solid after recrystallisation. Also, the phosphane oxide and phosphinic acid were obtained as yellow solids. In the syntheses of the secondary phosphanes, over-alkylated tertiary phosphanes, which were also new compounds, were commonly isolated in minor amounts as by-products. Some of them could be fully characterised but the others could not because of the insufficient amounts of the samples. Although the phosphanes were relatively unstable i.e. decomposed in solution over weeks, they could be purified by chromatography with a preparative TLC plate, eluting with light petroleum spirits or an appropriate mixture of organic solvents, and/or by recrystallization in air. Despite the attempts, obtaining satisfactory samples for some of the desired secondary and primary phosphanes was challenging. Satisfactory microanalytical data could only be obtained for **3**, **4**, and **14** although the NMR spectra of the samples sent for the analyses i.e. ³¹P-{¹H}, ¹H and ¹³C-{¹H} NMR spectra, were relatively clean. The compounds were, however, well characterised spectroscopically.

The secondary phosphanes were less air stable. The oxidative stabilities of the secondary phosphanes ranged from several weeks to months probably depending on the substituent on the phosphorus. The more electron-withdrawing the R group was the less stable the phosphane became (R = -CH₂C₆H₄NO₂ < -CH₃ < -C₆H₁₁).

The primary phosphanes all exhibited remarkable air-stability under ambient conditions. They were stable in solution at room temperature for more than 5 months

with little oxidation. There appears to be no or little correlation between the oxidative stabilities of the phosphanes and length of the alkyl chains.

³¹P NMR Studies on the Oxidative Stabilities of PhPH₂ and 2 in Solution: By simply adding ferrocene or **1** to the solutions, the air-sensitive primary phosphanes, PhPH₂ and **2** could be stabilised. The result of the experiment that PhPH₂ could also be stabilised with the antioxidants nitrosobutane and DPPH was consistent with the free radical cation theory for the oxidation mechanism of primary phosphanes proposed by some researchers^{75, 114}. Since ferrocene and **1** have been implied a free radical mechanism, ferrocene and the ferrocene moiety of **1** may be able to act as radical scavenger, inhibiting the radical chain reaction of primary phosphane oxidation to proceed further thereby stabilising the air-sensitive primary phosphanes.

The attempted syntheses of ferrocenyl arsanes with extended alkyl chains *via* the corresponding arsonic acids were unsuccessful. Only ferrocenylmethyl arsane **38** could be prepared *via* another synthetic route i.e. the corresponding dichloroarsine **39** which was synthesised by reaction of **40** with AsCl₃ in dry THF. Even though the number of ferrocenyl arsane prepared in the present study is very limited, the synthetic route may be applicable for those with extended alkyl chains because of the availability of the corresponding precursors Fc(CH₂)_nOCH₃ (n > 2).

The air stability of the primary arsane **38** was surprisingly low compared to the closely related analogue **41** which had been reported to exhibit a significant stability towards air oxidation. The significant decomposition of **38** was observed during work-up and purification in air by deposition of a grey solid. The attempted synthesis of the corresponding primary stibane **45** was unsuccessful.

2.4 Experimental

2.4.1 Synthesis of Ferrocenylmethyl Secondary Phosphanes; [Fe(η -C₅H₅)(η -C₅H₄CH₂PRH)] (R = C₆H₁₁ (3), CH₃ (4), *p*-CH₂(C₆H₄)NO₂) (5))

2.4.1.1 Synthesis of FcCH₂P(CH₂OH)Cy (7)

KOH (1.61 g, 28.7 mmol) was added to a solution of [(C₆H₁₁)P(CH₂OH)₃]Cl (7.12 g, 29.3 mmol) in MeOH (40 mL). The mixture was stirred for 1 h at room temperature before being added dropwise to a solution of **6** (3.60 g, 9.35 mmol) in MeOH (40 mL). The reaction mixture was heating to reflux for 21 h. After cooling, the solvent was reduced to about 8 mL and distilled H₂O (30 mL), Et₂O (70 mL) and NEt₃ (30 mL) were added. The mixture was stirred for 1 h. The aqueous layer was removed and re-extracted with Et₂O (30 mL). The combined organic layers were washed with distilled H₂O (3 × 20 mL) and then filtered. Removal of the solvent under reduced pressure gave **7** as a red oil (5.25 g, > 100 % contains impurities). ESI-MS (MeOH, cone voltage 20 V, with aq. AgNO₃ added) *m/z* 344 [*M*]⁺, 796 [2*M* + Ag]⁺. ³¹P-{¹H} NMR: δ -11.3 (*P*, s) ppm.

2.4.1.2 Synthesis of FcCH₂P(Cy)H (3)

Na₂S₂O₅ (2.44 g, 12.8 mmol) was added to a solution of **7** (5.25g, 15.3 mmol) in a two-phase solvent system consisting of distilled H₂O (60 mL) and light petroleum spirits (60 mL). The mixture was heating to reflux for 3 h in air. After cooling, the aqueous layer was removed and the organic layer was washed with distilled H₂O (3 × 20 mL). Removal of the solvent from the organic layer under reduced pressure gave a red oil (2.21 g, 75 % based upon the number of moles of **6** used; a trace of (C₆H₁₁)PH₂ was found only in the ³¹P NMR spectrum of the crude product {³¹P NMR: δ -110.2 ppm (*PH*₂, t, ¹*J*_{PH} = 194 Hz)}. The red oil was extracted with a solvent mixture of Et₂O (30 mL) and light petroleum spirits (30 mL) which resulted

in an immediate precipitation of a yellow solid which was collected by filtration, washed with cold Et₂O (2 mL) and identified by ¹H and ³¹P NMR spectroscopy and ESI-MS as **11** (0.15 g, 3 %; decomposition of **11** occurred over the period of 2 weeks in solution (in CDCl₃) at room temperature in a capped NMR tube; ³¹P NMR: δ -7.6 (s) ppm. ¹H NMR: δ 1.2 – 1.8 (C₆H₁₁, unresolved m, 11 H), 2.5 (CH₂, s, 4 H), 4.1 (CH, s, 18 H) ppm. ESI-MS (cone voltage of 20 V, with a drop of aqueous AgNO₃ solution added): *m/z* 620 [*M* + Ag]⁺, 1132 [2*M* + Ag]⁺).

The organic filtrates were combined and the solvents were removed under reduced pressure. The residue was subjected to chromatography with a preparative PLC plate, eluting with Et₂O/hexane (1 : 10). The orange band at R_f 0.91 gave the pure title compound as a red oil (0.55 g, 19 % based on **6** used) which solidifies at -18 °C. Calcd. for C₁₇H₂₃Fe₁P₁: C 64.99; H 7.38 %. Found: C 65.18; H 7.56 %. IR: *ν* 2268s (*P-H str*) cm⁻¹. ³¹P NMR: δ -41.1 (PH, d, ¹*J*_{PH} = 199 Hz) ppm. ¹H NMR: δ 1.3 – 1.7 (C₆H₁₁, unresolved m, 11 H), 2.7 (CH₂, d of m, ²*J*_{PH} = 37 Hz, 2 H), 3.1 (PH, d, ¹*J*_{PH} = 198 Hz), 4.06 (H₃, t, ³*J*_{HH} = 2 Hz, 2 H), 4.09 (H₂, unresolved m, 2 H), 4.1 (H₄, s, 5 H) ppm. ¹³C-{¹H} NMR: δ 19.8 (C_{H2}, d, ¹*J*_{PC} = 13 Hz), 27.0 (CH₂, d, ²*J*_{PC} = 8 Hz), 31.2 (CH₂, d, ¹*J*_{PC} = 7 Hz), 32.0 (br), 67.3 (C₃, s, CH), 68.3 (C₂, unresolved br, CH), 68.8 (C₄, s, CH), 87.0 (C₁, d, ²*J*_{PC} = 5 Hz, C) ppm. ESI-MS (cone voltage of 20 V, with a drop of aqueous AgNO₃ solution added): *m/z* 314 [*M*]⁺, 422 [*M* + Ag]⁺, 736 [2*M* + Ag]⁺.

2.4.1.3 Synthesis of FcCH₂P(Me)H (**4**)

MeI (0.13 mL, 2.08 mmol) was added dropwise to a solution of **8** (0.63 g, 2.16 mmol) in MeOH (15 mL). The mixture was stirred for 15 mins at 50 °C. The solvent was removed under vacuum and distilled H₂O (60 mL), light petroleum spirits (60 mL), NEt₃ (2 drops) and Na₂S₂O₅ (0.47 g, 2.47 mmol) were added sequentially. The mixture was heating to reflux for 3 h in air. After cooling, the aqueous layer was removed and re-extracted with light petroleum spirits (30 mL). The combined organic extracts were washed with distilled H₂O (4 × 20 mL). The solvent was reduced to 8 mL and cooled at -18 °C for 16 h. The yellow precipitate which was not identified

was filtered. The filtrate was concentrated to about 2 mL and subjected to chromatography with a preparative TLC plate, eluting with Et₂O/light petroleum spirits (1 : 10). The yellow band at R_f 0.86 gave the desired compound as a yellow oil (0.17 g, 33 %). Calcd. for C₁₂H₁₅FeP: C 58.57; H 6.14 %. Found: C 59.00; H 6.19%. IR: 2276s (*P-H str*) cm⁻¹. ³¹P NMR: δ -73.5 (PH, d, ¹J_{PH} = 199 Hz) ppm. ¹H NMR: δ 1.7 (CH₃, unresolved m, 3 H), 2.7 (CH₂, d of m, 2 H), 3.1 (PH, d of q, ¹J_{PH} = 194, ³J_{HH} = 4 Hz, 1 H), 4.06 (H₃, t, ³J_{HH} = 2 Hz, 2H), 4.08 (H₂, t, ³J_{HH} = 2 Hz, 2 H), 4.11 (H₄, s, 5 H) ppm. ¹³C-¹H NMR: δ 19.8 (CH₂, d, ¹J_{PC} = 14 Hz), 31.2 (CH₃, d, ¹J_{PC} = 7 Hz), 67.3 (C₃, s, CH), 68.3 (C₂, d, ³J_{PC} = 4 Hz, CH), 68.8 (C₄, s, CH), 87.0 (C₁, d, ²J_{PC} = 6 Hz, C) ppm.

2.4.1.4 Synthesis of FcCH₂P(CH₂C₆H₄NO₂)H (5)

A mixture of **8** (2.04 g, 6.98 mmol) and *p*-O₂NC₆H₄CH₂Br (1.82 g, 8.44 mmol) in MeOH (60 mL) was heating to reflux for 22 h. After cooling, the solvent was removed under vacuum. Distilled H₂O (30 mL), toluene (30 mL), NEt₃ (1 mL) and Na₂S₂O₅ (1.33 g, 7.01 mmol) were added. The mixture was heating to reflux for 5 h. After cooling, the aqueous layer was removed and re-extracted with toluene (60 mL). The combined organic layer was washed with distilled H₂O (5 × 20 mL) and then filtered. Removal of the solvent under reduced pressure gave a red solid (2.43 g). The residue was subjected to chromatography with a preparative TLC plate, eluting with CH₂Cl₂/light petroleum spirits (1 : 1), giving orange and yellow bands. Removal of the solvent of the orange band at R_f 0.57 gave **5** as a red oil (0.46 g, 18 %) which solidifies at -18 °C. Calcd. for C₁₈H₁₈Fe₁N₁O₂P₁: C 58.88; H 4.94; N 3.81 %. Found: C 59.63; H 4.92; N 3.95%. IR: 2278m (*P-H str*) 1515vs (*N-O str*), 1342vs (*N-O str*) cm⁻¹. ³¹P NMR: δ -49.1 (PH, d, ¹J_{PH} = 192 Hz) ppm. ¹H NMR: δ 2.6 (CH₂, m, 2 H), 3.0 (CH₂, m, 2 H), 3.4 (PH, d of p, ¹J_{PH} = 198 Hz, ³J_{HH} = 7 Hz, 1 H), 4.08 (H₃, unresolved m, 2 H), 4.10 (H₂, unresolved m, 2 H), 4.11 (H₄, s, 5 H), 7.3 (CH, d, ³J_{HH} = 8 Hz, 2 H), 8.1 (CH, d, ³J_{HH} = 8 Hz, 2 H) ppm. ¹³C-¹H NMR: δ 21.6 (CH₂, d, ¹J_{PC} = 14 Hz), 28.8 (CH₂, d, ¹J_{PC} = 17 Hz), 68.1 (C₃, s), 68.6 (C₂, d, ³J_{PC} = 4 Hz), 68.9 (C₄, s), 85.6 (C₁, d, ²J_{PC} = 7 Hz), 123.9 (CH, s), 129.3 (CH, d, ³J_{PC} = 4 Hz), 129.5 (C, s),

148.7 (\underline{C} , d, $^2J_{PC} = 3$ Hz) ppm. ESI-MS (MeOH): m/z 367.043 [M]⁺observed; 367.042 calcd. for C₁₈H₁₈Fe₁N₁O₂P₁.

The yellow band at R_f 0.33 gave **12** a red oil (0.02 g, 0.8 %). ³¹P NMR: δ -12.3 (\underline{P} , s) ppm. ¹H NMR: δ 2.5 (\underline{CH}_2 , q of d, $^4J_{HH} = 8$ Hz, 6 H), 4.03 (\underline{CH} , unresolved m, $^3J_{HH} = 2$ Hz, 4 H), 4.06 (\underline{CH} , unresolved m, $^3J_{HH} = 2$ Hz, 4 H), 4.08 (\underline{H}_4 , s, 10 H), 7.3 (\underline{CH} , d of d, $^3,^4J_{HH} = 8, 1$ Hz, 2 H), 8.1 (\underline{CH} , d, $^3J_{HH} = 9$ Hz, 2 H) ppm. ¹³C-¹H NMR: δ 27.9 (\underline{CH}_2 , d, $^1J_{PC} = 19$ Hz), 34.4 (\underline{CH}_2 , d, $^1J_{PC} = 21$ Hz), 67.7 (\underline{CH} , d, $^3J_{PC} = 4$ Hz), 68.9 (\underline{CH} , d, $^4J_{PC} = 3$ Hz), 68.9 (\underline{C}_5 , s, CH), 83.6 (\underline{C}_1 , d, $^2J_{PC} = 10$ Hz), 123.6 (\underline{CH} , s), 129.9 (\underline{CH} , d, $^3J_{PC} = 6$ Hz), 146.2 (\underline{C} , s), 147.0 (\underline{C} , d, $^2J_{PC} = 7$ Hz) ppm.

Another by-product **13** was obtained as a red solid (0.84 g, 24 %) from the orange fraction at R_f 0.66. Calcd. for C₂₅H₂₃Fe₁N₂O₄P₁: C 59.76; H 4.62; N 5.58 %. Found: C 59.79; H 4.78; N 5.71%. IR: 1513vs (*N-O str*), 1343vs (*N-O str*) cm⁻¹. ³¹P NMR: δ -8.7 (\underline{P} , s) ppm. ¹H NMR: δ 2.6 (\underline{CH}_2 , s, 2 H), 2.9 (\underline{CH}_2 , q, $^4J_{HH} = 19$ Hz, 4 H), 4.03 (\underline{CH} , unresolved m, 2 H), 4.08 (\underline{H}_5 , s, 5 H), 4.11 (\underline{CH} , unresolved m, 2H), 7.3 (\underline{CH} , d, $^3J_{HH} = 8$ Hz, 4 H), 8.1 (\underline{CH} , d, $^3J_{HH} = 8$ Hz, 4 H) ppm. ¹³C-¹H NMR: δ 27.7 (\underline{CH}_2 , d, $^1J_{PC} = 19$ Hz), 34.1 (\underline{CH}_2 , d, $^1J_{PC} = 19$ Hz), 68.0 (\underline{CH} , s), 68.9 (\underline{CH} , d, $^3J_{PC} = 3$ Hz), 69.0 (\underline{CH} , s), 82.2 (\underline{C} , d, $^2J_{PC} = 8$ Hz), 123.9 (\underline{CH} , s), 129.9 (\underline{CH} , d, $^3J_{PC} = 6$ Hz), 145.5 (\underline{C} , t, $^2J_{PC} = 4$ Hz), 146.5 (\underline{C} , s) ppm. ESI-MS (MeOH with aq. AgNO₃ added): m/z 502.074 [M]⁺observed; 502.073 calcd. for C₂₅H₂₃Fe₁N₂O₄P₁; 608.978 [$M + Ag$]⁺observed; 608.979 calcd. for C₂₅H₂₃Ag₁Fe₁N₂O₄P₁.

2.4.2 Syntheses of Ferrocenylalkyl Primary Phosphanes

2.4.2.1 Synthesis of Fc(CH₂)₄P(CH₂OH)₂ (**20**)

KOH pellets (1.85 g, 32.97 mmol) were added to a solution of [P(CH₂OH)₄]Cl (8.29 g, 34.80 mmol) in MeOH (19 mL). The mixture was stirred for 1 h before being added dropwise to a solution of **17** (3.63 g, 11.31 mmol) in MeOH (20 mL). The reaction mixture was heating to reflux for 21 h. After cooling, the solvent was removed under reduced pressure. Distilled H₂O (25 mL), Et₂O (60 mL) and NEt₃ (25

mL) were added. The solution was stirred for 1 h. The aqueous layer was removed and re-extracted with Et₂O (30 mL). The combined organic layer was washed with distilled H₂O (3 × 20 mL) and then filtered. Removal of the solvent under reduced pressure gave the title compound as a red oil (3.36 g, 89 %). Calcd. for C₁₆H₂₃Fe₁P₁O₂: C 57.49; H 6.94; N 0.00 %. Found: C 58.84; H 6.73; N < 0.2 %. ³¹P NMR: δ -22.7 (P, s) ppm. ¹H NMR: δ 1.6 (CH₂, m, 2 H), 1.7 (CH₂, m, 2 H), 1.8 (CH₂, m, 2 H), 2.4 (CH₂, m, 2 H), 4.05 (CH, m, 4 H), 4.10 (CH, s, 5 H), 4.2 (CH₂, d of m, ²J_{PH} = 85 Hz, 4 H) ppm. ¹³C-¹H NMR: δ 16.7 (d, ¹J_{PC} = 9 Hz, CH₂), 25.8 (d, ²J_{PC} = 15 Hz, CH₂), 29.3 (s, CH₂), 32.7 (d, ³J_{PC} = 12 Hz, CH₂), 61.9 (d, ¹J_{PC} = 21 Hz, CH₂), 67.1 (s, CH), 68.1 (s, CH), 68.5 (s, CH), 89.1 (C, s) ppm. ESI-MS (MeOH with a half drop of aqueous AgNO₃ added): *m/z* 334.078 [*M*]⁺ observed; 334.078 calcd. for C₁₆H₂₃Fe₁O₂P₁; 440.984 [*M* + Ag]⁺ observed; 440.983 calcd. for C₁₆H₂₃Ag₁Fe₁O₂P₁; 775.061 [*2M* + Ag]⁺ observed; 775.061 calcd. for C₃₂H₄₆Ag₁Fe₂O₄P₂.

2.4.2.2 Synthesis of Fc(CH₂)₄PH₂ (14)

Na₂S₂O₅ (0.03 g, 0.16 mmol) was added to a solution of **20** (0.07 g, 0.21 mmol) in a two-phase solvent system consisting of distilled H₂O (5 mL) and light petroleum spirits (5 mL). The mixture was heating to reflux for 2 h. After cooling, the aqueous layer was removed and re-extracted with light petroleum spirits (10 mL). The combined organic layer was washed with distilled H₂O (3 × 10 mL). Removal of the solvent under reduced pressure gave a red oil. The crude oil was subjected to chromatography with a preparative TLC plate, eluting with light petroleum spirits. Removal of the solvent of the yellow band at R_f 1.0 gave the title compound as a yellow oil (0.02 g, 35 %). IR: 2289s (*P-H str.*) cm⁻¹. ³¹P NMR: δ -136.9 (PH₂, t, ¹J_{PH} = 194 Hz) ppm. ¹H NMR: δ 1.5 – 1.6 (CH₂, m, 6 H), 2.3 (CH₂, t, ³J_{HH} = 7 Hz, 2 H), 2.7 (PH₂, d of t, ¹J_{PH} = 194 Hz, ³J_{HH} = 7 Hz, 2 H), 4.05 (CH, unresolved two singlets, 4 H), 4.1 (H₄, s, 5 H) ppm. ¹³C-¹H NMR: δ 13.7 (CH₂, d, ¹J_{PC} = 7 Hz), 29.2 (CH₂, s), 32.0 (d, ²J_{PC} = 6 Hz), 32.8 (CH₂, d, ³J_{PC} = 3 Hz), 67.1 (C₃, s, CH), 68.1 (C₂, s, CH), 68.5 (C₄, s, CH), 89.1 (C₁, s) ppm. GC-MS: *m/z* 56 [*Fe*]⁺, 121 [*CpFe*]⁺, 199 [*FcCH*₂]⁺, 274 [*M*]⁺. ESI-MS (CH₂Cl₂/MeOH): *m/z* 274.056 [*M*]⁺ observed; 274.056 calcd. for C₁₄H₁₉Fe₁P₁. A sample for elemental analysis was obtained by distillation under 10⁻⁶

torr at 65 °C for 12 h. Calcd. for C₁₄H₁₉Fe₁P₁: C 61.34; H 6.99 %. Found: C 61.64; H 6.61 %.

2.4.2.3 Synthesis of Fc(CH₂)₆P(CH₂OH)₂ (**21**)

KOH pellets (1.91 g, 34.04 mmol) were added to a solution of [P(CH₂OH)₄]Cl (7.71 g, 32.37 mmol) in MeOH (20 mL). The mixture was stirred for 1 h before being added dropwise to a solution of **18** (2.06 g, 5.89 mmol) in 95% EtOH (20 mL). The reaction mixture was heating to reflux for 20.5 h. After cooling, the solvent was removed under vacuum. Distilled H₂O (25 mL), Et₂O (40 mL) and NEt₃ (12 mL) were added. The solution was stirred for 2 h. The aqueous layer was removed and re-extracted with Et₂O (30 mL). The combined organic layer was washed with distilled H₂O (3 × 20 mL). Removal of the solvent under reduced pressure gave the title compound as a red oil (2.02 g, 95 %). Calcd. for C₁₈H₂₇Fe₁P₁O₂: C 59.67; H 7.52; N 0.00 %. Found: C 62.48; H 7.90; N < 0.2 %. ³¹P NMR: δ -22.9 (P, s) ppm. ¹H NMR: δ 1.4 – 1.5 (CH₂, m, 8 H), 1.8 (CH₂, m, 2 H), 2.3 (CH₂, t, ³J_{HH} = 8 Hz, 2 H), 4.04 (H_{2,3}, unresolved m, 4 H), 4.09 (H₄, s, 5 H), 4.2 (CH₂, d of m, ²J_{PH} = 92 Hz, 4 H) ppm. ¹³C-¹H NMR: δ 16.8 (d, ¹J_{PC} = 8 Hz, CH₂), 25.8 (d, ²J_{PC} = 15 Hz, CH₂), 29.3 (s, CH₂), 29.5 (s, CH₂), 31.0 (s, CH₂), 31.2 (d, ³J_{PC} = 12 Hz, CH₂), 61.9 (d, ¹J_{PC} = 20 Hz, CH₂), 67.0 (s, CH), 68.1 (s, CH), 68.5 (s, CH), 89.4 (C, s) ppm. ESI-MS (MeOH with a half drop of aqueous AgNO₃ added): *m/z* 362.108 [*M*]⁺ observed; 362.109 calcd. for C₁₈H₂₇Fe₁O₂P₁; 385.099 [*M* + *Na*]⁺ observed; 385.099 calcd. for C₁₈H₂₇Fe₁Na₁O₂P₁; 469.014 [*M* + *Ag*]⁺ observed; 469.014 calcd. for C₁₈H₂₇Ag₁Fe₁O₂P₁; 831.123 [*2M* + *Ag*]⁺ observed; 831.124 calcd. for C₃₆H₅₄Ag₁Fe₂O₄P₂.

2.4.2.4 Synthesis of Fc(CH₂)₆PH₂ (**15**)

Na₂S₂O₅ (1.08 g, 5.66 mmol) was added to a solution of **21** (2.04 g, 5.64 mmol) in a two-phase solvent system consisting of distilled H₂O (30 mL) and light petroleum spirits (30 mL). The mixture was heating to reflux for 4 h in air. After cooling, the aqueous layer was removed. The organic layer was washed with distilled H₂O (3 × 10 mL) and then filtered. Removal of the solvent under reduced pressure gave a red oil

(1.42 g, 83 %). Analytical samples were obtained by chromatography on a preparative TLC plate, eluting with Et₂O/light petroleum spirits (1 : 1). Removal of the solvent of the fraction at R_f 0.70 gave the title compound as a yellow oil. Calcd. for C₁₆H₂₃Fe₁P₁: C 63.58; H 7.68 %. Found: C 62.04; H 7.99 %. IR: 2283m (*P-H str.*) cm⁻¹. ³¹P NMR: δ -136.5 (PH₂, t of p, ¹J_{PH} = 195, ²J_{PH} = 6 Hz) ppm. ¹H NMR: δ 1.3 – 1.6 (CH₂, m, 10 H), 2.3 (CH₂, t, ³J_{HH} = 8 Hz, 2 H), 2.7 (PH₂, d of t, ¹J_{PH} = 195 Hz, ³J_{HH} = 7 Hz, 2 H), 4.05 (CH, unresolved m, ³J_{HH} = 2 Hz, 4 H), 4.09 (H₄, s, 5 H) ppm. ¹³C-¹H NMR: δ 13.7 (CH₂, d, ¹J_{PC} = 7 Hz), 29.2 (CH₂, s), 29.6 (CH₂, s), 30.5 (CH₂, d, ²J_{PC} = 6 Hz), 31.0 (CH₂, s), 32.9 (CH₂, d, ³J_{PC} = 4 Hz), 67.0 (CH, s), 68.1 (CH, s), 68.5 (CH, s), 89.4 (C, s) ppm. GC-MS: *m/z* 56 [*Fe*]⁺, 121 [*CpFe*]⁺, 199 [*FcCH*₂]⁺, 302 [*M*]⁺. ESI-MS (CH₂Cl₂/MeOH): *m/z* 302.088 [*M*]⁺ observed; 302.088 calcd. for C₁₆H₂₃Fe₁P₁.

2.4.2.5 Synthesis of Fc(CH₂)₁₁P(CH₂OH)₂ (22)

KOH pellets (3.40 g, 60.60 mmol) were added to a solution of [P(CH₂OH)₄]Cl (15.28 g, 64.15 mmol) in MeOH (20 mL). The mixture was stirred for 1 h before adding dropwise to a solution of **19** (8.68 g, 20.69 mmol) in MeOH (20 mL). The reaction mixture was heating to reflux for 20.5 h. After cooling, the solvent was reduced to ~13 mL under vacuum. Distilled H₂O (12 mL), Et₂O (34 mL) and NEt₃ (14 mL) were added. The solution was stirred for 2 h. The aqueous layer was removed and re-extracted with Et₂O (10 mL). The combined organic layer was washed with distilled H₂O (6 × 10 mL). Removal of the solvent under reduced pressure gave a red oil (8.29 g, 93%). Recrystallisation of the crude product by addition of light petroleum spirits (b.p. 40 – 60 °C) to a CH₂Cl₂–MeOH solution followed by cooling to -18 °C gave the title compound as a yellow solid. Calcd. for C₂₃H₃₇Fe₁O₂P₁: C 63.87; H 8.63; N 0.00 %. Found: C 63.95; H 8.76; N 0.47 %. ESI-MS (MeOH with a half drop of aqueous AgNO₃ added): *m/z* 432.186 [*M*]⁺ observed; 432.187 calcd. for C₂₃H₃₇Fe₁O₂P₁; 539.093 [*M* + Ag]⁺ observed; 539.092 calcd. for C₂₃H₃₇Ag₁Fe₁O₂P₁. ³¹P NMR: δ -22.7 (*P*, s) ppm. ¹H NMR: δ 1.4 – 1.5 (CH₂, m, 18 H), 1.8 (CH₂, m, 2 H), 2.3 (CH₂, t, ³J_{HH} = 8 Hz, 2 H), 4.04 (CH, m, 4 H), 4.09 (CH, s, 5 H), 4.2 (CH₂, d of m, ²J_{PH} = 89 Hz, 4 H) ppm. ¹³C-¹H NMR: δ 16.9 (d, ¹J_{PC} = 8 Hz, CH₂), 25.9 (d,

$^2J_{PC} = 15$ Hz, \underline{CH}_2), 28.2 – 31.1 (s, \underline{CH}_2), 31.3 (d, $^3J_{PC} = 12$ Hz, \underline{CH}_2), 61.8 (d, $^1J_{PC} = 20$ Hz, \underline{CH}_2), 67.0 (s, \underline{CH}), 68.1 (s, \underline{CH}), 68.5 (s, \underline{CH}), 89.6 (\underline{C} , s) ppm.

2.4.2.6 Synthesis of $\text{Fc}(\text{CH}_2)_{11}\text{PH}_2$ (**16**)

$\text{Na}_2\text{S}_2\text{O}_5$ (0.11 g, 0.57 mmol) was added to a solution of **22** (0.25 g, 0.64 mmol) in a two-phase solvent system consisting of distilled H_2O (10 mL) and light petroleum spirits (b.p. 40 – 60 °C) (10 mL). The mixture was heating to reflux for 3 h. After cooling, the solvents were removed with a syringe. The yellow precipitate was washed with distilled H_2O (4×10 mL). After drying under vacuum, the residue (0.26 g) was extracted with CH_2Cl_2 and filtered. The filtrate was subjected to chromatography with a preparative TLC plate, eluting with CH_2Cl_2 /light petroleum spirits (5 : 6). Removal of the solvent from the yellow fraction at R_f 0.93 gave the title compound as a yellow oil (0.06 g, 28 %). Calcd. for $\text{C}_{21}\text{H}_{33}\text{Fe}_1\text{P}_1$: C 67.73; H 8.94; N 0.00 %. Found: C 71.08; H 9.36; N < 0.2 %. IR: 2290m (*P-H str.*) cm^{-1} . ^{31}P NMR: δ -136.7 (\underline{PH}_2 , t of p, $^1J_{PH} = 195$, $^2J_{PH} = 6$ Hz) ppm. ^1H NMR: δ 1.3 – 1.5 (\underline{CH}_2 , m, 22 H), 2.3 (\underline{CH}_2 , t, $^3J_{HH} = 8$ Hz, 2 H), 2.7 (\underline{PH}_2 , d of t, $^1J_{PH} = 195$ Hz, $^3J_{HH} = 7$ Hz, 2 H), 4.04 (\underline{CH} , unresolved m, 4 H), 4.09 (\underline{CH} , s, 5 H) ppm. ^{13}C - $\{^1\text{H}\}$ NMR: δ 13.7 (\underline{CH}_2 , d, $^1J_{PC} = 7$ Hz), 29.2 (\underline{CH}_2 , s), 29.6 (\underline{CH}_2 , s), 30.6 (\underline{CH}_2 , d, $^2J_{PC} = 6$ Hz), 31.1 (\underline{CH}_2 , s), 32.9 (\underline{CH}_2 , d, $^3J_{PC} = 3$ Hz), 67.0 (\underline{CH} , s), 68.1 (\underline{CH} , s), 68.5 (\underline{CH} , s), 89.6 (\underline{C} , s) ppm. GC-MS: m/z 121 [CpFe] $^+$, 199 [FcCH_2] $^+$, 372 [M] $^+$. ESI-MS ($\text{CH}_2\text{Cl}_2/\text{MeOH}$): m/z 372.165 [M] $^+$ observed; 372.166 calcd. for $\text{C}_{21}\text{H}_{33}\text{Fe}_1\text{P}_1$.

2.4.2.7 Synthesis of $\text{Fc}(\text{CH}_2)_6\text{PH}_2\cdot\text{BH}_3$ (**34**)

$(\text{CH}_3)_2\text{S}\cdot\text{BH}_3$ (0.50 mL, 5.63 mmol) was added to a solution of **15** (0.05 g, 0.17 mmol) in dry hexane (10 mL) at -63.5 °C. The mixture was stirred at that temperature for 15 mins. The volatiles were removed under vacuum. A yellow solid initially precipitated out. It, however, turned to a yellow oil while being dried under vacuum for further 15 mins at room temperature. Recrystallisation of the residue from dry hexane at -18 °C gave the title compound as orange crystalline needles. The needles were washed with cold hexane (1 mL \times 2) at 0 °C (0.01 g, 26 %). Calcd. for

C₁₆H₂₆BF₂FeP: C 60.75; H 8.29 %. Found: C 60.84; H 8.19 %. IR: 3924w, 3092w, 2925s, 2855m, 2398m (unresolved), 2263w, 1636w,br, 1463m, 1104 – 1054s (unresolved), 913m, 829m, 805m, 723w, 670w, 489 – 461m (unresolved) cm⁻¹. ESI-MS (CH₂Cl₂/MeOH): *m/z* 316.119 [*M*]⁺ observed; 316.120 calcd. for C₁₆H₂₆B₁Fe₁P₁; 339.109 [*M* + Na]⁺ observed; 339.111 calcd. for C₁₆H₂₆B₁Fe₁Na₁P₁; 355.058 [*M* + K]⁺ observed; 355.084 calcd. for C₁₆H₂₆B₁Fe₁K₁P₁. ³¹P NMR: δ -52.3 (PH₂, broad t of m, ¹*J*_{PH} = 362 Hz, 2 H) ppm. ¹H NMR: δ 1.3 – 1.5 (CH₂, & BH₃, unresolved m, 13 H), 1.8 – 1.9 (CH₂, m, 2 H), 2.3 (CpCH₂, t, ³*J*_{HH} = 8 Hz, 2 H), 4.05 – 4.10 (CpH, s, 11 H), 4.5 (PH₂, d of sextet, ¹*J*_{PH} = 360, ³*J*_{HH} = 1 Hz) ppm. ¹³C-{¹H} NMR: δ 16.5 (CH₂PH₂, ¹*J*_{PC} = 35 Hz, CH₂), 28.9 (CpCH₂CH₂CH₂, s, CH₂), 28.9 (CH₂CH₂CH₂PH₂, d, ³*J*_{PC} = 6 Hz, CH₂), 29.5 (CpCH₂, s, CH₂), 30.2 (CH₂CH₂PH₂, d, ²*J*_{PC} = 11 Hz, CH₂), 31.0 (CpCH₂CH₂, s, CH₂), 67.2 (C₃, s, CH), 68.2 (C₂, s, CH), 68.7 (C₅H₅, s, CH), 89.5 (C₁, s) ppm.

A sample for X-ray crystallographic structural determination was obtained by recrystallisation from hexane at 0 °C. The concentrated solution of the compound in hexane was cooled inside a closed Dewar flask gradually from room temperature to 0 °C. The solvent was removed while cool and the single crystals were washed with cold hexane (1 mL × 2) at 0 °C and then dried under vacuum.

2.4.2.8 Synthesis of R_cCH₂P(CH₂OH)₂ (27)

KOH pellets (1.30 g, 23.13 mmol) were added to a solution of [P(CH₂OH)₄]Cl (5.37 g, 22.54 mmol) in MeOH (15 mL). The mixture was stirred for 1 h before being added dropwise to a solution of [R_cCH₂NMe₃⁺]I⁻ (1.95 g, 4.53 mmol) in MeOH (15 mL). The reaction mixture was heating to reflux for 20 h. After cooling, the solvent was removed under reduced pressure. Distilled H₂O (10 mL), Et₂O (25 mL) and NEt₃ (5 mL) were added. The solution was stirred for 1 h. The aqueous layer was removed and re-extracted with Et₂O (20 mL). The combined organic layer was washed with distilled H₂O (5 × 10 mL). Removal of the solvent under reduced pressure gave the title compound as a pale-yellow oil with some white solids (0.95g, 62 %). This was used in the synthesis of **24** without further purification or characterisation.

2.4.2.9 Synthesis of $RcCH_2PH_2$ (**24**)

$Na_2S_2O_5$ (0.54 g, 2.83 mmol) was added to a solution of **27** (0.95 g, 2.83 mmol) in a two-phase solvent system consisting of distilled H_2O (20 mL) and light petroleum spirits (25 mL). The mixture was heating to reflux for 3 h. After cooling, the aqueous layer was removed. The organic layer was washed with distilled H_2O (5×10 mL). Removal of the solvent from the organic layer under reduced pressure gave a pale-yellow oil with some white solids (0.34 g, 43 %). The crude product was purified by chromatography with a preparative TLC plate, eluting with CH_2Cl_2 /petroleum spirits (1 : 1). Removal of the solvent of the pale yellow fraction at R_f 0.76 gave the title compound as a pale-yellow oil (0.08 g, 10 %). Satisfactory microanalytical data could not be obtained. Calcd. for $C_{11}H_{13}P_1Ru_1$: C 47.65; H 4.73 %. Found: C 45.03; H 4.44%. IR: 2290m (*P-H str.*) cm^{-1} . ^{31}P NMR: δ -132.5 ($\underline{PH_2}$, t, $^1J_{PH} = 193$ Hz) ppm. 1H NMR: δ 2.5 ($\underline{CH_2}$, m, $^3J_{HH} = 4$ Hz, 2 H), 2.9 ($\underline{PH_2}$, d of t, $^1J_{PH} = 194$, $^3J_{HH} = 7$ Hz, 2 H), 4.5 (\underline{CH} , t, $^3J_{HH} = 2$ Hz, 2 H), 4.56 (\underline{CH} , s, 5 H), 4.57 (\underline{CH} , t, $^3J_{HH} = 2$ Hz, 2 H) ppm. ^{13}C - $\{^1H\}$ NMR: δ 14.0 ($\underline{CH_2}$, d, $^1J_{PC} = 8$ Hz), 69.5 (\underline{CH} , s), 70.7 (\underline{CH} , s), 70.9 (\underline{CH} , d, $^3J_{PC} = 3$ Hz), 92.6 (C, unresolved m) ppm. GC-MS: m/z 167 [$CpRu$] $^+$, 245 [$RcCH_2$] $^+$, 278 [M] $^+$. ESI-MS (MeOH): m/z 244.989 [$M - PH_2$] $^+$ observed; 244.989 calcd. for $C_{11}H_{11}Ru_1$; (MeOH with a drop of aqueous $AgNO_3$ added): m/z 384.885 [$M + Ag$] $^+$ observed; 384.884 calcd. for $C_{11}H_{13}Ag_1P_1Ru_1$.

A by-product which was tentatively identified as **28** was obtained as a white solid (0.05 g, 5 %) from the aqueous phase of the reaction mixture. ^{31}P NMR: δ 35.7 (\underline{PH} , d of t, $^1J_{PH} = 467$, $^2J_{PH} = 14$ Hz) ppm. 1H NMR: δ 3.0 ($\underline{CH_2}$, d of t, $^3J_{HH} = 13$, $^4J_{HH} = 4$ Hz, 2 H), 4.0 ($\underline{CH_2}$, m, 2 H), 4.5 (\underline{CH} , d, $^3J_{HH} = 1$ Hz, 2 H), 4.6 (\underline{CH} , s, 5 H), 4.7 (\underline{CH} , unresolved m, 2 H), 6.8 (\underline{PH} , broad d, $^1J_{PH} = 467$ Hz, 1 H) ppm. ^{13}C - $\{^1H\}$ NMR: δ 26.7 ($\underline{CH_2}$), 58.7 ($\underline{CH_2}$, d, $^1J_{PC} = 74$ Hz), 70.6 (\underline{CH}), 71.2 (\underline{CH}), 71.9 (\underline{CH}), 80.0 (C) ppm.

2.4.2.10 Synthesis of [CpFeC₅H₃(CH₂OH){CH₂P(CH₂OH)₂}] (31)

KOH pellets (0.79 g, 14.08 mmol) were added to a solution of [P(CH₂OH)₄]Cl (3.40 g, 14.27 mmol) in MeOH (20 mL). The mixture was stirred for 2 h before being added dropwise to a solution of [CpFeC₅H₃(CH₂OH)(CH₂NMe₃)⁺]I⁻ (1.25 g, 3.00 mmol) in MeOH (20 mL). The reaction mixture was heating to reflux for 20.5 h. After cooling, the solvent was reduced to about 2 mL. Distilled H₂O (12 mL), Et₂O (24 mL) and NEt₃ (3 mL) were added. The mixture was stirred for 1.5 h. The aqueous layer was removed and re-extracted with Et₂O (20 mL). The combined organic layer was washed with distilled H₂O (3 mL × 4) and then filtered. After removal of the solvent, the title compound was obtained as a mixture of a crystalline yellow solid and oil (0.85 g, 88 %). ³¹P NMR: δ -19.3 (P, septet, ²J_{PH} = 6 Hz) ppm. ¹H NMR: δ 3.1 (CH₂, m, 2 H), 4.05 (H_{2,3}, unresolved m, 3 H), 4.07 (H₄, s, 5 H), 4.26 (CH₂OH, d, ⁴J_{HH} = 2 Hz, 2 H), 4.29 (PCH₂OH, m, 4 H) ppm. ¹³C-{¹H} NMR: δ 16.6 (CH₂, d, ¹J_{PC} = 9 Hz), 60.9 (CH₂OH, d, ¹J_{PC} = 26 Hz), 66.4 (CH, s), 68.6 (CH₂OH, s), 69.9 (C_{2b}H, d, ³J_{PC} = 4 Hz), 70.0 (C₄H, s), 82.9 (C₁, ²J_{PC} = 8 Hz) ppm.

2.4.2.11 Synthesis of [CpFeC₅H₃(CH₂OH)(CH₂PH₂)] (32)

Na₂S₂O₅ (0.50 g, 2.63 mmol) was added to a solution of **31** (0.85 g, 2.63 mmol) in a two-phase solvent system consisting of distilled H₂O (15 mL) and petroleum spirits (25 mL). The mixture was heating to reflux for 3.5 h. After cooling, the mixture was extracted with CH₂Cl₂ (40 mL) and the aqueous layer was removed. The organic layer was washed with distilled H₂O (20 mL × 3). Removal of the solvent gave a yellow oil (0.39 g, 56 %). A strong garlic-like odour was noted. Attempted recrystallisation of the crude product from warm light petroleum spirits (10 mL) at -18 °C was unsuccessful. No precipitate could be obtained. Attempted elemental analysis on the crude product also gave an unsatisfactory result. Calcd. for C₁₂H₁₅O₁P₁Fe₁: C 54.98; H 5.77; N 0.00 %. Found: C 59.30; H 7.74; N < 0.2 %. IR: 2291m (*P-H str.*) cm⁻¹. ³¹P NMR: δ -129.8 (PH₂, t, ¹J_{PH} = 197 Hz) ppm. ¹H NMR: δ 2.7 (CH₂, m, 2 H), 2.9 (PH₂, d of m, ¹J_{PH} = 200; ³J_{HH} = 5 Hz, 2 H), 4.01 (CH, t, ³J_{HH} = 2 Hz, 2 H), 4.06 (CH, s, 5 H), 4.07 (CH, d, ³J_{HH} = 1 Hz, 1 H), 4.10 (CH₂OH, t, ³J_{HH}

= 6 Hz, 2 H), 4.11 (\underline{CH} , m, 2H) ppm. ^{13}C - $\{^1\text{H}\}$ NMR: (CDCl_3 , 100.62 MHz): δ 12.9 ($\underline{\text{CH}_2}$, d, $^1J_{\text{PC}} = 9$ Hz), 65.7 ($\underline{\text{CH}}$, s), 67.4 ($\underline{\text{CH}}$, $\underline{\text{CH}_2}$, unresolved m, $^3J_{\text{HH}} = 2$ Hz), 69.5 ($\underline{\text{CH}}$, s), 69.6 ($\underline{\text{CH}}$, d, $^3J_{\text{PC}} = 1$ Hz), 86.9 (C, d, $^2J_{\text{PC}} = 8$ Hz) ppm.

2.4.3 Synthesis of Ferrocenylmethyl Phosphane Oxide and Phosphinic Acid

2.4.3.1 Synthesis of $\text{FcCH}_2\text{P}(\text{O})\text{H}_2$ (30)

$\text{H}_2\text{NC}(\text{O})\text{NH}_2 \cdot \text{H}_2\text{O}_2$ (0.18 g, 1.91 mmol) was added to a solution of **1** (0.17 g, 0.72 mmol) in THF (7 mL) at 0 °C. To the mixture, MeOH (4 mL) was added dropwise with continuous stirring. Stirring was continued until all the urea-peroxide added was dissolved (approx. 10 mins). Distilled H_2O (20 mL) and CH_2Cl_2 (20 mL) were added and the organic layer was separated. The aqueous layer was re-extracted with CH_2Cl_2 (10 mL). The combined organic layer was washed with aq. NaOH (0.067 M, 10 mL \times 3) and then with distilled H_2O (5 mL \times 2). Removal of the solvent under vacuum gave the title compound as a yellow solid (0.80 g, 45 %). Attempted purifications by recrystallisation from a mixture of $\text{CH}_2\text{Cl}_2/\text{MeOH}$ or $\text{CH}_2\text{Cl}_2/\text{petroleum spirits}$ at -18 °C or by column-chromatography with silica gel, eluting with CH_2Cl_2 (100 %) or a mixture of $\text{CH}_2\text{Cl}_2/\text{MeOH}$ (95 : 5) were unsuccessful. The purest sample was obtained by column-chromatography, eluting with a mixture of $\text{CH}_2\text{Cl}_2/\text{MeOH}$ (95 : 5). Satisfactory microanalytical data could, however, not be obtained: Calcd. for $\text{C}_{11}\text{H}_{13}\text{O}_1\text{P}_1\text{Fe}_1$: C 53.24; H 5.28; N 0.00 %. Found: C 56.44; H 5.39; N 0.5 %. IR: 2390m ($P-H$ str.) cm^{-1} . ^{31}P NMR: δ 9.5 ($\underline{\text{PH}_2}$, t of t, $^1J_{\text{PH}} = 470$, $^2J_{\text{PH}} = 16$ Hz) ppm. ^1H NMR (300.13 MHz): δ 3.1 ($\underline{\text{CH}_2}$, d of t, $^2J_{\text{PH}} = 16$ $^3J_{\text{HH}} = 5$ Hz, 2 H), 4.11 ($\underline{\text{CH}}$, s, 2 H), 4.14 ($\underline{\text{CH}}$, s, 2 H), 4.18 ($\underline{\text{CH}}$, s, 5 H), 6.91 ($\underline{\text{PH}_2}$, d of t, $^1J_{\text{PH}} = 469$, $^3J_{\text{HH}} = 5$ Hz, 2 H) ppm. ^{13}C - $\{^1\text{H}\}$ NMR (75.47 MHz): δ 29.7 ($\underline{\text{CH}_2}$, s), 68.7 ($\underline{\text{CH}}$, s), 68.9 ($\underline{\text{CH}}$, d, $^3J_{\text{PC}} = 4$ Hz), 69.1 ($\underline{\text{CH}}$, s), 75.19 (C, s) ppm. ESI-MS (MeOH): m/z 270.999 [$M + \text{Na}$] $^+$ observed; 270.994 calcd. for $\text{C}_{11}\text{H}_{13}\text{Fe}_1\text{Na}_1\text{O}_1\text{P}_1$; 286.969 [$M + \text{K}$] $^+$ observed; 286.968 calcd. for $\text{C}_{11}\text{H}_{13}\text{Fe}_1\text{K}_1\text{O}_1\text{P}_1$; 518.999 [$2M + \text{Na}$] $^+$ observed; 518.999 calcd. for $\text{C}_{22}\text{H}_{26}\text{Fe}_2\text{Na}_1\text{O}_2\text{P}_2$.

2.4.3.2 Synthesis of FcCH₂P(O)(OH)H (36)

Synthesis With Oxalyl Chloride: Oxalyl chloride (0.21 mL, 2.19 mmol) was added by syringe to a solution of **1** (0.15 g, 0.65 mmol) in dry CH₂Cl₂ (10 mL). The mixture was heating to reflux for 2 h. After cooling, the volatiles were removed under vacuum. Distilled H₂O (10 mL) was added and the solution was stirred for 15 h. The solution was made basic by adding aq. NaOH (4.98 M, 2 mL) and filtered. The filtrate was then washed with CH₂Cl₂ (10 mL × 3). After the aqueous solution was acidified with concentrated HCl (3 mL), it was extracted with CH₂Cl₂ (10 mL × 2) and then filtered. Removal of the solvent under reduced pressure gave a brown oil. The ³¹P NMR spectroscopy suggested the formation of the desired product by a doublet of triplets at δ 36.3 ppm which was consistent with those in the earlier study⁷⁹. The signal was, however, only minor. The ³¹P NMR signal of the major product, which was not identified, was observed at δ 49.9 ppm as a pentet. The attempted separation of the two products by recrystallisation from CH₂Cl₂ at -18 °C was unsuccessful.

Synthesis With Triphosgene: A solution of triphosgene (0.07 g, 0.24 mmol) in dry CH₂Cl₂ (5 mL) was added to that of **1** (0.09 g, 0.40 mmol) in dry CH₂Cl₂ (2 mL). The mixture was heating to reflux for 1 h. After cooling, the organic solvent was removed under vacuum. Distilled H₂O (10 mL) was added and the solution was stirred overnight. The solution was made basic by adding aq. NaOH (5 M, 2 mL) and washed with CH₂Cl₂ (10 mL × 2). The aqueous phase was acidified with concentrated HCl (3 mL) and extracted with CH₂Cl₂ (10 mL × 2). Removal of the solvent under reduced pressure gave the desired compound **36** as a yellow solid (0.67 g, 64 %). Calcd. for C₁₁H₁₃Fe₁O₂P₁: C 50.02; H 4.96 %. Found: C 50.12; H 4.95 %. IR: 2899w and 2924w (*P-O-H* str.), 2378m and 2346m (*P-H* str.), 1181s (*P=O* str) cm⁻¹. ³¹P NMR: δ 36.9 (PH, d of t, ¹J_{PH} = 557, ²J_{PH} = 17 Hz) ppm. ¹H NMR: δ 2.9 (CH₂, d of d, ²J_{PH} = 15, ³J_{HH} = 2 Hz, 2 H), 4.14 (CH, s, 5 H), 4.15 (CH, m, ³J_{HH} = 2 Hz, 2 H), 4.20 (CH, m, ³J_{HH} = 1 Hz, 2 H), 7.0 (PH, d of t, ¹J_{PH} = 557, ³J_{HH} = 2 Hz, 1 H) ppm. ¹³C-¹H NMR: δ 31.8 (CH₂, d, ¹J_{PC} = 91 Hz), 68.4 (CH, s), 69.0 (CH, s), 69.3 (CH, d, ³J_{PC} = 4 Hz) ppm.

2.4.4 ^{31}P NMR Studies on Oxidative Stability of PhPH_2 and CamphylPH_2 (**2**) in Solution

2.4.4.1 ^{31}P NMR Investigation on Oxidative Stability of PhPH_2 in Solution with Added FcH or FcCH_2PH_2 (**1**)

Ferrocene (0.0144 g, 0.077 mmol) and **1** (0.0137 g, 0.059 mmol) were placed in a separate NMR tube and CDCl_3 (0.5 mL) was added. The tubes were gently shaken in order to completely dissolve the solids. To the two NMR tubes and one consisting of CDCl_3 (0.5 mL) (control), PhPH_2 (10 % in hexane, 0.02 mL, 0.16 mmol) was added under an N_2 atmosphere. After sealing the NMR tubes with a plastic lid, the samples were removed from the inert atmosphere into air and the first $^{31}\text{P}\{-^1\text{H}\}$ NMR spectrum was immediately recorded on each sample.

The oxidation of PhPH_2 in each sample was monitored at intervals by ^{31}P NMR spectroscopy with ^1H decoupled until the control was completely oxidised. Between the intervals, the NMR tubes were kept at room temperature in air with their plastic lids on. The solvent was occasionally refilled when necessary due to slow evaporation.

2.4.4.2 ^{31}P NMR Investigation on Oxidative Stability of CamphylPH_2 (**2**) in Solution with Added FcH and FcCH_2PH_2 (**1**)

Compound **2** was prepared according to the literature methods^{118, 128}. Ferrocene (0.0141 g, 0.076 mmol) and **1** (0.0146 g, 0.063 mmol) were placed in a separate NMR tube and CDCl_3 (0.5 mL) was added. The tubes were gently shaken in order to completely dissolve the solids. To the two tubes and one consisting of CDCl_3 (0.5 mL) (control), **2** (0.02 mL, 0.12 mmol) was added under an N_2 atmosphere. After sealing each NMR tube with a plastic lid, the samples were removed from the inert atmosphere into air and the first $^{31}\text{P}\{-^1\text{H}\}$ NMR spectrum was immediately recorded on each sample. The oxidation progress of **2** in each sample was monitored by ^{31}P -

{¹H} NMR spectroscopy until the control was fully oxidised. The solvent was occasionally filled due to slow evaporation.

2.4.4.3 ³¹P NMR Investigation on Oxidative Stability of PhPH₂ in Solution with Added Antioxidants

Nitrosobutane (0.01 g, 0.11 mmol) and 2,2-diphenyl-1-picrylhydrazyl free radicals, DPPH, (0.009 g, 0.02 mmol) were placed in a separate NMR tube and CDCl₃ (1 mL) was added. The tubes were gently shaken in order to completely dissolve the solids. To the two tubes and one consisting of CDCl₃ (0.5 mL) (control), PhPH₂ (10 % in hexane, 0.02 mL, 0.16 mmol) was added under an N₂ atmosphere. The oxidation of PhPH₂ in each sample was monitored for 3 months.

2.4.4.4 ³¹P NMR Investigation on Oxidative Stability of PhPH₂ in Solution with Added Phenylphosphinic Acid

Under an N₂ atmosphere, PhP(O)(OH)H (0.0135 g, 0.095 mmol) was placed in a NMR tube and deoxygenated dry CDCl₃ (1 mL) was added. To the tube and one consisting of deoxygenated dry CDCl₃ (1 mL) (control), PhPH₂ (10 % in hexane, 0.01 mL) was added under an N₂ atmosphere. After sealing with plastic NMR lids, the samples were removed from the inert atmosphere into air. The oxidation of PhPH₂ in each sample was monitored at intervals by ³¹P-¹H NMR spectroscopy. During the intervals, the samples were kept at room temperature in air with their lids on. The solvent was occasionally refilled using deoxygenated dry CDCl₃ under an N₂ atmosphere when necessary.

2.4.5 Synthesis of Ferrocenylalkyl Arsanes

2.4.5.1 Synthesis of FcCH₂AsCl₂ (39)

A solution of **40** generated by reaction of $\text{FcCH}_2\text{OCH}_3$ **47** (0.17 g, 0.74 mmol) with a small pieces of freshly cut Li metal (0.5 g) in dry THF (10 mL) at $-10\text{ }^\circ\text{C}$ for 3 h under an Ar atmosphere, was added slowly *via* a #2 frit to a solution of AsCl_3 (0.70 mL, 8.30 mmol) in dry THF (15 mL) at $0\text{ }^\circ\text{C}$ under an Ar atmosphere. The colour change of the solution from red to dark brown was observed upon the addition. The mixture was stirred at room temperature for 1.5 h. Removal of the solvent under vacuum gave the title compound as a dark brown oil. The crude product was extracted with dry Et_2O (30 mL) and the insoluble materials were filtered with a #4 frit. Removal of the solvent from the filtrate gave the crude **39** as a brown oil. The attempted crystallisation of the brown oil from Et_2O (8 mL)/dry hexane (1 mL) at $-18\text{ }^\circ\text{C}$ was unsuccessful. No precipitate could be obtained. ^1H NMR: δ 3.6 (CH_2 , s, 2H), 4.22 (H_4 , s, 5H), 4.23 (H_3 , m, 2H), 4.24 (H_2 , m, 2H) ppm. ^{13}C - $\{^1\text{H}\}$ NMR: δ 46.7 (CH_2 , s, CH_2), 69.0 (C_3 , s, CH), 69.1 (C_4 , s, CH), 69.6 (C_2 , s, CH), 78.7 (C_1 , s, C) ppm. ESI-MS (MeCN, +ve, at a capillary exit voltage of 100 V): m/z observed 308.912 [$M - \text{Cl}$] $^+$; calcd. 308.910 for $\text{C}_{11}\text{H}_{11}\text{As}_1\text{Cl}_1\text{Fe}_1$; (at 250 V): observed m/z 343.879 [M] $^+$; 343.879 calcd. for $\text{C}_{11}\text{H}_{11}\text{As}_1\text{Cl}_2\text{Fe}_1$. The darkening of the NMR sample was observed over the course of 24 days left at room temperature in air.

2.4.5.2 Synthesis of $\text{FcCH}_2\text{AsH}_2$ (**38**)

LiAlH_4 (0.20 g, 6.67 mmol) was added to a solution of **39** (the entire yield obtained as above) in dry Et_2O (50 mL) at $0\text{ }^\circ\text{C}$. The mixture was slowly brought to room temperature and stirred for 2.5 h. (addition of conc. HCl (36 %, 5 mL) at this stage to destroy the excess LiAlH_4 resulted in a very poor yield (i.e. $\sim 5\%$) of the title compound). The solvent was removed under vacuum and the residue was extracted with dry hexane (40 mL). The insoluble materials were filtered with a #4 frit. Removal of the solvent gave the title compound as a yellow oil (0.08 g, 40 %). IR: ν 2088 cm^{-1} (*As-H str.*). ESI-MS (MeOH, +ve, 90 V): m/z observed 275.959 [M] $^+$; calcd. 275.957 for $\text{C}_{11}\text{H}_{13}\text{As}_1\text{Fe}_1$. Although a half drop of aqueous AgNO_3 was also added, the expected silver adducts could not be observed. GC-MS: $m/z(\%)$ 56(8) [Fe] $^+$, 121(40) [FeCp] $^+$, 199(100) [FcCH_2] $^+$, 276(20) [M] $^+$. ^1H NMR: δ 2.5 (AsH_2 , t, $^3J_{\text{HH}} = 6\text{ Hz}$, 2 H), 2.7 (CH_2 , t, $^3J_{\text{HH}} = 6\text{ Hz}$, 2 H), 4.02 (H_3 , t, $^3J_{\text{HH}} = 2\text{ Hz}$, 2 H), 4.06

(\underline{H}_2 , t, $^3J_{HH} = 2$ Hz, 2 H), 4.09 (\underline{H}_4 , s, 5 H) ppm. ^{13}C - $\{^1\text{H}\}$ NMR: δ 12.6 ($\underline{\text{C}}_{\text{H}_2}$, s, CH_2), 67.3 ($\underline{\text{C}}_3$, s, CH), 67.6 ($\underline{\text{C}}_2$, s, CH), 68.8 ($\underline{\text{C}}_4$, s, CH), 89.7 ($\underline{\text{C}}_1$, s, C) ppm. The arsane proton signal was still observed after 24 h at 300 K in air. It, however, completely disappeared after 24 days at room temperature in air.

Attempted Chromatography and Recrystallisation: The chromatography of the crude product on a preparative TLC plate, eluting with light petroleum spirits (100 %) gave three yellow fractions at R_f 0.77, 0.23 and 0.08. After extraction with CH_2Cl_2 and removal of the solvent, the fractions gave a yellow oil and solid (R_f 0.77 a yellow oil, 0.013 g; R_f 0.23 a yellow solid, 0.004 g; R_f 0.08 a yellow solid, 0.009 g). ^1H NMR spectroscopy showed that the yellow oil from the R_f 0.77 fraction contained the desired compound. GC-MS also showed that the fraction at R_f 0.77 was a mixture of FcCH_3 (95 %) and **38** (5 %), that at R_f 0.23 was $(\text{FcCH}_2)_2$ (100 %) and no ions for that at R_f 0.08 which was probably not very volatile and no further characterisation was, therefore, carried out on that fraction. Recrystallisation of the yellow oil from the R_f 0.77 fraction from CH_2Cl_2 /light petroleum spirits or dry hexane at -18 °C gave a very fine yellow solid. The solid was, however, too fine to collect the solid with a #4 sintered glass or by centrifuge which appeared to have decomposed the compound to a grey solid.

2.4.5.3 Attempted Synthesis of $\text{Fc}(\text{CH}_2)_4\text{AsH}_2$ (**42**) from reaction of $\text{Fc}(\text{CH}_2)_4\text{As}(\text{O})(\text{OH})_2$ (**48**) with Zn/HCl

Arsenic(III) oxide (As_2O_3 , 0.03 g, 0.16 mmol) was dissolved in aqueous sodium hydroxide (2.20 mL, 4.62 mol L^{-1} , 10.17 mmol) and distilled H_2O (3 mL) was added. To this, compound **17** (0.10 g, 0.31 mmol) in CH_2Cl_2 (2 mL) was added and the CH_2Cl_2 was removed under reduced pressure. EtOH (1 drop) was added as a co-solvent. The mixture was heating to reflux under an N_2 atmosphere for 7 h. After cooling, the excess **17** was extracted with CH_2Cl_2 (10 mL), making the aqueous phase almost clear colourless. Acidification of the aqueous phase with aq. HCl (2 M, 30 mL) gave no precipitate. Removal of the solvent from the organic phase under reduced pressure gave a yellow oil. ^1H NMR spectroscopy in CDCl_3 and ESI-MS in

MeOH in positive ion mode showed that it was the unreacted **17**. Distilled H₂O (10 mL), light petroleum spirits (10 mL) and Zn powder (0.5 g) were added to the reaction flask containing the yellow oil. Under an N₂ atmosphere, conc. HCl (10 mL) was added dropwise. The organic phase was separated and removal of the solvent from the organic phase gave a yellow oil. ¹H NMR spectroscopy in CDCl₃ and ESI-MS in MeOH showed that it was **17**.

2.4.5.4 Attempted Synthesis of Fc(CH₂)₁₁AsH₂ (**44**) from reaction of Fc(CH₂)₁₁As(O)(OH)₂ (**49**) with Zn/HCl

In air, arsenic(III) oxide (As₂O₃, 0.64 g, 3.23 mmol) was dissolved in aqueous sodium hydroxide (3.90 mL, 5.07 mol L⁻¹, 19.77 mmol) and the solution was diluted with distilled H₂O (11 mL). This was added to a flask containing **19** (3.26 g, 7.52 mmol). EtOH (1.5 mL) was added as a co-solvent. The mixture was heating to reflux in air for 7 h. After cooling, the reaction mixture was extracted with CH₂Cl₂ (4 × 3 mL) to remove the unreacted bromide. The aqueous phase was acidified with conc. HCl (30 mL). No precipitate was obtained. Removal of the solvent from the aqueous phase under reduced pressure gave a significant amount of a white solid which was probably NaCl and a very small amount of a yellow oil. The yellow oil was extracted with MeOH and filtered. The extract was concentrated and cooled at -18 °C which gave a brown solid (0.004 g). The brown solid was dissolved in aq. NaOH (0.65 mL, 2.00 M, 1.30 mmol) and distilled H₂O (1 mL), light petroleum spirits (10 mL) and Zn powder (0.5 g) were added. Under an N₂ atmosphere, conc. HCl (10 mL) was added dropwise. The organic phase was separated and removal of the solvent from the organic phase gave a small amount of a yellow oil. ¹H NMR spectroscopy and ESI-MS showed that it was the unreacted **19**. The reaction was discontinued.

The reaction was repeated under an N₂ atmosphere. Arsenic(III) oxide (As₂O₃, 0.64 g, 3.23 mmol) was dissolved in aqueous sodium hydroxide (4.00 mL, 5.07 mol L⁻¹, 20.28 mmol) and distilled H₂O (5 mL) was added. This was added to a flask containing **19** (3.26 g, 7.52 mmol) in EtOH (20 mL). The mixture was heating to reflux under an N₂ atmosphere for 7 h. After cooling, the EtOH was removed under

reduced pressure and the residue was extracted with CH_2Cl_2 (4×5 mL) to remove the unreacted **19**. The aqueous phase was acidified with conc. HCl (30 mL). The resulting brown precipitate was filtered with a #4 sintered glass and dried in air. The brown solid (0.14 g) was dissolved in aq. NaOH (0.15 mol L^{-1} , 10 mL) and light petroleum spirits (10 mL) and Zn dust (0.25 g) were added. Under an N_2 atmosphere, conc. HCl (10 mL) was added dropwise. The mixture was stirred for 15 mins. The organic phase remained colourless. After the organic phase was separated and washed with distilled H_2O ($10 \text{ mL} \times 3$), removal of the solvent from the organic phase gave no coloured residue. The reaction was discontinued.

The reaction was repeated without EtOH as co-solvent. Arsenic(III) oxide (As_2O_3 , 0.13 g, 0.66 mmol) was dissolved in aqueous sodium hydroxide (3.24 mL, 2.00 mol L^{-1} , 6.48 mmol) and distilled H_2O (2 mL) was added. This was added to a flask containing **19** (0.57 g, 1.32 mmol). The mixture was heating to reflux in air for 6 h. After cooling, the reaction solution was acidified with conc. HCl (30 mL). The resulting brown precipitate was collected and dried in air. ESI-MS in MeOH showed no ions corresponding to the desired compound in either ion mode. ^1H and $^{13}\text{C}\{-^1\text{H}\}$ NMR spectroscopy did not suggest the formation of the desired compound either. The reaction was discontinued.

The longer reaction time i.e. > 20 h, the various concentrations of aq. NaOH and/or HCl (i.e. 1 mol L^{-1}), or the increased amount of EtOH did not give the arsonic acid either.

2.4.5.5 Attempted Synthesis of Ferrocenylmethyl Stibane

2.4.5.6 Attempted Synthesis of $\text{FcCH}_2\text{SbCl}_2$ (**46**)

Under an Ar atmosphere, a solution of **40** prepared from the reaction of **47** (1.46 g, 6.35 mmol) and freshly cut small pieces of Li metal (ca. 0.5 g) in dry THF (40 mL) at $-7 - 0$ °C for 3 h, was slowly added over the period of 30 mins, *via* a #4 frit to a solution of SbCl_3 (1.07 g, 4.69 mmol) in dry THF (30 mL). The mixture was stirred

for 1 h at that temperature. Removal of the solvent under vacuum at 0 °C gave a brown oil (4.66 g). This was used as obtained without further purification.

2.4.5.7 Attempted Synthesis of $\text{FcCH}_2\text{SbH}_2$ (45)

At 0 °C, LiAlH_4 (0.29 g, 7.63 mmol) was added to a solution of the brown oil (the entire yield obtained as above) in dry Et_2O (60 mL). The mixture was stirred for 3 h at that temperature. A significant amount of a metallic mirror was deposited on the wall of the reaction flask. The insoluble materials were filtered with a #4 frit. Removal of the solvent from the filtrate under vacuum at 0 °C gave a yellow semi-solid (1.87 g). ESI-MS (MeOH, +ve, 50 V): m/z observed 320.940 [$M - H$]⁺; calcd. 320.932 for $\text{C}_{11}\text{H}_{12}\text{Fe}_1\text{Sb}_1$ which was common type of ionisation for primary stibanes¹²⁵. IR spectroscopy showed a weak broad band at 1966w, br which was probably too high to be assigned for the Sb-H str (cf. $\sim 1880^{125} \text{ cm}^{-1}$). Despite the attempts, satisfactory NMR data could not be obtained.

2.4.6 X-Ray Crystallography

X-ray crystallographic structural data were collected by Dr. Tania Groutso at Auckland University in New Zealand.

Table 2-19: Bond lengths (Å) and angles (°) for 34

Lengths / Å		Angles / °			
Fe(1)-C(14)	2.0391(13)	C(14)-Fe(1)-C(13)	40.86(5)	C(6)-P(2)-H(5)	103.0(8)
Fe(1)-C(13)	2.0425(13)	C(14)-Fe(1)-C(24)	123.85(6)	B(1)-P(2)-H(5)	113.8(9)
Fe(1)-C(24)	2.0452(13)	C(13)-Fe(1)-C(24)	106.15(6)	H(4)-P(2)-H(5)	102.0(12)
Fe(1)-C(12)	2.0465(13)	C(14)-Fe(1)-C(12)	68.52(5)	P(2)-B(1)-H(1)	106.1(10)
Fe(1)-C(23)	2.0466(14)	C(13)-Fe(1)-C(12)	40.82(5)	P(2)-B(1)-H(2)	102.9(10)
Fe(1)-C(25)	2.0489(13)	C(24)-Fe(1)-C(12)	120.15(6)	H(1)-B(1)-H(2)	114.8(14)
Fe(1)-C(21)	2.0528(13)	C(14)-Fe(1)-C(23)	107.62(6)	P(2)-B(1)-H(3)	106.2(10)
Fe(1)-C(22)	2.0531(13)	C(13)-Fe(1)-C(23)	120.55(6)	H(1)-B(1)-H(3)	113.4(14)
Fe(1)-C(15)	2.0577(13)	C(24)-Fe(1)-C(23)	40.73(6)	H(2)-B(1)-H(3)	112.2(13)
Fe(1)-C(11)	2.0657(13)	C(12)-Fe(1)-C(23)	155.78(6)	C(11)-C(1)-C(2)	116.46(11)
P(2)-C(6)	1.8164(13)	C(14)-Fe(1)-C(25)	160.42(6)	C(1)-C(2)-C(3)	111.08(11)
P(2)-B(1)	1.9204(17)	C(13)-Fe(1)-C(25)	123.27(6)	C(4)-C(3)-C(2)	114.09(11)
P(2)-H(4)	1.305(19)	C(24)-Fe(1)-C(25)	40.73(5)	C(3)-C(4)-C(5)	112.22(11)
P(2)-H(5)	1.29(2)	C(12)-Fe(1)-C(25)	106.76(6)	C(6)-C(5)-C(4)	112.88(11)
B(1)-H(1)	1.074(18)	C(23)-Fe(1)-C(25)	68.44(6)	C(5)-C(6)-P(2)	113.65(9)
B(1)-H(2)	1.127(18)	C(14)-Fe(1)-C(21)	157.56(6)	C(12)-C(11)-C(15)	107.20(11)
B(1)-H(3)	1.11(2)	C(13)-Fe(1)-C(21)	160.52(6)	C(12)-C(11)-C(1)	124.22(12)
C(1)-C(11)	1.5040(18)	C(24)-Fe(1)-C(21)	68.49(5)	C(15)-C(11)-C(1)	128.46(12)
C(1)-C(2)	1.5227(18)	C(12)-Fe(1)-C(21)	124.33(6)	C(12)-C(11)-Fe(1)	68.95(7)
C(2)-C(3)	1.5301(17)	C(23)-Fe(1)-C(21)	68.41(6)	C(15)-C(11)-Fe(1)	69.42(7)
C(3)-C(4)	1.5260(18)	C(25)-Fe(1)-C(21)	40.63(6)	C(1)-C(11)-Fe(1)	129.75(9)
C(4)-C(5)	1.5286(18)	C(14)-Fe(1)-C(22)	122.01(6)	C(13)-C(12)-C(11)	108.80(11)
C(5)-C(6)	1.5281(18)	C(13)-Fe(1)-C(22)	156.71(6)	C(13)-C(12)-Fe(1)	69.44(7)
C(11)-C(12)	1.4282(18)	C(24)-Fe(1)-C(22)	68.50(6)	C(11)-C(12)-Fe(1)	70.40(7)
C(11)-C(15)	1.4287(18)	C(12)-Fe(1)-C(22)	161.63(6)	C(14)-C(13)-C(12)	107.57(12)
C(12)-C(13)	1.4260(18)	C(23)-Fe(1)-C(22)	40.70(6)	C(14)-C(13)-Fe(1)	69.44(7)
C(13)-C(14)	1.4247(19)	C(25)-Fe(1)-C(22)	68.36(6)	C(12)-C(13)-Fe(1)	69.74(7)
C(14)-C(15)	1.4286(18)	C(21)-Fe(1)-C(22)	40.60(6)	C(13)-C(14)-C(15)	108.12(12)
C(21)-C(25)	1.424(2)	C(14)-Fe(1)-C(15)	40.81(5)	C(13)-C(14)-Fe(1)	69.70(8)
C(21)-C(22)	1.424(2)	C(13)-Fe(1)-C(15)	68.59(5)	C(15)-C(14)-Fe(1)	70.29(7)
C(22)-C(23)	1.426(2)	C(24)-Fe(1)-C(15)	161.61(5)	C(14)-C(15)-C(11)	108.31(12)
C(23)-C(24)	1.424(2)	C(12)-Fe(1)-C(15)	68.15(5)	C(14)-C(15)-Fe(1)	68.90(8)
C(24)-C(25)	1.4248(19)	C(23)-Fe(1)-C(15)	125.52(6)	C(11)-C(15)-Fe(1)	70.03(7)
		C(25)-Fe(1)-C(15)	156.86(5)	C(25)-C(21)-C(22)	108.00(12)
		C(21)-Fe(1)-C(15)	122.27(5)	C(25)-C(21)-Fe(1)	69.54(7)
		C(22)-Fe(1)-C(15)	108.96(5)	C(22)-C(21)-Fe(1)	69.71(8)
		C(14)-Fe(1)-C(11)	68.70(5)	C(21)-C(22)-C(23)	107.92(12)
		C(13)-Fe(1)-C(11)	68.79(5)	C(21)-C(22)-Fe(1)	69.69(8)
		C(24)-Fe(1)-C(11)	155.77(6)	C(23)-C(22)-Fe(1)	69.41(8)
		C(12)-Fe(1)-C(11)	40.64(5)	C(24)-C(23)-C(22)	108.08(12)
		C(23)-Fe(1)-C(11)	162.28(5)	C(24)-C(23)-Fe(1)	69.58(8)
		C(25)-Fe(1)-C(11)	120.92(5)	C(22)-C(23)-Fe(1)	69.89(8)
		C(21)-Fe(1)-C(11)	107.98(5)	C(23)-C(24)-C(25)	107.90(12)
		C(22)-Fe(1)-C(11)	125.39(5)	C(23)-C(24)-Fe(1)	69.69(8)
		C(15)-Fe(1)-C(11)	40.54(5)	C(25)-C(24)-Fe(1)	69.77(7)
		C(6)-P(2)-B(1)	117.18(7)	C(21)-C(25)-C(24)	108.10(12)
		C(6)-P(2)-H(4)	104.0(8)	C(21)-C(25)-Fe(1)	69.84(8)
		B(1)-P(2)-H(4)	115.0(8)	C(24)-C(25)-Fe(1)	69.50(7)

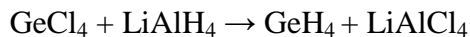
Chapter 3: Stabilisation Effects of Ferrocenylalkyl Groups on the Hydrides of the Heavier Group 14 Elements, Si, Ge, Sn

3.1 Introduction

3.1.1 Hydrides of Heavier Group 14 Elements

Silane, SiH₄, is a colourless and thermally stable gas at 25 °C¹. The substantial and rapid decomposition only occurs at ~450 °C^{1, 4}. Silane is, however, highly air-sensitive and ignites in air in the pure state¹. It can be prepared in good yields by reaction of halogeno silanes, alkoxy silanes or silica with suitable metal hydrides i.e. LiH, NaBH₄, LiAlH₄ and metal duteride i.e. LiAlD₄ in anhydrous organic solvents such as Et₂O and THF, diethylene glycol dimethyl ether. Higher yields are often obtained from reaction of silicon chlorides i.e. SiCl₄ or SiHCl₃ with ether-soluble metal hydrides such as LiAlH₄¹. SiH₄ generally reacts with K, Rb and Cs to form H₃SiM⁴.

Germane, GeH₄, is also a colourless and thermally stable gas at room temperature. It is less flammable than SiH₄ but still reacts vigorously towards air. The decomposition of the compound occurs slowly at 280 °C, producing a germanium mirror and hydrogen¹. Germane can be prepared by reaction of germanium tetrachloride or germanium tetra-alkoxides with metal hydrides and also with Li[Al(OBu^t)₃H] in anhydrous organic solvents (e.g. Et₂O, THF or dioxan)¹.



The Ge-H bond reacts in a similar manner to Si-H bond, including replacement of hydrogen with halogen (i.e. X₂, HX, RX, HgX₂) such as oxygen (i.e. O₂, OH⁻, RCOOH), sulfur (i.e. Ag₂S, RSH), nitrogen (i.e. NH₃), carbon (i.e. N₂CHR, LiR,

addition to alkene and alkyne), alkyl metals (e.g. in liquid ammonia or polyethers), transition metal complexes (e.g. $\text{HMn}(\text{CO})_5$)¹. The reactivity of GeH_4 compared to SiH_4 towards K, Rb and Cs to form H_3GeM^4 is also similar.

Stannane, SnH_4 , is a colourless pyrophoric gas. It is significantly more thermally unstable than SiH_4 and GeH_4 . It decomposes substantially at room temperature. The decomposition occurs even at $-50\text{ }^\circ\text{C}$ into elemental tin and hydrogen, giving a metallic tin mirror, which also catalyses the decomposition. Traces of grease or O_2 are also known to catalyse the decomposition of stannane even though a higher concentration of O_2 is said to inhibit it¹. Stannane can be prepared by reaction of SnCl_4 with LiAlH_4 in dry Et_2O at $-30\text{ }^\circ\text{C}$ ⁴. Stannane reacts in the similar manner as the corresponding silane and germane¹.

Very little is known about plumbane, PbH_4 . It is thermally too unstable to be of any use. The decomposition of the compound occurs at $-196\text{ }^\circ\text{C}$. Plumbane is thought to form in traces when Mg-Pb alloys are hydrolysed by acid or when Pb^{2+} salts are reduced cathodically⁴. Many attempts to prepare PbH_4 from alternate routes have been unsuccessful⁴. Unlike SnH_4 , PbH_4 doesn't form in aqueous media from PbBr_2 or $\text{NaPb}(\text{OH})_3$ with NaBH_4 or in aqueous HBr solution in Et_2O at $-140 - -78\text{ }^\circ\text{C}$ which gives SnH_4 in 84 % yield. Reaction of PbCl_4 with LiAlH_4 or $\text{Li}[\text{AlH}(\text{O}i\text{Bu})_3]$ or LiBH_4 does not provide PbH_4 either. It cannot be prepared by reaction of $\text{Pb}(\text{OMe})_4$ with $(\text{BH}_3)_2$ which successfully yields SnH_4 from $\text{Sn}(\text{OMe})_4$, mainly because $\text{Pb}(\text{OMe})_4$ cannot be prepared from lead(IV) compounds either by alcoholysis or by reaction with sodium methoxide¹. Hydrogenation of lead(II) compounds with metal hydride has not been successful in providing the hydrides either.

3.1.2 Organo-silanes, -germanes and -stannanes

While SiH_4 and GeH_4 are highly toxic and pyrophoric gases with unpleasant odours¹, most organo-silicon and -germanium hydrides, $\text{R}_{4-n}\text{EH}_n$ ($\text{E} = \text{Si}$ or Ge ; $n = 1 - 3$), are typically air-stable and only slowly decompose in air at room temperature. The corresponding stannanes are, however, more thermally unstable as well as air-

sensitive^{1, 39}. The decompositions of stannanes are detected by deposition of a metallic tin mirror¹²⁹. The thermal stability of organoderivatives of the hydrides of heavier group 14 elements decreases in the order of $R_{4-n}EH_n$ ($E = Si > Ge > Sn$; $n = 1 > 2 > 3$) and aryl analogues are more unstable than the corresponding alkyl ones^{1, 39}. Organogermanes are only slightly more thermally unstable than the corresponding silanes and decompose slowly at room temperature into hydrogen and organic or organogermanium compounds depending on the nature of the R groups bonded to the germanium.

The applications of the organoderivatives of the hydrides of heavier group 14 elements, especially organosilanes, are diverse, ranging from chemical vapour deposition of the elements onto material surfaces as superconductor at higher temperatures (i.e. at > 420 °C for Si)¹³⁰, coupling agent to adhere glass fibres to a polymer matrix or a bio-inert layer on a titanium implant, water repellents, masonry protection, control of graffiti, sealants, supersonic combustion ramjets to reducing agents and precursors in organic¹³⁰ and organometallic chemistry¹. Main uses of organo-germanes and -stannanes are also as intermediates in organic syntheses^{39, 131}.

3.1.3 Stabilisation of Hydrides of Heavier Group 14 Elements

Steric protection around the hydride centre can also be effective at stabilising primary germanes⁷⁶ and stananes¹³² (Figure 3-1).

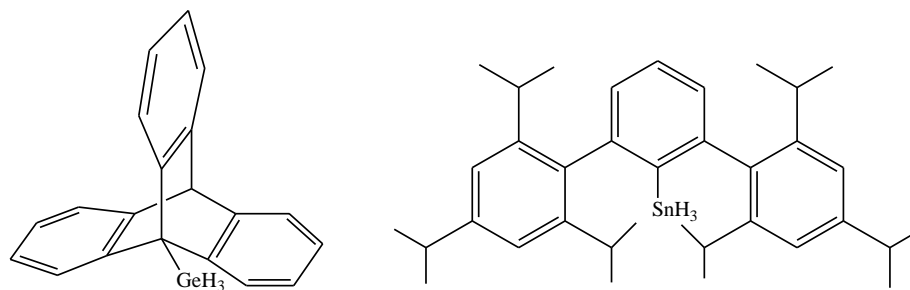
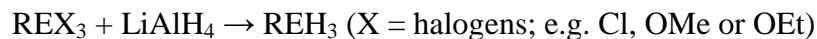


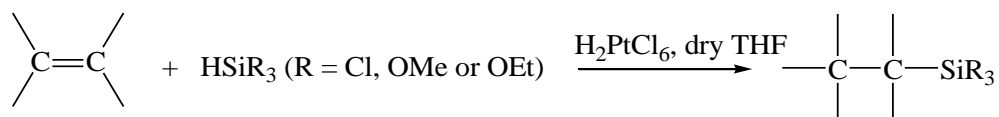
Figure 3-1: *Stable primary organo-germane and -stannane*

3.1.4 Synthesis of Hydrides of Heavier Group 14 Elements

The hydrides of the heavier group 14 elements are commonly prepared by reduction of the corresponding halides with lithium aluminium hydride^{129, 133}.

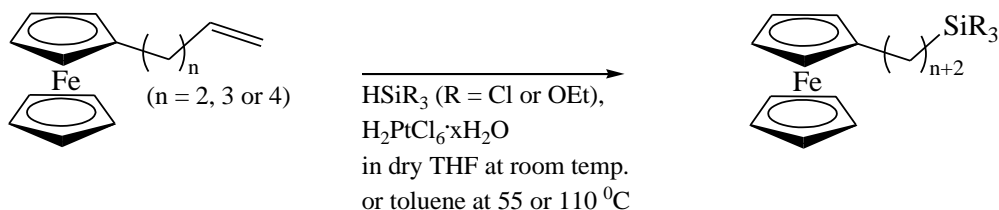


Hydrosilation of an alkene using a Pt catalyst¹³⁴ is well established for the synthesis of organosilanes. A trihalogenated silane can add to an alkene in a mild condition (i.e. room temperature) using a Pt catalyst (H_2PtCl_6) in dry THF (Scheme 3-1).



Scheme 3-1: Hydrosilation of alkene using a Pt catalyst

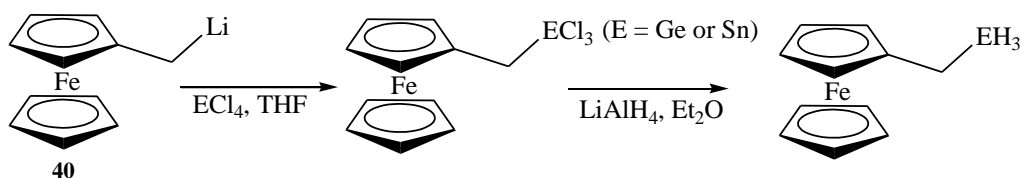
Hydrosilation of ferrocenyl alkenes, $\text{Fc}(\text{CH}_2)_n\text{CH}=\text{CH}_2$ ($n = 2, 3$ or 4) with trihalogenated silane, HSiR_3 ($\text{R} = \text{Cl}$ or OEt), catalysed by $\text{H}_2\text{PtCl}_6 \cdot x\text{H}_2\text{O}$ to give the corresponding trichloro or ethoxy silanes, $\text{Fc}(\text{CH}_2)_{n+2}\text{SiR}_3$ (Scheme 3-2), has been well known^{134, 135}. Reduction of the trihalogenated silanes with an appropriate reducing agent, i.e. metal hydride, should provide the corresponding silanes, $\text{Fc}(\text{CH}_2)_{n+2}\text{SiH}_3$. This approach was also employed in the present research.



Scheme 3-2: Hydrosilation of ferrocenyl alkenes with a Pt catalyst

For the synthesis of the corresponding germanium and tin halides, FcCH_2EH_3 ($\text{E} = \text{Ge}$ or Sn), the synthesis using ferrocenylmethyl lithium **40**¹²³ was adopted. The reaction of excess **40** with ECl_4 ($\text{E} = \text{Ge}$ or Sn) should give the corresponding trihalogenatedmethyl ferrocene, $\text{FcCH}_2\text{ECl}_3$. Reduction of the trihalogenatedmethyl

ferrocene with a suitable reducing agent such as lithium aluminium hydride should give the corresponding desired hydrides, FcCH_2EH_3 (Scheme 3-3).



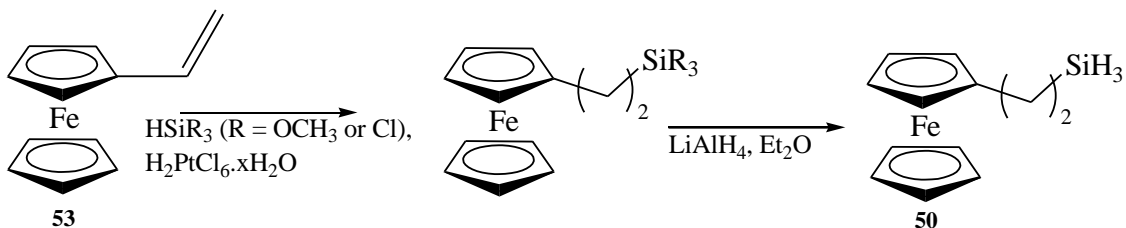
Scheme 3-3: Synthesis of FcCH_2EH_2 ($E = \text{Ge}$ or Sn) via $\text{FcCH}_2\text{ECl}_3$

This chapter describes the synthesis and characterisation of ferrocenylalkyl silane and germane and also the attempts to synthesise ferrocenylalkyl stannanes. The stabilities of the silane and germane under ambient conditions determined by NMR spectroscopy are also reported in the chapter.

3.2 Results and Discussion

3.2.1 Synthesis and Characterisation of Ferrocenylethyl Silane, $\text{FcCH}_2\text{CH}_2\text{SiH}_3$ (**50**)

A new silane, ferrocenylethyl silane **50**, could be prepared by reduction of the corresponding silicon halides, $\text{FcCH}_2\text{CH}_2\text{SiX}_3$ ($X = \text{Cl}$ **51** or OMe **52**) with LiAlH_4 . Compound **51** was obtained by a well-established hydrosilylation¹³⁶⁻¹³⁸ of the corresponding vinyl ferrocene, $\text{FcCH}=\text{CH}_2$ **53**, with HSiR_3 catalysed by a Pt catalyst generated *in situ* from hydrated H_2PtCl_6 (Scheme 3-4).



Scheme 3-4: Synthesis of **50**

Compound **53** was prepared using the literature methods^{139, 140} with minor modifications where required and confirmed by ¹H NMR spectroscopy. The ¹H NMR data were consistent with the literature values¹⁴⁰⁻¹⁴². The vinyl ferrocene **53** was purified prior to the subsequent reaction by column chromatography on silica-gel, eluting with hexane.

The literature conditions¹⁴⁰ for the synthesis of Fc(CH₂)₅SiCl₃ **54** also from a Pt-catalysed reaction of Fc(CH₂)₃CH=CH₂ **55** with HSiCl₃ were adopted for the synthesis of **51** due to the excellent yield of the synthesis i.e. 93 % reported.

3.2.1.1 Synthesis and Characterisation of Fc(CH₂)₂SiX₃ (X = Cl (**51**) and OMe (**52**))

Hydrosilation of **53** with HSi(OCH₃)₃ or HSiCl₃ catalysed by a dry THF solution of H₂PtCl₆·xH₂O, after removal of the unwanted volatiles under reduced pressure, yielded **51** and **52** as a viscous brown and red oil, respectively. The crude products were extracted with dry CH₂Cl₂ and the insolubles were removed by filtration. No further purification was carried out due to the extreme moisture-sensitivity of the desired compounds. They could also be only partially characterised by ESI- and/or GC-MS, IR and NMR spectroscopy because of the extreme instability of the compounds.

Despite the attempts, the mass spectrometric data for **51** could not be obtained by GC- or ESI-MS, which might not be surprising considering the instability of the compound. In the IR spectrum, the *Si-C* stretch for **51** could, however, be observed at ν 484 cm⁻¹ (Figure 3-2) as a medium peak which is a little lower than ν 587 cm⁻¹ for **54**¹⁴⁰.



Figure 3-2: Partial IR Spectrum of **51**

Better resolution could be achieved for the NMR spectra of **51** when the crude product was extracted with dry CH_2Cl_2 and the insoluble materials were filtered with a frit possibly due to the elimination of paramagnetic ferricinium species. The assignments of the ^1H and ^{13}C NMR chemical shifts were made according to the $^{1,2,3}J_{\text{CH}}$ and $^3J_{\text{HH}}$ correlations observed in the HMBC, HSQC and COSY NMR experiments as well as with reference to the literature values for **51**¹⁴⁰. The selected $^{1,2,3}J_{\text{CH}}$ and $^3J_{\text{HH}}$ correlations observed for **51** in the 2-D NMR experiments are shown in Figure 3-3.

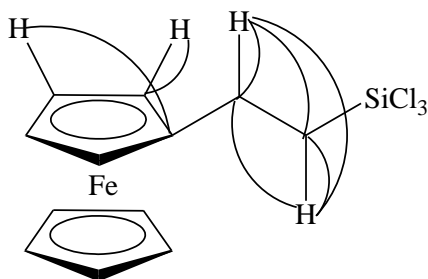


Figure 3-3: Selected $^{1,2,3}J_{\text{CH}}$ and $^3J_{\text{HH}}$ correlations observed for **51** in the HMBC, HSQC and COSY NMR experiments

The mass spectrometric data for **52** could be obtained by GC- and ESI-MS. In the GC mass spectrum, the molecular ion, $[M]^+$, as well as the ions corresponding to the fragmentation, $[\text{FcCH}_2]^+$, $[\text{CpFe}]^+$ and $[\text{Fe}]^+$, were observed. In the ESI mass spectrum, the molecular ion, $[M]^+$, (Figure 3-4) as well as the sodium adduct $[M + \text{Na}]^+$ were observed in the positive-ion mode using MeOH as a mobile phase with a drop of CH_2Cl_2 added to aid solubility.

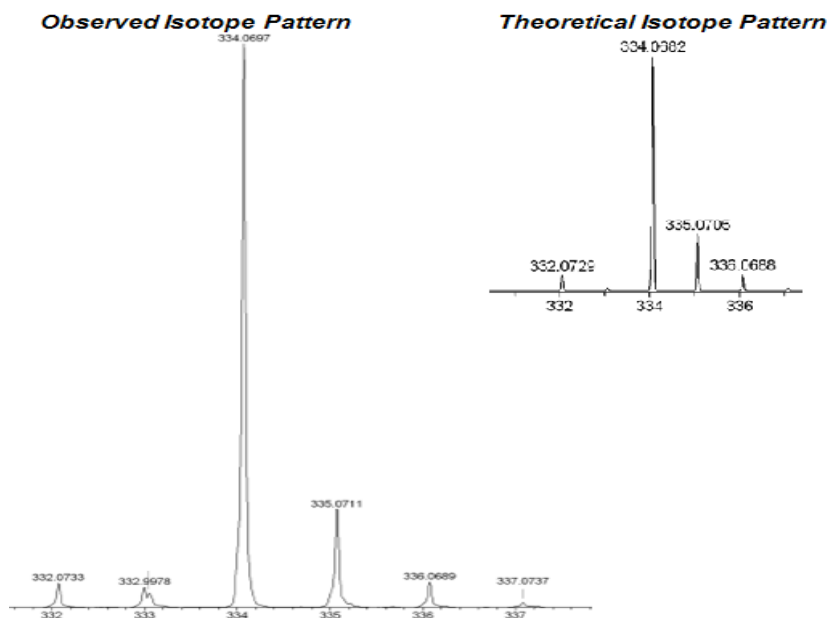


Figure 3-4: Partial ESI-MS of **52** showing the observed and theoretical $[M]^+$ ion ($M = 52$)

The NMR data for **52** were consistent with the literature values for $\text{PhCH}_2\text{Si}(\text{OCH}_3)_3$ ¹⁴³ and also comparable to those for $\text{Fc}(\text{CH}_2)_6\text{Si}(\text{OCH}_2\text{CH}_3)_3$ ¹⁴⁴. The CH_2Si and CpCH_2 proton signals appeared at δ 1.2 and δ 2.3 ppm, respectively, which showed $^{1,2,3}J_{\text{CH}}$ and $^3J_{\text{HH}}$ correlations to the respective carbon signals in the HMBC, HSQC and COSY NMR experiments. The selected $^{1,2,3}J_{\text{CH}}$ NMR correlations observed in the 2-D NMR experiments are shown in Figure 3-5. The SiOCH_3 proton signal was observed at δ 3.6 ppm which was comparable to the literature values for **55** and **56** (cf. δ 3.4 ppm for $\text{PhCH}_2\text{Si}(\text{OCH}_3)_3$ ¹⁴³ and δ 3.8 ppm for $\text{Fc}(\text{CH}_2)_6\text{Si}(\text{OCH}_2\text{CH}_3)_3$ ¹⁴⁴). The assignments of the chemical shifts were made according to the 2-D NMR data obtained by HMBC, HSQC and COSY NMR experiments as well as by comparison to the literature values for **55** and **56**.

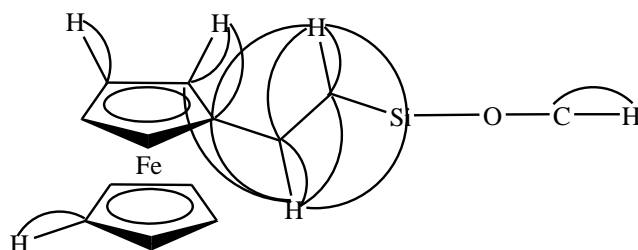


Figure 3-5: Selected $^{1,2,3}J_{\text{CH}}$ and $^3J_{\text{HH}}$ correlations observed for **52** in the HMBC, HSQC and COSY NMR experiments

Compound **52** seemed more stable than compound **51** and hence maybe a better precursor because more purifications could be performed on the compound which may be advantageous.

3.2.1.2 Synthesis of $\text{Fc}(\text{CH}_2)_2\text{SiH}_3$ (**50**)

Compound **51** was reduced with LiAlH_4 in dry Et_2O at $0\text{ }^\circ\text{C}$ under an N_2 atmosphere. After removal of the reaction solvent under reduced pressure, the residue was extracted with dry hexane and then the insoluble materials were filtered with a #4 frit. Removal of the solvent from the filtrate under reduced pressure gave **50** as a yellow oil in moderate yield (65 %).

Compound **50** could also be prepared by reduction of **52** with LiAlH_4 in dry Et_2O . After stirring the reaction mixture at room temperature under an N_2 atmosphere for 3.5 h, the supernatant was transferred into another Schlenk flask *via* a N_2 -filled syringe. To the solution, a 4 M HCl solution was slowly added at $0\text{ }^\circ\text{C}$ to destroy the excess LiAlH_4 . After stirring the solution for approximately 10 mins, the organic phase was washed with distilled H_2O . Removal of the solvent from the organic phase under reduced pressure at $25\text{ }^\circ\text{C}$ gave a yellow oil which exceeded the theoretical yield, suggesting that it contained impurities.

The attempted purification of the crude product by chromatography on a preparative TLC plate and recrystallisation from hexane at $-18\text{ }^\circ\text{C}$ were unsuccessful. No precipitate could be obtained from the recrystallisation which may not be surprising as compound **51** is probably very non-polar and hence very soluble in hexane.

3.2.1.3 Characterisation of $\text{Fc}(\text{CH}_2)_2\text{SiH}_3$ (**50**)

Compound **50** was characterised by IR, NMR spectroscopy and GC- and/or ESI-MS. The spectroscopic data were comparable to those for $\text{PhCH}_2\text{SiH}_3$, $\text{PhCH}_2\text{CH}_2\text{SiH}_3$ and $n\text{-C}_8\text{H}_{17}\text{SiH}_3$ in the literature¹⁴⁵. The selected spectroscopic data and those for

PhSiH₃, PhCH₂SiH₃, PhCH₂CH₂SiH₃ and *n*-C₈H₁₇SiH₃ adopted from the literature¹⁴⁵ for comparative purposes are summarised in Table 3-1.

	ν Si-H / cm^{-1}	δ SiH ₃ / ppm* ¹
PhSiH ₃ *	2156	4.4 / 4.3 ¹⁴⁵ (in CCl ₄)
PhCH ₂ SiH ₃ ¹⁴⁵	~2160 ¹⁴⁵ or 2150 ¹⁴³	3.7 (in CCl ₄) or 3.6 ¹⁴³
Ph(CH ₂) ₂ SiH ₃ ¹⁴⁵	~2160	3.4 (in CCl ₄)
50	2151	3.5
<i>n</i> -C ₈ H ₁₇ SiH ₃ ¹⁴⁵	~2160	3.5 (in CCl ₄)

*was available in the laboratory; the NMR data are recorded in CDCl₃ unless otherwise specified.

The Si-H stretch for **50** was observed at 2151 cm⁻¹ as a medium band (Figure 3-6) and is consistent with the literature values for PhCH₂SiH₃, PhCH₂CH₂SiH₃ and *n*-C₈H₁₇SiH₃ (Table 3-1).

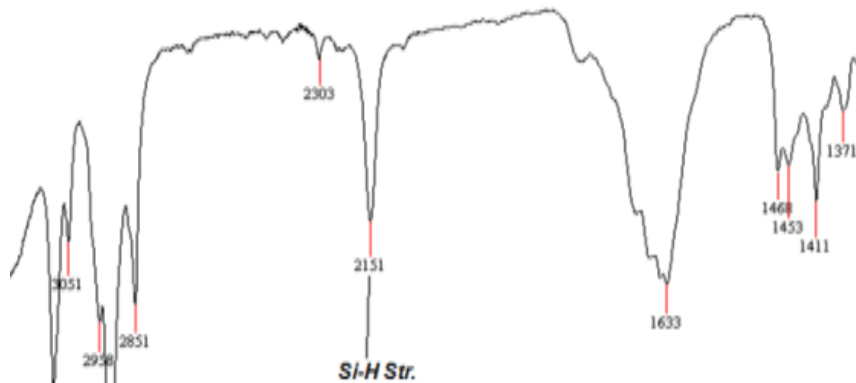


Figure 3-6: IR spectrum of **50**

The silane proton signal appeared at δ 3.5 ppm as a triplet with a $^3J_{HH}$ coupling constant of 4 Hz (Figure 3-7). The chemical shift is consistent with those listed in Table 3-1.

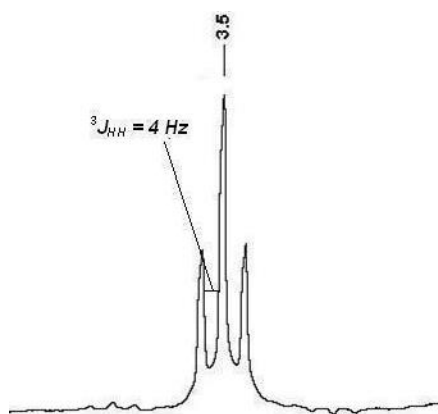


Figure 3-7: Partial ^1H NMR spectrum showing the δ Si-H Signal of **50**

The 2-D NMR data were also consistent with the structure of **50**. The selected $^{1,2,3}J_{\text{CH}}$ and $^3J_{\text{HH}}$ correlations observed for **50** in the HMBC, HSQC and COSY NMR experiments are shown Figure 3-8.

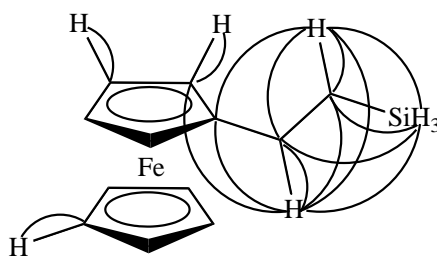


Figure 3-8: Selected $^{1,2,3}J_{\text{CH}}$ and $^3J_{\text{HH}}$ correlations observed for **50** in the HMBC, HSQC and COSY NMR experiments

The molecular ion, $[M]^+$, was observed in the positive ion mode of ESI-MS using MeOH as a mobile phase at capillary exit voltage of 80 V. The observed isotope distribution patterns agreed with the theoretical one (Figure 3-9).

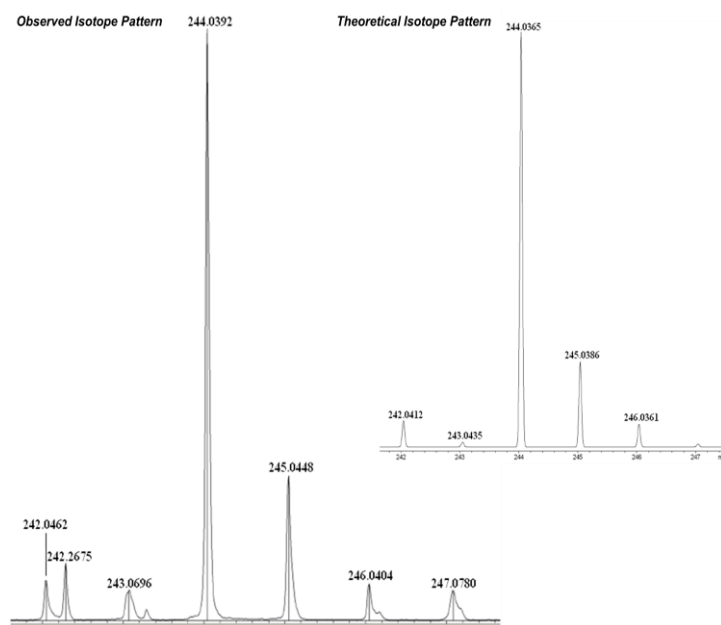
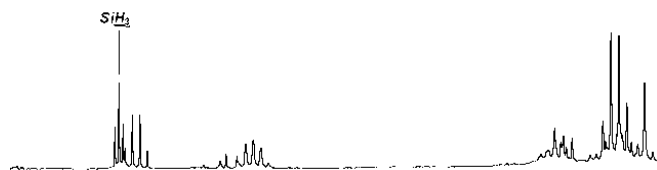


Figure 3-9: Partial ESI-MS of **50** showing the observed and theoretical $[M]^+$ ion ($M = 50$)

3.2.2 Air-Stability of $\text{Fc}(\text{CH}_2)_2\text{SiH}_3$ (**50**)

The air oxidation of **50** in CDCl_3 in a capped NMR tube in air at ambient temperature was monitored by ^1H NMR spectroscopy. The silane proton signal could be observed for 218 days with slight reduction in the intensity of the signal, suggesting that it was quite stable in air (Figure 3-10). This may not be surprising as monoalkylated silanes are usually stable in air at room temperature.

After 1 hour in Solution at Room Temperature in a Capped NMR Tube in Air



After 218 days in Solution at Room Temperature in a Capped NMR Tube in Air

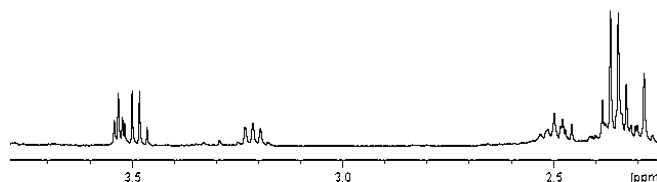
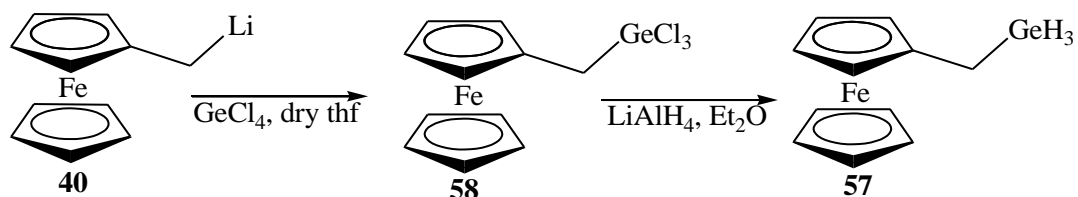


Figure 3-10: Partial ^1H NMR spectra showing the oxidation of **50** in CDCl_3 at room temperature in a capped NMR tube in air over 218 days

3.2.3 Synthesis and Characterisation of Ferrocenylmethyl Germane, $\text{FcCH}_2\text{GeH}_3$ (**57**)

Ferrocenylmethyl germane **57** was prepared analogously to the corresponding arsenic analogue **38** the synthesis of which is described in Chapter 2. The synthesis of **57** via the corresponding germanium halide, $\text{FcCH}_2\text{GeCl}_3$ **58**, is shown in Scheme 3-5.



Scheme 3-5: Synthesis of **57** via **58**

3.2.3.1 Synthesis and Characterisation of $\text{FcCH}_2\text{GeCl}_3$ (**58**)

The precursor **58**, which was also a new compound, was prepared from the reaction of **40** with GeCl_4 in dry THF (Scheme 3-5). After stirring the reaction mixture for 4 h

at room temperature under an Ar atmosphere, removal of the solvent from the mixture under reduced pressure yielded **58** as a dark brown oil and was used as obtained in the subsequent reaction without further purifications.

Compound **58** was partially characterised by ESI-MS and IR and NMR spectroscopy. In the IR spectrum, a weak band was observed at ν 422 cm^{-1} (Figure 3-11). Since *Ge-Cl* stretches often appear in the region (cf. ν 426 – 430 cm^{-1} for RGeCl_3 (R = Me, *i*-Pr, *n*-Bu, *sec*-Bu, *tert*-Bu, allyl, Ph or PhCH_2 ³⁹; ν 425 and 422 cm^{-1} for 2-trichlorogermylmethylbutanedioic acid and 3-trichlorogermylpentanedioic acid, respectively¹⁴⁶), the band may be assigned as the *Ge-Cl* stretch.

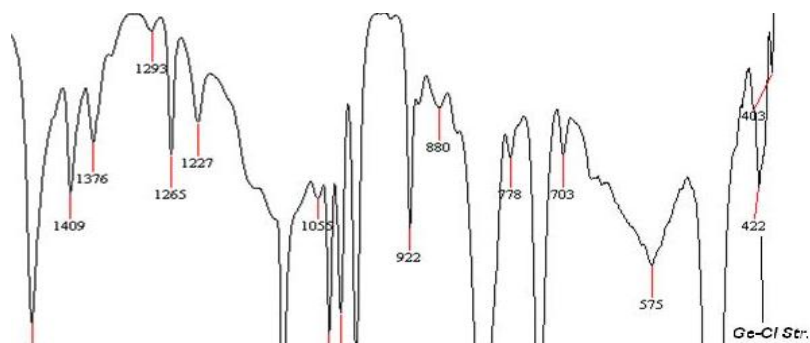


Figure 3-11: IR spectrum of **58**

The mass spectrometric data were obtained by ESI-MS using MeCN as a mobile phase. The corresponding ion was observed as $[\text{FcCH}_2\text{Ge}(\text{OH})\text{Cl}_2]^+$ (Figure 3-12). One of the chlorides had been replaced by an OH^- ion probably from the residual moisture in the solvent, giving the observed ion in the positive-ion mode. The observed and theoretical isotope distribution patterns also agreed.

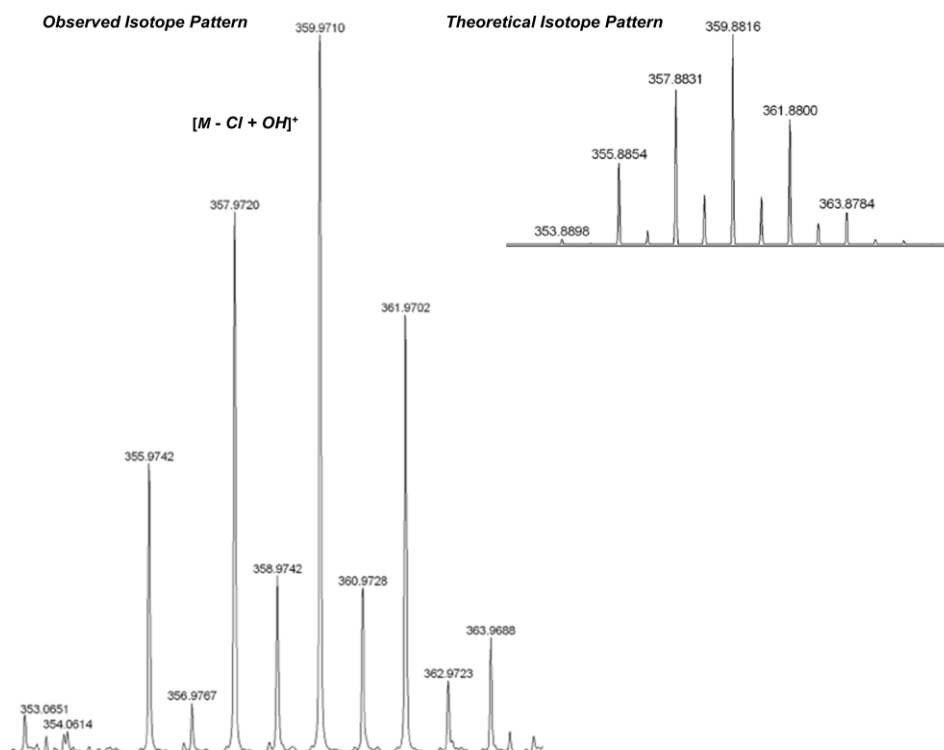


Figure 3-12: Partial ESI-MS of **58** showing the observed and theoretical $[M - Cl + OH]^+$ ion ($M = 58$)

The 2-D NMR data were also consistent with the structure of the expected compound. The assignments of the chemical shifts were made according to the 2-D data and the selected $^{1,2,3}J_{CH}$ correlations observed in the respective HMBC and HSQC NMR experiments are shown in Figure 3-13. The chemical shift of the methylene proton signal ($\text{FcCH}_2\text{GeCl}_3$) appeared at δ 3.3 ppm and is consistent with the literature value for $\text{PhCH}_2\text{GeCl}_3$ (δ 3.4 ppm)¹³⁵.

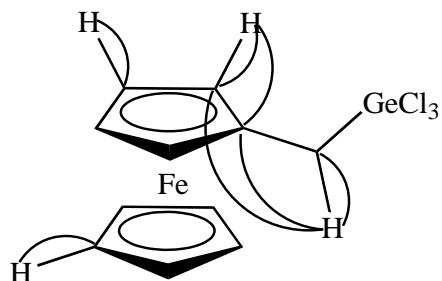


Figure 3-13: Selected $^{1,2,3}J_{CH}$ correlations observed for **58** in the HMBC and HSQC NMR experiments

3.2.3.2 Synthesis of $\text{FcCH}_2\text{GeH}_3$ (**57**)

Compound **57** was prepared by reduction of **58** prepared as above with LiAlH_4 in dry Et_2O . After stirring the reaction mixture at room temperature for 1 h under an N_2 atmosphere, the excess LiAlH_4 was destroyed by addition of aq. HCl at $0\text{ }^\circ\text{C}$ and then filtered with a #4 frit. Removal of the solvent from the filtrate gave a mixture of a yellow solid and oil. The mixture was extracted with hexane and the insoluble materials were filtered. Removal of the solvent from the filtrate gave **57** as a yellow oil in moderate yield (35 %).

After confirming the formation of the desired germane **57** by NMR spectroscopy which showed the germane proton signal at δ 3.7 ppm (see 3.2.3.3), attempts were made to purify the compound. The chromatography on a preparative TLC plate, eluting with CH_2Cl_2 gave three yellow fractions. ^1H NMR spectroscopy was carried out on each fraction. It, however, indicated that none contained the desired compound. It appeared that the germane had decomposed during the chromatography. Another sample was, therefore, freshly prepared. The crystallisation of the freshly prepared sample from the mixture of CH_2Cl_2 /hexane at $-18\text{ }^\circ\text{C}$ gave a very fine yellow precipitate which could not be collected because it was too fine to collect even with a #4 sintered glass. The solvents were, therefore, removed and the residue (a yellow oil) was extracted with hexane several times until the extract became clear. Removal of the solvent from the combined organic extracts under reduced pressure gave a yellow oil. ESI- and GC-MS and IR spectroscopy all indicated the presence of the desired compound in the oil. Another attempt was, therefore, made to crystallise the yellow oil from a 1 : 1 mixture of dry CH_2Cl_2 /hexane at $-18\text{ }^\circ\text{C}$. A mixture of a red solid and crystal were obtained after 3 weeks. ESI-MS indicated that the crystals were of the desired compound. The crystals were, therefore, sent for elemental analysis. Satisfactory microanalytical data could, however, not be obtained (i.e. calcd. for $\text{C}_{11}\text{H}_{14}\text{Fe}_1\text{Ge}_1$: C 48.10; H 5.14 %; found: C 63.43; H 5.42 %). The much higher percentage of the carbon composition than expected may suggest that there was still a lot of the organic solvent left in the sample. The crystals were unsuitable for X-ray

crystallographic structural determination either. The decomposition of the red crystals into grey solids after being stored for another 3 weeks at $-18\text{ }^{\circ}\text{C}$ in air were observed.

3.2.3.3 Characterisation of $\text{FcCH}_2\text{GeH}_3$ (**57**)

Since the purifications of **57** were not successful, the compound could only be partially characterised by IR and NMR spectroscopy and ESI-MS. The intensity of the peaks and signals corresponding to the desired compound was always stronger when recorded on a freshly prepared sample. The intensities decreased after handling under ambient conditions (i.e. in air or at room temperature), suggesting compound **57** was not so stable.

The Ge-H stretch appeared at 2030 cm^{-1} as a broad medium peak (Figure 3-14). The peak was in the expected region for the class of compounds concerned (cf. $\sim 2065\text{ cm}^{-1}$ for trihydrides of alkylgermanium³⁹).

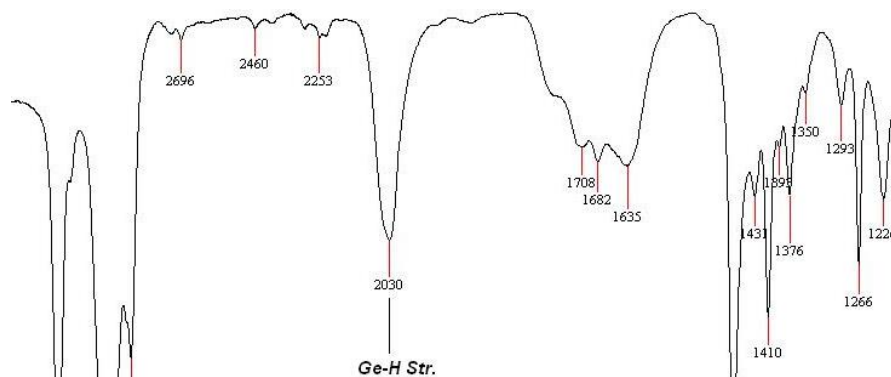


Figure 3-14: IR spectrum of **57**

The mass spectrometric data were obtained by ESI- and GC-MS. In the ESI mass spectrum, the molecular ion, $[M]^+$, was observed at capillary exit voltage of 100 V in the positive-ion mode (Figure 3-15). In the GC-MS spectrum, the molecular ion, $[M]^+$, which had the distinctive isotope pattern of a organogermanium compound, as well as the ions corresponding to common fragments of ferrocenylalkyl compounds, $[\text{FcCH}_2]^+$, $[\text{CpFe}]^+$ and $[\text{Fe}]^+$, were observed (Figure 3-16).

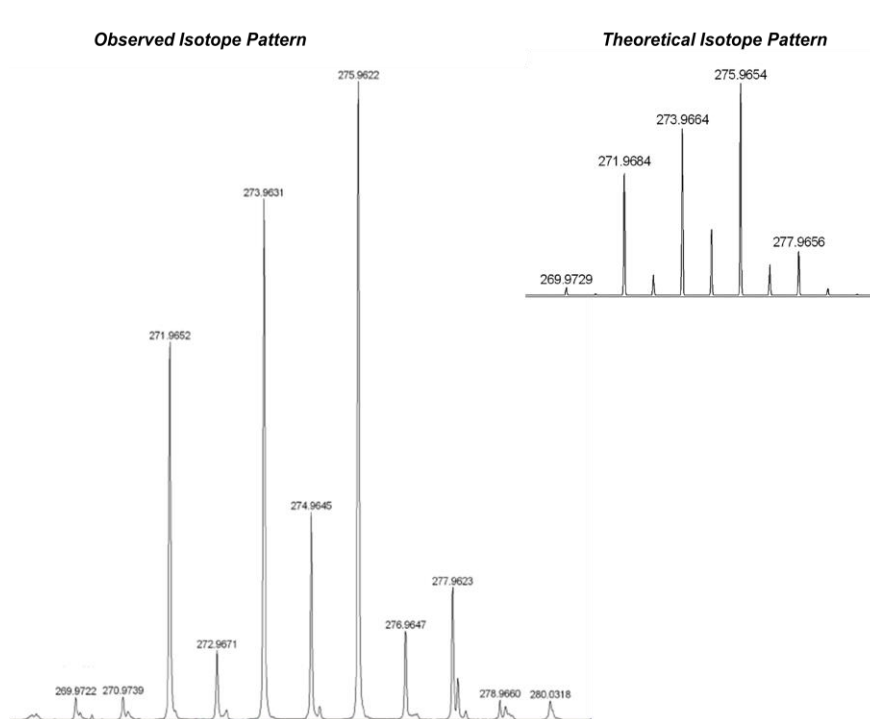


Figure 3-15: Partial ESI-MS of **57** showing the observed and theoretical $[M]^+$ ion ($M = 57$)

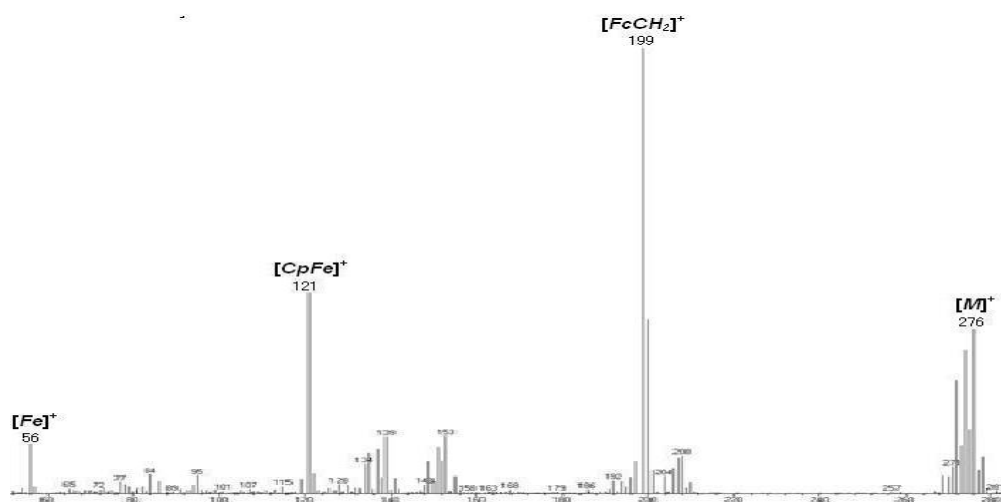


Figure 3-16: GC-MS of **57**

The germane proton NMR signal appeared at δ 3.7 ppm as a triplet with a $^3J_{HH}$ coupling constant of 3 Hz. The $^3J_{HH}$ coupling constant agrees with the literature value for EtGeH₃ (3 Hz³⁹). In the COSY NMR experiment, the $^3J_{HH}$ correlation between the germane proton, GeH₃, and methylene proton, CH₂, signals could also be observed (Figure 3-17). The ¹³C and 2-D NMR data were also consistent with the structure of the expected compound and the assignments of the chemical shifts were made according

to those 2-D NMR data. The selected $^{1,2,3}J_{CH}$ and $^3J_{HH}$ correlations observed in the respective HMBC, HSQC and COSY NMR experiments are shown in Figure 3-18.

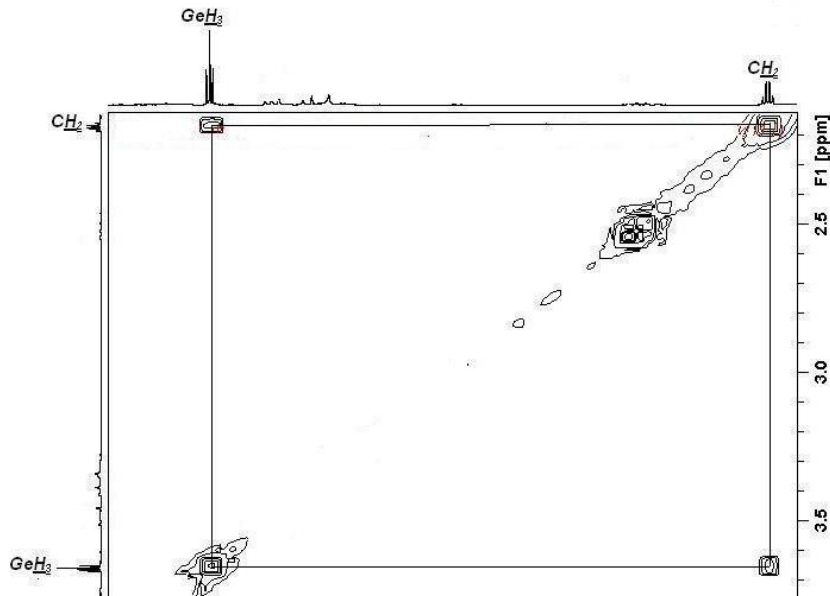


Figure 3-17: Partial COSY NMR spectrum of **57**

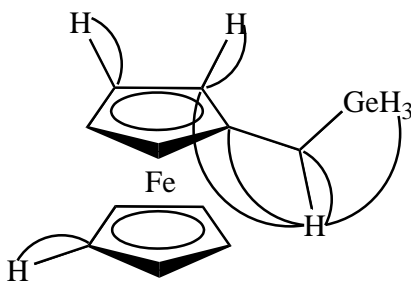


Figure 3-18: Selected $^{1,2,3}J_{CH}$ and $^3J_{HH}$ correlations observed for **57** in the HMBC, HSQC and COSY NMR experiments

3.2.4 Stability of $\text{FcCH}_2\text{GeH}_3$ (**57**)

The stability of **57** in solution (in CDCl_3) at room temperature in air was monitored by ^1H NMR spectroscopy. The sample was kept at room temperature in air with a plastic NMR lid on. The disappearance of the germane proton NMR signal was observed after 20 h at 300 K (Figure 3-19), suggesting that it was not so stable in solution at room temperature in air.

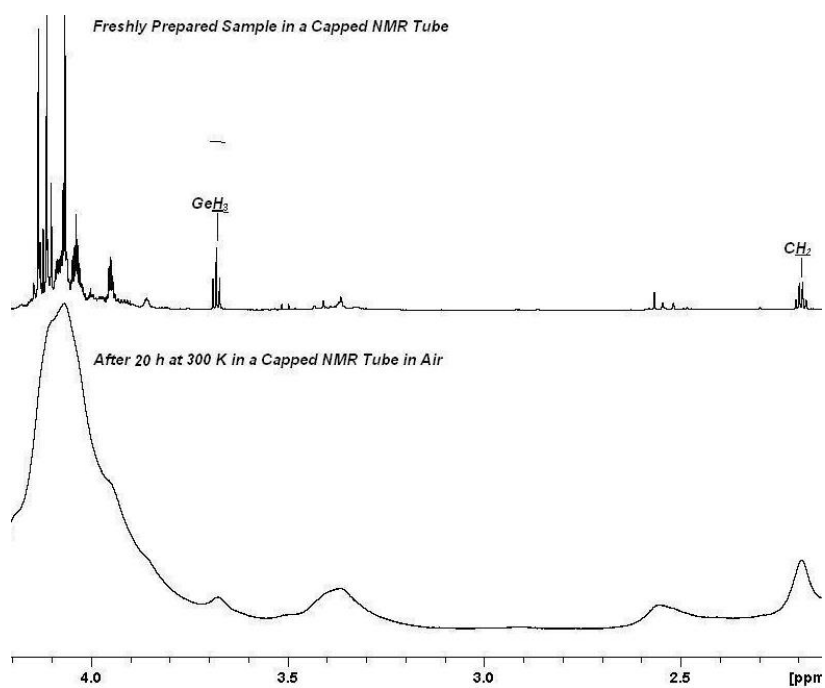
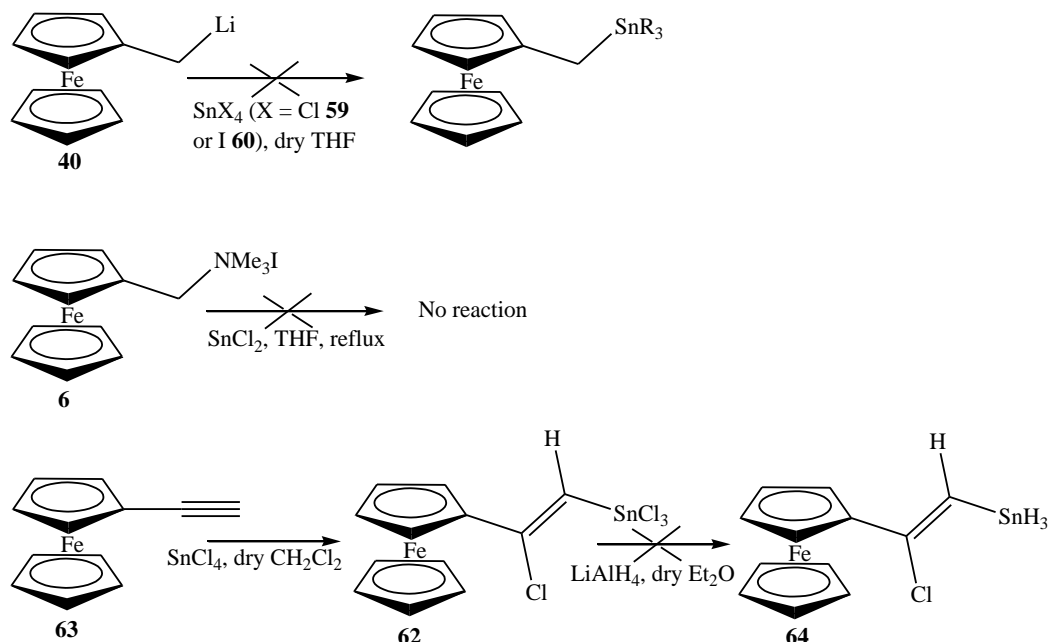


Figure 3-19: ^1H NMR spectra of **57** in solution at 300 K over 20 hours

3.2.5 Attempted Syntheses and Characterisations of Ferrocenylalkyl Stannane

Alkyl primary stannanes, RSnH_3 , can generally be prepared from the corresponding halides⁵¹. Attempts were, therefore, made to synthesise ferrocenylalkyl stannic halides, $\text{FcCH}_2\text{SnX}_3$ ($\text{X} = \text{Cl}$ **59** or I **60**), analogously to the corresponding arsenic **39** and germanium **58** halides, by reaction of FcCH_2Li **40** with SnX_4 or $[\text{FcCH}_2\text{NMe}_3]\text{I}$ **6** with SnI_4 halides. The attempts were, however, unsuccessful (Scheme 3-6). The reaction with SnCl_4 only afforded the undesired products i.e. FcCH_3 , $\text{FcCH}_2\text{CH}_2\text{Fc}$ or FcCH_2OH **73**, which were identified by GC-MS. The reaction with SnI_4 gave no new product. Only the precursor **6** was recovered unreacted. The ferrocenyl stannic halide **62** could, however, be prepared by reaction of **63**, which was available in the lab., with SnCl_4 . The corresponding stannane **64** could, however, not be obtained by reduction of **63** with LiAlH_4 . Since organo primary stannanes are generally extreme unstable⁵¹, it may have not been possible to confirm the formation even if the corresponding stannane **64** did form. This also suggests a $\text{Fc}(\text{CH}_2)_n$ moiety was not effective at stabilising primary organostannanes either.



Scheme 3-6: Attempted syntheses of ferrocenyl stannic halides and stannane

Despite the probable instability, attempts were made to confirm spectroscopically the formation of the desired stannane **64**. Primary organostannanes are typically extremely unstable⁵¹. They may, however, be identified spectroscopically. For example, ions corresponding to primary stannanes should exhibit unique Sn isotope distribution patterns¹⁴⁷ in mass spectra. Stannane proton NMR signals should appear between δ 4.8 – 5.8 and δ 3.0 – 5.0 ppm for alkyl and aryl stannanes, respectively²⁰, and also exhibit two Sn satellite peaks, arising from homonuclear coupling between the other two NMR active nuclei of Sn, with a $^1J^{117/119}_{SnH}$ coupling constant of ~1600 – 2200 Hz (typical for $R_{4-n}SnH_n$)^{132, 148} and also a $^3J_{HH}$ coupling constant of 1.6 – 2.8 Hz (typical for alkyl stannanes²⁰) in 1H NMR spectrum. A typical $\nu(Sn-H)$ stretch for R_3SnH_3 should appear at 1855 – 1880 cm^{-1} ^{51, 132, 148, 149}. The reference values used for the identification of **64** are summarised in Table 3-2.

Table 3-2: Selected reference spectroscopic values for primary stannanes

	MeSnH ₃	EtSnH ₃	BuSnH ₃	PhSnH ₃
IR / $\nu(Sn-H)$ cm^{-1}	1870	1869	Not given.	1880
1H NMR / $\delta(Sn-H)$ ppm	5.86	5.66	5.71	4.98
1H NMR / $^1J^{117/119}_{SnH}$ Hz	1770/1852	1710/1790	1716/1796	1836/1921

*All the data were adopted from the literatures⁵¹.

Neither of these above could be observed for the product isolated from the reaction of **62** with LiAlH_4 . Further investigation was, therefore, not carried out. The desired stannane may be too unstable to identify under ambient conditions.

3.2.5.1 Attempted Syntheses of $\text{FcCH}_2\text{SnX}_3$ ($\text{X} = \text{Cl}$ (**59**), **I** (**60**)) and by Reaction of FcCH_2Li (**40**) with SnX_4

The reactions of **40** with SnX_4 ($\text{X} = \text{Cl}$ or **I**) in dry THF gave a viscous brown oil which was identified as a mixture of FcCH_3 , $\text{FcCH}_2\text{CH}_2\text{Fc}$, **73** and unidentified impurities. Neither the expected ions nor signals for the desired compound could be observed by ESI-MS (in MeCN) or NMR (in CDCl_3) spectrum. Further reaction of the brown oil with SnCl_4 and then LiAlH_4 in dry Et_2O also confirmed no formation of the desired compound. A yellow oil obtained after removal of the solvent from the reaction mixture was analysed. Neither NMR spectroscopy nor GC- or ESI-MS on the oil showed the expected ions, signals or peaks that could be assigned for the desired compound. In the IR spectrum, there was, however, a weak peak at 1817 cm^{-1} (Figure 3-20) which might have been assigned as the *Sn-H* stretch for the desired stannane (cf. $\sim 1880\text{ cm}^{-1}$ for RSnH_3 ⁵¹) although further investigations would be needed to confirm the formation of the desired compound.

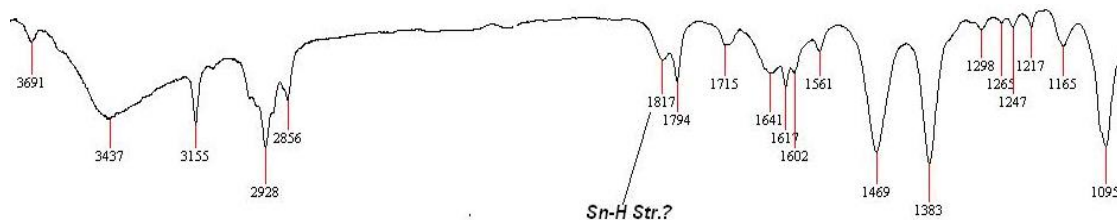


Figure 3-20: IR spectrum of the crude product from the reaction of **59** (assumed) with LiAlH_4

3.2.5.2 Attempted Synthesis of $\text{FcCH}_2\text{SnCl}_3$ (**59**) by Reaction of $[\text{FcCH}_2\text{NMe}_3]\text{I}$ (**6**) with SnCl_2

This reaction was carried out in order to investigate if $\text{FcCH}_2\text{NMe}_3^+$ would oxidatively add to SnCl_2 in a similar manner to PhCH_2Cl ⁵¹. The reaction of **6** with

SnCl₂ in dry THF either at room or reflux gave a yellow solid after removal of the reaction solvent. NMR spectroscopy on the crude product indicated that it was only unreacted **6**. ESI-MS also only showed the ions corresponding to **6** (i.e. m/z 258 [$M - I$]⁺) in the positive-ion mode. Further investigations were, therefore, not carried out.

3.2.5.3 Synthesis and Characterisation of 1-Trichlorostannyl-2-ferrocenyl-ethene (**62**)

During the course of the present study, a paper¹⁵⁰ which describes the synthesis of Ph(Cl)C=C(SnCl₃)H **61** in excellent yield has been published. With reference to the literature method¹⁵⁰, attempts were, therefore, made to prepare the corresponding ferrocenyl analogue, Fc(Cl)C=C(SnCl₃)H **62**, which could then be reduced to produce the desired primary stannane. The reaction of ferrocenylalkyne, FcC≡CH **63**, which was available in the lab., with SnCl₄ in dry CH₂Cl₂ under a N₂ atmosphere gave **62** (Figure 3-21) as a red solid in excellent yield (97 %). When removed from the inert atmosphere into air, the red solid immediately turned black, suggesting that it was extremely sensitive probably to moisture as expected for the class of compounds concerned i.e. RSnCl₃⁵¹ (spontaneously decomposes). The attempted ESI-MS in MeCN as a mobile phase and IR spectroscopy as KBr windows on the sample did not give any useful data. It could, however, only partially be characterised by NMR spectroscopy (see the next page) in a NMR tube sealed under vacuum using dry CDCl₃ (from a freshly opened bottle). The subsequent reduction of **62** with LiAlH₄ in dry Et₂O to reduce to the corresponding primary stannanes, Fc(Cl)C=CH(SnH₃) **64** or may be FcCH₂CH₂SnH₃ **65** (two possible products as LiAlH₄ may also reduce chloride) was, however, unsuccessful. Despite the attempts, no spectroscopic data that suggested the formation of the desired compounds could be obtained.

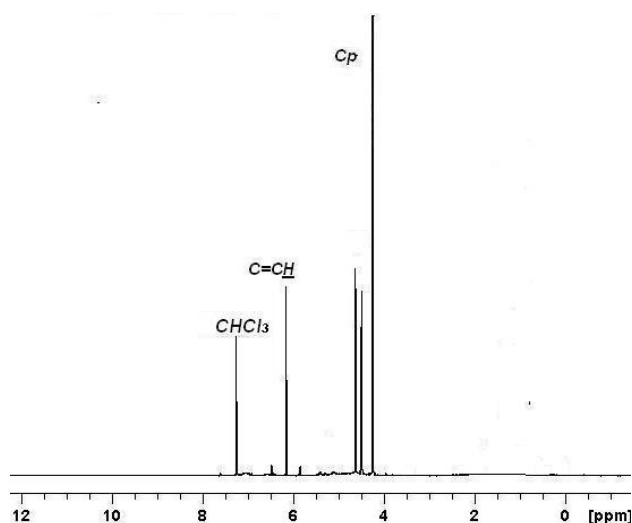


Figure 3-21: ^1H NMR spectrum of the crude product of **62**

The proton signal for the proton bonded *cis* to the SnCl_3 appeared at δ 6.2 ppm as a singlet with the $^{117/119}\text{Sn}$ satellites as doublets with a $^2J^{117/119}\text{SnH}$ coupling constants of 240 and 256 Hz, respectively (Figure 3-22) which were consistent for the class of compounds concerned and also with the fact that a $J_{119\text{SnH}}$ is generally greater than $J_{117\text{SnH}}$ ⁵¹. The Cp proton signals were shifted further downfield by δ 0.1 – 0.6 ppm which was consistent with the bonding to an alkene which was electron-withdrawing and hence deshielding. The ^{13}C and 2-D NMR data were also consistent with the structure of the expected compound (Figure 3-24).

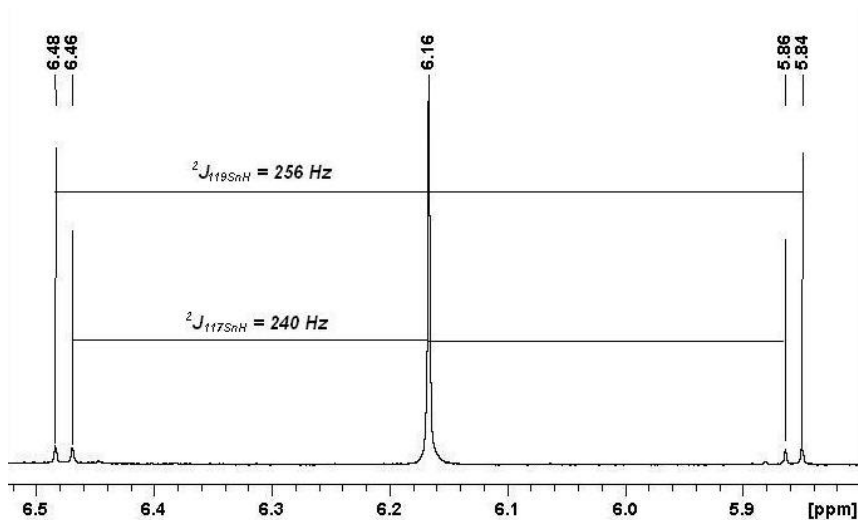


Figure 3-22: Partial ^1H NMR spectrum showing the alkene proton signal bonded *cis* to SnCl_3

Organotin trichlorides are generally highly moisture-sensitive⁵¹. The spontaneous decomposition of **62** in solution could be observed by ¹H NMR spectroscopy, the colour change of the NMR sample from brown to red and also precipitation of a black solid which may be elemental Sn. The C=CH proton NMR signal could not be observed after 2 hours if in a NMR tube sealed with a plastic lid in air (Figure 3-23).

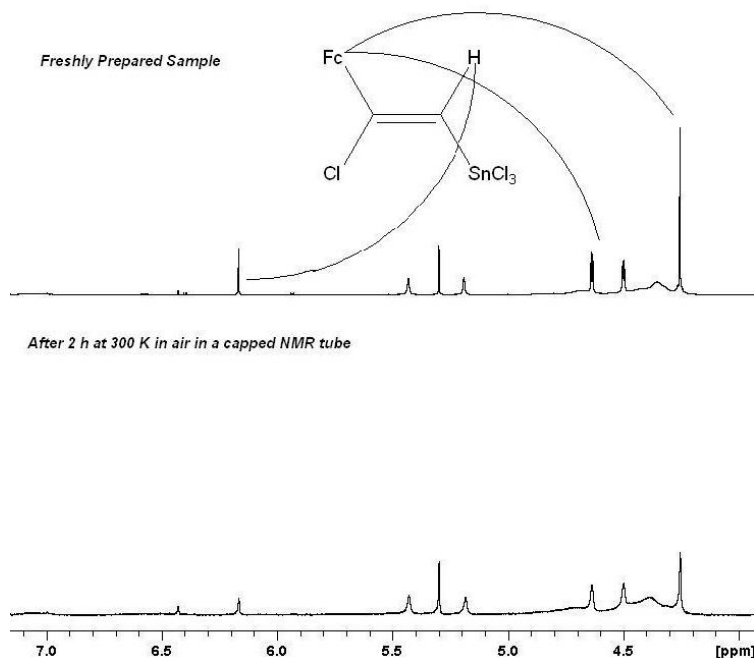


Figure 3-23: ¹H NMR spectrum showing the decomposition of **62** after 2 h at room temperature in air

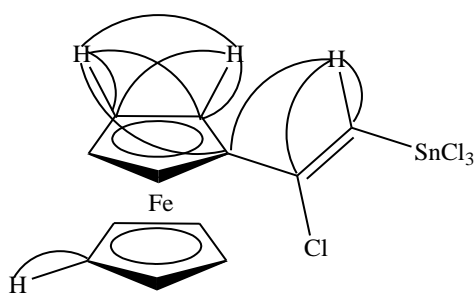


Figure 3-24: Selected ^{1,2,3}J_{CH} and ³J_{HH} correlations observed for **62** in the HMBC, HSQC and COSY NMR experiments

Although it was much slowed, the decomposition of **62** was observed even when the NMR sample was prepared under an inert atmosphere using dry and deoxygenated solvents followed by sealing under vacuum. The alkene proton signal completely

disappeared after 11 days at room temperature in the permanently sealed glass NMR tube under *vacuo* (Figure 3-25). This may suggest that **62** is also thermally unstable which may not be surprising for compounds of the heavier elements of the group¹.

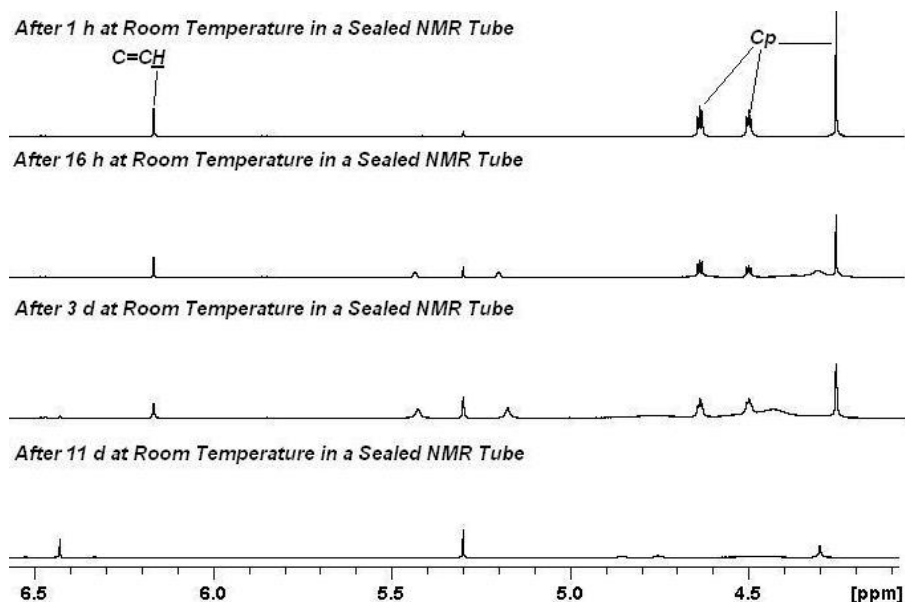


Figure 3-25: ¹H NMR spectrum showing the decomposition of **62** at room temperature in a sealed NMR tube over 11 days

3.2.5.4 Attempted Synthesis of $\text{Fc}(\text{Cl})\text{C}=\text{C}(\text{H})\text{SnH}_3$ (**64**) or $\text{Fc}(\text{CH}_2)_2\text{SnH}_3$ (**65**) via $\text{Fc}(\text{Cl})\text{C}=\text{C}(\text{H})\text{SnCl}_3$ (**62**)

The attempted synthesis of the corresponding primary stannane of **62** with LiAlH_4 in dry Et_2O was unsuccessful. Despite the attempts, no spectroscopic data including GC-MS, NMR and IR spectroscopy, that suggested the formation of the desired compounds could be obtained. After stirring the reaction mixture at 0 °C for 3 hours, removal of the solvent under reduced pressure gave a brown oil. The expected signals^{132, 148} could, however, not be observed by ¹H NMR spectroscopy in CDCl_3 . The oil turned into a green solid when brought to room temperature under an inert atmosphere after having been stored at -18 °C overnight during which time no notable change was observed. It may be possible that the desired compound decomposed by warming up to room temperature and/or storing impure because primary organostannanes are generally thermally unstable (i.e. RSnH_3 decompose at

$> 0\text{ }^{\circ}\text{C}^{51}$) and impurities may also catalyse the decomposition (an autocatalytic reaction may occur)⁵¹. Despite the observation of vigorous effervescence and colour change of the reaction mixture from red to dark brown after **62** and LiAlH_4 were reacted, the formation of the desired primary stannane could not be confirmed.

3.3 Conclusion

The ferrocenyl derivatives of heavier Group 14 element hydrides, ferrocenylethyl silane **50** and $\text{-methyl germane 57}$ as well as the corresponding halides **51**, **52** and **58**, could be prepared.

Hydrosilation of the vinyl ferrocene **53** with HSiX_3 ($\text{X} = \text{Cl}$ or OCH_3) catalysed by $\text{H}_2\text{PtCl}_6 \cdot x\text{H}_2\text{O}$ in dry THF yielded the corresponding silylated halides **51** and **52** in good yields. The corresponding germanium halide of **57** could be prepared from the reaction of **40** with GeCl_4 in dry THF analogously to the arsenic analogue **39**. The subsequent reduction of the respective halide with LiAlH_4 in dry Et_2O provided the desired hydrides **50** and **57** as a yellow oil in moderate to good yields. The halides and hydrides could not be fully characterised but were well characterised spectroscopically. Despite the attempts, satisfactory microanalytical and X-ray crystallographic structural data could not be obtained due to the difficulties in purifying and growing a single crystal of them.

Attempts to prepare ferrocenylalkyl stannanes were also unsuccessful. It was found difficult to prepare the corresponding tin halide **59** or **60**. The attempted synthesis by the reaction of **40** or **6** with SnX_4 ($\text{X} = \text{Cl}$ or I) or SnCl_2 , respectively, were unsuccessful. With reference to the recently published paper, a ferrocenyl stannic halide **62** could be obtained by reaction of **63** with SnCl_4 in dry CH_2Cl_2 in excellent yield. The stannic halide **62** was highly unstable, decomposed in solution within 2 hours at room temperature in air and could, therefore, only be partially characterised by NMR spectroscopy. The attempted synthesis of the corresponding primary stannane **64** or possibly **65** by reduction with LiAlH_4 was unsuccessful. No

spectroscopic data that suggested the formation of the desired compound could be obtained. A significant amount of a metallic mirror deposited on the wall of the reaction vessel during the reaction suggested the significant decomposition of either the halide or the corresponding hydride.

The stability of the hydrides of heavier Group 14 elements with ferrocenylalkyl moieties varied. While the silane **50** exhibited great stability in solution under ambient conditions, standing for over 7 months, the germane **57** decomposed during the work-up carried out in air or upon the storage over 6 weeks at $-18\text{ }^{\circ}\text{C}$. The incorporation of a $\text{Fc}(\text{CH}_2)_n$ ($n = 1$ or 2) group at the hydride centres of heavier Group 14 elements seemed, therefore, to have had little or no effect on their stabilities under ambient conditions. Since the hydrides of heavier Group 14 elements are often thermally unstable^{1, 39, 51} as well as air-sensitive, the thermal stability of compounds may be a more important factor than the oxidative stability for the overall stability of the Group 14 element hydrides. The incorporation of a $\text{Fc}(\text{CH}_2)_n$ group at the hydride centre may improve the air stability of primary phosphanes which are of lower oxidative stability, but not their thermal stability which may be a more important factor for stabilisation of heavier Group 14 element hydrides.

3.4 Experimental

3.4.1 Synthesis of $\text{Fc}(\text{CH}_2)_2\text{SiH}_3$ (**50**)

3.4.1.1 Synthesis of $\text{Fc}(\text{CH}_2)_2\text{Si}(\text{OMe})_3$ (**52**)

$\text{HSi}(\text{OCH}_3)_3$ (2.00 mL, 15.74 mmol) was added to a dry Schlenk flask containing **53** (0.18 g, 0.85 mmol). After the solid was fully dissolved, a solution (0.1 mL) of $\text{H}_2\text{PtCl}_6 \cdot x\text{H}_2\text{O}$ (0.01g) in dry THF (0.50 mL) was added dropwise. The mixture was stirred at room temperature for 24 h. Removal of the volatiles under vacuum gave a red oil. GC-MS: m/z 56(3%) $[\text{Fe}]^+$, 121(15%) $[\text{CpFe}]^+$, 199(10%) $[\text{FcCH}_2]^+$,

334(100%) $[M]^+$. ESI-MS (MeOH/CH₂Cl₂, +ve): m/z observed 334.068 $[M]^+$; calcd. 334.068 for C₁₅H₂₂FeO₃Si; observed 357.053 $[M + Na]^+$; calcd. 357.058 for C₁₅H₂₂FeNaO₃Si. ¹H NMR: δ 1.2 (CH₂CH₂Si, t, ³J_{HH} = 4 Hz, 2 H), 2.3 (CpCH₂CH₂, t, ³J_{HH} = 4 Hz, 2 H), 3.6 (OCH₃, s, 9 H), 4.06 (C₅H₄, unresolved m, 2 H), 4.09 (C₅H₄, unresolved m, 2 H), 4.12 (C₅H₅, s, 5 H) ppm. ¹³C-¹H NMR: δ 14.6 (CH₂CH₂Si, s, CH₂), 22.2 (CpCH₂CH₂, s, CH₂), 50.9 (OCH₃, s, CH₃), 67.2 (C₅H₄, s, CH), 68.6 (C₅H₅, s, C), 91.5 (C, s) ppm.

3.4.1.2 Synthesis of Fc(CH₂)₂SiH₃ (50) via Fc(CH₂)₂Si(OMe)₃ (52)

Compound **52** (0.02 g, 0.06 mmol) was added to a stirred solution of LiAlH₄ (0.20 g, 5.27 mmol) in dry Et₂O (30 mL). Effervescence was observed. The mixture was stirred at room temperature for 3.5 h and then left to settle. The supernatant was transferred into another clean empty Schlenk flask. Aqueous HCl (4 M, 20 mL) was slowly added at 0 °C, stirring. The solution was stirred at that temperature until the vigorous reaction had subsided (~10 mins). The ethereal solution was washed with distilled H₂O (10 mL × 5). Removal of the solvent under reduced pressure gave a yellow oil (0.06 g, > 100 % – includes impurities). GC-MS: m/z 56(10%) $[Fe]^+$, 121(40%) $[CpFe]^+$, 199(25%) $[FcCH_2]^+$, 244(100%) $[M]^+$. ¹H NMR: δ 3.5 (SiH₃, t, ³J_{HH} = 4 Hz, 3 H) ppm. IR: 2150m (Si–H str.) cm⁻¹.

3.4.1.3 Synthesis of Fc(CH₂)₂SiCl₃ (51)

HSiCl₃ (2.00 mL, 19.80 mmol) was added to a dry Schlenk flask containing **53** (0.47 g, 2.22 mol). After the solid was fully dissolved, a dry THF solution of H₂PtCl₆·xH₂O (0.25 mL, 0.1 M) was added dropwise to the mixture. The reaction mixture was stirred at room temperature for 6 h. Removal of the volatiles under vacuum at room temperature gave a viscous brown oil. Attempted ESI-MS in MeCN or MeOH as a mobile phase was unsuccessful. No expected ions could be observed in either ion mode. The resolution of the ¹H NMR spectrum of the crude product in CDCl₃ was also poor and unambiguous assignments could not be made. The brown oil was extracted with dry CH₂Cl₂ (40 mL) and the insoluble materials were filtered with a #4

frit. Removal of the solvent from the extract under vacuum gave a brown oil (0.53 g, > 100 % – includes impurities). IR: 484m (*Si-Cl str*) cm^{-1} . $^1\text{H NMR}$: δ 1.9 (CpCH_2 , unresolved m, 2 H), 3.8 (CH_2SiCl_3 , unresolved m, 2 H), 4.06 (C_5H_4 , unresolved m, 2 H), 4.08 (C_5H_4 , unresolved m, 2 H), 4.12 (C_5H_5 , unresolved m, 5 H) ppm. $^{13}\text{C}\{-^1\text{H}\}$ NMR: δ 25.6 (CpCH_2 , s, CH_2), 68.0 (CH_2Si , s, CH_2), 66.0 – 68.0 (CpC , s, CH), 89.6 (C , s) ppm. Attempted GC-MS was unsuccessful.

3.4.1.4 Synthesis of $\text{Fc}(\text{CH}_2)_2\text{SiH}_3$ (**50**) via $\text{Fc}(\text{CH}_2)_2\text{SiCl}_3$ (**51**)

To the entire yield of **51** obtained in 3.4.1.3, dry Et_2O (30 mL) was added. A white solid precipitated out. At 0 °C, LiAlH_4 (0.07 g, 1.84 mmol) was added. Effervescence was observed. The reaction mixture was stirred at that temperature for 3 h. After removal of the solvent under vacuum, the residue was extracted with dry hexane (50 mL). The solution was vigorously stirred for 15 mins and the insoluble materials were filtered with a #4 frit. Removal of the solvent from the filtrate gave the title compound as a red oil (0.35 g, 65 %). IR: ν 2151m (*Si-H str.*) cm^{-1} . $^1\text{H NMR}$: δ 1.0 (CH_2Si , m, 2 H), 2.5 (CpCH_2 , m, 2 H), 3.5 (SiH_3 , t, $^3J_{\text{HH}} = 4$ Hz, 3 H), 4.04 (H_3 , unresolved m, 2 H), 4.07 (H_2 , unresolved m, 2 H), 4.09 (H_4 , s, 5 H) ppm. $^{13}\text{C}\{-^1\text{H}\}$ NMR: δ 7.8 (CH_2SiH_3 , s, CH_2), 26.3 (CpCH_2 , s, CH_2), 67.0 (C_3 , s, CH), 67.6 (C_2 , CH), 68.4 (C_4 , CH), 91.0 (C_1 , C) ppm. ESI-MS (MeOH with a drop of CH_2Cl_2 added, 80 V, +ve): observed m/z 244.036 [M] $^+$; calcd. m/z 244.036 for $\text{C}_{12}\text{H}_{16}\text{Fe}_1\text{Si}_1$. GC-MS: ($M = \mathbf{50}$) m/z 56(100%) [Fe] $^+$, 121(93%) [CpFe] $^+$, 199(60%) [FcCH_2] $^+$, 244(95%) [M] $^+$.

3.4.2 Synthesis of $\text{FcCH}_2\text{GeH}_3$ (**57**)

3.4.2.1 Synthesis of $\text{FcCH}_2\text{GeCl}_3$ (**58**)

Under an Ar atmosphere, a solution of **40** generated from **47** (0.32 g, 1.39 mmol) and freshly cut small pieces of Li metal (0.5 g) in dry THF (10 mL) stirring at $-8 - 0$ °C for 40 mins, was added *via* a #2 frit to another Schlenk flask containing dry THF (30 mL). GeCl_4 (0.80 mL, 7.01 mmol) was added. The mixture was stirred at room

temperature for 4 h under an Ar atmosphere. Removal of the volatiles under vacuum gave a dark brown oil. IR: 3914w, 3093s, 2924s, 2854s, 1638s, 1465m, 1409m, 1376m, 1293w, 1265m, 1227m, 1105s, 1055m, 1038m, 1022m, 1000m, 922m, 880w, 818s, 778w, 737s, 703w, 662w, 575m,br, 483s, 422w cm^{-1} . ^1H NMR: δ 3.3 ($\underline{\text{C}}\underline{\text{H}}_2$, s, 2 H), 4.17 ($\text{C}_5\underline{\text{H}}_5$, s, 5 H), 4.23 ($\text{C}_5\underline{\text{H}}_4$, m, 4 H) ppm. ^{13}C - $\{^1\text{H}\}$ NMR: δ 35.5 ($\underline{\text{C}}\underline{\text{H}}_2$, s, CH_2), 69.1 ($\underline{\text{C}}_4$, s, CH), 69.3 ($\underline{\text{C}}_3$, s, CH), 69.5 ($\underline{\text{C}}_2$, s, CH), 77.3 ($\underline{\text{C}}_1$, s) ppm. ESI-MS (MeCN, +ve, 280 V): m/z observed 273.014 [FcCH_2Ge] $^+$; calcd. 272.941 for $\text{C}_{11}\text{H}_{11}\text{Fe}_1\text{Ge}_1$; observed 359.971 [$\text{FcCH}_2\text{Ge}(\text{OH})\text{Cl}_2$] $^+$; calcd. 359.882 for $\text{C}_{11}\text{H}_{12}\text{Cl}_2\text{Fe}_1\text{Ge}_1\text{O}_1$.

3.4.2.2 Synthesis of $\text{FcCH}_2\text{GeH}_3$ (**57**)

LiAlH_4 (0.12 g, 3.16 mmol) was added to a solution of **58** (the entire yield) obtained as above in dry Et_2O (50 mL). The mixture was stirred at room temperature for 1 h. At 0 $^\circ\text{C}$, aqueous HCl (36 %, 10 mL) was slowly added to the mixture. The solution was stirred at that temperature until the vigorous reaction had subsided (~10 mins). The insoluble solids were filtered with a #4 frit. Removal of the solvent from the filtrate under vacuum gave a mixture of a yellow solid and oil (0.23 g). The mixture was extracted with dry hexane (20 mL \times 2). Removal of the solvent from the combined organic extract under vacuum gave the title compound as a yellow oil (0.13 g, 35 %). IR: 2030m (Ge-H str) cm^{-1} . ESI-MS (CH_3CN or MeOH with a drop of CH_2Cl_2 added, +ve, 120.0 V): m/z observed. 275.963 [M] $^+$; 275.965 calcd. for $\text{C}_{11}\text{H}_{14}\text{Fe}_1\text{Ge}_1$. GC-MS: m/z 56(10) [Fe] $^+$, 121(46) [CpFe] $^+$, 199(100) [FcCH_2] $^+$, 276(45) [M] $^+$. ^1H NMR: δ 2.2 ($\underline{\text{C}}\underline{\text{H}}_2$, q, $^3J_{\text{HH}} = 3$ Hz, 2 H), 3.7 ($\text{Ge}\underline{\text{H}}_3$, t, $^3J_{\text{HH}} = 3$ Hz, 3 H), 4.04 ($\underline{\text{H}}_3$, unresolved m, 2 H), 4.07 ($\underline{\text{H}}_2$, & $\underline{\text{H}}_4$, unresolved m, 7 H) ppm. ^{13}C - $\{^1\text{H}\}$ NMR: δ 9.6 ($\underline{\text{C}}\underline{\text{H}}_2$, s, CH_2), 67.1 ($\underline{\text{C}}_3$, s, CH), 68.1 ($\underline{\text{C}}_2$, s, CH), 68.6 ($\underline{\text{C}}_4$, s, CH), 87.8 ($\underline{\text{C}}_1$, s, C) ppm.

A portion of the crude product was subjected to chromatography on a preparative TLC plate, eluting with CH_2Cl_2 in air. Three coloured fractions were separated; orange (major) at R_f 0.85, red (minor) at R_f 0.5, yellow (minor) at R_f 0.4. ^1H NMR spectroscopy on each fraction indicated that neither was the title compound.

Recrystallisation of the rest of the crude product from a 1 : 1 mixture of dry CH₂Cl₂ and hexane at –18 °C for 3 weeks gave a few red crystals (0.18 mg) which were confirmed to be **57** by ESI- and GC-MS and IR spectroscopy. They were, however, not suitable for X-ray crystallographic structural determination. Despite the attempts, satisfactory microanalytical data could not be obtained: Calcd. for C₁₁H₁₄Fe₁Ge₁: C 48.10; H 5.14 %. Found: C 63.43; H 5.42 %.

Recrystallisation of the crude product (freshly prepared) from dry CH₂Cl₂ (minimum amount)/dry hexane (excess) at room temperature gave an immediate precipitation of a brown/yellow solid. The precipitate was filtered with a #4 sintered funnel and the solvent from the filtrate was removed under vacuum. The residue was washed with cold dry hexane at 0 °C until the solvent was clear. The residue was then dissolved in dry CH₂Cl₂, giving a clear red solution which was confirmed as of **57** by ESI-MS and ¹H NMR spectroscopy, and transferred into an ampoule. After removing the solvent, the ampoule was sealed under vacuum and sent for elemental analysis. Satisfactory microanalytical data could not, however, be obtained.

3.4.3 Attempted Synthesis of Ferrocenylalkyl Stannane, FcCH₂SnH₃ (**66**)

3.4.3.1 Attempted Synthesis of FcCH₂SnCl₃ (**59**)

Under Ar atmosphere, a solution of **40** generated from **47** (0.22 g, 0.96 mmol) and a small pieces of freshly cut Li metal (0.02 g) in dry THF (10 mL), stirring at 0 – –8 °C under an Ar atmosphere for 1 h, was added *via* a #2 frit to a solution of SnCl₄ (0.50 mL, 4.27 mmol) in dry THF (15 mL) with suspension of white solid which was probably SnCl₄·(THF)₂ formed upon the addition of the SnCl₄ into dry THF. The mixture was stirred at room temperature for 4 h. After filtering the insoluble materials with a #2 frit under an Ar atmosphere, the volatiles were removed under vacuum at 20 – 37 °C. A brown solid, which instantly darkened upon exposure into air, was

obtained. ESI-MS (in MeCN) and ^1H NMR spectroscopy (in CDCl_3) did not suggest the formation of the desired compound.

3.4.3.2 Attempted Synthesis of $\text{FcCH}_2\text{SnH}_3$ (**66**) via $\text{FcCH}_2\text{SnCl}_3$ (**59**)

Dry Et_2O (30 mL) was added to the Schlenk flask containing the brown solid obtained as above. To the resulting clear yellow solution with suspension of a black solid, LiAlH_4 (0.10 g, 2.63 mmol) was added. Effervescence was observed. The reaction mixture was stirred at room temperature for 2.5 h. GC-MS on a sample from the mixture only showed the ions corresponding to FcCH_3 (m/z 200) and $(\text{FcCH}_2)_2$ (m/z 398), which were probably carried through from the previous reaction as they were common side-products of reaction using **40**. After leaving the solution to settle, the supernatant was transferred *via* a syringe into another clean dry Schlenk flask under an Ar atmosphere. The solvent was removed under vacuum, the residue was extracted with dry CH_2Cl_2 (20 mL) and then filtered with on a #4 sintered frit in air. Removal of the solvent from the filtrate under reduced pressure at room temperature gave a yellow-brown oil. IR spectroscopy showed a weak band at 1889 cm^{-1} which may be assigned as ν Sn–H stretch.

The crude product was subjected to chromatography on a preparative TLC plate, eluting with light petroleum spirits. Three yellow bands were separated. After extraction with CH_2Cl_2 , removal of the solvent from the extract under reduced pressure gave a yellow oil (R_f 0.72, 0.01 g), a yellow solid (R_f 0.44, 0.03 g) and yellow oil (R_f 0.31, 0.02 g). Stannane proton signal could not be observed on in the ^1H NMR spectrum of neither fraction. A broad weak band at 1889 cm^{-1} which may be assigned as Sn–H stretch, was observed on the yellow oil obtained from the fraction at R_f 0.72. The attempted recrystallisation of the yellow oil from CH_2Cl_2 /light petroleum spirits at $-18\text{ }^\circ\text{C}$ gave no precipitate.

3.4.3.3 Attempted Synthesis of $\text{FcCH}_2\text{SnI}_3$ (60) by Reaction of FcCH_2Li (40) with SnI_4

Under an Ar atmosphere, a solution of **40** generated from **47** (0.08 g, 0.35 mmol) and freshly cut small pieces of Li metal (0.1 g) in dry THF (10 mL), stirring at 0 – –7 °C for 40 mins, was added *via* #4 frit to that of SnI_4 (0.06 g, 0.09 mmol) in dry THF (10 mL). The mixture was stirred at room temperature for 1.15 h and the solvent was removed under vacuum. ^1H NMR spectroscopy (in CDCl_3), GC- (in CH_2Cl_2) and ESI-MS (in MeCN with a drop of CH_2Cl_2 added) on the residue did not show the expected ions or signals corresponding the desired compound. The residue was extracted with dry CH_2Cl_2 (30 mL) and the insoluble materials were filtered with a #4 frit. After concentrating the dark brown filtrate to ~5 mL under vacuum and then adding dry hexane (0.5 mL), the solution was cooled at –18 °C. No precipitate could be obtained. After removing the solvent, the residue was used in the subsequent reaction without further purification.

3.4.3.4 Attempted Synthesis of $\text{FcCH}_2\text{SnH}_3$ (66) *via* $\text{FcCH}_2\text{SnI}_3$ (60)

To the residue obtained as above, dry Et_2O (60 mL) was added. After LiAlH_4 (0.20 g, 5.26 mmol) was added at 0 °C, the mixture was stirred at that temperature for 3 h and then the solvent was removed under vacuum. The residue was extracted with dry hexane (40 mL) and the insoluble materials were filtered with a #4 frit. Removal of the solvent under vacuum gave a yellow solid (0.03 g). IR spectroscopy (using KBr windows) showed no band which could be assigned as *Sn-H* stretch. GC- and ESI-MS (in MeOH) also indicated no ions corresponding to the desired compound in either ion mode but those for FcCH_3 and $\text{FcCH}_2\text{CH}_2\text{Fc}$.

3.4.3.5 Attempted Synthesis of $\text{FcCH}_2\text{SnCl}_3$ (59) by Reaction of $[\text{FcCH}_2\text{NMe}_3]\text{I}$ (6) with SnCl_2

SnCl₂ (1.04 g, 5.48 mmol) was added to a solution of **6** (0.99 g, 2.57 mmol) in dry THF (20 mL), giving a clear orange solution. After stirring the mixture at room temperature overnight, removal of the solvent under vacuum gave a mixture of a yellow and white solid. ¹H NMR spectroscopy only showed the signals corresponding to **6**. The corresponding ions were also observed by ESI-MS in the positive ion mode.

SnCl₂ (0.90 g, 4.76 mmol) and dry THF (30 mL) were added to the recovered **6**. The mixture was heating to reflux for 4.5 h. ESI-MS (in MeCN) on a sample from the reaction mixture only showed the ions corresponding to **6** in the positive ion mode. The reaction was discontinued.

3.4.3.6 Synthesis of Fc(Cl)C=C(H)SnCl₃ (**62**)

SnCl₄ (0.10 mL, 0.85 mmol) was added to a solution of **63** (0.07 g, 0.33 mmol) in dry CH₂Cl₂ (20 mL). The solution darkened immediately upon addition of SnCl₄ and a precipitate, the colour of which could not be identified due to the dark solution, formed. The mixture was stirred at room temperature for 20 h and then cooled to 0 °C. The insoluble materials were filtered with a #4 frit. Removal of the volatiles under vacuum gave a red solid (0.15 g, 97 %). The red solid turned instantly black as soon as it was removed from an N₂ atmosphere into air. ESI-MS (in MeCN) showed ions exhibiting Sn and Cl isotopes in both ion modes, which could not, however, be identified. ¹H NMR spectroscopy (in CDCl₃) indicated that it was a pure **62**. ¹H NMR: δ 4.3 (C₅H₅, s, 5 H), 4.5 (H₃, t, ³J_{HH} = 2 Hz, 2 H), 4.6 (H₂, t, ³J_{HH} = 2 Hz, 2 H), 6.2 (C=CH, s, ²J^{117/119}_{SnH} = 240/256 Hz, 1 H) ppm. ¹³C-{¹H} NMR (300 MHz): δ 69.0 (C₃, s, CH), 70.9 (C₄, s, CH), 72.0 (C₂, s, CH), 82.0 (C₁, s, C), 115.8 (C=C(H)SnCl₃, s, C), 158.0 (Fc(Cl)C=C, s, C) ppm. After 2 h at 300 K in air, the signals corresponding to the title compound disappeared. The NMR sample also turned dark brown from red overnight and a black solid precipitated out. The disappearance of the signals could be slowed if the sample was prepared under an inert atmosphere using deoxygenated dry CDCl₃. Since the title compound was too unstable, no further characterisation was carried out.

3.4.3.7 Attempted Synthesis of $\text{Fc}(\text{Cl})\text{C}=\text{C}(\text{H})\text{SnH}_3$ (**64**)

To a solution of **62** (0.15 g, 0.32 mmol) in dry Et_2O (30 mL) at 0 °C, LiAlH_4 (0.20 g, 5.26 mmol) were added. Effervescence occurred and the solution turned dark brown shortly after. The mixture was stirred at that temperature for 3.5 h. Dry hexane (50 mL) was added and the insoluble materials were filtered with a #4 frit. Removal of the solvent under vacuum gave a brown oil (0.13 g). ^1H NMR spectroscopy (in CDCl_3) on the crude product gave a poorly resolved spectrum, probably due to impurities, which could not be interpreted. The precipitation of a black solid in the NMR sample was also observed after 18 h at room temperature in air.

After storing the rest of the crude product at -18 °C overnight, it was brought to room temperature under vacuum. The brown oil turned into a green solid. GC-MS and IR spectroscopy on the green solid showed no ions or bands which suggested the presence of the desired product. Deoxygenated dry hexane (40 mL) was added to the green solid and the extract was subjected to column-chromatography on silica-gel, eluting with a 1 : 1 mixture of dry hexane and ethyl acetate under an N_2 atmosphere. Removal of the solvent from the eluent under vacuum gave a mixture of a red solid and oil. IR spectroscopy and ESI-MS (in MeOH) on the mixture showed no ν *Sn-H* stretch or ions corresponding to the title compound in either ion mode. NMR spectroscopy (in CDCl_3) did not show the signals which could be assigned for the title product either.

Chapter 4: Stabilisation Effects of Ferrocenylalkyl Groups on the Hydrides of Heavier Group 16 Elements, Se, Te

4.1 Introduction

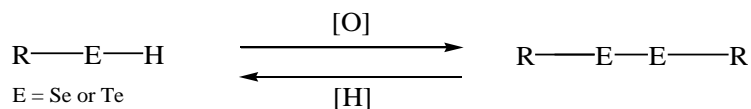
4.1.1 Hydrides of Heavier Group 16 Elements

Amongst the hydrides of the heavier Group 16 elements, thiol, H_2S , is best known. The hydrides of the heavier elements i.e. selenol, H_2Se , tellurol, H_2Te are, however, rare and little of their chemistry is known. The hydrides of the heavier elements are extremely toxic gases with noxious odours⁴. As for the hydrides of other heavier main group elements, the thermal stability of the hydride decreases from H_2S to H_2Po . While H_2Se is thermally stable up to 280 °C, H_2Te starts to decompose slowly at room temperature⁵. The hydrides of this group behave as very weak acids in an aqueous solution and the general reactivity increases with increasing atomic numbers⁵. Selenol and tellurol are also known as strong reducing agents⁵. The hydrides of this group can be made from their elements⁵.

4.1.2 Organo-selenols and -tellurols

Since organo-selenols and -tellurols, REH ($\text{E} = \text{Se}$ or Te), are often prepared *in situ* and reacted further¹⁵¹, very few examples of organo-selenols and -tellurols have been known. Recently, the syntheses of a series of highly unstable vinyl, allyl and propargyl selenols have been reported by Riague *et al.*¹⁵². Also, some unstable organo-tellurols including methane, ethene, 3-butene, vinyl, cyclopropane and cyclopropanemethane tellurols have also been known¹⁵³. Saturated selenols and tellurols are, however, rarely known¹⁵¹.

Organo-selenols and -tellurols, in particular of low molecular weights, as for the hydrides of other heavier main group elements, are extremely air-sensitive¹⁵¹. Organo-selenols and -tellurols are so highly air-sensitive that they must be handled under an inert atmosphere using deoxygenated solvent. The oxidation products of organo-thiols, -selenols¹⁵² and -tellurols are often the corresponding dichalcogenes, REER, which can be reduced back to the hydrides if appropriate reducing agents are used or under acidic conditions (Scheme 4-1)¹⁵¹. The dichalcogenides are commonly used as precursors to many organochalcogenide compounds^{151, 154, 155}. Organoditellurides such as (PhCH₂Te)₂ are also very powerful reducing reagents and often used in organic syntheses¹⁵¹.



Scheme 4-1: *Oxidation and reduction of organo-selenols and -tellurols and the corresponding dichalcogenides*

4.1.3 Stabilisation of Hydrides of Heavier Group 16 Elements

No stable organo-selenols or -tellurols except those sterically stabilised, i.e. {(CH₃)₃Si}₃SiTeH (Figure 4-1), have been reported. Since organo-selenium and -tellurium compounds are, in general, very useful and versatile precursors to many organo-selenium^{20, 156-158} and -tellurium compounds^{20, 151}, it would be of interest to synthesise stable selenols and tellurols without compromising their highly reactive hydride centres by sterically crowding.

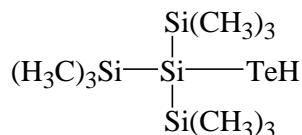
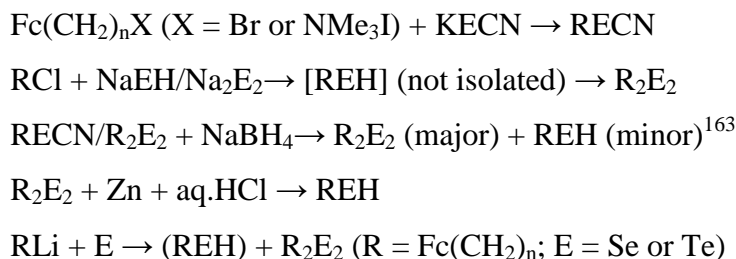


Figure 4-1: *Air-stable tellurol*

4.1.4 Synthesis of Organo-selenols and -tellurols

Ferrocene chalcogens of the type, FcEH, and disubstituted counterparts, Fe(C₅H₄EH)₂ (E = Se, Te)¹⁵⁹, are well known. They are often prepared from ferrocene, BuLi and elemental chalcogen. In contrast, compounds with (CH₂)_n spacers, Fc(CH₂)_nEH, are unknown for Se and Te. Our strategies to prepare ferrocenylalkyl selenols and tellurols were to prepare the corresponding dichalcogenides, Fc(CH₂)_nEE(CH₂)_nFc, from the corresponding halides, Fc(CH₂)_nX (X = Cl, Br or NMe₃⁺) and Na₂E₂ (E = Se¹⁶⁰ or Te^{160, 161}) generated *in situ* from elemental Se or Te with NaBH₄, and then reduce with a suitable reducing agent such as NaBH₄ to give Fc(CH₂)_nEH or to directly prepare by reactions of the corresponding halides with NaEH generated also *in situ* from elemental Se or Te¹⁶⁰ with NaBH₄. Alternatively, reduction of Fc(CH₂)_nECN prepared from Fc(CH₂)_nX (X = Cl, Br, NMe₃⁺) and KECN (E = Se or Te¹⁶²) with NaBH₄¹⁶³ or LiAlH₄/succinic acid^{152, 164} should as well give the desired compounds (Scheme 4-2).

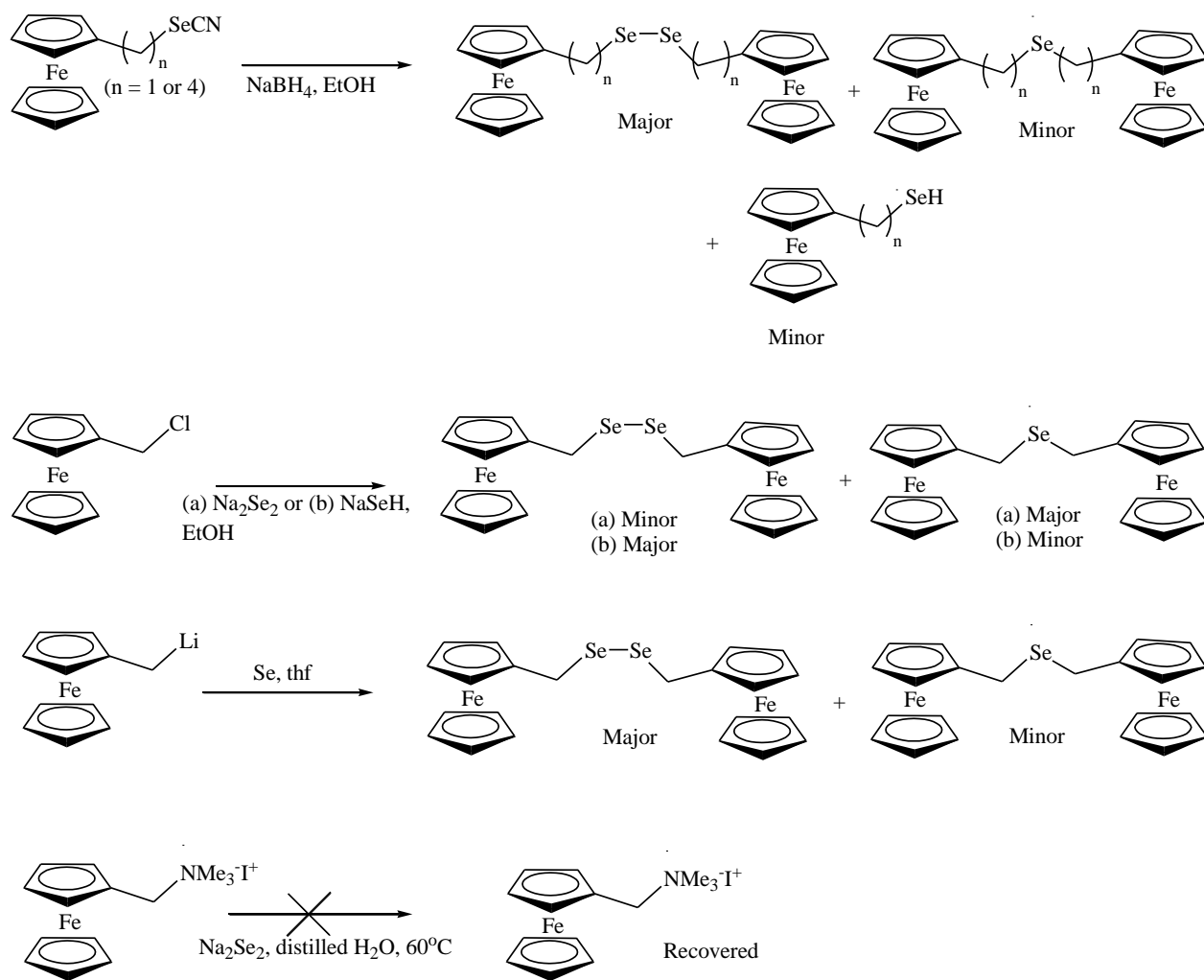


Scheme 4-2: Proposed synthetic routes to Fc(CH₂)_nEH (E = Se or Te)

This chapter reports the syntheses and characterisations of ferrocenylalkyl selenocyanates, Fc(CH₂)_nSeCN (n = 1 or 4), dichalcogenides, {Fc(CH₂)_nE}₂ (n = 1 or 4; E = Se or Te), and selenols Fc(CH₂)_nSeH (n = 1 or 4) and also the attempts to prepare FcCH₂TeCN **81** and FcCH₂TeH **80**. The corresponding ⁷⁷Se NMR study on the oxidative stability of PhSeH **78** in solution under ambient conditions with or without FcH added is also described.

4.2 Results and Discussion

4.2.1 Synthesis of Ferrocenylalkyl Selenols



Scheme 4-3: Attempted synthesis of ferrocenyl-methyl **72** and -butyl **74** selenols

n-Alkyl selenols are generally prepared by reduction of the corresponding diselenides, R_2Se_2 , or selenocyanates, RSeCN , with suitable reducing reagents such as $\text{LiAlH}_4/\text{succinic acid}$ ^{152, 164}, NaBH_4 ¹⁵⁶, Zn/HCl ¹⁵⁸ in appropriate organic solvent, or alternatively from the reaction of the corresponding halides with NaSeH ¹⁶⁰. There are also other alternate synthetic routes to *n*-dialkyl diselenides^{165, 166}.

The synthesis and attempted synthesis of ferrocenylalkyl selenols carried out in the present study are summarised in Scheme 4-3.

4.2.1.1 Synthesis of $\text{Fc}(\text{CH}_2)_n\text{SeCN}$ ($n = 1$ (**67**), **4** (**68**))

The synthesis of organoselenocyanates, RSeCN , by reaction of the corresponding halides, RSeX ($X = \text{Cl}$ or Br), with KSeCN is well established^{152, 157, 167}. The ferrocenylalkyl selenocyanates, $\text{Fc}(\text{CH}_2)_n\text{SeCN}$, were, therefore, prepared with reference to the literature methods with slight modifications where needed.

*Synthesis of FcCH_2SeCN **67**:* The mixture of **6** and KSeCN in distilled H_2O was heating to reflux under an N_2 atmosphere for 3.5 hours and then acidified with a 2 M HCl solution which resulted in immediate precipitation of a yellow solid. The aqueous phase and the precipitate were extracted with Et_2O which also led to the precipitation of a red solid. After washing the organic phase with distilled H_2O , drying over MgSO_4 and then filtering, removal of the solvent from the organic phase gave **67** as a red solid in poor yield (18 %). Recrystallisation of the red solid from $\text{Et}_2\text{O}/n$ -pentane at $-18\text{ }^\circ\text{C}$ afforded a mixture of a red solid and some red single crystals which were suitable for X-ray crystallographic structural determination (see later). Satisfactory microanalytical data on the mixture could not, however, be obtained (i.e. calcd. for $\text{C}_{12}\text{H}_{11}\text{Fe}_1\text{Se}_1\text{N}_1$: C 47.38; H 3.65; N 4.61 %; found: C 51.63; H 4.25; N 3.41 %). Since the found compositions of C and H atoms were higher than the expected values, there might still have been some organic solvents used during recrystallisation left in the sample.

*Synthesis of $\text{Fc}(\text{CH}_2)_4\text{SeCN}$ **68**:* The reaction conditions were adopted from the literature¹⁶⁷ which describes the syntheses of n -alkyl selenocyanates, $\text{CH}_3(\text{CH}_2)_n\text{SeCN}$ ($n = 4, 8, 10, 12$) in good to excellent yields. The mixture of $\text{Fc}(\text{CH}_2)_4\text{Br}$ **17** and KSeCN in dry DMF was stirred at $20\text{ }^\circ\text{C}$ for 17.5 hours. After hydrolysing with distilled H_2O , the aqueous phase was extracted with Et_2O and the organic phase was washed with distilled H_2O and dried over Na_2SO_4 . After filtering, removal of the solvent from the organic phase gave the crude title compound as a

yellow oil. Crystallisation of the crude product from Et₂O/*n*-pentane at -18 °C gave a pure **68** in good yield (78 %) as a yellow solid from which satisfactory microanalytical data could be obtained; Found C 52.09, H 5.07, N 3.94; Calcd. C 52.03, H 4.95, N 4.05 %. Recrystallisation of the yellow solid from *n*-pentane at -18 °C in an attempt to grow a single crystal gave a yellow crystal which was, however, not suitable for X-ray crystallographic structural determination.

4.2.1.2 Characterisation of Fc(CH₂)_nSeCN (n = 1 (**67**), 4 (**68**))

The selected IR and ¹³C-¹H NMR data for **67** and **68** are summarised in Table 4-1.

Table 4-1: Selected spectroscopic data for **67** and **68**

	IR / $\nu_{(C\equiv N)}$ cm ⁻¹	¹³ C- ¹ H NMR / δ_{CN} ppm
67	2140	102.8
68	2150	101.5

IR Spectroscopy: The $\nu(C\equiv N)$ stretches for **67** and **68** appeared at 2140 and 2150 cm⁻¹, respectively, as a medium to strong peak (Figure 4-2). The frequencies are consistent with those in the literatures i.e. 2149 – 2151 cm⁻¹ for CH₃(CH₂)_nSeCN¹⁶⁷ (n = 4, 8, 10, 12) and R(CH₂)_nSeCN^{152, 167} (R = HC≡C or H₂C=C=CH; n = 1 or 2).

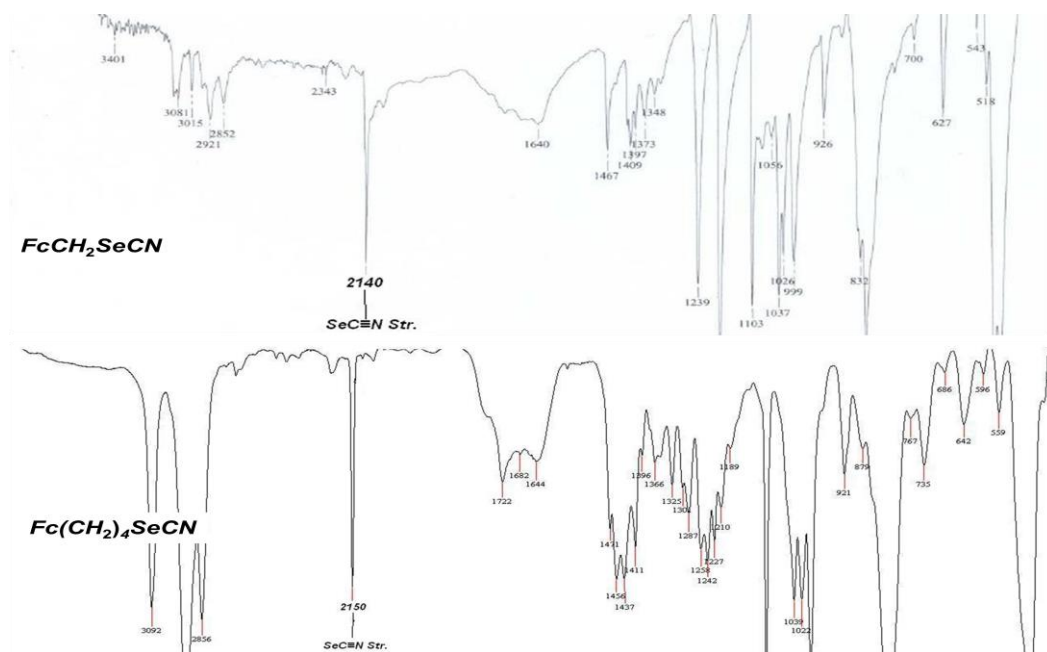


Figure 4-2: IR spectra showing the SeC≡N stretches of **67** and **68**

NMR Spectroscopy: The ^1H NMR chemical shifts for **68** were also comparable with the literature values for $\text{Fc}(\text{CH}_2)_6\text{SeCN}^{157}$ and $\text{CH}_3(\text{CH}_2)_4\text{SeCN}^{167}$ (i.e. δ 1.7 – 1.9 ($\underline{\text{CH}_2}$) cf. δ 1.3 – 1.9 ($\underline{\text{CH}_2}$, m, 6 H) 157 , δ 2.4 ($\text{Fc}\underline{\text{CH}_2}$) cf. δ 2.3 ($\text{Fc}\underline{\text{CH}_2}$, t, $^3J_{\text{HH}} = 7$ Hz, 2 H) 157 , δ 3.1 ($\underline{\text{CH}_2}\text{SeCN}$) cf. δ 3.1 ($\underline{\text{CH}_2}\text{SeCN}$, t, $^3J_{\text{HH}} = 7$ Hz, 2 H) 157 , δ 4.06 ($\text{C}_5\underline{\text{H}_4}$) cf. δ 4.04 ($\text{C}_5\underline{\text{H}_4}$, br,s, 4 H) 157 , δ 4.10 ($\text{C}_5\underline{\text{H}_5}$) cf. δ 4.09 ($\text{C}_5\underline{\text{H}_5}$, s, 5 H) 157 ppm). The selenocyanate carbon NMR signals for **67** and **68** were both observed at $\sim \delta$ 102 ppm (Table 4-1) which was consistent with the literature values (cf. $\sim \delta$ 101 ppm for $\text{R}(\text{CH}_2)_n\text{SeCN}$ ($\text{R} = \text{HC}\equiv\text{C}$ or $\text{H}_2\text{C}=\text{C}=\text{CH}$; $n = 1$ or 2) $^{152, 167}$. The 2-D NMR data were also consistent with the expected structures of **67** and **68**. The selected $^{1,2,3}J_{\text{CH}}$ correlations observed in the HMBC and HSQC NMR experiments are shown in Figure 4-3. The other correlations were either not observed or omitted for simplicity because the signals were heavily overlapped and definite assignments could not be made.

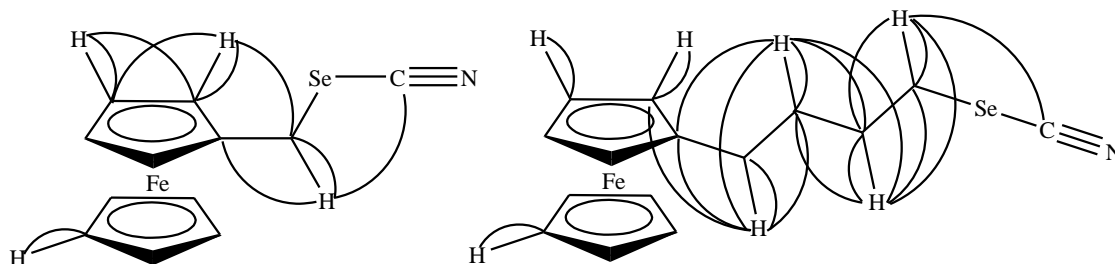


Figure 4-3: Selected $^{1,2,3}J_{\text{CH}}$ correlations observed in the HMBC and HSQC NMR experiments for **67** and **68**

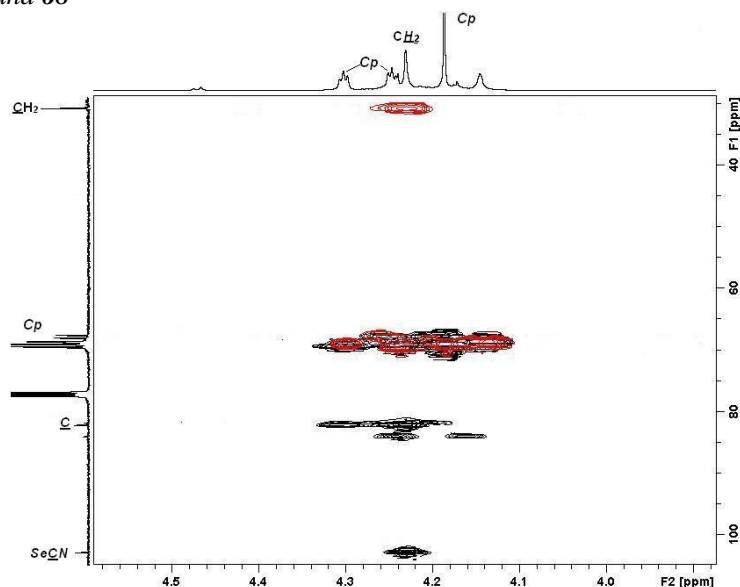


Figure 4-4: $^{1,2,3}J_{\text{CH}}$ correlations observed for **67** in the HMBC (in black) and HSQC (in red) NMR experiments

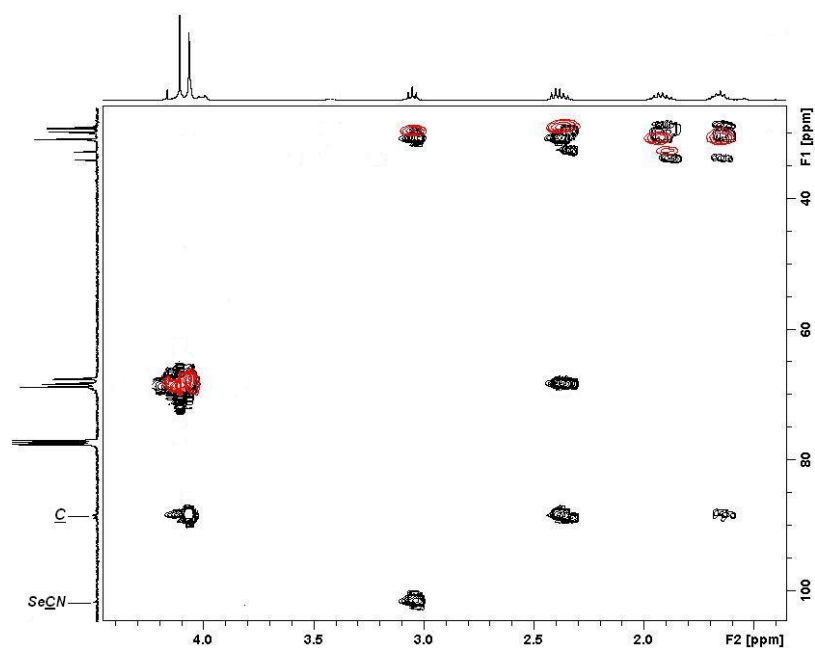


Figure 4-5: $^{1,2,3}J_{CH}$ correlations observed for **68** in the HMBC (in black) and HSQC (in red) NMR experiments

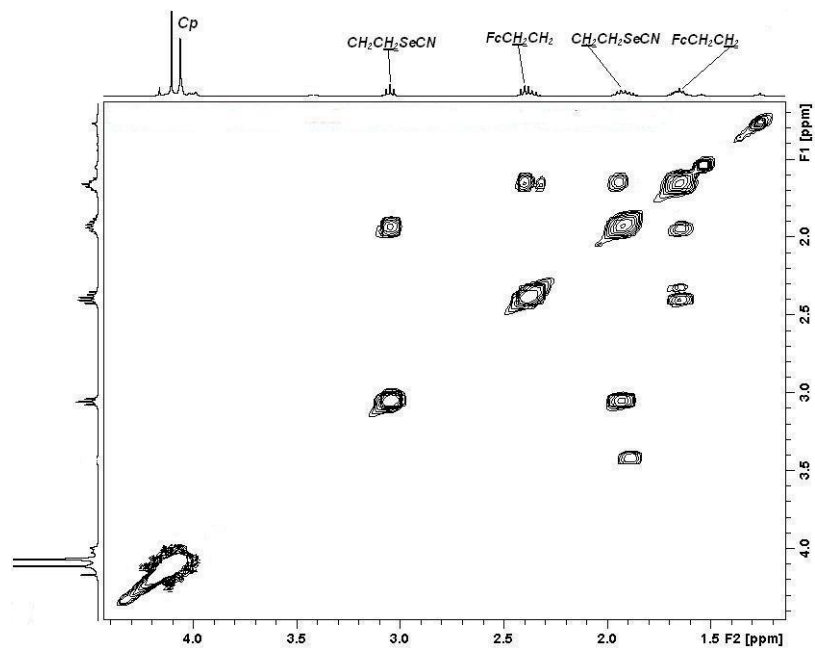


Figure 4-6: $^3J_{HH}$ correlations observed in the COSY NMR experiment for **68**

Mass Spectrometry: The mass spectrometric data for **68** could be obtained by ESI- and GC-MS. At a capillary exit voltage of 100 V, the molecular ion, $[M]^+$, (Figure 4-7) and the corresponding sodium adduct $[M + Na]^+$ were observed in the positive-ion mode of ESI-MS in MeOH as a mobile phase. GC-MS showed the $[M]^+$ ion as well as the ions corresponding to $[Fe]^+$, $[CpFe]^+$ and $[FcCH_2]^+$ produced by fragmentation of

the parent molecule (Figure 4-8) which are consistent with the hydrides of other heavier main group elements. Despite the attempt, the mass spectrometric data for **67** could not be obtained.

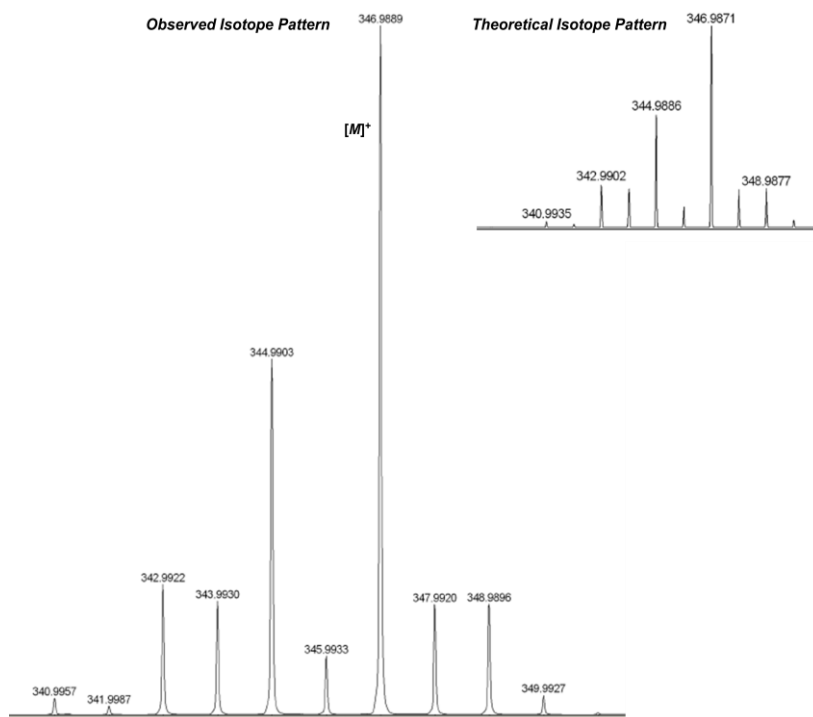


Figure 4-7: Partial ESI-MS showing the observed and theoretical $[M]^+$ ion of **68**

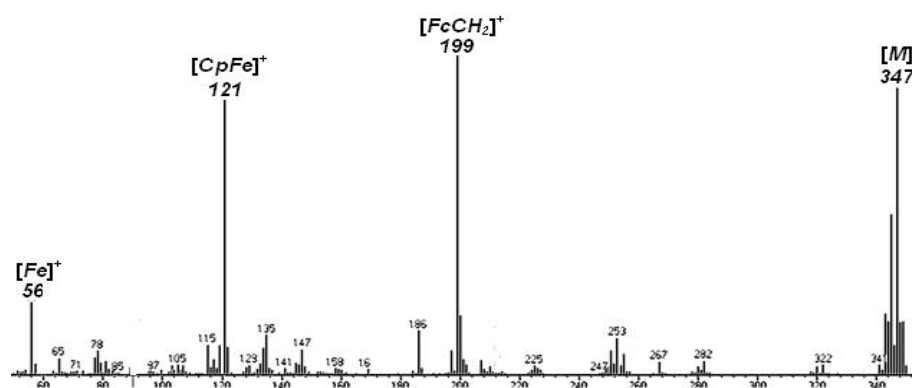


Figure 4-8: GC-MS of **68**

X-ray Crystallographic Structure of 67: A red crystal of **67** could be obtained by recrystallisation from Et_2O/n -pentane, cooling at -18 °C. Intensity data were obtained on a Bruker SMART diffractometer with Mo-K α X-rays and corrected for absorption

using a multi-scan procedure by Dr. Groutso at the University of Auckland. The structures were solved by direct methods and developed and refined on F_o^2 with Prof. Nicholson at the University of Waikato.

All calculations were with the SHELX97 programs^{103, 104} run under WinGX¹⁰⁵. Figures were generated with ORTEP-3¹⁰⁶. Figure 4-9 shows the crystal structure of **67** and Table 4-3 and Table 4-2 the selected bond parameters and crystal data and refinement details of **67**, respectively.

Table 4-2: *Crystal data and refinement details for 67*

67	
Empirical Formula	C ₁₂ H ₁₁ Fe ₁ N ₁ Se ₁
M _r	304.03
T / K	93(2)
Wavelength / Å	0.71073
Crystal System	Orthorhombic
Space Group	Pbca
a / Å	9.6105(5)
b / Å	9.1186(5)
c / Å	25.0515(13)
V / Å ³	2195.4(2)
Z	8
ρ / mg m ⁻³	1.840
μ / mm ⁻¹	4.651
F (000)	1200
Crystal Size / mm ³	0.16 × 0.08 × 0.08
θ range/ °	2.67 to 28.00
Limiting Indices	-12 ≤ h ≤ 12, -11 ≤ k ≤ 9, -32 ≤ l ≤ 32
Reflection Collected	14083
Unique Reflections	2629 [R _{int} 0.0354]
Completeness to θ ° (%)	28.00 (99.1)
Absorption Correction	Semi-empirical from equivalents
T _{max} and T _{min}	1.000 and 0.704
Refinement Method	Full-matrix least-squares on F ²
Data / Restraints / Parameters	2629 / 0 / 136
GoF on F ²	1.013
Final R Indices [I > 2σ(I)]	R ₁ 0.0241, wR ₂ 0.0552
R Indices (all data)	R ₁ 0.0387, wR ₂ 0.0614
Largest Diff. Peak and Hole / eÅ ⁻³	0.445 and -0.266

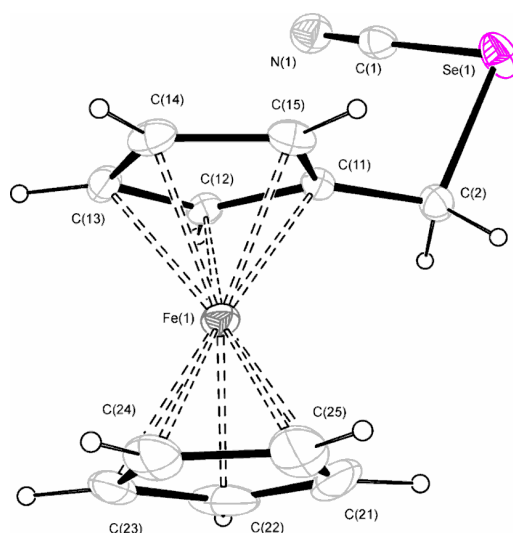


Figure 4-9: X-ray crystallographic structure of **67** showing the atom labelling scheme. Thermal ellipsoids are 50%, probability and H atoms are arbitrary circles.

Table 4-3: Selected bond lengths and angles for **67**

Bond Length / Å		Bond Angle / °	
Se(1)-C(1)	1.845(2)	C(1)-Se(1)-C(2)	94.82(9)
Se(1)-C(2)	1.999(2)	N(1)-C(1)-Se(1)	177.5(2)
N(1)-C(1)	1.146(3)	C(11)-C(2)-Se(1)	112.21(15)
C(2)-C(11)	1.477(3)	C(12)-C(11)-C(2)	125.12(19)
Cp C-C (range)	1.407(4) – 1.438(3)	C(15)-C(11)-C(2)	127.54(18)
Cp C-C (average)	1419	substituted Cp ring C-C-C range	107.31(18) – 108.45(18)
Fe-C (range)	2.033(3) – 2.048(2)	unsubstituted Cp ring C-C-C range	107.6(2) – 108.3(2)
Fe-C (average)	2.039		

The short N(1)-C(1) bond length of 1.146(3) Å (i.e. much shorter than that of 1.477(3) Å for C(2)-C(11)) is consistent with the triple bonding. The Se(1)-C(1) bond length of 1.845(2) Å is also shorter than the Se(1)-C(2) bond length of 1.999(2) Å by 0.154 Å which may be expected for a chemical bonding to an sp-hybridised carbon atom. The short bond could also arise from conjugation i.e. a resonance form of the type $\text{Se}^+=\text{C}=\text{N}^-$. The N-C-Se bond angle of 177.5(2)° is almost linear which is consistent with the triple bonding of the selenocyanate moiety. The C(1)-Se(1)-C(2) bond angle of 94.82(9) is, on the other hand, notably acute.

The C(11)-C(2) bond length and C(11)-C(2)-Se(2) angle of 1.477(3) Å and 112.21(15)°, respectively, were comparable to the literature values of 1.492(4) Å and 113.7° (no standard deviation was given in the literature), respectively, for **1**⁷⁸.

The Cp C–C bond lengths of 1.407(4) – 1.438(3) Å are in good agreement with those reported for other ferrocenylalkyl compounds (i.e. 1.420(2) – 1.4344(19) Å for **35**⁹⁰ and 1.379(7) – 1.428(6) Å **41**⁷⁹). The substituted and unsubstituted Cp ring C–C–C angles were found between 107.31(18) – 108.45(18) and 107.6(2) – 108.3(2)°, respectively, and are also consistent with the literature values of other ferrocenylalkyl compounds (i.e. 107.79(12) – 108.27(13) and 107.79(14) – 108.28(14)° for **35**⁹⁰ and 107.2(4) – 108.8(4) and 107.3(4) – 108.7(4)° **41**⁷⁹, respectively).

The C(12)–C(11)–C(2) and C(15)–C(11)–C(2) angles of 125.12(19) and 127.54(18)° are also consistent with the literature values of 126.18(13) and 126.03(13)° reported for **35**⁹⁰. The Fe–C bond lengths were found between 2.033(3) – 2.048(2) Å which are consistent with the literature values of 2.0371(16) – 2.0578(15) Å for **35**⁹⁰, of 2.022(3) – 2.042(2) Å for **1**⁷⁸ and also of 2.032(4) – 2.045(4) Å for **41**⁷⁹.

4.2.1.3 Synthesis of (FcCH₂Se)₂ (**69**) by Reaction of FcCH₂Li (**40**) with Elemental Se

The reaction of FcLi with elemental Se in dry THF to give (FcSe)₂ is well known¹⁵⁹. The synthesis of **69** was, therefore, attempted referring to the literature method¹⁵⁹ using **40** as precursor. Compound **40** was synthesised using the literature method reported by Nesmeyanov and co-workers¹²³. The mixture of **47**, which was obtained using the synthetic routes described in the literatures^{93, 168}, and freshly cut small pieces of elemental Li in dry THF was stirred at –10 to 0 °C under an Ar atmosphere for 30 mins. The solution turned deep red, indicating the formation of **40**. The resulting red solution of **40** was filtered with a #4 frit into another Schlenk flask containing Se powder under an Ar atmosphere. The reaction mixture was stirred at room temperature under an Ar atmosphere for 1 hour. After removal of the solvent from the resulting brown solution with a suspension of excess black Se powder, the residue was extracted with CH₂Cl₂ and the extract was subjected to flash-chromatography on silica-gel, eluting with dry hexane. Removal of the solvent from the eluent gave a mixture of an orange solid (major) and a yellow solid and oil (minor). ¹H NMR spectroscopy of the mixture indicated that it contained about 1 : 0.2

mixture of the desired diselenide **69** (major) and the corresponding selenide, $(\text{FcCH}_2)_2\text{Se}$ **70** (minor). The ratio was determined by comparison of the integrals for the corresponding CH_2 proton signals i.e. if the integrals of the proton signals corresponding to the CH_2 protons for **69** and **70** were 20 and 4, respectively, there were about 5 : 1 ratio of **69** and **70**, respectively, present in the mixture.

Despite the attempts, it was difficult to isolate either **69** or **70**. The attempted chromatography of the mixture on a preparative TLC plate or on a column packed with silica gel, eluting with the various ratios of CH_2Cl_2 -hexane mixtures was unsuccessful. The decomposition of **69** into **70** and elemental Se was indicated by deposition of a black solid on the plate or column and also by the changes in the ratio of the respective CH_2 proton signals in the ^1H NMR spectrum which was recorded after the chromatography. The more chromatography, especially on a preparative TLC plate, was performed, the more decomposition of **69** could be observed (Figure 4-10).

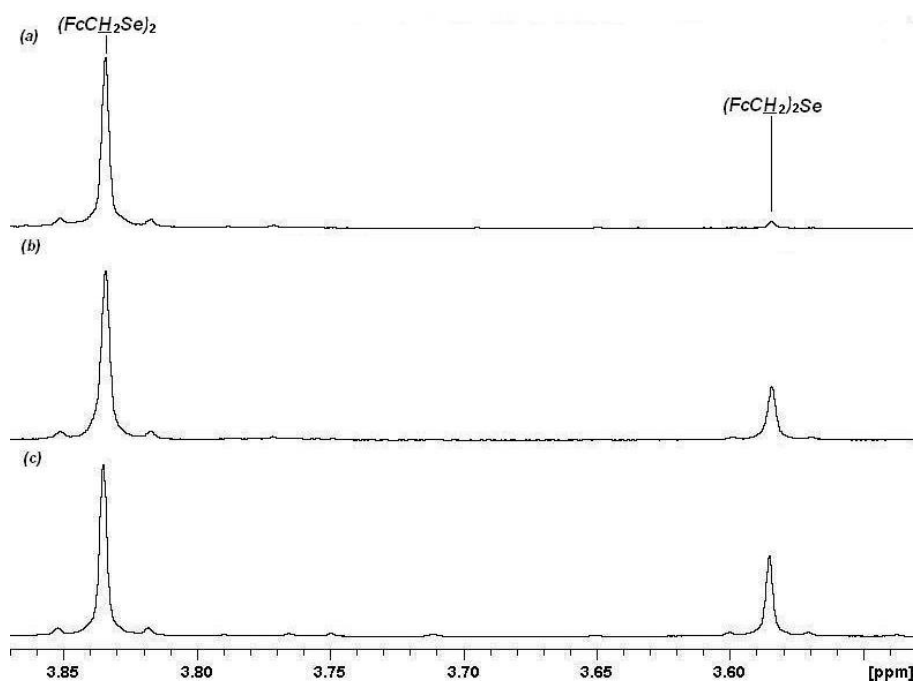


Figure 4-10: ^1H NMR spectra showing the decomposition of **69** into **70** after multiple chromatography on preparative TLC plates: (a) the crude product, (b) after 1st chromatography, (c) after 2nd chromatography

Neither did handling under a N₂ atmosphere nor using deoxygenated and dry solvent prevent the decomposition of **69**, suggesting that it was not due to air or moisture. When a sample of **69** was kept in dark (wrapped with aluminum foil) at -18 °C for 2 months, only slight decomposition of **69** could be observed (Figure 4-11), suggesting that it could be light sensitive.

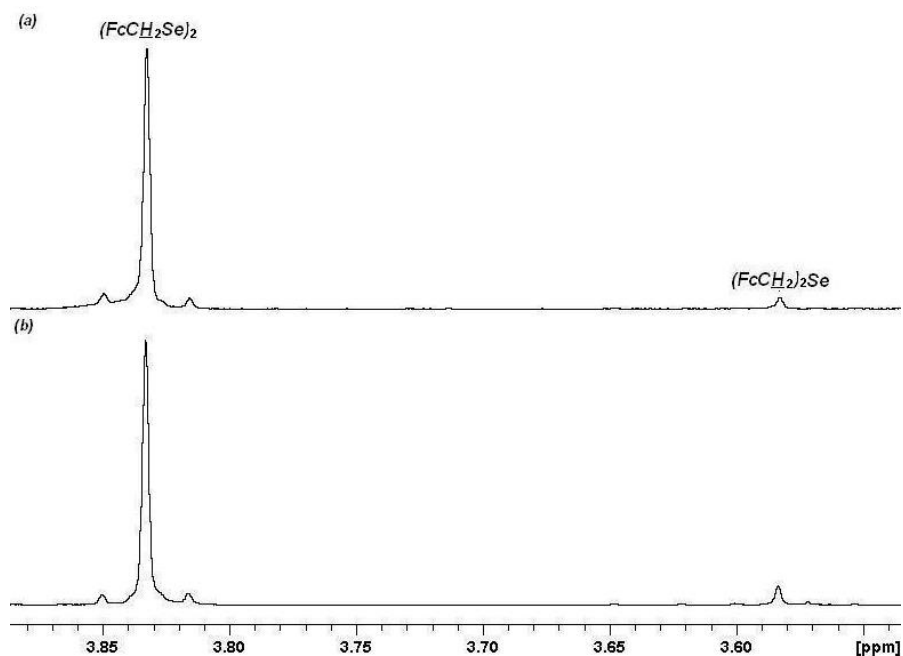


Figure 4-11: ¹H NMR spectra showing the decomposition of **69** into **70** (a) before the storage (b) after storage at -18 °C for 2 months

The attempted recrystallisation of the mixture from CH₂Cl₂/hexane or hexane at -18 °C was not successful either, although the purest sample of each compound could be obtained by recrystallisation from hexane at -18 °C. The diselenide **69** was first recrystallised out as an orange solid. After removing **69** by filtration, further concentrating the filtrate and cooling to -18 °C, the corresponding selenide **70** also precipitated out as a yellow solid. Although the samples had the least amount of the other compound, satisfactory microanalytical data for the samples could not be obtained.

Photochemical reaction of (PhCH₂Se)₂ with UV irradiation to quantitatively produce (PhCH₂)₂Se and elemental Se has been reported by Chu *et al.*¹⁶⁹. Photolysis of diorganodiselenides, R₂Se₂, in solution i.e. benzene or acetonitrile, to the

corresponding selenide upon exposure to a UV light has also been known¹⁶⁹⁻¹⁷². These studies may suggest that **69** be also light sensitive. The spontaneous decomposition of **69** might, therefore, have been caused by the prolonged exposure to room ceiling light during the work-up and purification. The further decomposition occurred during and after the chromatography on a preparative TLC plate probably due to the photochemical rearrangement reaction of **69** into **70** under room ceiling light. Recrystallisation afforded a much purer sample of each compound probably because the exposure of **69** to light was kept minimal while being stored in the freezer in dark.

4.2.1.4 Attempted Synthesis of (FcCH₂Se)₂ (**69**) by Reaction of [FcCH₂NMe₃]I (**6**) with Na₂Se₂

The synthesis of dibenzyl diselenide, (PhCH₂Se)₂, from the reaction of the corresponding chloride, PhCH₂Cl, with an aqueous or ethanolic solution of Na₂Se₂, generated from NaBH₄ and Se powder, has been reported by Klayman *et al.*¹⁶⁰. The synthesis of **69** according to the literature method using **6** as precursor was, therefore, attempted. The ethanolic solution of **6** and Na₂Se₂ (generated *in situ* from NaBH₄ and Se powder) was stirred at 60 °C for 72 h, precipitating a yellow solid. After filtering, the yellow solid was extracted with CH₂Cl₂. After filtering the insoluble materials, removal of the solvent afforded again a yellow solid. ESI-MS and NMR spectroscopy on the yellow solid both indicated that it was only **6** recovered unreacted (74 % recovery yield) (Figure 4-12).

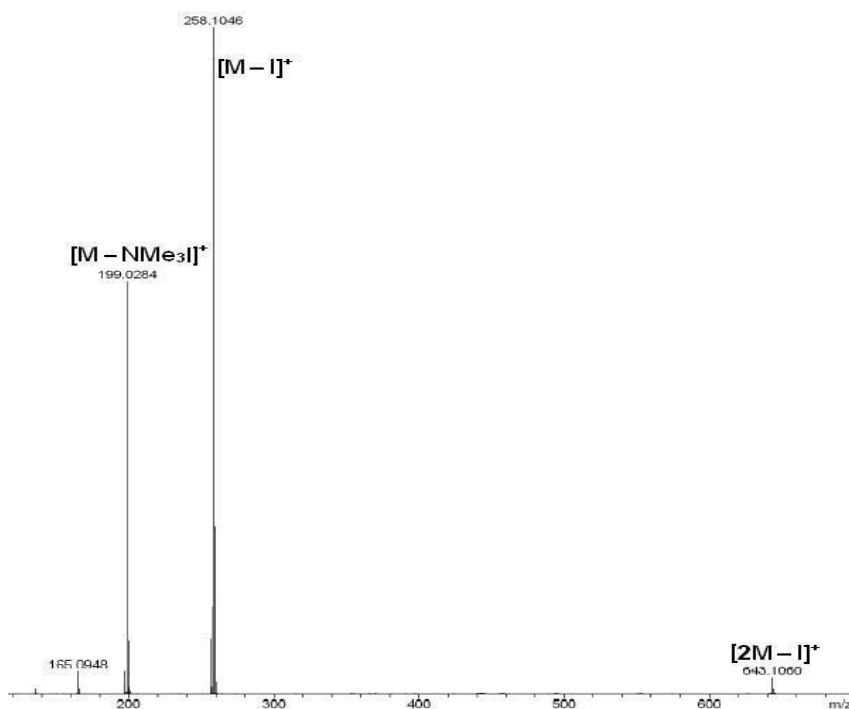


Figure 4-12: ESI-MS of the product (a yellow solid) from the reaction of $[FcCH_2NMe_3]I$ **6** with Na_2Se_2 ($M = 6$)

4.2.1.5 Synthesis of $(FcCH_2Se)_2$ (**69**) by Reaction of $FcCH_2Cl$ (**71**) with Na_2Se_2

Since compound **69** could not be obtained from **6**, this reaction was carried out using **71** as the starting compound as described in the literature¹⁶⁰. Compound **71**, which was prepared according to the literature methods^{93, 173} and used as obtained without further purifications after the volatiles had been removed under reduced pressure, was added to a red ethanolic solution of Na_2Se_2 prepared as before. The mixture was stirred at room temperature for 17.5 h. After filtering, the yellow solid was washed with distilled H_2O and then extracted with Et_2O . Removal of the ether under reduced pressure gave a yellow oil. 1H NMR spectroscopy on the yellow oil indicated that it was an approximately 1 : 2 mixture of **69** and **70**, respectively (determined as before by comparison of the integrals of the respective CH_2 proton signals (Figure 4-13)). Since the reaction yielded the unwanted side-product **70** as the major product, further investigations into this synthetic route were not carried out.

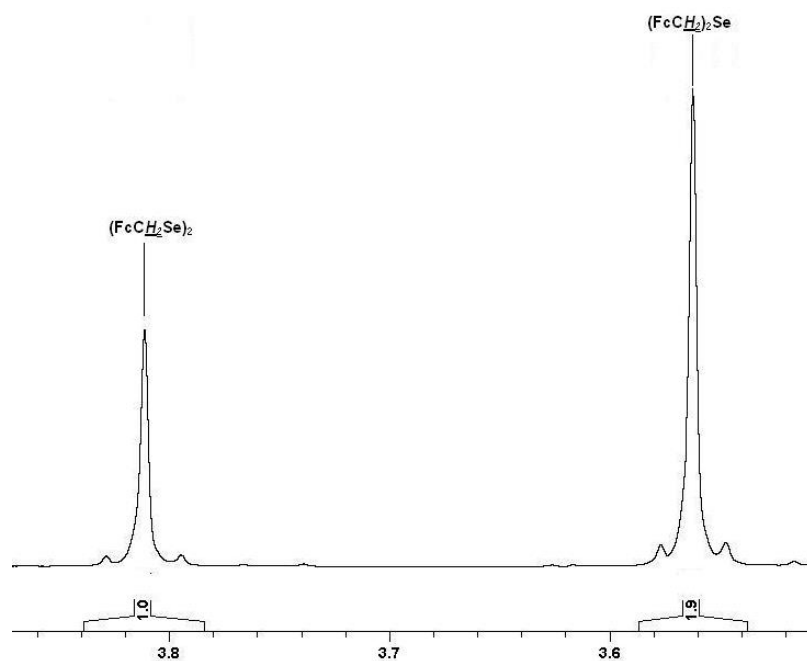


Figure 4-13: ^1H NMR Spectrum of the crude product from the reaction of FcCH_2Cl **71** with Na_2Se_2

4.2.1.6 Attempted Synthesis of FcCH_2SeH (**72**) by Reaction of FcCH_2Cl (**71**) with NaSeH

The synthesis of PhCH_2SeH from PhCH_2Cl with NaSeH has been reported in the literature¹⁶⁰. This attempted synthesis of **72** was, therefore, carried out using the method¹⁶⁰. Compound **71**, which was prepared as before, was added to a colourless ethanolic solution of NaSeH generated from Se powder and NaBH_4 in EtOH at $0\text{ }^\circ\text{C}$ as described in the literature¹⁶⁰. The mixture was stirred at room temperature for 18.5 h. After acidifying with 1.8 M HCl , the solution was stirred at room temperature for 2 h. The aqueous phase was extracted with CHCl_3 and the insoluble materials were filtered. Removal of the solvent from the filtrate under reduced pressure gave a yellow solid. ^1H NMR spectroscopy on the yellow solid indicated that it was an approximately 2.5: 1 mixture (determined as before) of **69** (27 % yield based on FcCH_2OH **73** used^{93, 173}) and **70**, respectively. No selenol proton signal for the desired compound, which is expected to appear at around $\delta -0.09$ ppm (for PhCH_2SeH ¹⁶⁰) could be observed.

4.2.1.7 Synthesis of Fc(CH₂)_nSeH (n = 1 (**72**), 4 (**74**)) by Reaction of Fc(CH₂)_nSeCN (n = 1 (**67**), 4 (**68**)) with NaBH₄

A high yielding synthesis of *n*-hexylselenol (75 % yield) by the reaction of *n*-hexylselenocyanate and NaBH₄ in EtOH at 20 °C for 0.25 h and the subsequent acid hydrolysis has been reported by Krief *et al.*¹⁶⁷. The syntheses of Fc(CH₂)_nSeH (n = 1 **72** or 4 **74**) from the corresponding Fc(CH₂)_nSeCN (n = 1 **67** or 4 **68**) with NaBH₄ were, therefore, carried out.

When excess NaBH₄ was added to a solution of **67** in absolute EtOH at room temperature under an N₂ atmosphere, the sudden colour change of the reaction mixture from red to yellow was observed after around 30 seconds. After adding extra NaBH₄ in order to ensure the completion of the reaction, the mixture was stirred for further 2 mins and hydrolysed with distilled H₂O which led to the immediate precipitation of a yellow solid. The precipitate was extracted with Et₂O and the ether extract was washed with distilled H₂O and dried over MgSO₄. After filtering, removal of the solvent from the organic phase gave a yellow solid (~50 % yield based upon the number of moles of **69**). ¹H NMR spectroscopy on the solid indicated that it was nearly pure diselenide **69**. No selenol proton NMR signal could be observed. The signal should have appeared around δ -0.09 ppm as a triplet with a ³J_{HH} coupling constant of around 6.5 Hz with reference to the literature values for PhCH₂SeH¹⁶⁰, was observed.

However, when the reaction was repeated and the crude product after removing the solvent from the reaction mixture under reduced pressure was immediately analysed without carrying out the subsequent work-ups, the selenol proton signal could be observed at δ -0.06 ppm as a triplet with a ³J_{HH} coupling constant of 6 Hz and also with two satellites with a ¹J_{SeH} with a coupling constant of 42 Hz (Figure 4-14). The signal could, however, not be observed when the ¹H NMR spectrum was recorded after the subsequent work-ups were carried out as before even though they were carried out under an N₂ atmosphere using deoxygenated solvent.

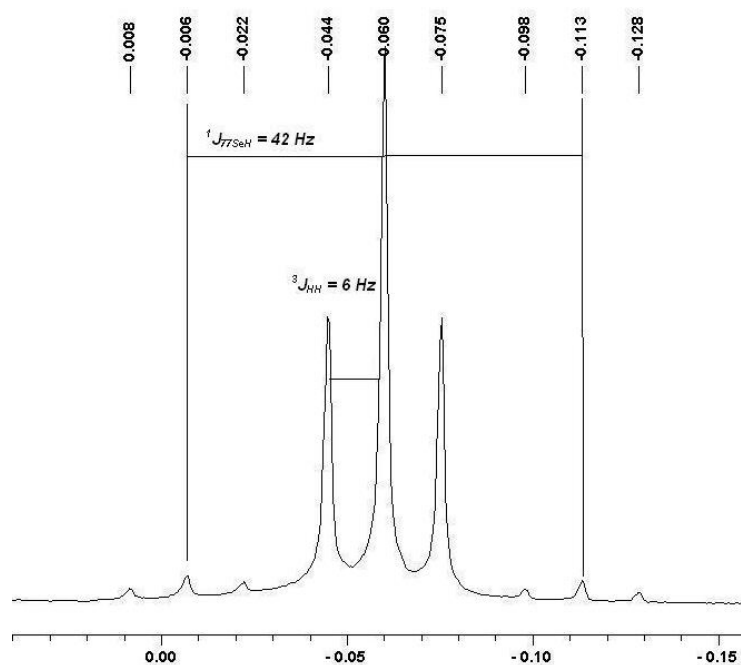


Figure 4-14: Partial ^1H NMR spectrum showing the selenol proton signal of **72**

The butyl analogue of **72** could also be prepared using the selenocyanate **68**. Excess NaBH_4 (> 2 eq.) was added to a solution of **68** in absolute EtOH and stirred at 20 °C under an N_2 atmosphere for 15 minutes. After hydrolysing with distilled H_2O , the solution was extracted with light petroleum spirits and the organic phase was washed with distilled H_2O , dried over Na_2SO_4 and filtered. Removal of the solvent from the organic phase gave an orange oil. ^1H NMR spectroscopy showed that the orange oil was again mostly the corresponding diselenide, $\{\text{Fc}(\text{CH}_2)_4\text{Se}\}_2$ **75**. However, in the ^1H NMR spectrum, the selenol proton signal could also be observed at δ -0.7 as a triplet with a $^3J_{\text{HH}}$ coupling constant of 7 Hz (Figure 4-15). The signal was, nevertheless, minor compared to those corresponding to the diselenide **75**. As for the attempted synthesis of **72** from **67**, the corresponding diselenide **75** was quantitatively obtained (~46 % yield) by the reaction and the amount of the selenol **74** formed was only minor. Moreover, the selenol proton NMR signal could not be observed after 18 h at 300 K in a capped NMR tube in air, suggesting that it was not stable.

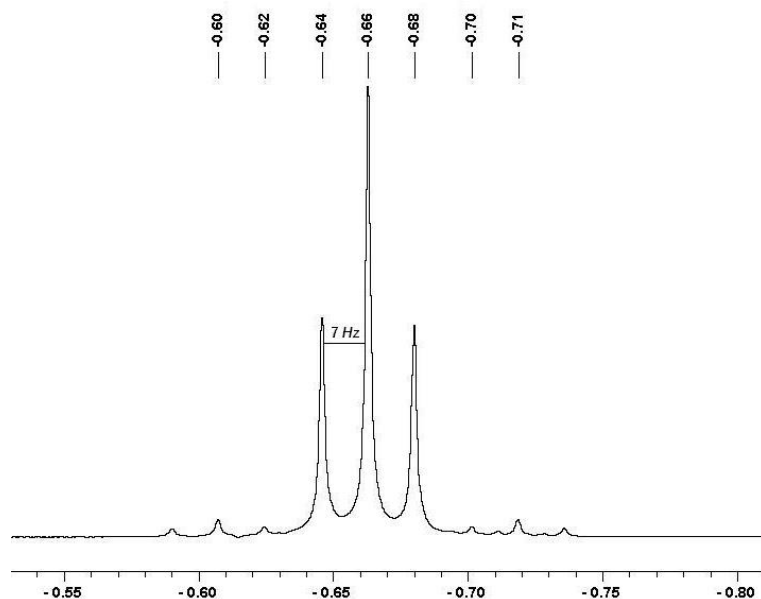
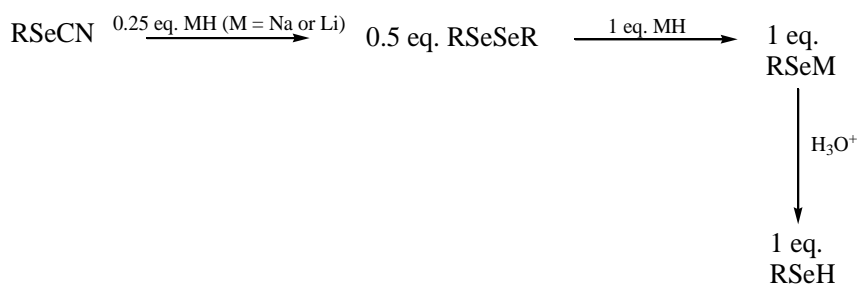


Figure 4-15: Partial ^1H NMR spectrum showing the selenol proton signal of **74**

Reduction of organoselenocyanates with metal hydrides such as NaH, LiHBEt₃, LiBH₄ or NaBH₄ generally yields the corresponding diselenides quantitatively^{157, 167}. The corresponding selenol was thought to form as intermediate. Krief *et al.*¹⁶⁷, however, argue that the reaction proceeded in a manner in which organoselenocyanate was first reduced by metal hydride to give the corresponding metal salt, RSeM, which would then react with unreacted RSeCN to produce the corresponding diselenide, RSeSeR, which would be the major product if the reaction is carried out with less than 1.25 molar equivalent of a metal hydride. If excess metal hydride, MH (M = Na or Li) i.e. at least > 1.25 eq. in total is used, the diselenide produced will be further reduced to give the corresponding selenolate, RSeM, the acid hydrolysis of which will then give the corresponding selenol (Scheme 4-4).



Scheme 4-4: Proposed reaction of organoselenocyanate with metal hydride to give the corresponding organoselenol by Krief *et al.*¹⁶⁷

Since NaBH₄ was always used in excess (> 1.5 eq.) in the syntheses of **72** and **74**, the quantitative formation of the corresponding diselenides may not be explained by the insufficient amount of the metal hydride used. Since organoselenols are typically air-sensitive and readily undergo oxidation to yield the corresponding diselenides¹⁵¹, the diselenides obtained in these syntheses might have been due to the oxidation of the desired selenols into the corresponding diselenides owing to their instability towards air oxidation which were also exhibited by the disappearance of the selenol proton signal in the ¹H NMR spectrum over a relatively short period of time i.e. overnight left in solution at room temperature in air.

Attempts to grow a single crystal of either compound by recrystallisation from a mixture of dry CH₂Cl₂ and hexane at -18 °C were unsuccessful. No precipitates could be obtained.

4.2.1.8 **Synthesis of FcCH₂SeH (72) by Reaction of (FcCH₂Se)₂ (69) with Zn under Acidic Conditions**

A high yielding synthesis of PhSeH **78** (~99 %) by reduction of (PhSe)₂ **79** with zinc dust in two-solvent system consisting of Et₂O and H₂O under acidic conditions has been described by Santi *et al.*¹⁵⁸ The synthesis of **72** from the corresponding diselenide **69** (see earlier for the preparations) using these literature conditions was, therefore, carried out.

When concentrated HCl solution was added dropwise to a solution of **69** in a two-solvent system consisting of Et₂O/distilled H₂O with a suspension of Zn powder¹⁵⁸, vigorous effervescence was observed. The reaction mixture was stirred until the vigorous reaction had subsided (~2 hours). The aqueous phase was removed with a syringe and the solvent from the remaining organic phase was then removed under reduced pressure, giving a mixture of a yellow solid (major) and oil (minor). ¹H NMR spectroscopy on the mixture showed that it contained major amounts of **69** and **70**, and only a minor amount of **72** (approximately 4 : 3.75 : 1 molar ratio of **69**, **70** and

72, respectively, appeared to have been present in the product. The ratio was determined by comparison of the integrals of the respective CH₂ proton NMR signals (Figure 4-16) i.e. the ratio between the integrals of the CH₂ proton NMR signals for **69**, **70** and **72** should be 2 : 2 : 1 if equimolar amounts of each was present). The selenol proton NMR signal again completely disappeared after the work-up was carried out in air i.e. the crude product was extracted with Et₂O and washed with distilled H₂O even though it was carried out under an N₂ atmosphere using deoxygenated solvents.

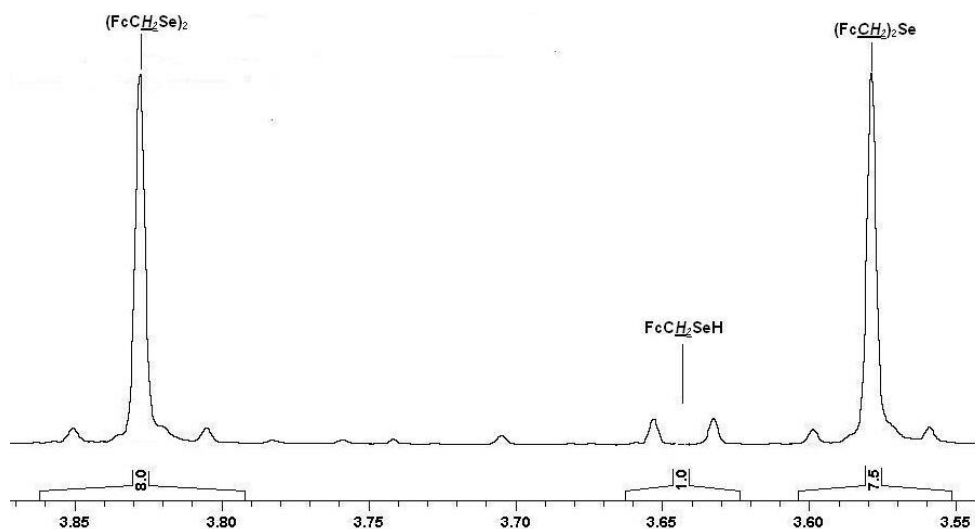


Figure 4-16: Partial ¹H NMR spectrum showing an approximately 4 : 1 : 3.75 mixture of **69**, **72** and **70**, respectively

4.2.1.9 Synthesis of FcCH₂SeH (**72**) by Reduction of (FcCH₂Se)₂ (**69**) with NaBH₄

A 75%-yielding synthesis of FcSe(*n*-C₇H₁₅) via the corresponding selenol, FcSeH, generated *in situ* by reduction of (FcSe)₂ with NaBH₄ in EtOH at 0 °C under an Ar atmosphere has been reported by Kumar *et al.*¹⁵⁶ Although the selenol was not isolated in the literature synthesis¹⁵⁶, due to the excellent yield of the derivative (i.e. a 75 % yield for FcSe(*n*-C₇H₁₅)), the synthesis of **72** was carried out using the literature method¹⁵⁶.

The mixture of **69** and NaBH₄ in EtOH was stirred at 0 °C for 2 minutes and then at room temperature for further 2 minutes under an N₂ atmosphere. Removal of the

solvent under reduced pressure gave a yellow solid. GC-MS showed a trace amount of **72**. The attempts to isolate the desired compound were, however, unsuccessful.

4.2.1.10 Summary

Ferrocenylmethyl selenol **72** could be prepared by reduction of the corresponding diselenide **69** with Zn/HCl in H₂O/Et₂O at room temperature or with NaBH₄ in EtOH at 0 °C or of **67** with NaBH₄ in EtOH at 0 °C. Ferrocenylbutyl selenol **74** could also be prepared by reduction of the corresponding selenocyanate **68** with NaBH₄ in EtOH at 0 °C. Although the formation of the desired selenols was indicated by NMR spectroscopy, they were only in trace or minor amounts and could not be isolated due to their instabilities under ambient conditions.

For the synthesis of the diselenide **69**, since it was difficult to separate from the corresponding selenide **70**, it may be more desirable to synthesise it from the reaction of **67** with NaBH₄ or of **40** with Se powder which provided the least amount of **70** (Figure 4-17). The other synthetic pathways gave the selenide **70** in quantitative yields. For the synthesis of the diselenide **75**, a pure sample, for which satisfactory microanalytical data could be obtained, could be prepared by reaction of the corresponding selenocyanate **68** with NaBH₄.

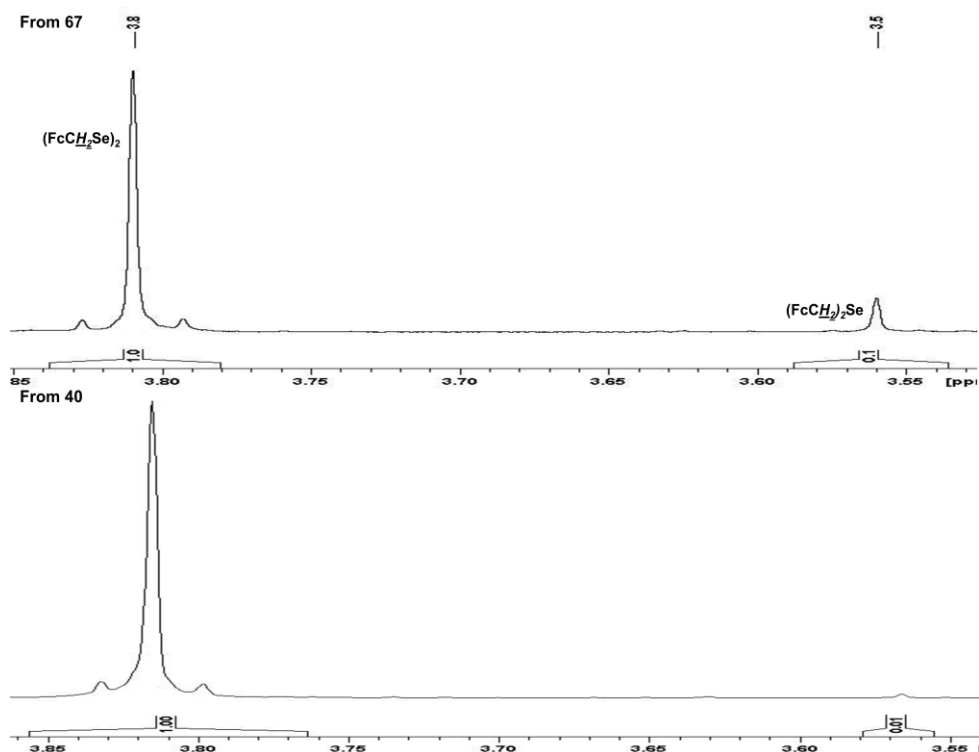


Figure 4-17: ^1H NMR Spectra of **69** (the crude product) obtained from reaction of FcCH_2SeCN **67** with NaBH_4 and of FcCH_2Li **40** with elemental Se

4.2.1.11 Characterisation of $(\text{FcCH}_2\text{Se})_2$ (**69**), $(\text{FcCH}_2)_2\text{Se}$ (**70**) and $(\text{FcCH}_2)_2\text{Se}_3$ (**76**)

The synthesis of **69** via an alternative synthetic route¹⁶⁵ had been reported during the course of the present study. Compound **69** could, therefore, be characterised by comparison to the literature values where applicable. The diselenide **69** and selenide **70** were obtained as orange and yellow solids, respectively. The formation of the triselenide **76** could also be observed but only by ESI-MS (see Figure 4-22). Due to the difficulties in obtaining pure samples of **69** and **70**, they could only partially be characterised by ^{77}Se , ^1H and $^{13}\text{C}\{-^1\text{H}\}$ NMR spectroscopy and ESI-MS. The ^{77}Se NMR data for **69** and **70** are summarised in Table 4-4.

Table 4-4: The ^{77}Se NMR signals for **69** and **70**

	^{77}Se NMR / δ ppm
69	391.5 (t, $^2J_{\text{SeH}} = 13$ Hz)
70	332.7 (t, $^2J_{\text{SeH}} = 11$ Hz)

The ^{77}Se NMR signals for **69** and **70** could be observed in the expected region for the class of compounds concerned^{152,174} i.e. $\sim \delta$ 398 – δ 412 ppm (several chemical shifts are reported for $(\text{PhCH}_2\text{Se})_2$ ¹⁷⁵ even though all were recorded in CDCl_3 and δ 333 ppm in CDCl_3 for $(\text{PhCH}_2)_2\text{Se}$ ¹⁷⁵. ^{77}Se NMR signals for dialkylselenides generally appear further upfield than those for the corresponding diselenide, $\text{R}_2\text{Se}_2 > \delta$ ^{77}Se ppm $>$ R_2Se ¹⁷⁵. The ^{77}Se NMR signal for **70** also appeared further upfield by δ 59 ppm than that for **69** which was consistent with the trend. The selenium in **69** is more deshielded than that in **70** because of the chemical bonding to another Se in **69** while to alkyl in **70**.

In the proton-coupled mode, the ^{77}Se NMR signal for **69** appeared as a triplet with a $^2J_{\text{SeH}}$ coupling constant of 13 Hz and that for **70** appeared as a five-line multiplet with a $^2J_{\text{SeH}}$ coupling constant of 11 Hz (Figure 4-18) which are both consistent with the class of compounds concerned i.e. $^2J_{\text{SeH}} = 4 - 16$ Hz¹⁷⁵ for aliphatic selenides in general). The ^{77}Se NMR signal for **70** was a five-line multiplet instead of a triplet as observed for **69**, which suggested that the CH_2 protons in **70** were not completely magnetically equivalent.

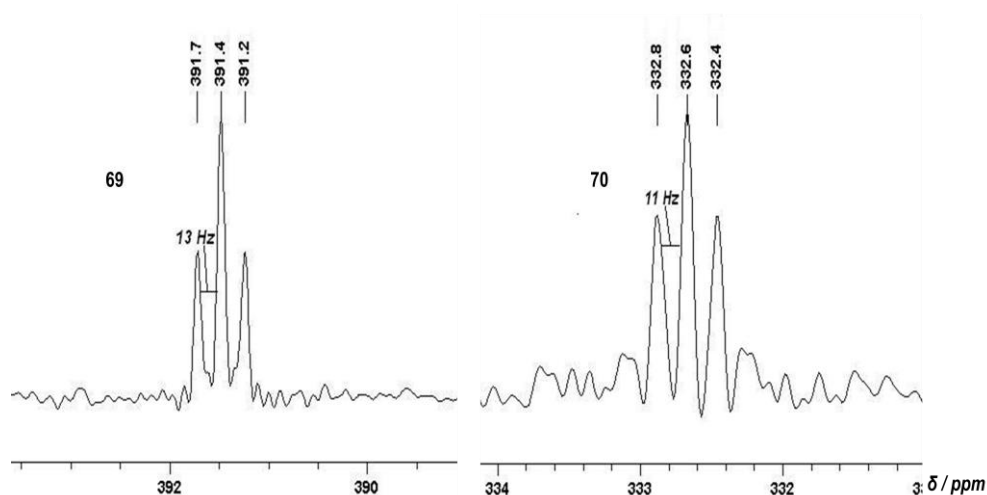


Figure 4-18: ^{77}Se NMR spectra showing the δ ^{77}Se NMR signals of **69** and **70** in the proton-coupled mode

The 2-D NMR data for **69** and **70** were also consistent with the structures of the expected compounds. The selected $^{1,2,3}J_{\text{CH}}$ correlations observed in the HMBC and

HSQC NMR experiments are shown in Figure 4-19. The absence of the second Se in **70** could clearly be indicated in the HMBC spectrum by the presence of a correlation at δ 23.4 ppm (in black) between the CH₂ protons and the CH₂ carbon of the CH₂ group at the other side of the Se atom.

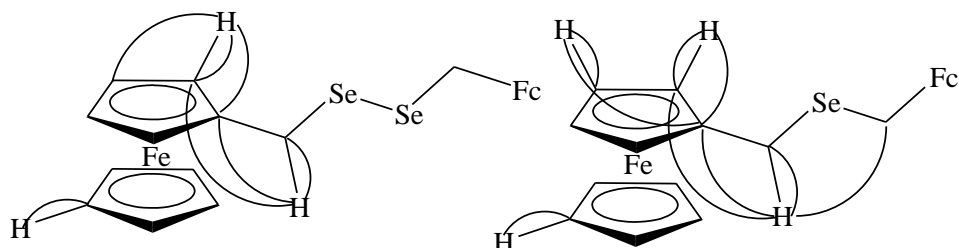


Figure 4-19: Selected $^{1,2,3}J_{CH}$ correlations observed for **69** and **70** in the HMBC and HSQC NMR experiments

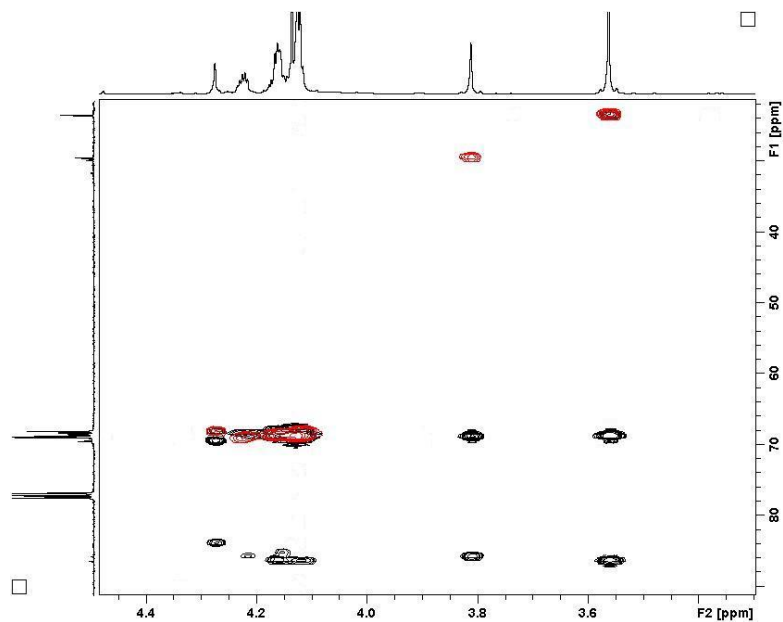


Figure 4-20: $^{1,2,3}J_{CH}$ correlations observed for **69** and **70** in the HMBC and HSQC NMR experiments

The assignments of the chemical shifts were made according to the 2-D NMR data and also by reference to the literature values i.e. the ^1H NMR data for **69** and **70** are consistent with those reported in the literatures^{153,165}.

Mass spectrometric data for **69** and **70** were obtained as a mixture by ESI-MS using MeOH as a mobile phase. At capillary exit voltage of 100 V, the molecular ions, $[M]^+$

($M = 69$ or 70) (Figure 4-21), and also the sodium and potassium adducts, $[M + Na]^+$ and $[M + K]^+$, (Table 4-5) could be observed in the positive-ion mode. Minor ions corresponding to **76** (Table 4-5; Figure 4-21) were also observed in the positive-ion mode although no other spectroscopic data for **76** could be obtained due to the insufficient amount.

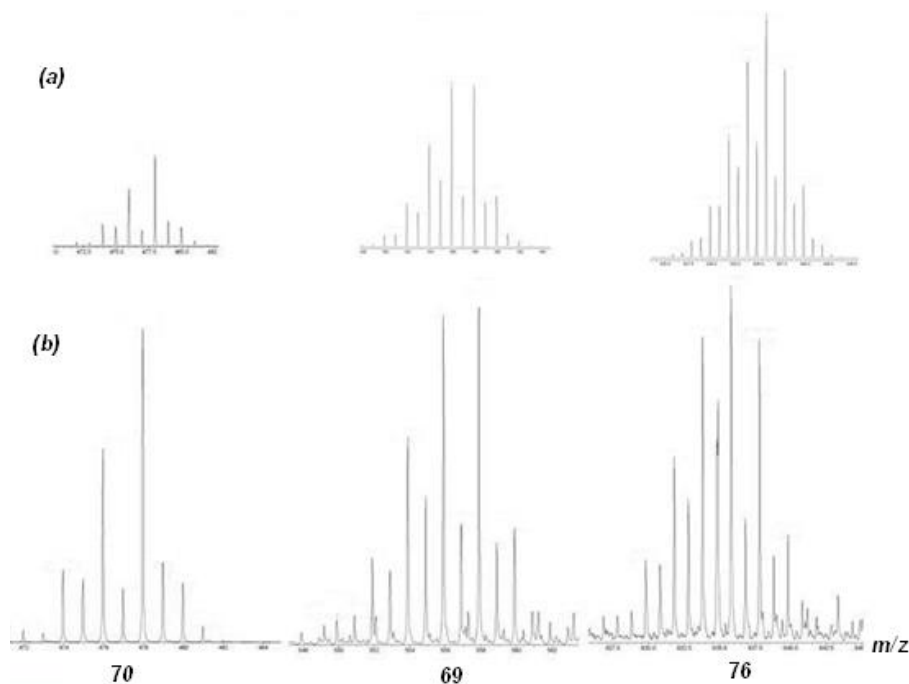


Figure 4-21: Partial ESI spectra showing the (a) theoretical and (b) observed $[M]^+$ ions of **69**, **70** and **76**

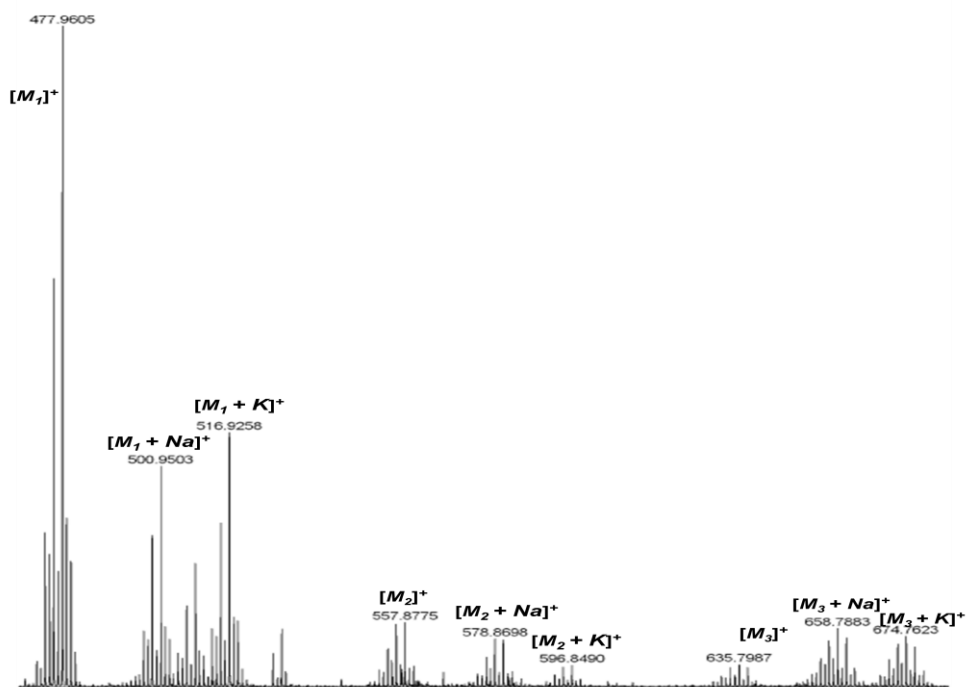


Figure 4-22: ESI-MS of the mixture of **70** ($= [M_1]$), **69** ($= [M_2]$) and **76** ($= [M_3]$)

<i>m/z</i> (MeOH, 100 V)	70	69	76
$[M]^+$	477.960 (477.958)	557.877 (557.874)	637.794 (637.791)
$[M + Na]^+$	500.950 (500.947)	580.867 (580.864)	660.786 (660.780)
$[M + K]^+$	516.925 (516.921)	596.849 (596.838)	676.759 (676.754)

*calculated *m/z* in brackets

The GC-MS data for **70** could also be obtained with the ions corresponding to the fragmentation of the parent ion (Figure 4-23).

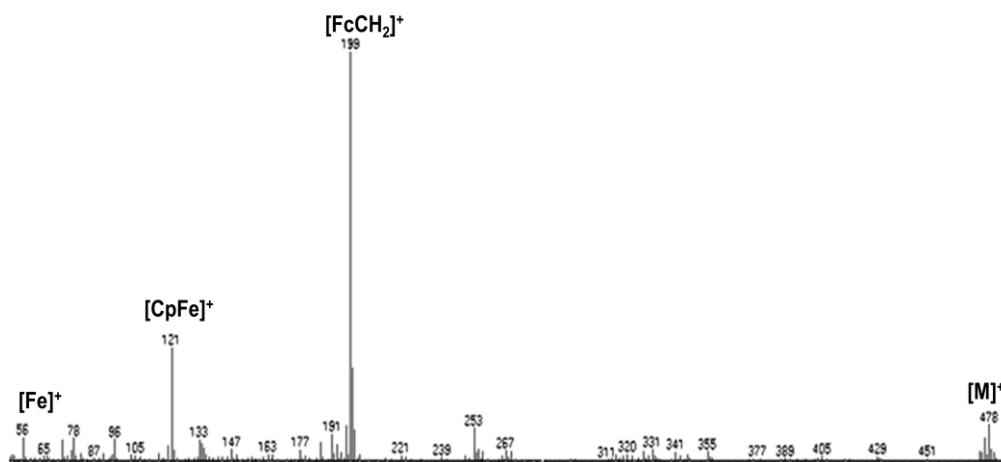


Figure 4-23: GC-MS of **70**

Despite the attempts, satisfactory microanalytical data for **69** (i.e. calcd. for $C_{22}H_{22}Fe_2Se_2$: C 47.52; H 3.99 %; found: C 33.83; H 2.89 %) and **70** (i.e. calcd. for $C_{22}H_{22}Fe_2Se_1$: C 55.39; H 4.65 %; found: C 50.38; H 4.40 %) could not be obtained. Attempts to obtain single crystals of **70** and **76** were also unsuccessful (the X-ray crystallographic structure of **69** had already been reported¹⁶⁵).

4.2.1.12 Characterisation of $\{Fc(CH_2)_4Se\}_2$ (**75**) and $\{Fc(CH_2)_4\}_2Se$ (**77**)

Ferrocenylbutyl diselenide **75** was characterised by ^{77}Se , 1H and $^{13}C\{-^1H\}$ NMR spectroscopy and ESI-MS. Satisfactory microanalytical data for **75** i.e. Found: C 52.93; H 5.63 %; Calcd. C 52.53; H 5.35 %, could be obtained on the orange oil after removal of the solvent from the organic phase which had been washed with distilled

H₂O and dried over Na₂SO₄ after extracting of the aqueous phase of the reaction mixture, and the sample was sent in a sealed ampoule under vacuum as precaution. The corresponding selenide **77** could also be observed but only by ESI-MS. Since the NMR analysis for **77** was carried out as a mixture of **77** and **75**, some signals were indistinguishable with those for **75** because of the similarities in their structures. Unambiguous assignments for **77** could, therefore, not be made due to the signal overlapping.

The ⁷⁷Se NMR signal for **75** appeared at δ 306.1 ppm as expected for the class of compounds concerned i.e. δ 200 – 600 ppm for C–Se–Se in general¹⁷⁵; δ 346 ppm for (*n*-C₄H₉Se)₂⁵⁹ both were recorded in CDCl₃). The signal was shifted further upfield by δ 86 ppm than that for **69** i.e. δ 392 ppm which may be expected due to the greater distance between the selenium atom and ferrocene, the latter of which is deshielding, and also probably due to shielding from the saturated aliphatic carbons which could shift a signal further upfield. The ⁷⁷Se NMR signal for **77** could not be observed probably because of the insufficient amount of **77** in the sample in order to acquire a decent ⁷⁷Se NMR spectrum. In the proton-coupled mode, the ⁷⁷Se NMR signal for **75** appeared at δ 305.9 ppm as an unresolved multiplet with a ²*J*_{SeH} coupling constant of 8 Hz (Figure 4-24) which was slightly smaller than that observed for **69** i.e. 13 Hz. It was, however, within the range expected for ²*J*_{SeH} couplings between aliphatic hydrogen and selenium i.e. 4 – 16 Hz in general¹⁷⁵.

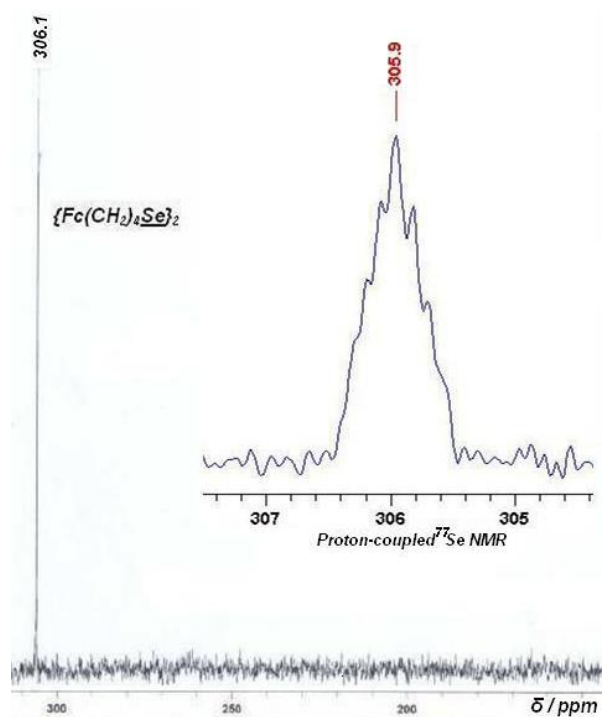


Figure 4-24: Partial ^{77}Se NMR Spectra showing the δ ^{77}Se NMR signals of **75** in proton-coupled and -decoupled modes

^1H NMR spectroscopy was also recorded. The ^1H NMR chemical shifts for **75** were comparable to the literature values reported for a close analogue, $\{\text{Fc}(\text{CH}_2)_6\text{Se}\}_2$ ¹⁵⁷. The 2-D NMR data were also consistent with the structure of the expected compound. The selected $^{1,2,3}J_{\text{CH}\&\text{HH}}$ correlations observed for **75** in the HMBC, HSQC and COSY NMR experiments are shown in Figure 4-19.

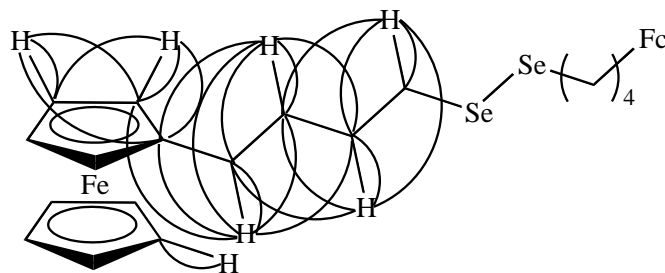


Figure 4-25: Selected $^{1,2,3}J_{\text{CH}\&\text{HH}}$ correlations observed for **75** in the HMBC, HSQC and COSY NMR experiments

The mass spectrometric data for **75** and **77** could be obtained by ESI-MS using MeOH as a mobile phase. At a capillary exit voltage of 100 V, the molecular ions, $[M]^+$ ($M = \mathbf{75}$ or $\mathbf{77}$), were observed in the positive-ion mode (Table 4-6). The isotope

distribution patterns agreed with the theoretical ones (Figure 4-26). The corresponding triselenide was not observed.

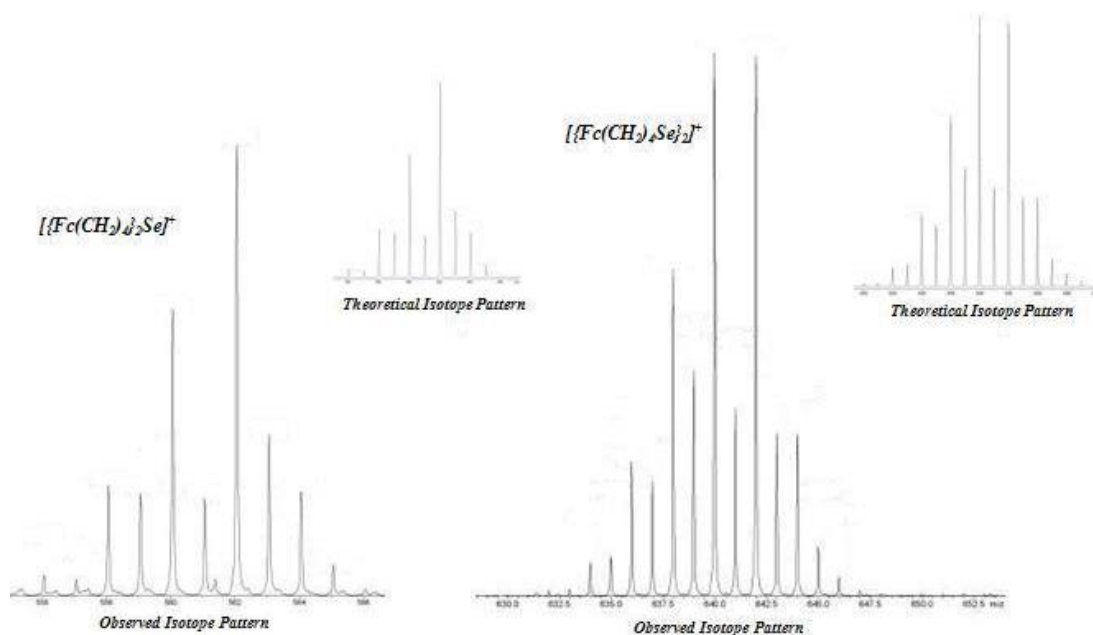


Figure 4-26: Partial ESI-MS showing the observed and theoretical $[M]^+$ ions of **75** and **77**

Table 4-6: ESI mass spectrometric data for 75 and 77		
	75	77
$[M]^+ / m/z$	641.967 (calcd. 641.968)	562.050 (calcd. 562.052)

4.2.1.13 Characterisation of $\text{Fc}(\text{CH}_2)_n\text{SeH}$ ($n = 1$ (**72**), **4** (**74**))

Due to the instability of **72** and **74**, they could only partially be characterised by ^{77}Se , ^1H and $^{13}\text{C}\{-^1\text{H}\}$ NMR and IR spectroscopy and ESI mass spectrometry. The selected spectroscopic data are summarised in Table 4-7. Some known alkyl and aryl selenols are also included for comparative purposes.

Table 4-7: Selected spectroscopic data for 72 and 74				
	$^{77}\text{Se}\{-^1\text{H}\}$ NMR / δ	^1H NMR (SeH) / δ	Se-H str. / $\nu \text{ cm}^{-1}$	$[M]^+ / m/z$
	ppm	ppm		
$(\text{C}_3\text{H}_5)\text{SeH}^{153}$	96.4	0.19	2250m	Not given.
$\text{PhCH}_2\text{SeH}^{160}$	Not given	-0.09	Not given.	Not given.
72	80.0 (s)	-0.06	Could not be obtained.	278 (calcd. 278)
74	-13.7 (s)	-0.66	2248m	321.991 (calcd. 321.991)

* all NMR data were recorded in CDCl_3 .

NMR spectroscopy was recorded under an inert atmosphere. The NMR samples were prepared under a N₂ atmosphere using deoxygenated dry solvents and sealed permanently under vacuum for these compounds unless otherwise specified. The ⁷⁷Se NMR signals for alkyl selenols (C–Se–H) generally appear between δ –200 – δ 300 ppm¹⁷⁵. The large range in chemical shift of ⁷⁷Se NMR signal is very common in ⁷⁷Se NMR spectroscopy¹⁷⁵. ⁷⁷Se NMR signal of selenol is generally observed much further upfield than the corresponding diselenide which often appears between δ 200 – δ 550 ppm¹⁷⁵. The selenol selenium signals for **72** and **74** could also be observed at δ 80.5 and –13.7 ppm, respectively, and were further upfield by about δ 300 ppm than those for the corresponding diselenides **69** and **75** i.e. δ 391.4 and 306.1 ppm, respectively, respectively, and were all in the expected region for the class of compounds concerned¹⁷⁵.

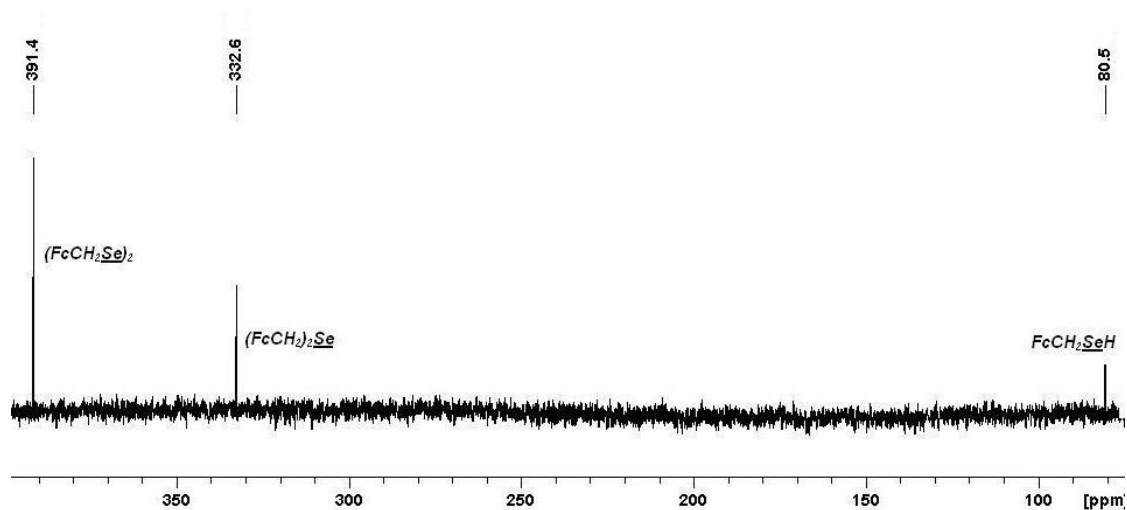


Figure 4-27: ⁷⁷Se-¹H NMR spectrum of a mixture of **69**, **70** and **72**

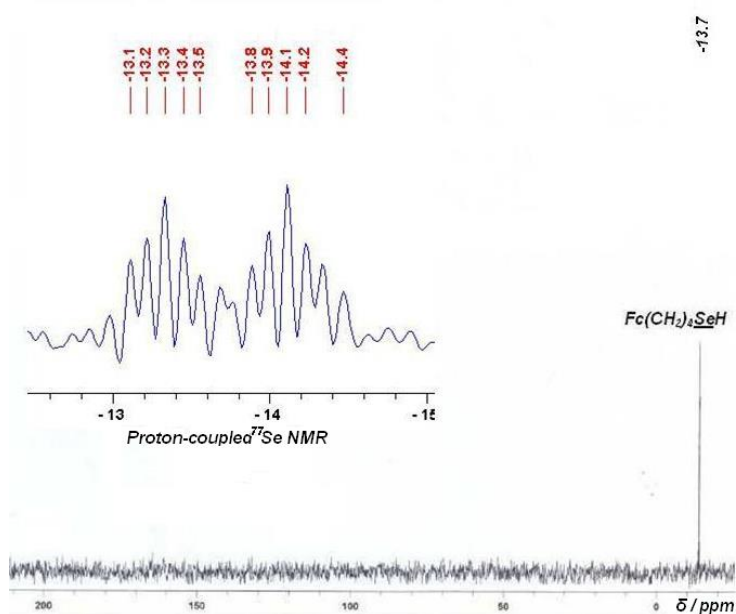


Figure 4-28: Partial ^{77}Se NMR spectrum showing the $\delta^{77}\text{Se}$ NMR signals of **74** in proton-coupled and -decoupled modes

The selenol selenium signal for **74** appeared further upfield by δ 93.7 ppm than that for the corresponding diselenide **72**, suggesting that the selenium in **74** was more shielded than that in **72** which might have been expected considering the greater distance between the selenium and ferrocene, the latter of which was deshielding due to the aromatic ring currents because of which benzene chemical shifts are downfield. Since the hydrides ($\text{C}-\text{Se}-\text{H}$) are those with the most strongly shielded selenium nuclei among the type¹⁷⁵, without deshielding from adjacent groups, the signals appear further upfield and this was consistent for **72** and **74** and the corresponding mono- and di-selenides. In the ^1H -coupled mode, both the ^{77}Se signals for **72** and **74** could be observed as a doublet of multiplets with $^1J_{\text{SeH}}$ coupling constants of 41 and 44 Hz, respectively. The coupling constants were consistent for the class of compounds concerned (cf. $^1J_{\text{SeH}} = 41 - 58$ Hz for aliphatic and aromatic selenols)^{152, 174}.

In the ^1H NMR spectra, the selenol proton signals for **72** and **74** were observed at δ -0.06 and δ -0.66 ppm, respectively, as triplets with $^3J_{\text{HH}}$ coupling constants of ~ 7 Hz (Figure 4-29). The chemical shifts were comparable with those for PhCH_2SeH ¹⁶⁰ (Table 4-7). The selenol proton signal for **72** appeared slightly shifted further upfield

by about δ 0.03 ppm than that for $\text{PhCH}_2\text{SeH}^{160}$ which was consistent with the fact that a FcCH_2 moiety was less electron-withdrawing than the benzyl counterpart, PhCH_2 . The proton bonded to the selenium in **72** may, therefore, be less deshielded than that in PhCH_2SeH . The ^1H and ^{77}Se NMR signals for **74** were also comparable with those for **72**.

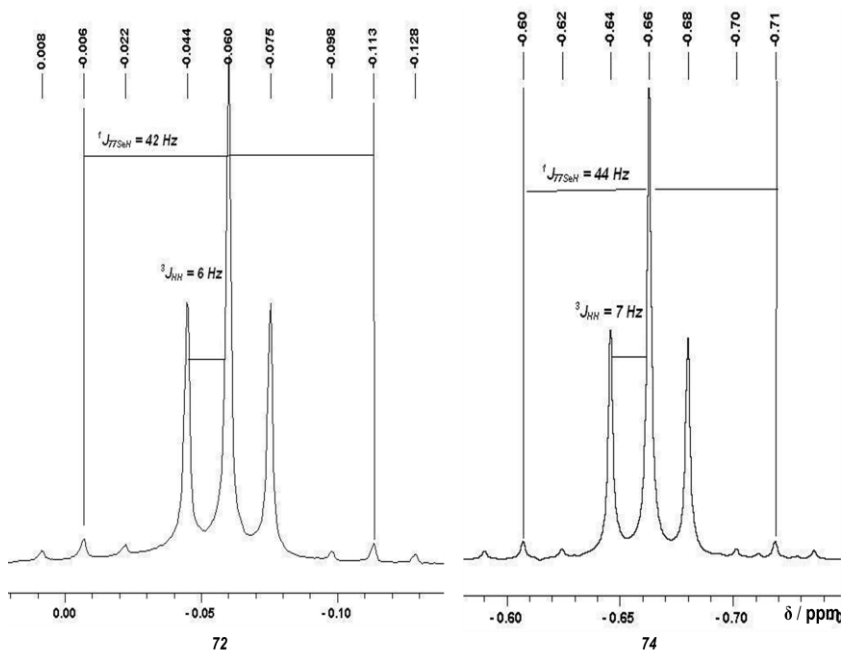


Figure 4-29: Partial ^1H NMR spectra showing the selenol proton signals for **72** and **74**

The ^{13}C and 2-D NMR data including HMBC, HSQC and COSY NMR experiments were also consistent with the structures of the expected compounds. The assignments of the ^1H and ^{13}C chemical shifts were made according to the 2-D NMR data. In the COSY NMR experiment (Figure 4-30), the $^3J_{\text{HH}}$ correlations between the selenol proton and methylene protons were observed for both **72** and **74** which are consistent with their molecular structures. The selected $^{1,2,3}J_{\text{CH}}$ correlations observed for **72** and **74** in the respective HMBC and HSQC NMR experiments are shown in Figure 4-33. Two-dimensional NMR correlations where definitive assignments could not be made due to overlapping of the signals are omitted in Figure 4-33.

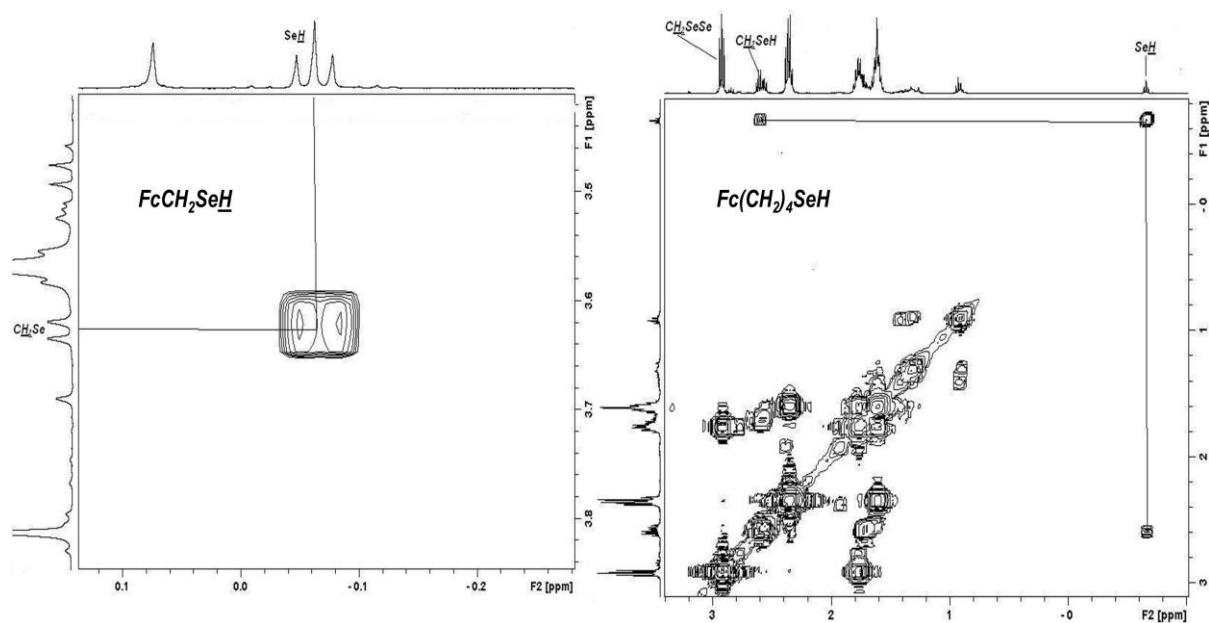


Figure 4-30: Selected $^3J_{HH}$ correlation between the selenol proton and CH_2 proton signals observed for **72** and **74** in the COSY NMR experiment

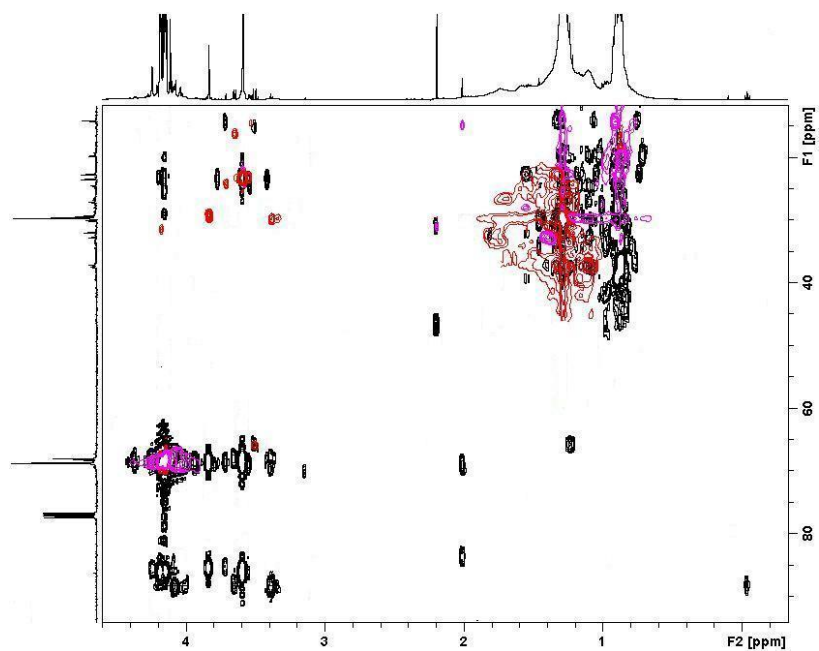


Figure 4-31: $^{1,2,3}J_{CH}$ correlations observed for **72** in the HMBC (in black) and HSQC (in red and pink) NMR experiments

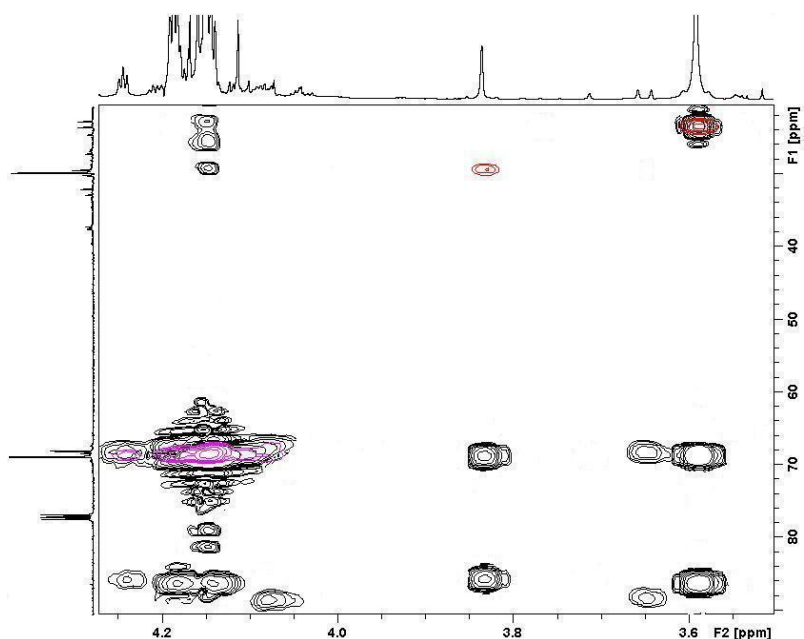


Figure 4-32: $^{1,2,3}J_{CH}$ correlations between the CH_2 and adjacent proton signals observed for **72** in the HMBC (in black) and HSQC (in red (CH_2 protons) and pink (CH protons)) NMR experiments

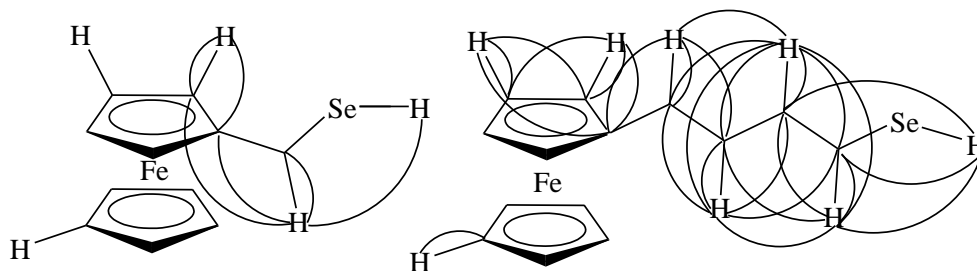


Figure 4-33: Selected $^{1,2,3}J_{CH}$ correlations observed for **72** and **74** in the HMBC, HSQC and COSY NMR experiments

IR spectroscopy was recorded as their neat states i.e. oils placed between KBr windows and in air. The ν (Se–H) stretch for **74** could be observed at 2248 cm^{-1} as a medium-intensity band, which was consistent with that reported for C_3H_5SeH (ν 2250 cm^{-1})¹⁵³. IR spectroscopy could not be recorded for **72** because the compound was too unstable.

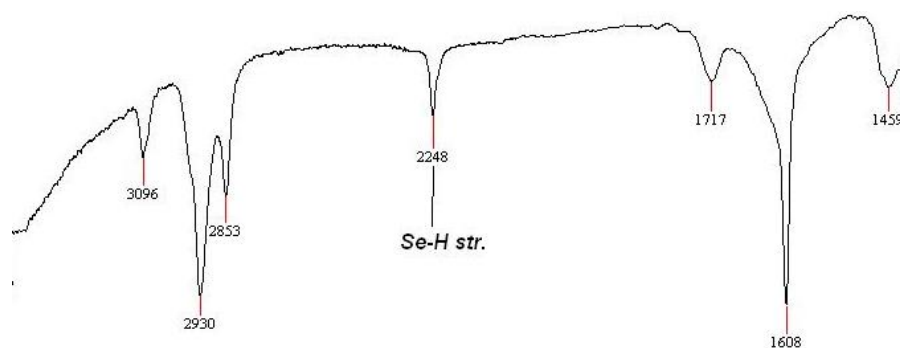


Figure 4-34: IR Spectrum showing the Se–H stretch of **74**

The mass spectrometric data for **72** could be obtained by GC-MS. The molecular ion, $[M]^+$ ($M = 72$), could be observed with those corresponding to $[Fe]^+$, $[CpFe]^+$ and $[FcCH_2]^+$ produced by fragmentation of the parent molecule (Figure 4-35). The mass spectrometric data for **74** could be obtained by both GC- and ESI-MS in MeOH as a mobile phase. At a capillary exit voltage of 100 V, the $[M]^+$ ion ($M = 74$; m/z observed 321.991; calcd. 321.991 for $C_{14}H_{18}Fe_1Se_1$) was observed in the positive-ion mode (Figure 4-36). GC-MS also showed the parent ion with the expected isotope distribution patterns (Figure 4-35).

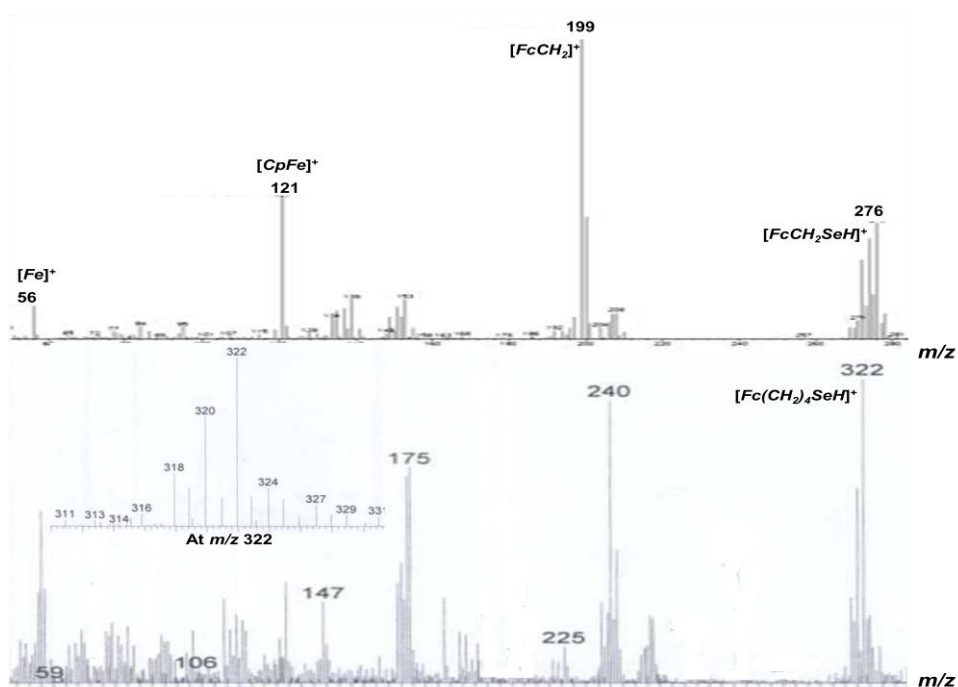


Figure 4-35: GC-MS of **72** and **74**

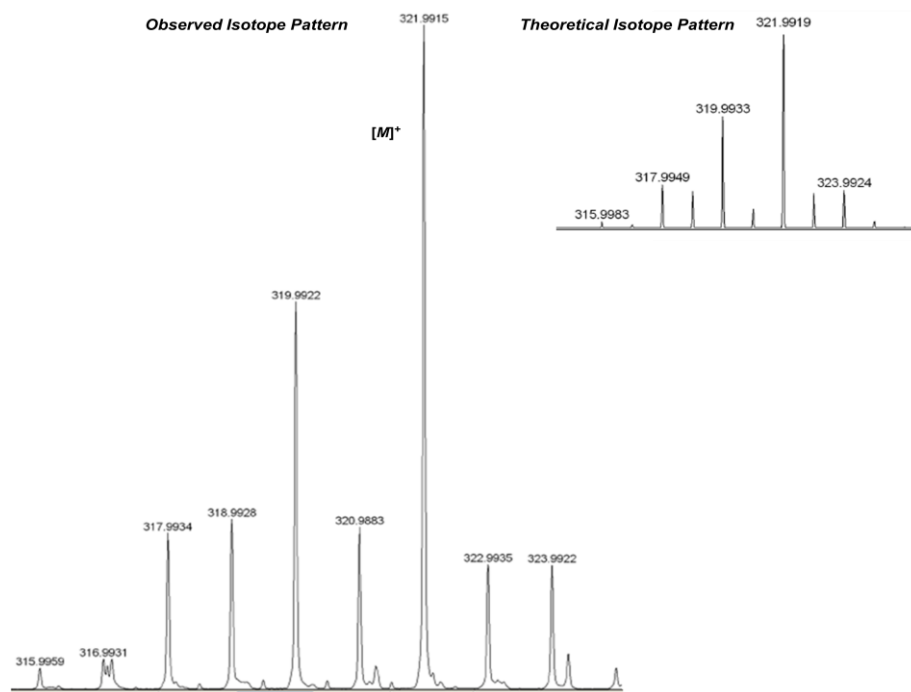


Figure 4-36: Partial ESI-MS showing the observed and theoretical $[M]^+$ ions of **74**

Although the attempts were made, single crystals of **72** and **74** could not be obtained.

4.2.1.14 Air-stability of $\text{Fc}(\text{CH}_2)_n\text{SeH}$ ($n = 1$ (**72**), 4 (**74**))

The stability of **72** in solution (in CDCl_3) at room temperature in a capped NMR tube in air was monitored by ^1H NMR spectroscopy by the disappearance of the CH_2 proton signal. After 5 days, a slight decrease and also increase in the intensities of the CH_2 proton signals for **72** and the oxidation product i.e. $(\text{FcCH}_2\text{Se})_2$, respectively, were observed (Figure 4-37), indicating the instability of the compound under ambient conditions. Since the selenol proton signal could not be observed after carrying out the work-up i.e. washing the organic phase containing **72** with deoxygenated distilled H_2O several times and drying over Na_2SO_4 under an N_2 atmosphere, and the strongest intensity of the selenol proton signal could always be observed for the crude product of a freshly prepared sample, the selenol **72** seemed more unstable as the neat state than in solution.

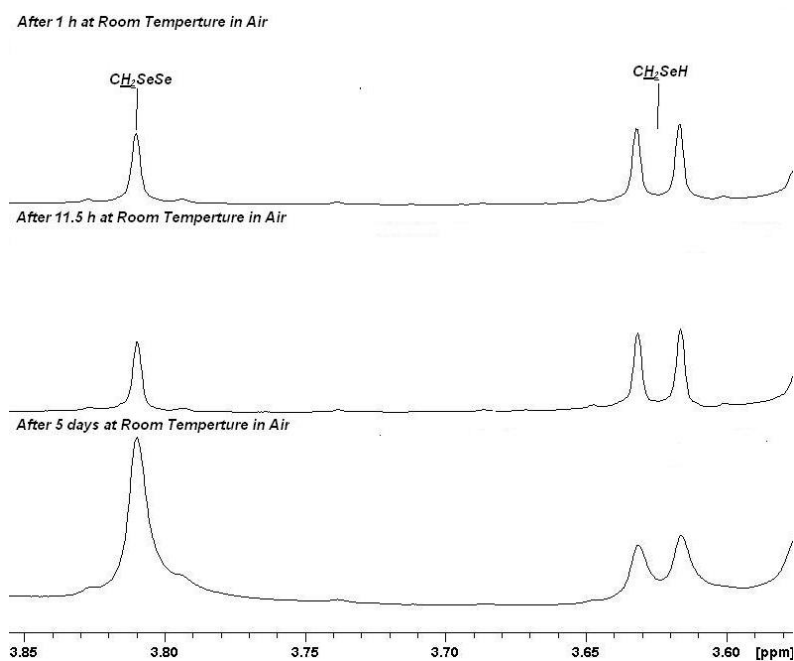


Figure 4-37: ^1H NMR spectra showing the air oxidation of **72** in CDCl_3 at room temperature in a capped NMR tube in air over 5 days

The air oxidation of **74** was also monitored by IR spectroscopy and also ^1H NMR spectroscopy as the neat state and in solution, respectively. IR spectroscopy was recorded on the crude product (a yellow oil) as a thin liquid film placed between KBr windows. Between the recordings, the windows were open and left exposed to air for seconds. The disappearance of the ν Se-H stretch at 2248 cm^{-1} was observed over a period of 10 mins (Figure 4-38).

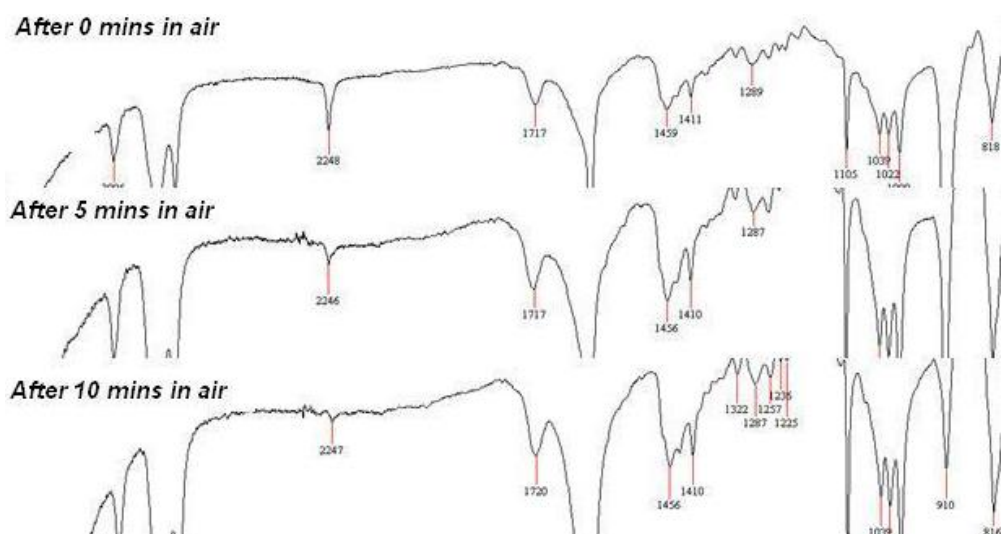


Figure 4-38: IR spectra showing the air oxidation of **74** in the neat state at room temperature by disappearance of the Se-H stretch

The oxidation of **74** in solution (i.e. CDCl_3) was monitored by ^1H NMR spectroscopy. The sample was left with a plastic NMR lid on at room temperature in air. The selenol proton signal could not be observed after 3 days (Figure 4-39). Even though a direct comparison can not be made due to the non-equimolar amount of each selenol used, **74** appeared to be less air-stable than **72** whose selenol proton signal could be observed for more than 5 days under the similar conditions.

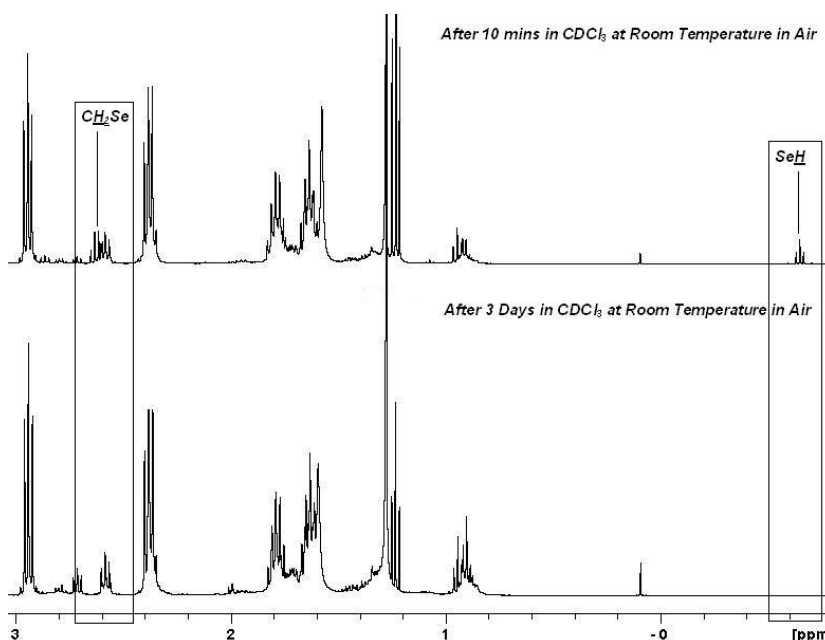


Figure 4-39: ^1H NMR spectra showing the air oxidation of **74** in solution (in CDCl_3) at room temperature in a capped NMR tube

Primary selenols could not to be stabilised by incorporation of a $\text{Fc}(\text{CH}_2)_n$ moiety into the hydride centres. They were as air-sensitive as may be expected for the class of compounds concerned.

4.2.2 ^{77}Se NMR Study on Effect of Ferrocene on Oxidative Stability of Phenyl Selenol (**78**) in Solution

This ^{77}Se NMR study was carried out in order to investigate if the stabilisation effect of ferrocene observed for the ^{31}P NMR studies on PhPH_2 in Chapter 2 would be extended to other heavier main group element hydrides. The ^{77}Se NMR signals for

PhSeH **78** and the corresponding diselenide, Ph₂Se₂ **79**, the latter of which was the oxidation product, appeared at δ 145 and δ 463 ppm, respectively. The oxidation of **78** could, therefore, be monitored by the changes in the intensity of the signals in the ⁷⁷Se-¹H NMR spectra. The NMR samples were prepared under a N₂ atmosphere. Equimolar amounts of **78** were placed in separate NMR tubes containing one millilitre of deoxygenated CDCl₃. To one of the tubes, excess ferrocene (~5 times equimolar amount) was added. After sealing the tubes with NMR plastic lids, they were removed from the inert atmosphere into air. The first ⁷⁷Se-¹H NMR spectra were recorded immediately after the preparations. The oxidation progress of **78** was monitored by ⁷⁷Se-¹H NMR spectroscopy until fully oxidised (i.e. the disappearance of the signal could be observed). During the intervals, the samples were placed on a rack placed in a fumehood at room temperature in air with their lid on. The solvents were occasionally filled due to the loss by slow evaporation in the same manner as the samples were prepared i.e. under an inert atmosphere using deoxygenated solvent. The integrals of the ⁷⁷Se NMR signals for **78** were set as the reference values (i.e. 1) and that for **79** was determined accordingly using the function of the TopSpin software. The integrals were then converted into percentages by dividing the integral of **79** by that of **78** followed by multiplication by 100. The calculated percentages (the vertical axis) were plotted as a graph against time (the horizontal axis) (Figure 4-40). The selected ⁷⁷Se-¹H NMR spectra of the control sample and the one with added ferrocene are also shown in Figure 4-41 and Figure 4-42, respectively.

Air Oxidation of 78 in Solution

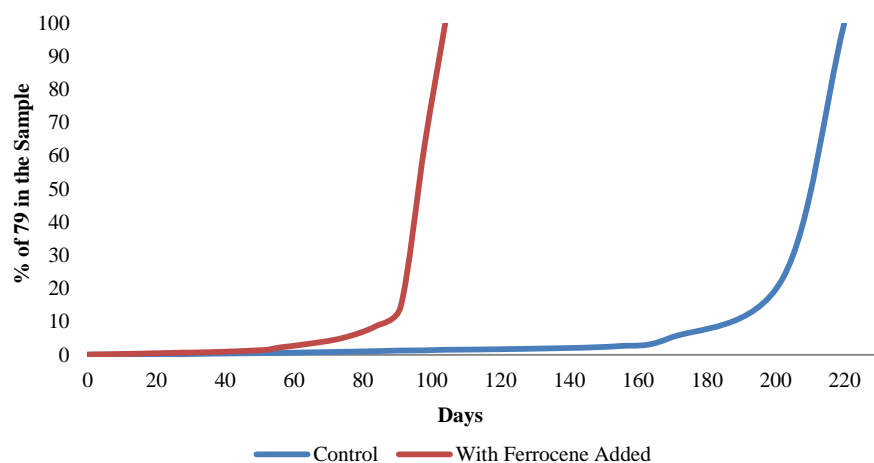


Figure 4-40: % of 79 in the sample against time

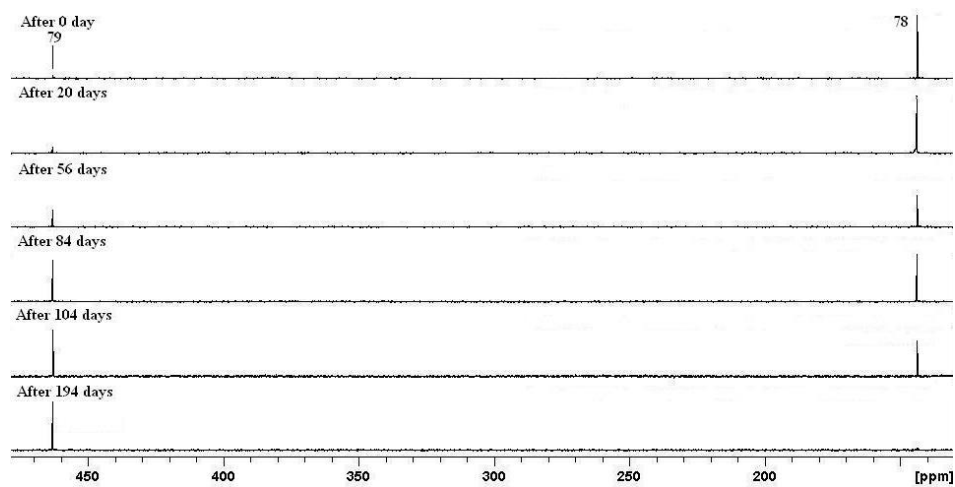


Figure 4-41: Selected ^{77}Se - $\{^1\text{H}\}$ spectra showing the oxidation of 78 in CDCl_3 at room temperature in air in a capped NMR tube

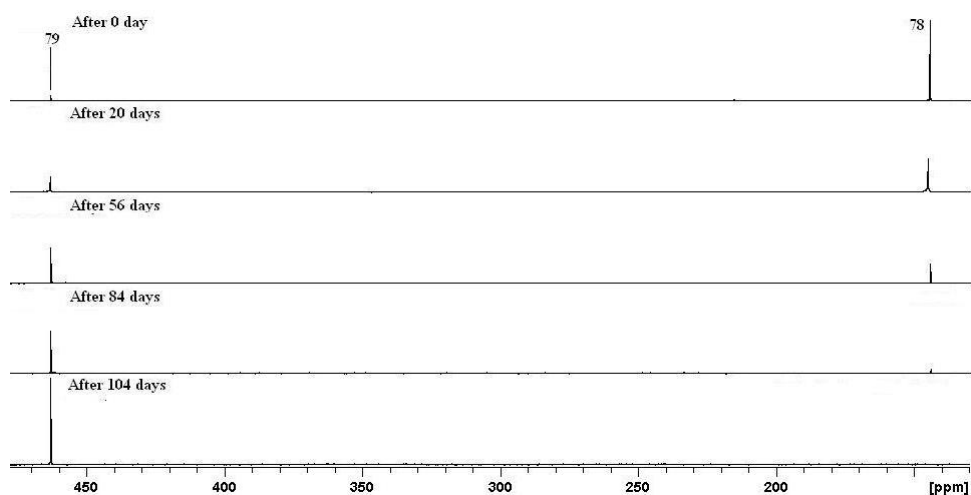
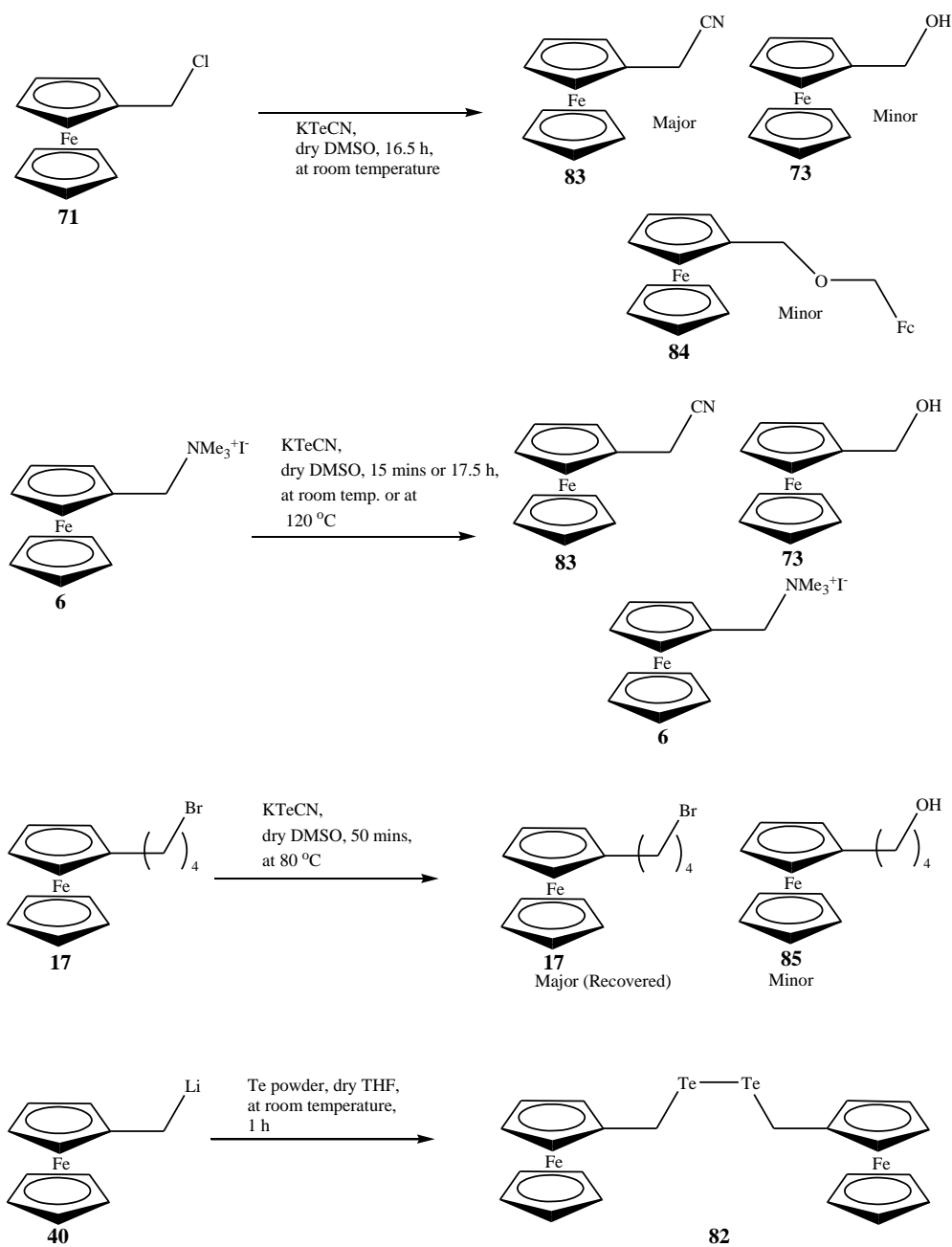


Figure 4-42: Selected ^{77}Se - $\{^1\text{H}\}$ spectra showing the oxidation of 78 in CDCl_3 at room temperature in air in a capped NMR tube with added FcH

As clearly seen from the figures above, the complete oxidation of **78** in CDCl_3 with ferrocene added was observed after ~3 months while that of **78** without ferrocene was after more than 6 months. The result of the study was contrary to that of the corresponding ^{31}P NMR study on PhPH_2 (see 2.2.4.4 for results and discussion). As discussed earlier (see 2.2.4.7), ferrocene might be able to act as a free radical inhibitor in solution, preventing the air oxidation of primary phosphanes. Therefore, although it was not clear why, the oxidation of **78** was almost twice as rapid as that of **78** in solution by itself when ferrocene was added to the solution, the result of the study showed that the selenol **78** could not be stabilised by simple addition of ferrocene as it could for the corresponding primary phosphane, PhPH_2 . The result of the study may, therefore, suggest that the oxidation of organoselenols does not involve the formation of free radicals. It may, tentatively, be concluded that the ferrocene stabilisation effect cannot be extended to selenols.

4.2.3 Attempted Synthesis of Ferrocenylmethyl Tellurol (**80**)

Attempts were made to synthesise a tellurol with a $\text{Fc}(\text{CH}_2)_n$ moiety i.e. FcCH_2TeH **80**, analogously to the corresponding selenol. The attempted syntheses of FcCH_2TeCN **81** and **80** and the synthesis of $(\text{FcCH}_2\text{Te})_2$ **82** are summarised in Scheme 4-5:



Scheme 4-5: Attempted synthesis of **81** and synthesis of **82**

4.2.3.1 Synthesis of KTeCN (**86**)

The literature method¹⁶² was adopted for the synthesis of KTeCN. A mixture of freshly ground KCN and Te powder in dry DMSO was stirred at 100 – 120 °C for 4 h under an N₂ atmosphere. The resulting pale yellow solution which was consistent with the literature description was used as obtained in the subsequent reaction.

4.2.3.2 Attempted Synthesis of FcCH₂TeCN (**81**) by Reaction of FcCH₂Cl (**71**) with KTeCN (**86**)

Under an N₂ atmosphere, a pale yellow solution of **86** was added dropwise to a dry DMSO solution of **71**. After stirring the mixture at room temperature for 16.5 h, the mixture was hydrolysed with distilled H₂O at 0 °C, which deposited a quantitative amount of elemental Te. After filtering, washing the yellow solid with distilled H₂O and then extracting with Et₂O, the organic phase was washed with distilled H₂O and then dried on MgSO₄·3H₂O. Removal of the solvent under reduced pressure gave a yellow-orange crystalline solid. GC-MS indicated that it contained a mixture of **83** (major), **73** (major) and **84** (minor). IR spectroscopy also showed a medium peak at 2251 cm⁻¹ which may arise from the C≡N stretch of **83** (cf. ~2220 cm⁻¹ for FcCN¹⁷⁶). It would have been too high for **81** compared to the literature values reported for PhCH₂TeCN (~2150 – 2180 cm⁻¹ ^{162, 177}). Since TeCN⁻ may easily dissociate into elemental Te and CN⁻, **71** reacted with CN⁻, giving FcCN quantitatively.

4.2.3.3 Attempted Synthesis of FcCH₂TeCN (**81**) by Reaction of [FcCH₂NMe₃]I (**6**) with KTeCN (**86**)

Under an N₂ atmosphere, a pale yellow solution of **86** was added dropwise to a solution of **6** in dry DMSO. After stirring the mixture at room temperature for 15 mins or at 120 °C for 17.5 h, the mixture was hydrolysed with distilled H₂O. This resulted in precipitation of a black solid which was probably by the decomposition of excess **86** into elemental Te and CN⁻. The subsequent filtration of the black solid gave a clear orange filtrate. The GC-MS analysis on the filtrate showed that it was a mixture of **83** (major) and **73** (minor). The HRMS analysis on the filtrate in MeOH also showed the ions corresponding to **6** i.e. *m/z* 258.095 [*M* – I]⁺; 643.072 [2*M* – I]⁺ (*M* = **6**) dominating in the positive-ion mode. Flash-chromatography of the filtrate on silica gel, eluting with CH₂Cl₂ and removal of the solvent from the eluent collected gave an orange solid which was also identified as **83** (36 % yield) by IR spectroscopy

(ν 2247 cm^{-1} ($\text{C}\equiv\text{N}$ str.)) and GC-MS (i.e. 225 $[\text{M}]^+$; 121 $[\text{CpFe}]^+$; 56 $[\text{Fe}]^+$ ($M = \mathbf{83}$)). Neither spectroscopic data suggested the formation of the desired compound.

4.2.3.4 Attempted Synthesis of $\text{Fc}(\text{CH}_2)_4\text{TeCN}$ (**87**) by Reaction of $\text{Fc}(\text{CH}_2)_4\text{Br}$ (**17**) with KTeCN (**86**)

Under an N_2 atmosphere, a pale yellow solution of **86** was added dropwise to a solution of **17** in dry DMSO at 40 °C. The solution immediately turned black from yellow upon the addition. After stirring at 80 °C for 50 mins, the mixture was hydrolysed with distilled H_2O at 0 °C and extracted with hexane and then with CH_2Cl_2 . Flash chromatography of the combined organic extracts on a silica gel, eluting with CH_2Cl_2 followed by removal of the solvent under reduced pressure gave a mixture of a red oil (major) and yellow solid (minor). The GC-MS analysis on the mixture indicated that it was a mixture of unreacted **17** (major) and **85** (minor).

4.2.3.5 Synthesis of $(\text{FcCH}_2\text{Te})_2$ (**82**) by Reaction of FcCH_2Li (**40**) with Te powder

With reference to the literature methods^{159, 178} for the synthesis of $(\text{FcTe}_2)_2$, the methyl analogue **82** could be prepared. Under an Ar atmosphere, a dry THF solution of **40** was added to another reaction flask containing Te powder. After stirring the mixture at 0 °C for 1 h in the dark, the solvent was removed under vacuum and the residue was extracted with CH_2Cl_2 . The organic extract was chromatographed on a silica gel, eluting with dry CH_2Cl_2 under an Ar atmosphere. Removal of the solvent from the eluent collected under reduced pressure gave **82** as a red solid in moderate yield (32 %). Further chromatography of the red solid on a preparative TLC plate in air or recrystallisation from dry CH_2Cl_2 at -18 °C in dark did not provide a purer sample but led to the decomposition probably by the reaction with light (see later). Despite the attempts, satisfactory samples for elemental analysis and X-ray crystallographic structural determination could not be obtained.

Photochemical decomposition of **83** into elemental Te could also be observed on storage especially in solution state and also during the chromatography on a TLC plate under ceiling room light in air. A fine black solid precipitated out in the solution and also on the plate if the sample was left exposed to ceiling room light. A sample was also prepared under an inert atmosphere using dry and deoxygenated solvent. However, it did not prevent the spontaneous formation of a black solid from forming. Keeping the sample wrapped in aluminium foil did, however, appear to stop further deposition of the black solid. The photochemical lability of dibenzyl ditelluride is well known^{170, 171, 179}. Brown *et al.*¹⁷⁰ studied the photolysis of diorganoditellurides in solution using R_2Te_2 ($R = Et$ or CH_2Ph), irradiating with ultraviolet light. The reformation of the ditellurides, losing an elemental Te, to produce the corresponding telluride, R_2Te , and elemental Te, quantitatively upon exposure to the ultraviolet irradiation was observed. Spencer *et al.*¹⁷¹ and Suzuki *et al.*¹⁷⁷ also reported the spontaneous decomposition of $(PhCH_2Te)_2$. The latter group also reported the spontaneous decomposition of all the dibenzyl ditellurides with different substituents on the aromatic rings that they made, upon storage. They claimed that the more electron-withdrawing the organic substituents on the aromatic rings were the more stable the ditelluride would be. Since there are not strongly electron-withdrawing substituents around the tellurium in **82** and the corresponding dibenzyl ditelluride is also quite light sensitive, it may not be surprising that **82** was also quite light sensitive. The photochemical decomposition of **82** may also be supported by the presence of the signals corresponding to $(FcCH_2)_2Te$ **88** in the 1H NMR spectrum. While the CH_2 proton signal at δ 4.1 ppm corresponding to **82** disappeared with time, a new proton signal developed at δ 3.8 ppm. Further 2-D NMR analysis showed that the correlations between the newly developed proton signals were consistent with the structure of **88** (Figure 4-43). The ESI-MS analysis also showed the corresponding ion as $[M + Na]^+$ ($M = \mathbf{88}$) in the positive ion mode.

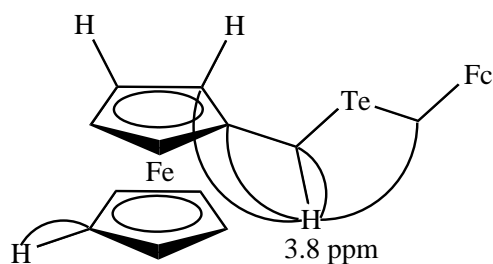


Figure 4-43: Selected $^{1,2,3}J_{CH}$ correlations observed for **88** in the HMBC and HSQC NMR experiments

4.2.3.6 Characterisation of $(\text{FcCH}_2\text{Te})_2$ (**82**) and $(\text{FcCH}_2)_2\text{Te}$ (**88**)

Compound **82** and **88** could be characterised by ESI-MS and NMR spectroscopy; selected NMR and ESI-MS data are shown in Table 4-8. Those for the corresponding benzyl analogues from the literatures are also included in the table for comparative purposes.

Table 4-8: Selected ESI-MS and NMR data for $(\text{PhCH}_2\text{Te})_2$, $(\text{PhCH}_2)_2\text{Te}$, **82** and **88**

	$^{13}\text{C}\{-^1\text{H}\}$ NMR ($\underline{\text{C}}\text{H}_2$) / δ ppm	^1H NMR ($\underline{\text{C}}\text{H}_2$) / δ ppm	$[\text{M} + \text{Na}]^+$ / m/z
$(\text{PhCH}_2\text{Te})_2$	6.6 ¹⁷¹	4.2 ¹⁷⁷	Not given.
$(\text{PhCH}_2)_2\text{Te}$	Not given.	4.0 ¹⁷¹	Not given.
82	3.5	4.1	
88	2.5	3.8	

The CH_2 proton and carbon signals for **82** appeared as singlets at δ 4.1 and δ 3.5 ppm, respectively. Both signals were shifted further upfield by δ 0.1 and δ 3.1 ppm, respectively, than those for $(\text{PhCH}_2\text{Te})_2$. Since a phenyl ring is more electron-withdrawing and hence deshielding than ferrocene, the shift towards further upfield is consistent with the desired compounds. The CH_2 proton signal for **88** appeared further upfield by δ 0.3 ppm than that for **82** which was also consistent with the shift observed for the corresponding benzyl analogues. The 2-D NMR data were also consistent with the structures of the expected compounds. The selected $^{1,2,3}J_{CH}$ correlations observed in the HMBC and HSQC NMR experiments for **88** and **82** are shown in Figure 4-43 and Figure 4-44, respectively, and also in Figure 4-45.

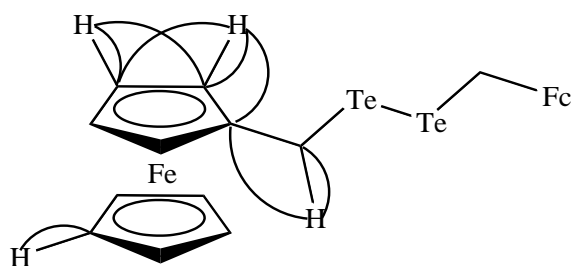


Figure 4-44: Selected $^{1,2,3}J_{CH}$ correlations observed in the HMBC and HSQC NMR experiments for **82**

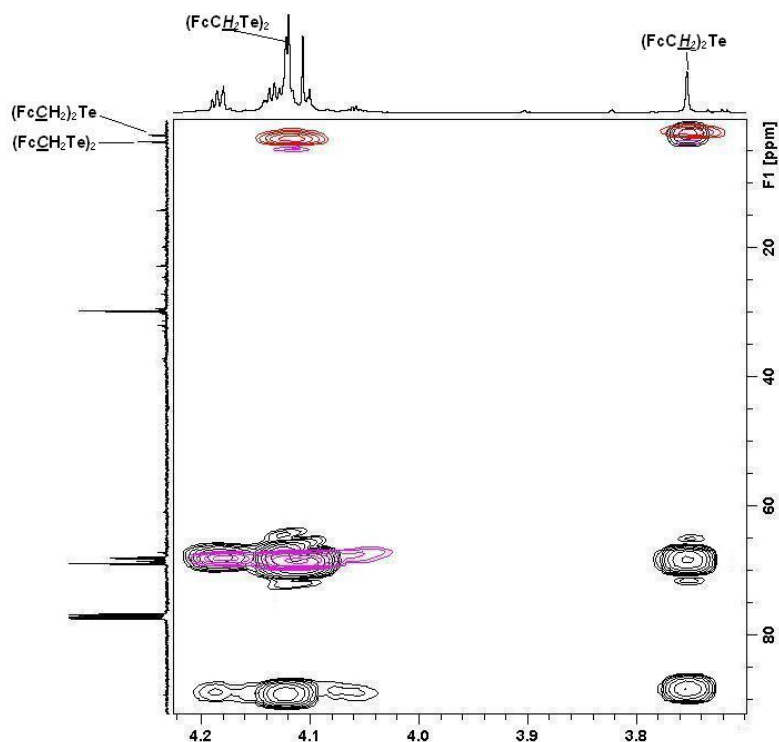


Figure 4-45: $^{1,2,3}J_{CH}$ correlations between the CH_2 proton and Cp carbons observed in the HMBC (in black) and HSQC (in red) NMR experiments for **82** and **88**

The $^{2,3}J_{CH}$ correlations between the CH_2 proton (H_5) and the CH_2 carbon (C_5), the quaternary carbon (C_1) and CH carbon (C_2) observed for **82** and **88** are shown in Figure 4-45 (the atom labelling is referring the atom labelling scheme in Figure 2-3). Although the di- and mono-tellurides **82** and **88** were obtained as a mixture and could not be separated, their 1H and ^{13}C NMR signals could be distinguished by using their $^{2,3}J_{CH}$ correlations observed in HMBC and HSQC NMR experiments. Since the $^3J_{CH}$ correlation between the H_5 proton and C_5 carbon signals was only observed for the telluride **88**, but not for the ditelluride **82** due to the absence of CH_2 group in a 3 σ -

bond distance, the H₅ proton and C₅ carbon signals could be assigned unambiguously for **88**. By using the ^{2,3}J_{CH} correlations from the H₅ proton and C₅ carbon signals, definitive assignments of the rest of the signals could also be made. The absence of the ³J_{CH} correlation between the H₅ proton and C₅ carbon signals was also observed for the mixture of the corresponding selenide **70** and diselenide **69** and assignments for their ¹H and ¹³C NMR signals were also made accordingly.

The mass spectrometric data for **82** and **88** were obtained as a mixture by ESI-MS using MeOH as a mobile phase. At a capillary exit voltage of 80 V, although the [M]⁺ ions for both **82** and **88** could not be observed, the corresponding sodium adducts, [M + Na]⁺ (M = **82** or **88**), could be observed in positive ion mode (Figure 4-46).

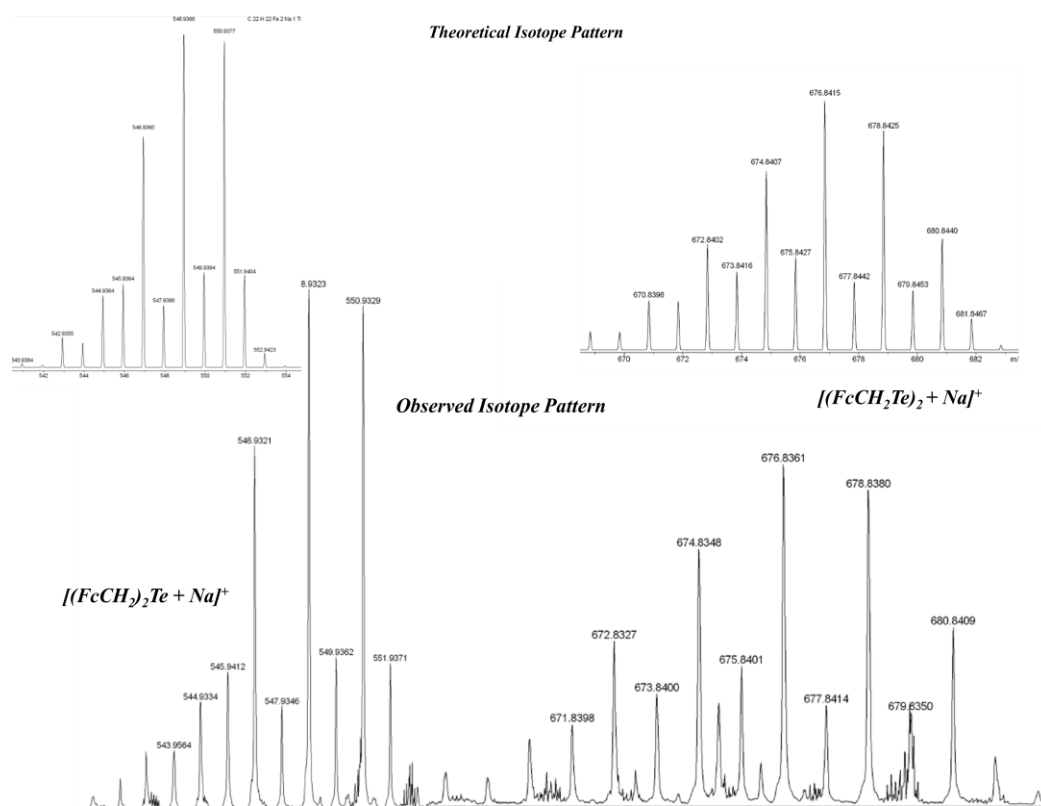
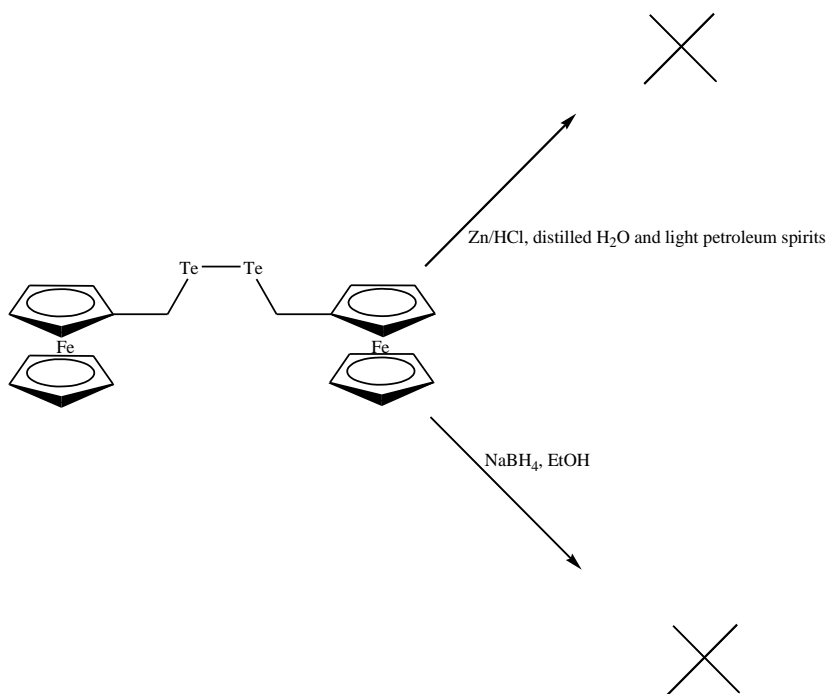


Figure 4-46: Partial ESI-MS showing the observed and theoretical [M + Na]⁺ ions of **82** and **88**

Due to the extreme instability of **82** i.e. the spontaneous decomposition under room light, microanalytical and X-ray crystallographic structural data for **82** could not be obtained. The compound spontaneously decomposed into the corresponding telluride and elemental Te upon handling.

4.2.3.7 Attempted Synthesis of FcCH₂TeH (80)

Organotellurium compounds derived from RTeH are known⁷². However, the intermediate species, RTeH, has not been isolated⁷². Alkyl tellurols are usually generated *in situ* by reduction of the corresponding ditellurides, RTeTeR, most commonly with NaBH₄ in EtOH. Attempts were, therefore, made to prepare the corresponding tellurol **80** by reaction of **82** with NaBH₄, with reference to the literature method¹⁵⁴ for the synthesis of PhCH₂TeH never isolated from (PhCH₂Te)₂ with NaBH₄, or using Zn/HCl analogously to the corresponding selenol **72**. The determination of the formation of the desired compound was made by the presence of the tellurol proton signal which should appear at δ -5 - -2 ppm¹⁵³ in ¹H NMR spectrum or Te-H band at ~2000 cm⁻¹¹⁵³ in IR spectrum. The attempted syntheses are summarised in Scheme 4-6.



Scheme 4-6: Attempted synthesis of **80** via **82**

4.2.3.8 Attempted Synthesis of FcCH₂TeH (**80**) by Reduction of (FcCH₂Te)₂ (**82**) with Zn/HCl

Stirring a mixture of **82** and Zn powder in dry Et₂O with aqueous HCl added at room temperature for 3 h provided a mixture of a yellow and red solid. Neither GC-MS, ¹H NMR nor IR spectroscopy on the mixture suggested the formation of the desired compound. Further investigations were, therefore, not carried out.

4.2.3.9 Attempted Synthesis of FcCH₂TeH (**80**) by Reduction of (FcCH₂Te)₂ (**82**) with NaBH₄

Reduction of **82** with NaBH₄ to give **80** was not successful either. A mixture of **82** and NaBH₄ in absolute EtOH was stirred at room temperature for 3 hours under an N₂ atmosphere. Neither did GC- and ESI-MS on the reaction mixture nor also GC- and ESI-MS, NMR and IR spectroscopy on the yellow oil obtained after the work-up suggested the formation of **80**.

4.3 Conclusion

Ferrocenyl-methyl and -butyl selenols **72** and **74** could be prepared by the reactions of the corresponding selenocyanates, Fc(CH₂)_nSeCN (n = 1 **67** or 4 **68**), with NaBH₄ or the corresponding diselenide, {Fc(CH₂)_nSe}₂ (n = 1 **69** or 4 **75**), with Zn/HCl or NaBH₄. The selenols could be characterised by NMR and IR spectroscopy and GC- and/or ESI-MS. The selenols were both air-sensitive and oxidised in air. The ⁷⁷Se NMR study on the effect of ferrocene on the oxidative stability of **78** in solution also showed that, unlike the corresponding ³¹P NMR study on PhPH₂ in Chapter 2, simple addition of ferrocene did not stabilise **78** in solution or rather accelerated the oxidation.

Attempts to prepare **80** analogously to the corresponding selenol **72** were unsuccessful. The attempted synthesis of the corresponding tellurocyanate **81** by

reaction of the corresponding halides **71**, **17** or **6** with **86** according to the literature method for the synthesis of $\text{PhH}_2\text{TeCN}^{162}$ was unsuccessful. The corresponding ditelluride **82** could, however, be synthesised by reaction of **40** with elemental Te. The subsequent reduction of **82** with NaBH_4 or Zn/HCl did not, however, give the desired tellurol **80**. The spectroscopic data did not suggest the formation of the desired compound. Even if the tellurol had been formed, it were probably too reactive to isolate under ambient conditions. The formation of the tellurol may be proved by derivatisation *in situ* as organotellurols are used as intermediate in many organic syntheses.

Therefore, it may be concluded that organo-selenols including **72**, **74** and **78** and -tellurol **80** cannot be stabilised by simply addition of ferrocene in solution or incorporation at their hydride centres. It may, therefore, also be concluded that heavier Group 16 element hydrides cannot be stabilised by incorporation of a $\text{Fc}(\text{CH}_2)_n$ group into the hydride centre or simple addition of ferrocene into the solution. For heavier Group 16 element hydrides, thermodynamic factors i.e. thermodynamically unstable due to weak element-hydrogen bond for heavier elements of the group, may be more important in the stability of the compounds.

Even though only a limited number of Group 16 element hydrides were prepared, the reaction precursors including $\text{Fc}(\text{CH}_2)_n\text{SeCN}$ ($n = 1$ **67** or 4 **68**), $\{\text{Fc}(\text{CH}_2)_n\text{Se}\}_2$ ($n = 1$ **69** or 4 **75**), $\{\text{Fc}(\text{CH}_2)_n\}_2\text{Se}$ ($n = 1$ **70** or 4 **77**) and **82** were also new and their synthetic routes may be useful for future studies.

4.4 Experimental

4.4.1 Synthesis of Ferrocenylalkyl Selenols, $[\text{Fe}(\eta\text{-C}_5\text{H}_5)\{\eta\text{-C}_5\text{H}_4(\text{CH}_2)_n\text{SeH}]$ ($n = 1$ (**72**) or 4 (**74**))

4.4.1.1 Synthesis of (FcCH₂Se)₂ (**69**) from FcCH₂Li (**40**) with Elemental Se

Under an Ar atmosphere, a solution of **40** generated from the reaction of FcCH₂OMe **47** (0.61 g, 2.65 mmol) with freshly cut, small pieces of Li metal (excess) in dry THF (5 mL), stirring at 0 °C for 30 mins, was filtered with a #4 frit into another Schlenk flask containing Se powder (0.95 g, 12.04 mmol). The mixture was stirred at room temperature for 1 h. The solvent was removed under reduced pressure. The residue was extracted with dry CH₂Cl₂ (30 mL × 2). The combined organic extract was subjected to column chromatography on silica-gel (60 – 80 mesh size), packed with dry hexane, eluted with dry hexane. Removal of the solvent from the eluent collected under reduced pressure at 20 °C gave a mixture of an orange solid (major) and a yellow solid and oil (minor) (0.68 g, 46 % (based upon the number of moles of **69**)). ¹H NMR spectroscopy on the mixture in CDCl₃ showed that it was an approximately 1 : 0.2 mixture of **69** and **70**, respectively (determined by comparison of the integrals of the respective CH₂ proton signals).

The mixture was chromatographed on a preparative TLC plate, eluting with a 1 : 1 mixture of dry CH₂Cl₂ and hexane. Three coloured bands were separated; a weak yellow band at R_f 0.92, a strong orange band at R_f 0.85, a broad yellow band at R_f 0.43. After extraction with CH₂Cl₂, removal of the solvent from the fraction at R_f 0.85 yielded a mixture of an orange solid (major) and yellow oil (minor) (0.26 g). ¹H NMR spectroscopy showed that it was an approximately 1 : 0.3 mixture of **69** and **70**, respectively. Removal of the solvent from the fraction at R_f 0.43 gave a red oil (0.11 g). ¹H NMR spectroscopy and ESI-MS both indicated that it was unreacted **47**. The mixture of **69** and **70** obtained from the fraction at R_f 0.85 was further chromatographed on a preparative TLC plate, eluting with a 4 : 9 mixture of CH₂Cl₂ and hexane, respectively. A black solid precipitated out on the plate during the chromatography. Two coloured bands, orange (major) and yellow (minor), were separated. The major orange fraction at the top was collected. After extraction with CH₂Cl₂, removal of the solvent from the fraction gave a mixture of a red solid (major)

and yellow oil (minor) (0.19 g). ^1H NMR spectroscopy showed that it was an approximately 1 : 0.5 mixture of **69** and **70**, respectively.

Recrystallisation of the 1 : 0.5 mixture of **69** and **70** from CH_2Cl_2 with hexane added at $-18\text{ }^\circ\text{C}$ gave an orange solid. ^1H NMR spectroscopy indicated that it was an approximately 1 : 0.04 mixture of **69** and **70**, respectively (the purest sample of **69** could ever be obtained even though satisfactory microanalytical data could not be obtained: Calcd. for $\text{C}_{22}\text{H}_{22}\text{Fe}_2\text{Se}_2$: C 47.52; H 3.99 %; Found: C 33.83; H 2.89 %). After removing and washing the orange solid with cold hexane (1 mL \times 2) at $0\text{ }^\circ\text{C}$, the combined filtrate was concentrated. Cooling the solution again at $-18\text{ }^\circ\text{C}$ afforded a yellow solid which was identified by ^1H NMR spectroscopy as the purest sample of **70** which could ever be obtained although satisfactory microanalytical data could not be obtained: Calcd. for $\text{C}_{22}\text{H}_{22}\text{Fe}_2\text{Se}_1$: C 55.39; H 4.65 %; Found: C 50.38; H 4.40 %.

69: ^{77}Se NMR: δ 391.5 (t, $^2J_{\text{SeH}} = 13\text{ Hz}$) ppm. ^1H NMR: δ 3.8 (FcCH $\underline{2}$, t, $^4J_{\text{HH}} = 6\text{ Hz}$, 4 H), 4.13 (C $\underline{5}$ H $\underline{5}$, s, 10 H), 4.16 (H $\underline{3}$, t, $^3J_{\text{HH}} = 2\text{ Hz}$, 4 H), 4.22 (H $\underline{2}$, t, $^3J_{\text{HH}} = 2\text{ Hz}$, 4 H) ppm. ^{13}C - $\{^1\text{H}\}$ NMR: δ 29.4 (FcCH $\underline{2}$, s, CH $_2$), 68.3 (C $\underline{3}$, s, CH), 68.7 (C $\underline{2}$, s, CH), 68.8 (C $\underline{4}$, s, CH), 85.7 (C $\underline{1}$, s) ppm. ESI-MS (MeOH, +ve, at 100 V): m/z observed 557.877 [M] $^+$; calcd. 557.874 for $\text{C}_{22}\text{H}_{22}\text{Fe}_2\text{Se}_2$; observed 580.867 [$M + \text{Na}$] $^+$; calcd. 580.864 for $\text{C}_{22}\text{H}_{22}\text{Fe}_2\text{Na}_1\text{Se}_2$; observed 596.849 [$M + \text{K}$] $^+$; calcd. 596.838 for $\text{C}_{22}\text{H}_{22}\text{Fe}_2\text{K}_1\text{Se}_2$. **70**: ^{77}Se NMR: δ 332.7 (t, $^2J_{\text{SeH}} = 11\text{ Hz}$) ppm. ^1H NMR: δ 3.6 (FcCH $\underline{2}$, t, $^4J_{\text{HH}} = 6\text{ Hz}$, 4 H), 4.12 (H $\underline{3}$ & H $\underline{4}$, unresolved m, 14 H), 4.16 (H $\underline{2}$, t, $^3J_{\text{HH}} = 2\text{ Hz}$, 4 H) ppm. ^{13}C - $\{^1\text{H}\}$ NMR: δ 23.4 (FcCH $\underline{2}$, s, CH $_2$), 68.3 (C $\underline{3}$, s, CH), 68.7 (C $\underline{2}$, s, CH), 68.8 (C $\underline{4}$, s, CH), 86.3 (C $\underline{1}$, s) ppm. GC-MS: m/z 56(6) [Fe] $^+$, 121(30) [CpFe] $^+$, 199(100) [FcCH_2] $^+$, 478(10) [M] $^+$. ESI-MS (MeOH, +ve, at 100 V): m/z observed 477.960 [M] $^+$; calcd. 477.958 for $\text{C}_{22}\text{H}_{22}\text{Fe}_2\text{Se}_1$; observed 500.950 [$M + \text{Na}$] $^+$; calcd. 500.947 for $\text{C}_{22}\text{H}_{22}\text{Fe}_2\text{Na}_1\text{Se}_1$; observed 516.925 [$M + \text{K}$] $^+$; calcd. 516.921 for $\text{C}_{22}\text{H}_{22}\text{Fe}_2\text{K}_1\text{Se}_1$. **76** (only observed by ESI-MS on the mixture of **69** and **70**): ESI-MS (MeOH, +ve, at 100 V): m/z observed 637.794 [M] $^+$; calcd. 637.791 for $\text{C}_{22}\text{H}_{22}\text{Fe}_2\text{Se}_3$; observed 660.786 [$M + \text{Na}$] $^+$; calcd. 660.780 for $\text{C}_{22}\text{H}_{22}\text{Fe}_2\text{Na}_1\text{Se}_3$; observed 676.759 [$M + \text{K}$] $^+$; calcd. 676.754 for $\text{C}_{22}\text{H}_{22}\text{Fe}_2\text{K}_1\text{Se}_3$.

4.4.1.2 Synthesis of FcCH₂SeCN (67)

Excess KSeCN was added to a solution of **6** (3.00 g, 7.79 mmol) in distilled H₂O (30 mL). The mixture was heating to reflux for 3.5 h. After cooling, aq. HCl (2 M, 7.00 mL) was slowly added. A yellow solid immediately precipitated out. The aqueous phase was extracted with Et₂O (80 mL & 20 mL) which also led to the precipitation of a red solid. The combined organic extract was washed with distilled H₂O (20 mL × 3) and dried over MgSO₄. After filtering, removal of the solvent from the organic phase under reduced pressure gave the title compound as a red solid (0.44 g, 18 %). Recrystallisation of the red solid from Et₂O/*n*-pentane at –18 °C afforded a mixture of a red solid and a few red single crystals. The X-ray crystallographic structural data for the title compound were obtained on the red single crystal. Despite the attempts, satisfactory microanalytical data on the mixture could not be obtained. Calcd. for C₁₂H₁₁Fe₁Se₁N₁: C 47.38; H 3.65; N 4.61 %. Found: C 51.63; H 4.25; N 3.41 %. IR: ν 2140m (C≡N str.) cm⁻¹. ¹H NMR: δ 4.19 (C₅H₅, s, 5 H), 4.23 (FcCH₂, s, 2 H), 4.25 (H₃, t, ³J_{HH} = 2 Hz, 2 H), 4.30 (H₂, t, ³J_{HH} = 2 Hz, 2 H) ppm. ¹³C-¹H NMR: δ 30.8 (CpCH₂, s), 68.9 (CH, s), 69.0 (CH, s), 69.4 (CH, s), 82.1 (C, s), 102.8 (SeC≡N, s) ppm.

4.4.1.3 Synthesis of FcCH₂SeH (72) by Reaction of (FcCH₂Se)₂ (69) with Zn/HCl

Concentrated HCl (36 %, 5 mL) was added dropwise to a solution of **69** (0.01 g, 0.02 mmol) in a two-phase solvent system consisting of Et₂O (20 mL) and distilled H₂O (8 mL) with suspension of Zn powder (1.00 g, 15.29 mmol). Effervescence was observed. The mixture was stirred at room temperature until the vigorous reaction had subsided (approximately 2 h). The aqueous phase was removed *via* a syringe and the solvent from the organic phase was removed under reduced pressure (washing the organic phase with distilled H₂O would result in oxidation of the title compound to the corresponding diselenide regardless of using deoxygenated distilled H₂O). ¹H NMR spectroscopy on the residue consisting of a mixture of a yellow solid (major) and oil (minor) in deoxygenated CDCl₃ in a sealed NMR tube showed that it was an

approximately 1 : 8 : 7 mixture of **72**, **69** and **70**, respectively (determined based upon the comparison of the integrals of the respective CH₂ proton signal). Despite the attempts, IR and ESI-MS data could not be obtained. A single crystal could not be grown either. ⁷⁷Se NMR: δ 80.5 (d of m, ¹J_{SeH} = 41 Hz) ppm. ¹H NMR: δ -0.06 (SeH, t, ³J_{HH} = 6 Hz, 1H), 3.6 (FcCH₂, d, ³J_{HH} = 6 Hz, 2 H), 4.18 (H₃, t, ³J_{HH} = 2 Hz, 2H), 4.14 (H₄, s, 5 H), 4.22 (H₂, t, ³J_{HH} = 2 Hz, 2 H) ppm. GC-MS: (*M* = **72**): 56(8) [Fe]⁺, 121(50) [CpFe]⁺, 199(100) [FcCH₂]⁺, 278(8) [*M*]⁺.

4.4.1.4 Attempted Synthesis of (FcCH₂Se)₂ (**69**) by Reaction of [FcCH₂NMe₃]I (**6**) with Na₂Se₂

A solution of NaBH₄ (0.60 g, 15.86 mmol) in distilled H₂O (0.75 mL) was added to a suspension of Se powder (0.43 g, 5.45 mmol) in distilled H₂O (10 mL). The mixture was stirred at room temperature until the initial vigorous reaction had subsided (approximately 15 mins). Another portion of Se powder (0.91 g, 11.52 mmol) was added. The mixture was stirred at room temperature for 15 mins and then at 80 °C for 2 mins. After cooling, **6** (4.80 g, 12.47 mmol) was added. The mixture was warmed to 60 °C, stirred at that temperature for 72 h and then allowed to stand overnight. The yellow solid was filtered, washed thoroughly with distilled H₂O (50 mL × 5) and dried under reduced pressure at 40 °C. The solid was extracted with CH₂Cl₂ (100 mL) and the insoluble materials were filtered. Removal of the solvent from the organic phase under reduced pressure gave a yellow solid. ¹H and ¹³C-{¹H} NMR spectroscopy and ESI-MS showed that it was unreacted **6** (3.53 g, 74 % recovery yield). ESI-MS (MeOH, +ve, *M* = **6**): *m/z* 258.065 [*M* - I]⁺; 643.063 [2*M* - I]⁺.

4.4.1.5 Attempted Synthesis of (FcCH₂Se)₂ (**69**) by Reaction of FcCH₂Cl (**71**) with Na₂Se₂

A half of a NaBH₄ solution (0.46 g, 12.16 mmol) in distilled H₂O (20 mL) was added, with rapid stirring, into a Schlenk flask containing Se powder (0.96 g, 12.16 mmol). The solution turned nearly colourless. After the initial vigorous reaction had subsided, the rest of the NaBH₄ solution was added, giving a red solution. The mixture was

stirred at room temperature for 15 mins and at 40 °C for 2 mins. After cooling, **71** prepared from **73** (1.75 g, 8.08 mmol) and oxalyl chloride (3.00 mL, 34.38 mmol) in dry CH₂Cl₂ (20 mL) (the CH₂Cl₂ and excess oxalyl chloride had been removed before the addition), was added. The reaction mixture was stirred at room temperature for 17.5 h. The yellow solid was filtered, washed with distilled H₂O (10 mL) and then extracted with Et₂O (20 mL × 2). Removal of the solvent from the extract under reduced pressure gave a yellow oil (0.15 g) which was identified by ¹H NMR spectroscopy as an approximately 1 : 2 mixture of **69** and **70**, respectively.

4.4.1.6 Attempted Synthesis of FcCH₂SeH (**72**) from Reaction of FcCH₂Cl (**71**) with NaSeH

While cooling in an ice bath, absolute EtOH (10 mL) was added into a Schlenk flask containing a mixture of Se powder (0.29 g, 3.67 mmol) and NaBH₄ (0.16 g, 4.23 mmol). The mixture was stirred until the solution became nearly colourless. **71** (0.70 g, 2.99 mmol) was added and the ice bath was removed. The reaction mixture was stirred at room temperature for 18.5 h and then allowed to stand for 2 h. The mixture was made acidic by adding a solution of conc. HCl (36 %, 0.05 mL) in distilled H₂O (10 mL). The solution was stirred for 2 h before being extracted with CHCl₃ (30 mL). After filtering the insoluble materials, removal of the solvent from the organic phase under reduced pressure gave a yellow solid (0.47 g). ¹H NMR spectroscopy on the yellow solid showed that it was an approximately 2.5: 1 mixture of **69** and **70**, respectively (determined by comparison of the integrals of the respective CH₂ proton signal).

4.4.1.7 Synthesis of FcCH₂SeH (**72**) by Reaction of (FcCH₂Se)₂ (**69**) with NaBH₄

NaBH₄ (0.16 g, 4.23 mmol) was added to a solution of **69** (0.15 g, 0.27 mmol) in absolute EtOH (10 mL) at 0 °C and the reaction mixture was stirred for 2 mins. After removing the ice bath, the mixture was stirred for 2 mins. Removal of the solvent

under reduced pressure gave a yellow solid. GC-MS was immediately carried out and showed a trace amount of **72**.

4.4.1.8 Synthesis of FcCH₂SeH (**72**) by Reaction of FcCH₂SeCN (**67**) with NaBH₄

First Attempt: NaBH₄ (0.20 g, 5.29 mmol) was added to a solution of **67** (0.07 g, 0.23 mmol) in absolute EtOH (10 mL). The mixture was stirred at room temperature for around 30 s at which a sudden colour change of the reaction mixture to yellow from red was observed. After adding extra NaBH₄ (0.20 g, 5.29 mmol), the mixture was stirred for further 2 mins and then hydrolysed with distilled H₂O (10 mL). A yellow solid immediately precipitated out. The yellow precipitate was extracted with Et₂O (20 mL) and the aqueous phase was re-extracted with Et₂O (20 mL). The combined organic phase was washed with distilled H₂O (10 mL × 3) and dried over MgSO₄. After filtering, removal of the solvent from the organic phase under reduced pressure gave a yellow solid (0.06 g, 50 %). ¹H NMR spectroscopy showed that it was almost pure **69**.

Second Attempt: NaBH₄ (0.05 g, 1.32 mmol) was added to a solution of **67** (0.05 g, 0.16 mmol) in EtOH (10 mL) at 0 °C. The mixture was stirred for 5 mins, then brought to room temperature and stirred for further 2 mins in which time the mixture suddenly turned yellow from red. The mixture was hydrolysed with distilled H₂O (2 mL) and the aqueous phase was removed with a syringe. Removal of the solvent from the organic phase under reduced pressure gave a mixture of a yellow and white solid (excess NaBH₄) (0.10 g). The ¹H NMR analysis on the mixture indicated that it was a mixture of **69** (major) and **72** (trace). Despite the attempts, the *ν* Se-H stretch could not be observed in the IR spectrum probably due to the insufficient amount of **72**. The mixture was extracted with Et₂O (20 mL), washed with distilled H₂O (10 mL × 3) and dried over MgSO₄. After filtering, removal of the solvent under reduced pressure gave a yellow solid. ¹H NMR spectroscopy on the yellow solid showed no signals corresponding to **72** but those corresponding to **69**.

4.4.1.9 Synthesis of Fc(CH₂)₄SeCN (68)

A solution of Fc(CH₂)₄Br **17** (1.32 g, 4.11 mmol) in dry DMF (10 mL) was added to a solution of KSeCN (0.59 g, 4.10 mmol) in dry DMF (30 mL). The mixture was stirred partially immersed in an oil bath maintained at 20 °C for 17.5 h. The mixture was hydrolysed with distilled H₂O (10 mL) and extracted with Et₂O (20 mL × 2). The combined organic extract was washed with distilled H₂O (10 mL × 3) and dried over Na₂SO₄. After filtering, the solvent was removed under reduced pressure, giving a yellow oil. Recrystallisation of the yellow oil from Et₂O/*n*-pentane at -18 °C gave a pure title compound as a yellow solid (1.12 g, 78 %). Calcd. for C₁₅H₁₇FeNSe: C 52.03; H 4.95; N 4.05 %; Found: C 52.09; H 5.07; N 3.94%. IR: ν 2150 cm⁻¹ (C≡N str.) ⁷⁷Se-¹H NMR: δ 158.8 (SeCN, s) ppm. ¹H NMR: δ 1.7 (FcCH₂CH₂, m, 2 H), 1.9 (CH₂CH₂SeCN, m, 2 H), 2.4 (FcCH₂, t, ³J_{HH} = 8 Hz, 2 H), 3.1 (CH₂SeCN, t, ³J_{HH} = 7 Hz, 2 H), 4.06 (C₅H₄, s, 4 H), 4.10 (C₅H₅, s, 5 H) ppm. ¹³C-¹H NMR: δ 29.0 (FcCH₂, s, CH₂), 29.5 (CH₂Se, s), 30.66 (CH₂CH₂Se, s), 30.69 (FcCH₂CH₂, s, CH₂), 67.4 (C₃, s, CH), 68.2 (C₂, s, CH), 68.6 (C₅H₅, s, CH), 88.2 (C₁, s), 101.5 (SeCN, s, C) ppm. ESI-MS (MeOH, +ve, at 100 V): *m/z* observed 346.988 [M]⁺; calcd. 346.987 for C₁₅H₁₇Fe₁N₁Se₁; observed 369.978 [M + Na]⁺; calcd. 369.976 for C₁₅H₁₇Fe₁N₁Na₁Se₁. GC-MS: *m/z* 56(50) [Fe]⁺, 121(100) [CpFe]⁺, 199(85) [FcCH₂]⁺, 347(80) [M]⁺.

4.4.1.10 Synthesis of Fc(CH₂)₄SeH (74) by Reaction of Fc(CH₂)₄SeCN (68) with NaBH₄

NaBH₄ (0.05 g, 1.32 mmol) was added in one portion to a solution of **68** (0.16 g, 0.48 mmol) in absolute EtOH (10 mL). The mixture was stirred at 20 °C for 15 mins. After hydrolysing with distilled H₂O (15 mL), the aqueous phase was extracted with petroleum spirits (20 mL × 2). The combined organic phase was washed with distilled H₂O (20 mL × 2), dried over Na₂SO₄ and then filtered. Removal of the solvent from the organic phase under reduced pressure gave an orange oil (0.14 g, 46 % (based on the number of moles of **75**). ¹H NMR spectroscopy showed that it was an approximately 1 : 1 mixture of **75** and **74** (determined by comparison of the integrals

of the respective CH₂ proton signal adjacent to the selenium). After 18 h at 300 K in a capped NMR tube in air, the selenol proton signal completely disappeared. Attempts to grow a single crystal of either compound from dry CH₂Cl₂ with hexane added at -18 °C were unsuccessful. No precipitate could be obtained.

74: ESI-MS (MeOH, +ve, at 100 V): *m/z* observed 321.991 [*M*]⁺; calcd. 321.991 for C₁₄H₁₈Fe₁Se₁. ⁷⁷Se NMR: δ -13.7 (SeH, d of m, ¹*J*_{SeH} = 44, ²*J*_{SeH} = 6 Hz) ppm. ¹H NMR: δ -0.7 (SeH, t, ³*J*_{HH} = 7 Hz, 1 H), 1.6 (FcCH₂CH₂, m, 2 H), 1.7 (CH₂CH₂Se, m, 2 H), 2.4 (FcCH₂, t, ³*J*_{HH} = 8 Hz, 2 H), 2.6 (CH₂Se, m, ³*J*_{HH} = 7 Hz, 2 H), 4.05 (C₅H₄, m, ³*J*_{HH} = 2 Hz, 4 H), 4.10 (C₅H₅, s, 5 H) ppm. ¹³C-{¹H} NMR: δ 17.6 (CH₂Se, s, CH₂), 29.0 (FcCH₂, s, CH₂), 31.0 (FcCH₂CH₂, s, CH₂), 33.9 (CH₂CH₂Se, s, CH₂), 67.1 (C₃, s, CH), 68.1 (C₂, s, CH), 68.5 (C₄, s, CH), 89.0 (C₁, s, C) ppm. **77:** ESI-MS (MeOH, +ve, at 100 V): *m/z* observed 562.050 [*M*]⁺; calcd. 562.052 for C₂₈H₃₄Fe₂Se₁. **75:** IR: 3922m, 3091s, 2928s, 2853s, 1757m, 1707m, 1680m, 1637m, 1472m, 1456m, 1437m, 1410m, 1353w, 1287w, 1225m, 1235m, 1225m, 1199m, 1174w, 1105s, 1039m, 1022m, 1000s, 922m, 817s, 736m, 596w, 485s cm⁻¹. Calcd. for C₂₈H₃₄Fe₂Se₂: C 52.53; H 5.35 %; Found: C 52.93; H 5.63 %. The sample for elemental analysis was sent packed in an ampoule sealed under vacuum as precaution. ESI-MS (MeOH, +ve, at 100 V): *m/z* observed 641.967 [*M*]⁺; calcd. 641.968 for C₂₈H₃₄Fe₂Se₂. ⁷⁷Se NMR: δ 306.1 (Se, m, ²*J*_{SeH} = 8 Hz) ppm. ¹H NMR: δ 1.6 (FcCH₂CH₂, m, 4 H), 1.8 (CH₂CH₂Se, m, 4 H), 2.4 (FcCH₂, t, ³*J*_{HH} = 8 Hz, 4 H), 2.9 (CH₂Se, t, ³*J*_{HH} = 7 Hz, 4 H), 4.05 (C₅H₄, m, 8 H), 4.10 (C₅H₅, s, 10 H) ppm. ¹³C-{¹H} NMR: δ 29.1 (FcCH₂, s, CH₂), 30.0 (CH₂Se, s, CH₂), 30.8 (CH₂CH₂Se, s, CH₂), 30.9 (FcCH₂CH₂, s, CH₂), 67.1 (C₃, s, CH), 68.1 (C₂, s, CH), 68.5 (C₄, s, CH), 88.9 (C₁, s, C) ppm.

4.4.1.11 ⁷⁷Se NMR Study on Effect of Ferrocene on Oxidative Stability of PhSeH (78) in Solution

Two clean and dry NMR tubes were placed in a Schlenk flask under an N₂ atmosphere. Ferrocene (0.07 g, 0.38 mmol) was added into one of the tubes and deoxygenated dry CDCl₃ (1 mL) and the selenol **78** (90 %, 0.01 mL, 0.08 mmol) were added to both tubes. After sealing the tubes with plastic NMR lids, they were

removed from the inert atmosphere into air. The air oxidation of **78** in the samples was monitored by $^{77}\text{Se}\{-^1\text{H}\}$ NMR spectroscopy at intervals until completed. During the intervals, the samples were kept on a rack placed in a fumehood at room temperature in air with their lids on. Additional NMR solvents were occasionally added due to the loss by slow evaporation. The additions were carried out in the same manner as for the sample preparations i.e. under an N_2 atmosphere using deoxygenated solvent.

4.4.2 Attempted Synthesis of Ferrocenylmethyl Tellurol (**80**)

4.4.2.1 Attempted Synthesis of FcCH_2TeCN (**81**) by Reaction of FcCH_2Cl (**71**) with (**86**)

Compound **86** was generated by stirring a mixture of freshly ground KCN (1.27 g, 19.50 mmol) and Te powder (2.52 g, 19.70 mmol) in dry DMSO (20 mL) at 100 – 120 °C for 4 h. After cooling and then adding extra dry DMSO (30 mL), the resulting pale yellow solution of **86** was added dropwise to a solution of **71** (3.70 g, 15.80 mmol) in dry DMSO (60 mL). The reaction mixture was stirred at room temperature for 16.5 h. While cooling in an ice bath, the mixture was hydrolysed with distilled H_2O (250 mL) and then filtered with a #4 sintered glass in air. The yellow solid was washed with distilled H_2O (10 mL) and then extracted with Et_2O (10 mL). The aqueous phase was re-extracted with Et_2O (50 mL \times 3). The combined organic phase was washed with distilled H_2O (50 mL \times 3) and dried on $\text{MgSO}_4 \cdot 3 \text{H}_2\text{O}$. After filtering, removal of the solvent from the organic phase under reduced pressure gave an orange crystalline solid (0.92 g). The GC-MS analysis indicated that it was a mixture of **73** (major) (m/z 56 [Fe^+], 121 [CpFe^+], 186 [FcH^+], 199 [$\text{M} - \text{OH}^+$], 216 [M^+]), **83** (major) (m/z 56 [Fe^+], 121 [CpFe^+], 225 [M^+]) and **84** (minor) (m/z 56 [Fe^+], 121 [CpFe^+], 186 [FcH^+], 199 [$\text{M} - \text{OH}^+$], 414 [M^+]). IR: ν 2251w ($\text{C}\equiv\text{N str}$) cm^{-1} .

4.4.2.2 Attempted Synthesis of FcCH₂TeCN (**81**) by Reaction of [FcCH₂NMe₃]I (**6**) with (**86**)

First Attempt: A pale yellow dry DMSO solution of **86** (5.00 mL, 3.46 mmol) was added dropwise to a solution of **6** (1.34 g, 3.48 mmol) in dry DMSO (20 mL). The mixture turned dark brown from orange and then back to orange while being stirred at room temperature for a few minutes. The mixture was stirred at room temperature for further 15 mins before being hydrolysed with distilled H₂O (15 mL) which led to an immediate precipitation of a black solid. After filtering the black solid with a #4 sintered glass in air, a clear orange filtrate was obtained. The GC-MS analysis on the filtrate showed that it was a mixture of **73** (minor) (m/z 56 [Fe]⁺, 121 [CpFe]⁺, 186 [FcH]⁺, 199 [M – OH]⁺, 216 [M]⁺) and **83** (major) (m/z 56 [Fe]⁺, 121 [CpFe]⁺, 225 [M]⁺).

Second Attempt: The reaction mixture of **86** and **6** in dry DMSO was stirred at 120 °C for 17.5 h. The solution darkened with time. After cooling, the mixture was hydrolysed with distilled H₂O (15 mL). The resulting black precipitate was filtered with a #4 sintered glass in air and the residue was washed with distilled H₂O (10 mL × 3). The clear orange filtrate was extracted with CH₂Cl₂ (30 mL) and then with hexane (70 mL). Removal of the solvent from the combined organic extract under reduced pressure gave an orange solid (0.32 g). The GC-MS analysis showed that it was again a mixture of **73** (minor) and **83** (major). IR: ν 2247 cm⁻¹ (C≡N str.)

4.4.2.3 Attempted Synthesis of Fc(CH₂)₄TeCN (**87**) by Reaction of Fc(CH₂)₄Br (**17**) with (**86**)

A pale yellow dry DMSO solution of **86** (5.00 mL, 3.46 mmol) was added dropwise to a solution of **17** (0.86 g, 2.68 mmol) in dry DMSO (40 mL) at 40 °C. The mixture immediately turned black upon the addition. The mixture was stirred at 80 °C for 50 mins and then, while cooling in an ice bath, hydrolysed with distilled H₂O (10 mL). The aqueous phase was extracted with dry hexane (15 mL) and then with CH₂Cl₂ (50 mL). The combined organic extract was subjected to chromatography on a silica gel,

eluting with CH₂Cl₂. Removal of the solvent from the eluent under reduced pressure gave a mixture of a red oil (major) and a yellow solid (minor). The GC-MS analysis on the mixture indicated that it was a mixture of **17** (major) and **85** (minor).

4.4.2.4 Synthesis of (FcCH₂Te)₂ (**82**)

Under an Ar atmosphere, a solution of FcCH₂Li **40** prepared from FcCH₂OMe **47** (0.48 g, 2.09 mmol) and freshly cut small pieces of Li metal (excess) in dry THF (20 mL) at 0 °C for 3 h, was filtered *via* a #4 frit into another Schlenk containing Te powder (0.87 g, 6.82 mmol). The mixture was stirred at 0 °C for 1 h in dark. The solvent was removed under vacuum and the residue was extracted with dry CH₂Cl₂ (60 mL). After filtering the insoluble materials with a #4 frit under an Ar atmosphere, removal of the solvent under reduced pressure gave a red solid. The red solid was extracted with dry CH₂Cl₂ and the extract was subjected to column chromatography on silica-gel, eluting with dry CH₂Cl₂ under an Ar atmosphere. Removal of the solvent from the eluent under reduced pressure gave the title compound as a red solid (0.44 g, 32 %).

The red solid was further chromatographed on a preparative TLC plate in air, eluting with CH₂Cl₂. The major orange-red band was collected and extracted with CH₂Cl₂. Removal of the solvent from the extract under reduced pressure gave a red solid. ¹H NMR on the red solid showed that it was still a mixture of **82** and impurities. Recrystallisation of the red solid from dry CH₂Cl₂ at -18 °C in dark gave a red solid. **82**: ¹H NMR: δ 4.11 (H₄, s, 10 H), 4.12 (CH₂, unresolved s, 4 H), 4.13 (H₃, t, ³J_{HH} = 2 Hz, 4 H), 4.18 (H₂, t, ³J_{HH} = 2 Hz, 4 H) ppm. ¹³C-{¹H} NMR: δ 3.5 (CH₂, s, CH₂), 68.2 (C₂, s, CH), 68.6 (C₃, s, CH), 68.9 (C₄, s, CH), 89.2 (C₁, s, C) ppm. ESI-MS (MeOH with a drop of CH₂Cl₂ added, +ve, at 80 V): *m/z* observed 680.840 [*M* + *Na*]⁺; calcd. 680.843 for C₂₂H₂₂Fe₂Na₁Te₂. **88**: ¹H NMR: δ 3.8 (CH₂, s, 10 H), 4.10 (H₄, s, 10 H), 4.13 (H₃, t, ³J_{HH} = 2 Hz, 4 H), 4.18 (H₂, t, ³J_{HH} = 2 Hz, 4 H) ppm. ¹³C-{¹H} NMR: δ 2.5 (CH₂, s, CH₂), 68.3 (C₂, s, CH), 68.5 (C₃, s, CH), 68.9 (C₄, s, CH), 88.4 (C₁, s, C) ppm. ESI-MS (MeOH with a drop of CH₂Cl₂ added, +ve, at 80 V): *m/z*

observed 550.932 [$M + Na$]⁺; calcd. 550.937 for C₂₂H₂₂Fe₂Na₁Te₁; 566.903 [$M + K$]⁺; calcd. 566.911 for C₂₂H₂₂Fe₂K₁Te₁.

4.4.2.5 Attempted Synthesis of FcCH₂TeH (**80**) by Reaction of (FcCH₂Te)₂ (**82**) with Zn/HCl

Aq. HCl (1 M, 5.00 mL) was added dropwise to a solution of **82** (0.36 g, 0.55 mmol) in dry Et₂O (20 mL) with suspension of Zn powder (0.10 g, 1.53 mmol). Little effervescence was observed. The mixture was stirred at room temperature for 3 h. The aqueous phase was removed with a syringe and removal of the solvent from the remaining organic phase under reduced pressure gave a mixture of a yellow and red solid. Neither GC-MS nor ¹H NMR spectroscopy showed the ions and signals corresponding to the title compound.

4.4.2.6 Attempted Synthesis of FcCH₂TeH (**80**) by Reaction of (FcCH₂Te)₂ (**82**) with NaBH₄

NaBH₄ (0.20 g, 5.26 mmol) was added in small portions to a solution of **82** (0.36 g, 0.55 mmol) in absolute EtOH (20 mL). The mixture was stirred at room temperature for 3 h. The GC- and ESI-MS analysis on the mixture did not show the corresponding ions. The solvent was removed under reduced pressure and the residue was extracted with dry CH₂Cl₂ (30 mL). After filtering the insoluble matters with a #3 frit, removal of the solvent under reduced pressure gave a yellow oil. Neither GC-, ESI-MS, NMR nor IR spectroscopy showed the desired ions or signals.

4.4.3 X-Ray Crystallography

X-ray crystallographic structural data were collected by Dr. Tania Groutso at Auckland University in New Zealand.

Table 4-9: Bond lengths (Å) and angles (°) for **67**

Lengths / Å			
Fe(1)-C(21)	2.033(3)	C(21)-Fe(1)-C(12)	125.41(12)
Fe(1)-C(22)	2.033(3)	C(22)-Fe(1)-C(12)	107.96(10)
Fe(1)-C(15)	2.034(2)	C(15)-Fe(1)-C(12)	68.89(8)
Fe(1)-C(11)	2.0353(19)	C(11)-Fe(1)-C(12)	41.27(8)
Fe(1)-C(25)	2.038(2)	C(25)-Fe(1)-C(12)	162.34(11)
Fe(1)-C(14)	2.040(2)	C(14)-Fe(1)-C(12)	68.67(9)
Fe(1)-C(23)	2.042(2)	C(23)-Fe(1)-C(12)	120.97(9)
Fe(1)-C(13)	2.043(2)	C(13)-Fe(1)-C(12)	40.59(8)
Fe(1)-C(12)	2.0439(19)	C(21)-Fe(1)-C(24)	68.00(11)
Fe(1)-C(24)	2.048(2)	C(22)-Fe(1)-C(24)	68.11(11)
Se(1)-C(1)	1.845(2)	C(15)-Fe(1)-C(24)	124.16(9)
Se(1)-C(2)	1.999(2)	C(11)-Fe(1)-C(24)	161.21(9)
N(1)-C(1)	1.146(3)	C(25)-Fe(1)-C(24)	40.28(10)
C(2)-C(11)	1.477(3)	C(14)-Fe(1)-C(24)	107.02(10)
C(11)-C(15)	1.426(3)	C(23)-Fe(1)-C(24)	40.58(10)
C(11)-C(12)	1.438(3)	C(13)-Fe(1)-C(24)	120.78(10)
C(12)-C(13)	1.418(3)	C(12)-Fe(1)-C(24)	156.07(9)
C(13)-C(14)	1.425(3)	C(1)-Se(1)-C(2)	94.82(9)
C(14)-C(15)	1.420(3)	N(1)-C(1)-Se(1)	177.5(2)
C(21)-C(22)	1.413(5)	C(11)-C(2)-Se(1)	112.21(15)
C(21)-C(25)	1.415(5)	C(15)-C(11)-C(12)	107.31(18)
C(22)-C(23)	1.414(4)	C(15)-C(11)-C(2)	127.54(18)
C(23)-C(24)	1.418(3)	C(12)-C(11)-C(2)	125.12(19)
C(24)-C(25)	1.407(4)	C(15)-C(11)-Fe(1)	69.44(11)
Angles / °			
C(21)-Fe(1)-C(22)	40.65(13)	C(12)-C(11)-Fe(1)	69.69(11)
C(21)-Fe(1)-C(15)	121.34(11)	C(2)-C(11)-Fe(1)	124.66(15)
C(22)-Fe(1)-C(15)	156.96(11)	C(13)-C(12)-C(11)	108.06(18)
C(21)-Fe(1)-C(11)	107.78(10)	C(13)-C(12)-Fe(1)	69.67(11)
C(22)-Fe(1)-C(11)	121.49(10)	C(11)-C(12)-Fe(1)	69.04(10)
C(15)-Fe(1)-C(11)	41.02(8)	C(12)-C(13)-C(14)	108.21(19)
C(21)-Fe(1)-C(25)	40.67(13)	C(12)-C(13)-Fe(1)	69.74(12)
C(22)-Fe(1)-C(25)	68.37(13)	C(14)-C(13)-Fe(1)	69.44(12)
C(15)-Fe(1)-C(25)	107.32(10)	C(15)-C(14)-C(13)	107.96(19)
C(11)-Fe(1)-C(25)	124.67(9)	C(15)-C(14)-Fe(1)	69.38(13)
C(21)-Fe(1)-C(14)	156.23(13)	C(13)-C(14)-Fe(1)	69.69(13)
C(22)-Fe(1)-C(14)	161.18(11)	C(14)-C(15)-C(11)	108.45(18)
C(15)-Fe(1)-C(14)	40.80(9)	C(14)-C(15)-Fe(1)	69.82(12)
C(11)-Fe(1)-C(14)	69.03(9)	C(11)-C(15)-Fe(1)	69.54(11)
C(25)-Fe(1)-C(14)	120.49(12)	C(22)-C(21)-C(25)	108.0(2)
C(21)-Fe(1)-C(23)	68.34(11)	C(22)-C(21)-Fe(1)	69.69(15)
C(22)-Fe(1)-C(23)	40.61(10)	C(25)-C(21)-Fe(1)	69.85(16)
C(15)-Fe(1)-C(23)	160.83(10)	C(21)-C(22)-C(23)	108.1(3)
C(11)-Fe(1)-C(23)	156.75(9)	C(21)-C(22)-Fe(1)	69.66(16)
C(25)-Fe(1)-C(23)	68.30(10)	C(23)-C(22)-Fe(1)	70.01(14)
C(14)-Fe(1)-C(23)	123.98(9)	C(22)-C(23)-C(24)	107.6(2)
C(21)-Fe(1)-C(13)	161.89(13)	C(22)-C(23)-Fe(1)	69.38(13)
C(22)-Fe(1)-C(13)	124.65(11)	C(24)-C(23)-Fe(1)	69.93(13)
C(15)-Fe(1)-C(13)	68.73(9)	C(25)-C(24)-C(23)	108.3(2)
C(11)-Fe(1)-C(13)	69.03(8)	C(25)-C(24)-Fe(1)	69.49(13)
C(25)-Fe(1)-C(13)	155.73(12)	C(23)-C(24)-Fe(1)	69.48(12)
C(14)-Fe(1)-C(13)	40.87(8)	C(24)-C(25)-C(21)	107.9(3)
C(23)-Fe(1)-C(13)	107.15(9)	C(24)-C(25)-Fe(1)	70.24(13)
		C(21)-C(25)-Fe(1)	69.48(15)

Chapter 5: Overall Conclusion

Ferrocenylalkyl groups were very effective at stabilising primary phosphanes i.e. $\text{Fc}(\text{CH}_2)_n\text{PH}_2$ ($n = 1, 2, 4, 6$ or 11) for a considerably long period of time i.e. 3 – 10 months. The ease of handling was greatly improved. They could be purified and handled in air using non-deoxygenated solvent without causing significant oxidation. The crystallinity of the compound could, however, not be improved for those with extended alkyl spacers i.e. $n > 4$. They were isolated as oils.

Secondary phosphanes with a ferrocenylmethyl moiety i.e. FcCH_2 had appropriate stability in air. They could be purified in air using non-deoxygenated solvent and handled without causing significant oxidation. For long-term stability, the most stable ones were those with an electron-releasing substituent on the phosphorus atom i.e. CH_3 and C_6H_{11} . The least air-stable was the one with an electron-withdrawing substituent i.e. $\text{CH}_2(\text{C}_6\text{H}_4)\text{NO}_2$ bonded to the phosphorus atom.

Tertiary phosphanes could be isolated as by-products from the syntheses of the secondary phosphanes and were less stable than the corresponding secondary phosphanes although they could be purified and handled in air using non-deoxygenated solvent. Therefore, a FcCH_2 moiety was not very effective at stabilising tertiary phosphanes either.

An primary arsane with a FcCH_2 moiety i.e. $\text{FcCH}_2\text{AsH}_2$ was surprisingly air-sensitive, considering that the ethyl analogue i.e. $\text{FcCH}_2\text{CH}_2\text{AsH}_2$ had been reported as completely air stable. Handling of the compound in air during the purification caused significant oxidation and a satisfactory sample for elemental analysis and also for X-ray crystallography could not be obtained. Considering that a $\text{Fc}(\text{CH}_2)_n$ moiety could stabilise a number of primary phosphanes, which supposedly by inhibition of the formation of the corresponding radical cations upon air oxidation, it may suggest that the air oxidation of primary arsanes does not involve the formation of free radical cations. Therefore, in order to stabilise primary arsanes, different stabilisation

strategies may be needed. Or the incorporation of only one CH₂ spacer between the ferrocene and the hydride centre may not be suffice for effective stabilisation of a primary arsane because, with two CH₂ spacers, the arsane seemed air stable. Further studies may, however, be needed.

The ruthenocenyl analogue of primary phosphane i.e. RuCH₂PH₂ could also be prepared and exhibited appreciative air stability under ambient conditions. However, the ruthenocenyl analogue was significantly more air sensitive than the corresponding ferrocenyl counterpart i.e. FeCH₂PH₂ which was stable in air for > 1 year. It completely oxidised in solution in air in about 4 months. Since the ease and readily reversible redox property of ferrocene may be responsible for the stabilisation effect, the air sensitivity of the ruthenocenyl analogue may be accounted by the higher oxidation potential and also the irreversible redox chemistry of the ruthenocenium cation of ruthenocene.

When a small amount of either FeH or FeCH₂PH₂ added to a CDCl₃ solution of air-sensitive primary phosphane, PhPH₂ or CamphylPH₂, their stability towards air oxidation could greatly be improved. While PhPH₂ in solution itself was completely oxidised in 78 days, that with less than a half molar equivalent of either of the compounds added i.e. 0.48 and 0.37 moles of Fe and FeCH₂PH₂, respectively, showed no or little sign of oxidation for nearly at least a half year. Furthermore, after 7 months having been in solution in air, there were still significant amounts of PhPH₂ remained un-oxidised in both solutions. An analogous ³¹P NMR experiment carried out using another air-sensitive primary phosphane i.e. CamphylPH₂ in order to investigate if or not the stabilisation effect would be extended to other air-sensitive primary phosphanes also showed that the simple addition of either FeH or FeCH₂PH₂ was effective at stabilising the primary phosphane as well. While CamphylPH₂ in solution itself was completely oxidised after 6 months under the analogous conditions to the corresponding ³¹P NMR experiments using PhPH₂, the oxidation of CamphylPH₂ in solution with either of the additives added (0.63 and 0.53 moles of Fe and FeCH₂PH₂, respectively, with respect to 1 mole of CamphylPH₂) was

significantly slowed. Ferrocene and FcCH_2PH_2 , therefore, could also stabilise air-sensitive primary phosphanes by simply being added to their solutions.

The oxidation of PhPH_2 could also be inhibited by addition of a small amount of an anti-oxidant i.e. 0.69 and 0.13 moles of nitrosobutane and 2,2-diphenyl-1-picrylhydrazyl free radicals, DPPH, respectively, with respect to 1 mole of PhPH_2 . The ^{31}P NMR experiments showed that, after 3.5 months, while almost half of the PhPH_2 in solution itself had been oxidised, no or little oxidation occurred for the samples with either of the anti-oxidants added. The result was consistent with the free radical cation mechanism of primary phosphane air oxidation suggested by other researchers.

These ^{31}P NMR experiments may suggest that air-sensitive primary phosphanes could also be stabilised by simple addition of either ferrocene, its derivatives such as FcCH_2PH_2 , or an antioxidant to their solutions. Ferrocene and its derivatives have been known to act as anti-oxidant. Therefore, they may be able to inhibit the air-oxidation of primary phosphanes by preventing the formation of free radical cations which is thought to form during the air oxidation of primary phosphanes. This stabilisation strategy may be advantageous over the others because there is no chemical bonding to the hydride centre which may compromise the chemistry of the reactive hydride centres and also no synthesis steps are required. Also, it is very easy to utilise.

Despite the attempts, the ferrocenylmethyl halide, $\text{FcCH}_2\text{SnCl}_2$, and also the corresponding stibane, $\text{FcCH}_2\text{SbH}_2$, could not be prepared. Therefore, the stabilisation effect of a FcCH_2 moiety on primary stibanes could not be investigated.

Ferrocenylethyl silane, $\text{FcCH}_2\text{CH}_2\text{SiH}_3$, could be prepared using a well-established hydrosilation followed by reduction with LiAlH_4 . The silane was stable in solution in air for at least 7 months, which might not be surprising because mono-alkylated silanes are usually stable under ambient conditions i.e. at room temperature in air.

Ferrocenylmethyl germane, $\text{FcCH}_2\text{GeH}_3$, could be prepared analogously to the arsenic analogue, $\text{FcCH}_2\text{AsH}_2$. The germane was reasonably stable in air at room temperature. It could be characterised by IR, ESI- and also GC-MS under ambient conditions. The decomposition of the compound in solution could, however, be observed after 20 hours at 300 K in air (in a NMR machine) by broadening of the corresponding signals in the ^1H NMR spectrum. Also, the deposition of a grey solid during the work-up in air and also upon the storage in the freezer for about 6 weeks suggested that the germane was not so stabilised.

Ferrocenylalkyl stannanes could not be prepared although it might have been because of the extreme instability of the precursors, the corresponding stannic halides. Therefore, the stability of primary stannanes with a FcCH_2 moiety could not be investigated.

Although the desired selenols, FcCH_2SeH and $\text{Fc}(\text{CH}_2)_4\text{SeH}$, could be obtained, their stability in air could not be improved. The former oxidised spontaneously in solution in air i.e. over 5 days but more rapidly during the work-up in air. The latter as the neat state was almost completely oxidised over 10 minutes upon exposure to air or after 3 days in solution with a NMR plastic cap on.

The oxidation of PhSeH could not be inhibited by addition of ferrocene to the solution either. About 5 molar equivalents of ferrocene were added to one of the solutions containing PhSeH . The oxidation of PhSeH in solution with FcH added was in fact more rapid than that without FcH added and the result was contrary to that of the corresponding ^{31}P NMR experiment. While the selenol in solution with Fc added was completely oxidised after 3.5 months, it required about 6.5 months for that without FcH added to be completely oxidised to the corresponding diselenide. The addition of FcH increased the oxidation rate of PhSeH . The result may suggest that the oxidation of PhSeH does not involve the formation of free radical cations and hence the readily reversible redox property of ferrocene is not useful for stabilising selenols against air oxidation.

Ferrocenyl-methyl and -butyl tellurols, FcCH_2TeH and $\text{Fc}(\text{CH}_2)_4\text{TeH}$, could not be obtained analogously to the corresponding selenols. Hence, the stabilisation effect of a $\text{Fc}(\text{CH}_2)_n$ moiety on tellurols could not be investigated.

In conclusion, since the hydrides of the heavier elements of the groups i.e. RAsH_2 , RGeH_3 and RSeH could not be effectively stabilised by incorporation of a $\text{Fc}(\text{CH}_2)_n$ moiety to the hydride centre, it may be concluded that it is only effective at stabilising primary phosphanes, RPH_2 , by prevention of the corresponding free radical cation formation upon air oxidation probably by the ability of the ferrocenium cation of ferrocene to readily undergo reversible redox reactions the reactivity of which can also be increased by the electron-donating substituent such as an alkyl group on the cyclopentadienyl ring and a CH_2 group can also act itself as electron-insulator thereby maybe participating in stabilisation of the phosphane hydride centre. Thermal stability i.e. a weaker element and hydrogen bond in the hydrides of heavier elements may be a more important factor than oxidative stability for the overall stabilisation of hydrides of heavier elements of the groups. Therefore, the hydrides of the heavier element hydrides might not have been able to be stabilised by the anti-oxidant property of ferrocenylalkyl moieties.

Stabilisation by simple addition of FcH or **1** to a solution of air-sensitive primary phosphane may have its advantages in ease of use, no synthetic process required and only a small amount needed to stabilise the hydride. Since ferrocene sublimes easily, it may also be removed easily as well if not needed. Ferrocene is also inert and may not interfere with reactions. On the other hand, incorporation of a FcCH_2 group at the hydride centre may stabilise the phosphane as the neat state i.e. crystal and oil etc. under ambient conditions and does not require a solvent. It may also, therefore, be of interest to determine their reactivity towards reactions in order to see if or not the chemistry of the hydride centre had been compromised by the incorporation. .

Although the hydrides of heavier elements of the groups except for primary phosphanes could not be stabilised by incorporation of a $\text{Fc}(\text{CH}_2)_n$ group at their hydride centres, the synthetic routes to new hydrides of the heavier main group

elements could be established. The hydrides could be prepared and may also be used as reagents in organic syntheses for future studies.

Chapter 6: General Experimental Procedures and Materials

6.1 General Experimental Techniques

Oxygen or moisture-sensitive compounds were handled under an inert atmosphere of dry nitrogen using standard Schlenk line techniques¹⁸⁰. For highly moisture-sensitive compounds, the glassware were dried in an oven at 120 °C overnight and cooled in desiccators containing dry self-indicating silica gel under vacuum prior to use. Unless, otherwise specified, the reactions in the present study were carried out under a stream of an N₂ atmosphere using standard Schlenk line techniques and dry deoxygenated solvents. The work-ups were performed at room temperature in air unless otherwise stated. Dry solvents were obtained from PureSolv (solvent purification system model SP-SD-5) which supplies dry deoxygenated solvents suitable for the moisture and oxygen sensitive chemical reactions just prior to use as required.

The reaction mixtures were heated in a silicone oil bath with a thermostatted heating coil or directly on a magnetic stirrer with a thermostatted heating coil.

Elemental analyses were performed at the University of Otago at the Campbell Microanalytical Laboratory.

6.1.1 Schlenk Line

Schlenk line manipulation was performed following an established Schlenk line procedure¹⁸⁰. The solvents were degassed by inducing boiling at low pressures and introducing dry gaseous dinitrogen several times. The solvents were removed and concentrated by inducing boiling at low pressures and the products were dried at low pressures for appropriate duration of time.

6.1.2 Chromatography

Thin layer chromatography was performed on a 70×15 mm TLC strip cut out from a 200×200 mm TLC aluminium sheet of Merck Kieselgel 60 F₂₅₄ silica gel purchased from Merck and eluted in a beaker containing a solvent mixture of an appropriate ratio.

Preparative thin layer chromatography (TLC) plates were prepared by the established method as follows. Silica gel (140 g, Merck Kieselgel 60 PF₂₅₄) was mixed with distilled water (250 mL) and the mixture was shaken vigorously to make a smooth slurry. The slurry was deposited on a 200×200 mm glass plate to a depth of 1 – 1.5 mm, allowed to air dry overnight and then activated in an oven at 120 °C for at least 24 hours. The plate was removed for atmospheric equilibration at least 18 hours prior to use. A UV lamp employing the wavelengths of 254 and 312 nm was used to view the colourless or pale coloured fractions which were not otherwise visible under a room light.

The samples were dissolved in CH₂Cl₂ or appropriate solvent for the compound to be dissolved and specified in the appropriate section, and applied at the bottom of a TLC plate as a thin line by a glass pipette. The plate was developed in a tank containing a solvent mixture of an appropriate ratio. The desired bands were removed by scraping with a steel knife and the products were extracted with CH₂Cl₂ in a sintered glass (SINTA GLASS 2, 3 or 4), which was dried overnight in an oven at 120 °C and allowed to cool under reduced pressure prior to use, and collected in a round-bottomed flask in air. The solvents were removed under reduced pressure using rotary evaporator or Schlenk line.

Flash chromatography was carried out in air unless, otherwise, stated, on a column packed with a dry silica gel of 60 – 80 mesh size, by introducing the samples in solvent and eluting with appropriate solvent or a solvent mixture of appropriate ratio.

The desired eluent(s) was collected and the solvent was removed under reduced pressure.

6.2 Instrumentation

6.2.1 FTIR Spectroscopy

Fourier Transform Infrared Spectroscopy (FTIR) was performed on a Digilab Scimitar FTS 2000 series spectrometer using Varian Resolution software version 4.1.0.101 or Perkin Elmer Precisely Spectrum 100 FT-IR spectrometer using Spectrum software version 6.3.1.0132. Solid state IR was carried out as a KBr disc prepared by finely grinding sample with a KBr powder dried in an oven at 100 °C and pressured in a device at 8 tons for several minutes. The IR spectra of oil samples were obtained as a thin liquid film between KBr windows.

6.2.2 ESI-Mass Spectrometry

Low resolution electrospray ionisation mass spectrometry (ESI-MS) was performed on a Fisons Instruments VG Platform II mass spectrometer using MassLynx software version 2.0. The samples were run in MeOH as a mobile phase at 60 °C as the source temperature and also cone voltage of 20 V unless, otherwise, specified, in both positive and negative ion modes. The isotope pattern spectra were obtained with a low and high mass resolution (LM and HM resolution) of 13.5 – 15 and a gain of 4000 in the spectral window of m/z 20 within the desired peak. Samples were introduced into the spectrometer *via* a 10 µL sample loop using a Thermo Separation Products SpectraSystem P1000 LC pump at a flow rate of 0.02 mL min⁻¹.

High-resolution mass spectrometry (HR-MS) was carried out on a Bruker Daltonics MicrOTOF spectrometer using DataAnalysis software version 3.3. The capillary exit voltage was varied in order to maximise spectrum quality.

The samples were run in MeOH or in MeCN (especially for moisture sensitive compounds) as a mobile phase and also, as required, with a half or quarter drop of aqueous AgNO₃ (0.1 M, *ca.* 1 mmol mL⁻¹ of sample solution) added to aid ionisation to generate charged silver complexes *in situ*, following the established method⁹⁵ for ESI-MS characterisation of ferrocenyl compounds⁹⁵. A few drops of CH₂Cl₂ (drum grade) was also added when the compounds were not readily soluble in MeOH¹⁸¹. Ion assignments were assisted by comparison of observed and calculated *m/z* values as well isotope distribution patterns¹⁸².

6.2.3 GC-Mass Spectrometry

Gas chromatography mass spectrometry was performed on a Hewlett-Packard 5890 Series 1 gas chromatograph coupled to a Hewlett-Packard 5973 Series Mass Selective Detector, operating at 70 eV, using a HP1 column containing cross-linked methylsilicone gum, 24 m × 0.2 mm × 0.33 μm film thickness. The sample was injected using a HP 7683A Autosampler as a CH₂Cl₂ or MeOH solution and eluted using a 50 – 295 °C temperature ramp, at a rate of 50 °C min⁻¹ from 100 – 150 °C and 10 °C min⁻¹ from 150 – 295 °C with a 2.25 min solvent delay. The samples were freshly prepared prior to analysis either in MeOH or CH₂Cl₂ (drum grade or unless, otherwise stated.).

6.2.4 NMR Spectroscopy

Nuclear magnetic resonance (NMR) was performed on a Bruker Avance DRX 300 or a Bruker Avance DRX 400 spectrometer using Topspin software version 1.3 or a Bruker300AVR or a Bruker400AVR using TopSpin software version 3.0.

The ¹H NMR spectra were obtained on a Bruker Avance DRX 300 or a Bruker Avance DRX 400 spectrometer using Topspin software version 1.3 or a Bruker300AVR or a Bruker400AVR using TopSpin software version 3.0, operating at 300.13 (for Bruker 300 series) or 400.13 (for Bruker 400 series) MHz. The ¹³C-¹H NMR spectra were recorded on a Bruker Avance DRX 300 or a Bruker Avance

DRX 400 spectrometer using Topspin software version 1.3 or a Bruker300AVR or a Bruker400AVR using TopSpin software version 3.0, operating at 75.48 (for the Bruker 300 series) or 100.62 (for the Bruker 400 series) MHz. The chemical shifts were referenced to residual solvent lines and reported in ppm. Solvents were assigned the following chemical shifts values with respect to external tetramethylsilane, Me₄Si: CDCl₃, 7.26 (¹H), 77.06 (¹³C); D₂O, 3.5 (MeOH, ¹H) 49.3 (MeOH, ¹³C).

The ³¹P and ³¹P-¹H NMR spectra were recorded on a Bruker Advance DRX 300 using Topspin software version 1.3, operating at 121.49 MHz or a Bruker300AVR or a Bruker400AVR using TopSpin software version 3.0, operating at 161.97 MHz. The chemical shifts were reported in ppm relative to an external reference of 85 % *orthophosphoric acid* (δ 0.0 ppm). The following values of acquisition delay in seconds (Aq + D₁) were used in the studies on the oxidative stability of primary phosphanes; 2.0 sec. in PhPH₂ with antioxidants added (see 2.2.4.6), PhPH₂ with FcH or **1** added (see 2.2.4.4), and **2** with FcH or **1** added (see 2.2.4.5).

Both ⁷⁷Se and ⁷⁷Se-¹H NMR spectra were recorded on a Bruker300AVR, operating at 57.26 MHz. The chemical shifts were reported relative at **79** (δ 463 ppm)¹⁷⁵. The acquisition delay of 25.2 seconds (Aq + D₁) was used for the study on the oxidation of **78** (see 4.2.2).

Deuterated chloroform (CDCl₃) was used as solvent unless otherwise specified. The CDCl₃ was obtained from Aldrich, of 99.8 atom % D grade and used as received or dried over 4Å molecular sieves (activated at 300 °C for at least 8 hours, cooled in an evacuated desiccator overnight and stored at 120 °C until needed.) for at least 24 h for moisture sensitive compounds. Deoxygenated CDCl₃ was obtained using the standard Schlenk line technique by repeating induction of boiling at low pressures and introduction of dry gaseous N₂ several times, cooling over an ice bath in order to minimise the loss of solvent. Acid samples were dissolved in NaOD-D₂O solution, prepared by reaction of a small amount of Na (~ 1 – 3 mg) with excess D₂O (~ 2 mL).

Oxygen- and moisture-free NMR samples were prepared by dissolving the air- and moisture-sensitive compounds directly in the reaction vessels in which they were obtained after the solvent had been removed, with deoxygenated dry NMR solvent (CDCl_3) and transferring the dissolved samples into clean dry NMR tubes placed in a Schlenk flask under an N_2 atmosphere, *via* a N_2 -filled dry glass syringe. After sealing with plastic NMR lids, the NMR samples were removed under an N_2 atmosphere into air. For the compounds which were highly sensitive to air or moisture, the NMR tubes were sealed permanently under vacuum. After the sample preparations under an N_2 atmosphere as above, the samples were immediately placed under vacuum and frozen in a Dewar containing liquid N_2 . After deoxygenating several times by repeating warming to room temperature under static vacuum and freezing under active vacuum in a liquid N_2 , the tubes were sealed with a flame under active vacuum while frozen.

Two-dimensional NMR experiments were used to unambiguously assign spectra. The 1-D and 2-D NMR experimental data such as COSY, HSQC, HMBC, DEPT, Seltocsy (1-D), HETCOR, were recorded as required. Assignments were also aided by comparison to the literature values if available or to those for analogous compounds.

6.2.5 X-ray Crystallography

For full X-ray crystal structure determinations (XRD), intensity data were collected at the University of Auckland or the University of Canterbury. The X-ray intensity data were collected on a Siemens SMART CCD diffractometer using standard procedures and software. The structures were solved by direct methods, developed and refined on F^2 using the SHELX program¹⁰³ running under the WINGX^{105, 183}.

Preliminary investigations were also carried out by precession photography using nickel-filtered $\text{Cu-K}\alpha$ X-ray radiation which allowed the determination of space group and unit cell dimensions and also an indication of crystal quality as appropriate.

6.3 Chemicals

6.3.1 Reaction Solvents

Unless, otherwise, specified, the solvents used were LR grades or better, obtained from commercial suppliers and used as received unless otherwise stated: MeOH, EtOH, Et₂O, CH₂Cl₂, THF, hexane, pentane, heptane, toluene, EtOAc, CHCl₃, MeCN. Light petroleum spirits refer to the fraction of boiling point range 60 – 80 °C unless otherwise stated. Distilled H₂O refers to singly distilled H₂O. Dry solvents were obtained from Solvent Purification System (SPS).

6.3.2 Commercial Chemicals

The following chemicals were obtained from commercial sources and used as supplied: Ferrocene (Aldrich); 2,2-Diphenyl-1-picrylhydrazyl free radical, DPPH, (Aldrich); [P(CH₂OH)₄]Cl as Retardol C as an 80 % w/w aqueous solution (Albright & Wilson Ltd., Oldbury, UK); CH₃I (May and Baker Ltd., Dagenham, UK); *p*-NO₂(C₆H₄)CH₂Br (BDH); KOH pellets (Ajax. Finechem. Pty Ltd., Auckland, New Zealand); NEt₃ (Aldrich); Na₂S₂O₅ (Ajax Finechem. Pty Ltd., Auckland, New Zealand); Me₂S·BH₄ (2 M solution in THF, Aldrich); DMSO (dried over 4 Å molecular sieve) (Aldrich); (CH₃)₃COK (Aldrich); As₂O₃ (BDH); NaOH (Ajax Finechem. Pty Ltd., Auckland, New Zealand); Zn powder (Ajax Chemicals, Auburn, Australia); 36 % HCl (Ajax Finechem Pty Ltd., Auckland, New Zealand); H₂NC(O)NH₂·H₂O₂ (Aldrich); oxalyl chloride (Aldrich); triphosgene (Aldrich); 30 % H₂O₂ (Ajax Finechem Pty Ltd., Auckland, New Zealand); 85 % *orthophosphoric acid* (Aldrich); D₂O (Aldrich); PhPH₂ *ca.* 10 % weight in hexane (Aldrich); CDCl₃ (Aldrich); KSeCN (Aldrich); DMF (Ajax Finechem. Pty Ltd., Auckland, New Zealand); Se powder (Fluka AG: Buchs SG); MgSO₄ (Ajax Finechem Pty Ltd., Auckland, New Zealand); Na₂SO₄ (Aldrich); NaBH₄ (Aldrich); KCN (Aldrich); Te powder (BDH); silica gel mesh size 60 – 80 (Merck); Li metal (BDH); HSiCl₃ (Aldrich); H₂PtCl₆·xH₂O (BDH); HSi(OMe)₃ (Aldrich); LiAlH₄ (Aldrich);

PhP(O)(OH)H (Aldrich); PhSeH **78** (Aldrich); AsCl₃ (Aldrich); GeCl₄ (Strem Chemicals. Inc. Newburyport, MA, U.S.A.); SnCl₄ (BDH); SnCl₂ (Aldrich); SnI₄ (Aldrich); SbCl₃ (Aldrich); (PhSe)₂ **79** (Aldrich).

6.3.3 Synthesised Compounds

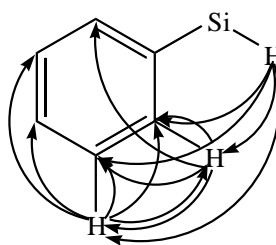
The following compounds were prepared *via* the literature procedures: nitrosobutane¹⁸⁴; (C₆H₁₁)P(CH₂OH)₃⁺Cl⁻ (recrystallised in isopropyl alcohol (IPA)); [FcCH₂NMe₃]I **6**⁹³; FcCH₂P(CH₂OH)₂ **8**⁹²; Fc(CH₂)₄Br **17**⁹⁶; Fc(CH₂)₆Br **18**⁹⁷; Fc(CH₂)₁₁Br **19**⁹⁸; FcCH=CH₂ **53** (purified by column chromatography on silica-gel, eluting with dry hexane)^{139, 185}; PhSiH₃¹⁸⁶; [CpFeC₅H₃(CH₂OH)(CH₂NMe₃)]⁺T⁻ **33**¹⁰¹; FcCH₂PH₂ **1**⁷⁸; [Ru(η⁵-C₅H₅)₂] **25**⁹⁹; [RcCH₂NMe₃]⁺T⁻ **26**¹⁰⁰; camphylPH₂ **2**¹¹⁸; FcCH₂Cl **71**¹⁷³; FcCH₂OH **73**^{93, 187}; FcC(O)CH₃¹⁸⁸; FcCH₂OMe **47**^{168, 189}; FcCH₂Li **40**^{122, 123}; Fc(CH₂)₄CH=CH₂^{140, 144}; FcC≡CH **63** (a gift from Prof. Michael Bruce, University of Adelaide).

Unless otherwise stated, the compounds were stored at -18 °C.

6.3.4 Other Compounds

Although the following compounds were synthesised during the course of this research, they were not used or used only as reference to aid for spectral assignments.

PhSiH₃ (colourless liquid/oil): IR (as a thin film between KBr windows in a IR cell): 3137vw, 3069w, 3054w, 3021w, 2922w, 2852w, 2156s (*Si-H* str), 1954w, 1881w, 1816w, 1703w, 1638w, 1591w, 1554w, 1484w, 1429m, 1384w, 1331w, 1282w, 1165w, 1117m, 1075w, 916vs, 873w, 750w, 698s, 678w, 643s cm⁻¹. ¹H NMR (at 400 MHz, CDCl₃): δ 4.36 (SiH₃, d, ¹J_{SiH} = 5.6 Hz, 3 H), 7.47 (unresolved m, 3 H), 7.71 (unresolved m, 2 H) ppm. ¹³C-{¹H} NMR (100 MHz, CDCl₃): δ 128.16 (C₃, s, CH), 129.85 (C₄, s, CH), 135.89 (C₂, s, CH) ppm.



[Fe(η -C₅H₅){ η -C₅H₄(CH₂)₉CH=CH₂}] 89 (a new compound): Under a N₂ atmosphere, with vigorous stirring, **19** (0.50 g, 1.19 mmol) was added to a deoxygenated solution of (CH₃)₃COK (0.28 g, 2.50 mmol) in dry DMSO (7 mL). The mixture was stirred at 37 °C for 24 h before being extracted with hexane (150 mL). After filtering, the extract was washed thoroughly with distilled H₂O (50 mL \times 5) and the solvent was removed under reduced pressure. Flash chromatography of the residue on silica gel, eluting with hexane followed by removal of the solvent from the eluent under reduced pressure gave the title compound as a yellow oil (135.9 mg, 34 %). Calcd. for C₂₁H₃₀Fe₁: C 74.54; H 8.94; N 0.00 %. Found: C 76.33; H 9.45; N < 0.2 %. IR: 3927w, 3093s, 2925vs, 2853vs, 1821vw, 1754vw, 1681w, 1640s (C=C str.^{140, 190}, 1464s, 1440s, 1412m, 1367w, 1301vw, 1226w, 1106s, 1039m, 1021m, 1000s, 909s, 853w, 816s, 722w, 636w, 484s cm⁻¹. ¹H NMR: δ 0.9 (CH₂, unresolved m, 2 H), 1.4 (CH₂, m, ³J_{HH} = 7 Hz, 4 H), 1.5 (CH₂, m, ³J_{HH} = 7 Hz, 4 H), 2.0 (CH₂, q, ³J_{HH} = 3 Hz, 2 H), 2.3 (CH₂, t, ³J_{HH} = 8 Hz, 2 H), 4.03 (CH, d, ³J_{HH} = 2 Hz, 2 H), 4.05 (CH, d, ³J_{HH} = 2 Hz, 2 H), 4.09 (CH, s, 5 H), 5.0 (CH=CH₂, m, ³J_{HH} = 2 Hz, 2 H), 5.8 (CH=CH₂, m, ³J_{HH} = 5 Hz, 1 H) ppm. ¹³C-{¹H} NMR: δ 29.0 (CH₂, s), 29.2 (CH₂, s), 29.5 (CH₂, m), 31.2 (CH₂, s), 33.9 (CH₂, s), 67.0 (CH, s), 68.1 (CH, s), 68.5 (CH, s), 89.7 (C, s), 114.1 (CH=CH₂, s), 139.3 (CH=CH₂, s) ppm. ESI-MS (MeOH, +ve): *m/z* 338.173 [*M*]⁺ observed; 338.169 calcd. for C₂₁H₃₀Fe₁.

References

1. Wiberg, E.; Amberger, E., *Hydrides of The Elements of Main Groups I-IV*. Elsevier Publishing Company: New York, 1971.
2. Johnson, M. W.; Sándor, E.; Arzi, E., *Acta Crystallographica* **1975**, 8, 1998–2003.
3. Abraham, L., *Marvell and Alchemy*. Aldershot Scolar Press: 1990.
4. Cotton, F. A.; Wilkinson, G.; Murillo, C. A.; Bochmann, M., *Advanced Inorganic Chemistry*. 6 ed.; John Wiley & Sons, Inc. : New York, 1999.
5. Massey, A. G., *Main Group Chemistry*. 2 ed.; John Wiley & Sons, Ltd. : New York, 2000.
6. Berger, A. Organogermanium, -tin, and -silicon hydrides, U.S. Patent. 1968.
7. Hooton, K. A., *Organogermanium compounds, Preparative Inorganic Reactions*. 1968; Vol. 4.
8. Murphy, P. J., *Organophosphorus Reagents A Practical Approach in Chemistry*. Oxford University Press: New York, 2004.
9. Kosolapoff, G. M.; Maier, L., *Organic Phosphorus Compounds*. Wiley-Interscience: New York, 1972; Vol. 1.
10. Xie, J.; Huang, J.-S.; Zhu, N.; Zhou, Z.-Y.; Che, C.-M., *Chemistry: A European Journal* **2005**, 11, 2405.
11. Boeré, R. T.; Masuda, J. D., *Canadian Journal of Chemistry* **2002**, 80, 1607.
12. Doak, G. O.; Freedman, L. D., *Organometallic compounds of arsenic, antimony and bismuth*. Wiley-Interscience: New York, 1970.
13. Breunig, H. J.; Ghesner, M. E.; Lork, E., *Zeitschrift Für Anorganische Und Allgemeine Chemie* **2005**, 631, 851.
14. Wieber, M., *Handbook of Inorganic Chemistry. Sb Organoantimony Compounds, part 2*. Springer: Berlin, 1981.
15. Akiba, K. Y.; Yamamoto, Y., *The Chemistry of Organic Arsenic, Antimony and Bismuth Compounds*. Wiley: Chichester, 1994.
16. Cross, W. I.; Godfrey, S. M.; McAuliffe, C. A.; Mackie, A. G.; Pritchard, R. G., *Chemistry of Arsenic, Antimony and Bismuth*. Blackie Academic and Professional: London, 1998.

17. Breunig, H. J.; Ghesner, M. E.; Lork, E.; Issleib, K.; Balszuweit, A., *Zeitschrift Für Anorganische Und Allgemeine Chemie* **1975**, 418, 158.
18. Issleib, K.; Balszuweit, A., *Zeitschrift Für Anorganische Und Allgemeine Chemie* **1976**, 419, 87.
19. Twamley, B.; Hwang, C.-S.; Hardman, N. J.; Power, P. P., *Journal of Organometallic Chemistry* **2000**, 609, 152.
20. Wilkinson, G.; Stone, F. G. A.; Abel, E. W., *Comprehensive Organometallic Chemistry The Synthesis, Reactions and Structures of Organometallic Compounds*. Pergamon Press: New York., 1982; Vol. 2.
21. Aylett, B. J., *Silicon hydrides and their derivatives*. Academic Press: New York, 1968; Vol. 11.
22. MacDiarmid, A. G., *New Pathways in Inorg. Chem.* Cambridge University Press: London, 1968.
23. MacDiarmid, A. G., *Quarterly Review* **1956**, 10, 208.
24. Bulgakova, S. A.; Mazanova, L. M.; Semenov, V. V.; Semchikov, Y. D., *European Polymer Journal* **2007**, 43, 644.
25. Kornev, A. N.; Semenov, V. V. Method of preparing organosilicon hydrides, U.S.S.R. Patent. 1992.
26. Chalk, A. J.; Harrod, J. F., *Journal of the American Chemical Society* **1965**, 87, 1133.
27. Nguyen, B., T. Hydrosilation with platinum free neat copper containing catalysts, U.S. Patent. 2004.
28. Shi, M.; Nicholas, K. M., *Journal of Chemical Research* **1997**, 11, 400.
29. Helmy, R.; Wenslow, R. W.; Fadeev, A. Y., *Journal of the American Chemical Society* **2004**, 126, 7595.
30. Denmark, S. E.; Ober, M. H., *Aldrichimica Acta* **2003**, 36, 75.
31. Weidman, T. W.; Joshi, A. M., *Applied Physics Letters* **1993**, 62, 372.
32. Chernyshev, E. A.; Korshunov, A. I., In *Gazofaznye Vysokotemp. Metody Sint. Kremniorg. Monomerov*, 1978; p 5.
33. Minoura, Y.; Shiina, K. E., Y., *Kogyo Kagaku Zasshi* **1965**, 68, 1155.
34. Michalska, Z. M., *Transition Metal Chemistry (Dordrecht, Netherlands)* **1980**, 5, 125.

35. Haszeldine, R. N.; Parish, R. V.; Riley, B. F., *Journal of the Chemical Society, Dalton Transactions* **1980**, 5, 705.
36. Kali-Chemie, A.-G. Organosilanes, Patent. 1957.
37. Bulten, E. J. Ph.D Thesis. State University of Utrecht, Utrecht, 1969.
38. Harmer, H. R.; Laubengayer, A. W., *Germanium and germanium compounds*. 2 ed.; Kirk-Othmer Encycl. Chem. Technol.: 1966; Vol. 10.
39. Lesbre, M.; Mazerolles, P.; Satge, J., *The Organic Compounds of Germanium*. John Wiley & Son: New York, 1971.
40. West, R., *Journal of the American Chemical Society* **1953**, 75, 6080.
41. Lopatina, V. S.; Sheverdina, N. I.; Derkach, O. Y.; Kocheshov, K. A. Organotellurium compounds, U.S.S.R. Patent. 1979.
42. Van Dyke, C. H.; Bulkowski, J. E.; Viswanathan, N., *Inorganic and Nuclear Chemistry Letters* **1971**, 7, 1057.
43. Seyferth, D.; Hopper, S. P., *Journal of Organometallic Chemistry* **1970**, 23, 99.
44. Massol, M.; Satge, J.; Lesbre, M., *Journal of Organometallic Chemistry* **1969**, 17, 25.
45. Riviere, P.; Satge, J., *Comptes Rendus des Seances de l'Academie des Sciences, Serie C: Sciences Chimiques* **1968**, 267, 267.
46. Massol, M.; Satge, J.; Lesbre, M., *Comptes, Rendus des Seances de l'Academie des Sciences, Serie C: Sciences Chimiques* **1966**, 262, 1806.
47. Leigh, W. J.; Harrington, C. R., *Journal of the American Chemical Society* **2005**, 127, 5084.
48. Orlov, N. A.; Bochkarev, L. N.; Nikitinsky, A. V.; Kropotova, V. Y.; Zakharov, L. N.; Fukin, G. K.; Khorshev, S. Y., *Journal of Organometallic Chemistry* **1998**, 560, 21.
49. Subashi, E.; Rheingold, A. L.; Weinert, C. S., *Organometallics* **2006**, 25, 3211.
50. Dakternieks, D.; Schiesser, C.; Perchnyonok, T.; Duthie, A. M. Preparation of organogermanium compounds and methods for their use, PCT international application Patent. 2004.
51. Neumann, W. P., *The organic chemistry of tin* John Wiley & Sons: London, New York, 1970.
52. Akhtar, M.; Clark, H. C., *Canadian Journal of Chemistry* **1968**, 46, 2165.

53. Dodero, V. I.; Mitchell, T. N.; Podesta, J. C., *Organometallics* **2003**, 22, 856.
54. Helliwell, M.; Thomas, E. J.; Townsend, L. A., *Journal of the Chemical Society. Perkin Transactions 1* **2002**, 10, 1286.
55. Faranoi, M. B.; Koll, L. C.; Mandolesi, S. D.; Zuniga, A. E.; Podesta, J. C., *Journal of Organometallic Chemistry* **2000**, 613, 236.
56. Terstiege, I.; Maleczka, R. E. J., *Journal of Organic Chemistry* **1999**, 64, 342.
57. Reifenberg, G. H.; Considine, W. J., *Organometallics* **1993**, 12, 3015.
58. Becker, W. E.; Cook, S. E., *Journal of the American Chemical Society* **1960**, 82, 6264.
59. Van der Kerk, G. J. M.; Noltes, J. G.; Luijteo, J. G. A., *Journal of Applied Chemistry* **1957**, 7, 356.
60. Juenge, E. C.; Hawkes, S. J.; Snider, T. E., *Journal of Organometallic Chemistry* **1973**, 51, 189.
61. Martynov, A. V.; Sereckina, S. G.; Mirskova, A. N., *Izvestiya Akademii Nauk SSSR, Seriya Khimicheskaya* **1990**, 8, 1865.
62. Chehayber, J. M.; Drake, J. E., *Inorganica Chimica Acta*. **1986**, 111, 51.
63. Comasseto, J. V.; Gariani, R. A.; Princival, J. L.; Dos Santos, A. A.; Zinn, F. K., *Journal of Organometallic Chemistry* **2008**, 693, 2929.
64. Sashida, H.; Ohyanagi, K.; Minoura, M.; Akiba, K., *Journal of the Chemical Society Perkin Transactions 1* **2002**, 5, 606.
65. Tucci, F. C.; Chieffi, A.; Comasseto, J. V.; Marino, J. P., *Journal of Organic Chemistry* **1996**, 61, 4975.
66. Comasseto, J. V.; Ling, L. W.; Petraghani, N.; Stefani, H. A., *Synthesis* **1997**, 373.
67. Dabdoub, M. J.; Dabdoub, V. B.; Comasseto, J. V.; Petraghani, N., *Journal of Organometallic Chemistry* **1986**, 308, 211.
68. Takahashi, H.; Ohe, K.; Uemura, S.; Sugita, N., *Nippon Kagaku Kaishi* **1987**, 1508.
69. Ohe, K.; Takahashi, H.; Uemura, S.; Sugita, N., *Journal of Organometallic Chemistry* **1987**, 52, 4859.
70. Uemura, S.; Fukuzawa, S. I.; Patil, S. R., *Journal of Organometallic Chemistry* **1983**, 243, 9.

71. Barros, S. M.; Dabdoub, M. J.; Dabdoub, V. M. B.; Comasseto, J. V., *Organometallics* **1989**, 8, 1661.
72. Jang, W. B.; Oh, D. Y.; Lee, C.-W., *Tetrahedron Letters* **2000**, 41, 5103.
73. Pillarsetty, N.; Kannan, R.; Katti, K. V.; Barnes, C. L., In *225th ACS National Meeting*, New Orleans, LA, U.S, 2003.
74. Pillarsetty, N.; Ramaiah, K. P.; Gali, H.; Katti, K. V.; Barnes, C. L., In *222nd ACS National Meeting*, Chicago, IL, U.S, 2001.
75. Hiney, R. M.; Higham, L. J.; Müller-Bunz, H.; Gilheany, D. G., *Angewandte Chemie International Edition* **2006**, 45, 7248.
76. Brynda, M.; Geoffroy, M.; Bernardinelli, G., *Chemical Communications* **1999**, 961.
77. Prabhu, K. R.; Kishore, P. N.; Gali, H.; Katti, H. V., *Current Science* **2000**, 78, 431.
78. Goodwin, N. J.; Henderson, W.; Nicholson, B. K.; Fawcett, J.; Russell, D. R., *Journal of Chemical Society, Dalton Transactions* **1999**, 1785.
79. Henderson, W.; Alley, S. R., *Journal of Organometallic Chemistry* **2002**, 656, 120.
80. Togni, A.; Hayashi, T., *Ferrocenes: homogeneous catalysis, organic synthesis, materials science*. VCH Publishers: New York 1995.
81. Štěpnička, P., *Ferrocenes : ligands, materials and biomolecules*. John Wiley: Hoboken, N.J., 2008.
82. Tschirschwitz, S.; Loennecke, P.; Reinhold, J.; Hey-Hawkins, E., *Angewandte Chemie International Edition* **2005**, 44, 2965.
83. Limburg, C.; Lönnecke, P.; Gómez-Ruiz, S.; Hey-Hawkins, E., *Organometallics* **2010**, 29, 5427.
84. Buerger, J. F.; Togni, A., *Organometallics* **2011**, 30, 4742.
85. Bettermann, G.; Krause, W.; Riess, G.; Hofmann, T., "Phosphorus Compounds Inorganic" in *Ullmann's Encyclopedia of Industrial Chemistry*. Wiley-VCH: Weinheim, 2002.
86. Holleman, A. F.; Wiberg, E., *Inorganic Chemistry*. Academic Press: San Diego, 2001.
87. Kalio, R.; Lönnecke, P.; Hey-Hawkins, E., *Journal of Organometallic Chemistry* **2008**, 693, 590.

88. Schmidbaur, H.; Weidenhiller, G.; Steigelmann, O.; Mueller, G., *Chemische Berichte* **1990**, 123, 285.
89. Dell'anna, M. M.; Mastroilli, P.; Nobile, C. F.; B., C.-C.; Englert, U.; Peruzzini, M., *Dalton Transactions* **2008**, 43, 6005.
90. Pet, M. A.; Cain, M. F.; Hughes, R. P.; Glueck, D. S.; Golen, J. A.; Rheingold, A. L., *Journal of Organometallic Chemistry* **2009**, 694, 2279.
91. Bruker, A. B.; Grinshtein, E. I.; Raver, K. R.; Balashova, L. D.; Soborovskii, L. Z., *Khim. Primen. Fosfororg. Soedin., Tr. Vses. Konf. 3rd* **1972**, 285.
92. Goodwin, N. J.; Henderson, W.; Nicholson, B. K.; Sarfo, J. K.; Fawcett, J.; Russell, D. R., *Journal of the Chemical Society, Dalton Transactions* **1997**, 4377.
93. Lednicer, D.; Hauser, C. R., *N,N*-Dimethylaminomethylferrocene Methiodide. In *Organic Syntheses Collective*, 1973; Vol. V, p 434.
94. O'Neil, M. J., *The Merck index : an encyclopedia of chemicals, drugs, and biologicals*. Merck Research Laboratories: Whitehouse Station, N.J. , 2001.
95. Henderson, W.; Olsen, G. M., *Polyhedron* **1998**, 17, 577.
96. Hai Wang, C. J. Y.; Wan, Y.; Yowanto, H.; Kim, J. C.; Donilon, L. H.; Tao, C.; Strong, M.; Chong, Y., *Journal of Organic Chemistry* **2001**, 66, 2937.
97. Zotti, G.; Zecchin, S.; Schiavon, G., *Chemistry of Materials* **1995**, 7, 2309.
98. Tazaki, M.; Okada, K.; Yakata, K.; Nakano, K.; Sakai, M.; Yonemitsu, T., *Phosphorus, Sulfur, and Silicon and the Related Elements* **2000**, 167, 239.
99. Kündig, E. P.; Monnier, F. R., *Advanced Synthesis & Catalysis* **2004**, 346, 901.
100. Gossel, M. C.; Hamilton, D. G.; Fuller, J. I.; Millan-Barios, E., *Journal of the Chemical Society, Dalton Transactions* **1997**, 3471.
101. Alley, S. R. Ph.D Thesis. University of Waikato, Hamilton, 2001.
102. Cowley, A. H.; Damasco, M. C., *Journal of American Chemical Society* **1971**, 93, 6815.
103. Sheldrick, G. M. *SHELX-97 Programs for the Solution and Refinement of Crystal Structures (Release 97-2)*, University of Göttingen, Germany, 1997.
104. Sheldrick, G. M., *Acta Crystallographica A64* **2008**, 112.
105. Farrugia, L. J., *Journal of Applied Crystallography* **1999**, 32, 837.
106. Farrugia, L. J., *Journal of Applied Crystallography* **1997**, 30, 565.

107. Kosolapoff, G. M.; Maier, L., *Organic Phosphorus Compounds*. John Wiley & Sons, Inc.: New York, 1972; Vol. 4.
108. Kuwana, T.; Bublitz, D. E.; Hoh, G., *Journal of American Chemical Society* **1960**, 82, 5811.
109. Rausch, M. D.; Fischer, E. O.; Grubert, H., *Journal of American Chemical Society* **1960**, 82, 76-82.
110. Hildebrandt, A.; Rüffer, T.; Erasmus, E.; Swarts, J. C.; Lang, H., *Organometallics* **2010**, 29, (21), 4900–4905.
111. Nemykin, V. N.; Rohde, G. T.; Barrett, C. D.; Hadt, R. G.; Bizzarri, C.; Galloni, P.; Floris, B.; Nowik, I.; Herber, R. H.; Marrani, A. G.; Zaroni, R.; Loim, N. M., *Journal of American Chemical Society* **2009**, 131, (41), 14969–14978.
112. Gale, R. J.; Job, R., *Inorganic Chemistry* **1981**, 20, (1), 42–45.
113. Sato, M.; Kudo, A.; Kawata, Y.; Saitoh, H., *Chemical Communications* **1996**, 1, 25-6.
114. Stewart, B.; Harriman, A.; Higham, L. J., *Organometallics* **2011**, 30, 5338.
115. Alley, S. R.; Henderson, W., *Journal of Organometallic Chemistry* **2001**, 637-639, 216.
116. Narasimhan, P. T.; Rogers, M. T., *The Journal of Physical Chemistry* **1961**, 34, 1049.
117. Stafford, S. L.; Baldeschwieler, J. D., *Journal of the American Chemical Society* **1961**, 83, 4473.
118. Berrigan, R. A.; Russell, D. K.; Henderson, W.; Leach, M. T.; Nicholson, B. K.; Woodward, G.; Harris, C., *New Journal of Chemistry* **2001**, 25, 322.
119. Higham, L. J.; Hudson, H. R., *The Chemistry of Organophosphorus Compounds*. Wiley: New York, 1990; Vol. 1.
120. Imrie, C., *Applied Organometallic Chemistry* **1993**, 7, 181.
121. Baker, R. J.; Brym, M.; Jones, C.; Waugh, M., *Journal of Organometallic Chemistry* **2004**, 689, 781.
122. Kondo, T.; Yamamoto, k.; Omura, T.; Kumada, M., *Journal of Organometallic Chemistry* **1973**, 60, 287.
123. Nesmeyanov, A. N.; Perevalova, E. G.; Ustynyuk, Y. A., *Doklady Akademii Nauk SSSR* **1960**, 133, 1105.

124. Phadnis, P. P.; Jain, V. K.; Klein, A.; Weber, M.; Kaim, W., *Inorganica Chimica Acta* **2003**, 346, 119.
125. Serre, S. L.; Guillemin, J.-C., *Journal of Organic Chemistry* **1998**, 63, 59.
126. Quick, A. J.; Adams, R., *Journal of the American Chemical Society* **1922**, 44, 805.
127. Dork, G. O.; Freedman, L. D., *Organometallic compounds of arsenic, antimony and bismuth*. Wiley-Interscience: New York, 1970.
128. Henderson, W.; Leach, M. T.; Nicholson, B. K.; Wilkins, A. L.; Hoye, P. A. T., *Polyhedron* **1998**, 17, 3747.
129. Greenwood, N. N.; Earnshaw, A., *Chemistry of the Elements*. 2 ed.; Butterworth-Heinemann: Oxford, 1997.
130. Anderson, H. H.; Grebe, L. R., *Journal of the American Chemical Society* **1961**, 26, 2006.
131. Davies, A. G.; Gielen, M.; Pannell, K. H., *Tin Chemistry*. Wiley: London, 2008.
132. Saito, M.; Hashimoto, H.; Tajima, T.; Ikeda, M., *Journal of Organometallic Chemistry* **2007**, 692, 2729.
133. Finholt, A. E.; Bond, A. C.; Schlesinger, H. I., *Journal of the American Chemical Society* **1947**, 69, 1199.
134. Fischer, A. K.; West, R. C.; Rochow, E. G., *Journal of the American Chemical Society* **1954**, 76, 5878.
135. Kluska, M.; Pypowski, K.; Chrzęścik, I.; Gadzała-Kopciuch, R.; Witkowska-Krajewska, E., *Critical Reviews in Analytical Chemistry* **2010**, 40, 30.
136. Speier, J. L.; Webster, J. A.; Barnes, G. H., *Journal of the American Chemical Society* **1957**, 79, 974.
137. Speier, J. L.; Saam, J. C., *ibid* **1958**, 80, 4104.
138. Bank, H. M.; Saam, J. C.; Speier, J. L., *Journal of Organometallic Chemistry* **1964**, 29, 792.
139. Joly, K. M.; Gleixner, R. M.; Simpkins, S. M. E.; Coe, D. M.; Cox, L. R., *Tetrahedron* **2007**, 63, 761.
140. Kondo, Y.; Miyazawa, K.; Kunugi, Y.; Takahashi, Y.; Miyazawa, H.; Miyao, K.; Tsukagoshi, T.; Yoshino, N., *Journal of Oleo Science* **2003**, 52, 505.

141. Li, J.; Wang, L.; Liu, J.; Evmenenko, G.; Dutta, P.; Marks, T. J., *Langmuir* **2008**, 24, 5755.
142. Carroll, M. A.; White, A. J. P.; Widdowson, D. A.; Williams, D. J., *Journal of the Chemical Society, Perkin Transactions 1* **2000**, 1551.
143. Eaborn, C.; Hancock, A. R.; Stańczyk, W. A., *Journal of Organometallic Chemistry* **1981**, 218, 147.
144. Audebert, P.; Sallard, S.; Sadki, S., *Journal of Physical Chemistry B* **2003**, 107, 1321.
145. Sakurai, H.; Shoji, M.; Yajima, M.; Hosomi, A., *Synthesis* **1983**, 598.
146. Gill, R.; Mazhar, M.; Mahboob, S.; Siddiq, M., *Polymer (Korea)* **2008**, 32, 239.
147. Brinckman, F. E.; Stone, F. G. A., *Journal of Inorganic and Nuclear Chemistry* **1959**, 11, 24.
148. Strenalyuk, T.; Samdal, S.; Møllendal, H.; Guillemin, J.-C., *Organometallics* **2006**, 25, 2626.
149. Neumann, V. W. P.; Niermann, H., *Justus Leibigs Annalen der Chemie* **1962**, 653, 164.
150. Czełuśniak, I.; Jachimowska, M.; Szymańska-Buzar, T., *Journal of Organometallic Chemistry* **2011**, 696, 3023.
151. Mingos, D. M. P.; Crabtree, R. H., *Comprehensive Organometallic Chemistry III Volume 9 Applications I: Main Group Compounds in Organic Synthesis*. Elsevier: London, 2007.
152. Riague, E. H.; Guillemin, J.-C., *Organometallics* **2002**, 21, 68.
153. Khater, B.; Gullemin, J.-C.; Bajor, G.; Veszpréml, T., *Inorganic Chemistry* **2008**, 47, 1502.
154. Ohira, N.; Aso, Y.; Otsubo, T.; Ogura, F., *Chemistry Letters* **1984**, 853.
155. Detty, M. R.; Murray, B. J.; Smith, D. L.; Zumbulyadis, N., *Journal of the American Chemical Society* **1983**, 105, 875.
156. Kumar, S.; Helt, J. P.; Autschbach, J.; Detty, M. R., *Organometallics* **2009**, 28, 3426.
157. Lee, Y.; Morales, G. M.; Yu, L., *Angewandte Chemie International Edition* **2005**, 44, 4228.
158. Santi, C.; Santoro, S.; Testaferri, L.; Tiecco, M., *Synlett* **2008**, 10, 1471.

159. Herberhold, M.; Leitner, P., *Journal of Organometallic Chemistry* **1987**, 336, 153.
160. Klayman, D. L.; Griffin, T. S., *Journal of the American Chemical Society* **1973**, 95, 197.
161. Goodman, M. M.; Knapp, F. F. J., *Organometallics* **1983**, 2, 1106.
162. Spencer, H. K.; Lakshmikantham, M. V.; Cava, M. P., *Journal of the American Chemical Society* **1977**, 99, 1470.
163. Krief, A.; Dumont, W.; Robert, M., *Chemical Communications* **2005**, 2167.
164. Guillemin, J.-C.; Bajor, G.; Riague, E. H.; Khater, B.; Veszpréml, T., *Organometallics* **2007**, 26, 2507.
165. Ahmar, S.; Nitschke, C.; Vijayaratnam, N.; MacDonald, D. G.; Fensk, D.; Corrigan, J. F., *New Journal of Chemistry* **2011**, 35, 2013.
166. Stoner, G. G.; Williams, R. W., *Journal of the American Chemical Society* **1948**, 70, 1113.
167. Krief, A.; Delmotte, C.; Dumont, W., *Tetrahedron* **1997**, 53, 12147.
168. Delacroix, O.; Andriamihaja, B.; Picart-Goetgheluck, S.; Brocard, J., *Tetrahedron* **2004**, 60, 1549.
169. Chu, J. Y. C.; Marsh, D. G.; Guenther, W. H. H., *Journal of the American Chemical Society* **1975**, 97, 4905.
170. Brown, D. H.; Cross, R. J.; Millington, D., *Journal of Organometallic Chemistry* **1977**, 125, 219.
171. Spencer, H. K.; Cava, M. P., *Journal of Organic Chemistry* **1977**, 42, 2937.
172. Stanley, W.; Van De Mark, M. R.; Kumler, P. L., *Journal of the Chemical Society. Chemical Communications* **1974**, 700.
173. Zeng, Z.; Torriero, A. A. J.; Belousoff, M. J.; Bond, A. M.; Spiccia, L., *Chemistry: A European Journal* **2009**, 15, 10988.
174. Luthra, N. P.; Boccanfuso, A. M.; Dunlap, R. B.; Odom, J. D., *Journal of Organometallic Chemistry* **1988**, 354, 51.
175. Duddeck, H., *Pergamon, Progress in NMR Spectroscopy* **1995**, 27, 1.
176. Nemykin, V. N.; Maximov, A. Y.; Kuposov, A. Y., *Organometallics* **2007**, 26, 3138.
177. Suzuki, H.; Miyoshi, K.; Osuka, A., *Nippon Kagaku Kaishi* **1981**, 3, 472.

178. Mugesh, G.; Panda, A.; Kumar, S.; Apte, S. D.; Singn, H. B.; Butcher, R. J., *Organometallics* **2002**, 21, 884.
179. Gautheron, B.; Tainturier, G.; Degrand, C., *Journal of the American Chemical Society* **1985**, 107, 5579.
180. Shriver, D. F.; Drezdson, M. A., *The Manipulation of Air-Sensitive Compounds*. John Wiley & Sons: New York, 1986.
181. Henderson, W.; McIndoe, J. S.; Nicholson, B. K.; Dyson, P. J., *Journal of the Chemical Society, Dalton Transactions* **1998**, 519.
182. Arnold, L. J., *Journal of Chemical Education* **1992**, 69, 811.
183. Farrugia, L. J. *WinGX – Version 1.64.05*, Department of Chemistry, University of Glasgow.
184. Terada, S.; Kuruma, K.; Konaka, R., *Journal of the Chemical Society, Perkin II* **1973**, 1252.
185. Wang, Y.-P.; Lin, T.-S.; Shyu, R.-S.; Hwu, J.-M., *Journal of Organometallic Chemistry* **1989**, 371, 57.
186. McIndoe, J. S. Ph.D. Thesis. University of Waikato, 1998.
187. Lednicer, D.; Mashburn, T. A. J.; Hauser, C. R., Hydroxymethylferrocene. In *Organic Syntheses Collective*, 1960; Vol. 40, p 52.
188. Davis, J.; Vaughan, D. H., *Journal of Chemical Education* **1995**, 72, 266.
189. Krasnikova, E. M.; Moskalenko, A. I.; Kopaeva, N. A.; Boev, V. I., *Russian Journal of General Chemistry* **2003**, 73, 1468.
190. Valderrama, M. I. R.; Vázquez García, R. A.; Klimova, T.; Klimova, E.; Ortiz-Frade, L.; Martínez García, M., *Inorganica Chimica Acta* **2008**, 361, 1597.

List of Compounds

1	FcCH ₂ PH ₂	27	RcCH ₂ P(CH ₂ OH) ₂
2	CamphylPH ₂	28	RcCH ₂ P(O)(CH ₂ OH)H
3	FcCH ₂ P(Cy)H	29	FcCH ₂ P(O)(CH ₂ OH)OH
4	FcCH ₂ P(Me)H	30	FcCH ₂ P(O)H ₂
5	FcCH ₂ P(CH ₂ C ₆ H ₄ NO ₂)H	31	{CpFeC ₅ H ₃ (CH ₂ OH)}{CH ₂ P(CH ₂ OH) ₂ }
6	[FcCH ₂ NMe ₃]I	32	{CpFeC ₅ H ₃ (CH ₂ OH)}(CH ₂ PH ₂)
7	FcCH ₂ P(Cy)(CH ₂ OH)	33	[{CpFeC ₅ H ₃ (CH ₂ OH)}(CH ₂ NMe ₃)]I
8	FcCH ₂ P(CH ₂ OH) ₂	34	Fc(CH ₂) ₆ PH ₂ ·BH ₃
9	FcCH ₂ P(Me)(CH ₂ OH)	35	FcCH ₂ PH ₂ ·BH ₃
10	FcCH ₂ P(CH ₂ C ₆ H ₄ NO ₂)(CH ₂ OH)	36	FcCH ₂ P(O)(OH)H
11	(FcCH ₂) ₂ P(Cy)	37	CamphylP(O)(OH)H
12	(FcCH ₂) ₂ P(CH ₂ C ₆ H ₄ NO ₂)	38	FcCH ₂ AsH ₂
13	FcCH ₂ P(CH ₂ C ₆ H ₄ NO ₂) ₂	39	FcCH ₂ AsCl ₂
14	Fc(CH ₂) ₄ PH ₂	40	FcCH ₂ Li
15	Fc(CH ₂) ₆ PH ₂	41	Fc(CH ₂) ₂ AsH ₂
16	Fc(CH ₂) ₁₁ PH ₂	42	Fc(CH ₂) ₄ AsH ₂
17	Fc(CH ₂) ₄ Br	43	Fc(CH ₂) ₆ AsH ₂
18	Fc(CH ₂) ₆ Br	44	Fc(CH ₂) ₁₁ AsH ₂
19	Fc(CH ₂) ₁₁ Br	45	FcCH ₂ SbH ₂
20	Fc(CH ₂) ₄ P(CH ₂ OH) ₂	46	FcCH ₂ SbCl ₂
21	Fc(CH ₂) ₆ P(CH ₂ OH) ₂	47	FcCH ₂ OMe
22	Fc(CH ₂) ₁₁ P(CH ₂ OH) ₂	48	Fc(CH ₂) ₄ As(O)(OH) ₂
23	Fc(CH ₂) ₂ PH ₂	49	Fc(CH ₂) ₁₁ As(O)(OH) ₂
24	RcCH ₂ PH ₂	50	Fc(CH ₂) ₂ SiH ₃
25	RcH	51	Fc(CH ₂) ₂ SiCl ₃
26	[RcCH ₂ NMe ₃]I	52	Fc(CH ₂) ₂ Si(OMe) ₃

53	Fc(H)C=CH_2	72	FcCH_2SeH
54	$\text{Fc(CH}_2)_5\text{SiCl}_3$	73	FcCH_2OH
55	$\text{PhCH}_2\text{Si(OMe)}_3$	74	$\text{Fc(CH}_2)_4\text{SeH}$
56	$\text{Fc(CH}_2)_6\text{Si(OEt)}_3$	75	$\{\text{Fc(CH}_2)_4\}_2\text{Se}_2$
57	$\text{FcCH}_2\text{GeH}_3$	76	$(\text{FcCH}_2)_2\text{Se}_3$
58	$\text{FcCH}_2\text{GeCl}_3$	77	$\{\text{Fc(CH}_2)_4\}_2\text{Se}$
59	$\text{FcCH}_2\text{SnCl}_3$	78	PhSeH
60	$\text{FcCH}_2\text{SnI}_3$	79	$(\text{PhSe})_2$
61	$\text{Ph(Cl)C=C(SnCl}_3\text{)H}$	80	FcCH_2TeH
62	$\text{Fc(Cl)C=C(SnCl}_3\text{)H}$	81	FcCH_2TeCN
63	$\text{FcC}\equiv\text{CH}$	82	$(\text{FcCH}_2)_2\text{Te}_2$
64	$\text{Fc(Cl)C=C(SnH}_3\text{)H}$	83	FcCH_2CN
65	$\text{Fc(H)C=C(SnH}_3\text{)H}$	84	$(\text{FcCH}_2)_2\text{O}$
66	$\text{FcCH}_2\text{SnH}_3$	85	$\text{Fc(CH}_2)_4\text{OH}$
67	FcCH_2SeCN	86	KTeCN
68	$\text{Fc(CH}_2)_4\text{SeCN}$	87	$\text{Fc(CH}_2)_4\text{TeCN}$
69	$(\text{FcCH}_2\text{Se})_2$	88	$(\text{FcCH}_2)_2\text{Te}$
70	$(\text{FcCH}_2)_2\text{Se}$	89	$\text{Fc(CH}_2)_9(\text{H)C=CH}_2$
71	FcCH_2Cl		